July 2019

Design, Synthesis and Study of Functional Amphiphilic Polymers and Their Applications

Huan He

Design, Synthesis and Study of Functional Amphiphilic Polymers and Their Applications

A Dissertation Presented

by

HUAN (JOY) HE

Submitted to the Graduate School of the
University of Massachusetts Amherst in partial fulfillment
of the requirements for the degree of

DOCTOR OF PHILOSOPHY

MAY 2019

Department of Chemistry

Design, Synthesis and Study of Functional Amphiphilic Polymers and Their Applications

A Dissertation Presented

by

HUAN (JOY) HE

Approved as to style and content by:

_____
Sankaran Thayumanavan, Chair

_____
Richard W. Vachet, Member

_____
Min Chen, Member

_____
Kathleen F. Arcaro, Member

_____
Richard W. Vachet, Department Head
Department of Chemistry

DEDICATION

To my parents (Youde He and Shuzhen Zhen), my sister (Rui He), my husband (Bin Liu) and my son (Ivan Liu).

ACKNOWLEDGMENTS

I would firstly like to thank the Chemistry Department at University of Massachusetts Amherst for accepting me in the Doctoral program. I would like to thank my advisor, Professor Sankaran Thayumanavan for taking me in working for his excellent research group. I will always be grateful for his patience, guidance, his constant effort in making his students critical thinkers and his intelligence which has been an inspiration towards me being a better thinker, a better scientist.

I would like to thank my committee members, Professor Richard Vachet, Professor Min Chen and Professor Kathleen F. Arcaro, for their suggestions, guidance, and insight into my prospectus, ORP and all my projects.

I would like to thank my mentor Dr. Ambata Poe and Dr. Rajasekhar Reddy Rami Reddy who took the time and effort to guide me from my first year when I was struggling with the projects in hand. I will always be indebted towards their mentorship and friendship. Next, I would like to thank the fantastic people I collaborated with in all my projects who gave the projects a different direction with their insightful suggestions and contributed to my research: Mahalia Adelina Corazon Serrano (Mac), Bin Liu, Ziwen Jiang, Meizhe Wang, Bo Zhao, Dr. Rajasekhar Reddy Rami Reddy, and Dr. Subramani Swaminathan.

I would like to thank our group assistant Karen Hakala for her constant help and support, and selfless love she bestows upon all the Thai group members. I would like to thank the staff from chemistry department: JMS, Viki, Ryan, Bob and Marv for all their help in making my life and research much easier here in Amherst.

I would like to thank all my friends at UMass who helped me throughout the journey with their cheer and support. My classmates, lab mates and friends for life, Dr. Priyaa Prasad and Dr. Poornimar Rangadurai were part of my journey here at Amherst from the beginning; Dr. Kishore

Raghupathi, Vikash Kumar, Piyachai Khomein, Wardah Ejaz, Dr. Hui Wang, Dr. Krishna Raghupathi, Dr. Jiaming Zhuang and every other past and current Thai group member – you have been amazing and thank you for the cheer and laugh. I would also like to thank all my friends I met outside the lab – Qinfang Sun, Xin Li, Monifa Fahie, Xuni Li, Chengfeng Ren. I would like to thank my undergrad friends from China for their constant support and friendship – Cuiping Zhang, Yawei Li, Dejing Liu, Shuang Yang and many more.

I would like to thank my parents and parents-in-law, my sister and sister-in-law for their selfless and generous love, encouragement and support. I would like to thank my best friend and also my husband, Bin Liu, for his endless love and criticism that has helped me changed into who I am today. Having known him for almost 14 years of my life is a great pleasure. Last but not least, I would like to thank my son, Ivan Liu, for his blind love, faith, and trust that has motivated me enormously and taught me never to give up. All achievements seem insignificant without friends and family. Thank you all once again for being in my life and making it memorable.

ABSTRACT

DESIGN, SYNTHESIS AND STUDY OF FUNCTIONAL AMPHIPHILIC POLYMERS AND THEIR APPLICATIONS

MAY 2019

HUAN (JOY) HE

B.S., NANKAI UNIVERSITY

M.S., NANKAI UNIVERSITY

Ph.D., UNIVERSITY OF MASSACHUSETTS AMHERST

Directed by: Professor Sankaran Thayumanavan

Amphiphilic homopolymers with high densities of functional groups are synthetically challenging. Thiol-yne nucleophilic click reactions have been investigated to introduce multiple functional groups in polymers with high density. An electron deficient alkyne group bearing methacrylate monomer was polymerized using reversible addition−fragmentation chain-transfer (RAFT) polymerization. Subsequently, the electron deficient alkyne group on polymer side chain was readily reacted with a thiol reagent using triethylamine (TEA) as the organocatalyst. This reaction was found to be very efficient under mild conditions. The resultant homopolymer bearing thiol vinyl ether functional groups could perform a second thiol addition with a stronger base, such as triazabicyclodecene (TBD), to prepare multifunctional homopolymers. This stepwise addition process was monitored by different techniques. The fidelity of this method was demonstrated by attaching four different functionalities, including both hydrophobic and hydrophilic moieties. Also, a novel polymerization method was developed using same thiol-yne nucleophilic addition strategy. Typically, two bi-functional thiol-based monomers with activated alkyne termini differencing in their linker length can be prepared and polymerized utilizing this strategy. Under mild conditions, monomers can be polymerized conveniently to yield linear structures with high

molecular weights. The polymerization conditions were optimized by screening various catalysts, solvents, temperatures, reaction time, and monomer concentrations. This new methodology efficiently yields polymers with high molecular weight. Moreover, the resulting polymer contains alkene backbone that acts as a functional handle for further modifications. For example, it can be subjected to a second thiol species to achieve multi-functional capabilities. These post-modified polymers with dithioacetal units in their backbone degrade in the presence of reactive oxygen species, providing the opportunity to design functional materials with stimuli responsive features.

TABLE OF CONTENTS

Page

LIST OF FIGURES

Figure Page

LIST OF SCHEMES

Scheme Page

CHAPTER

1. INTRODUCTION

1.1 Introduction

Amphiphilic polymers preparation and their self-assembly have been studied for many decades due to their various morphologies formation into ordered structures at the molecular scale and morphological transitions upon internal and/or external stimuli. Well controlled radical polymerization method combined with highly efficient click chemistry reactions could enable facile synthesis of complex polymer architecture. Based on polymer skeleton, amphiphilic polymers could be classified as block copolymer[1], random copolymer[2], brush polymer[3], star-shaped polymer[4], and dendrimers[5], etc. Through well-chosen monomer with different chemistry characteristics, control over polymer molecular weight, and design of macromolecular architecture, amphiphilic polymers can be used for numerous applications. These applications include but are not limited to biomedical, micro electrical, optical, lithographic and photonic materials[6–11].

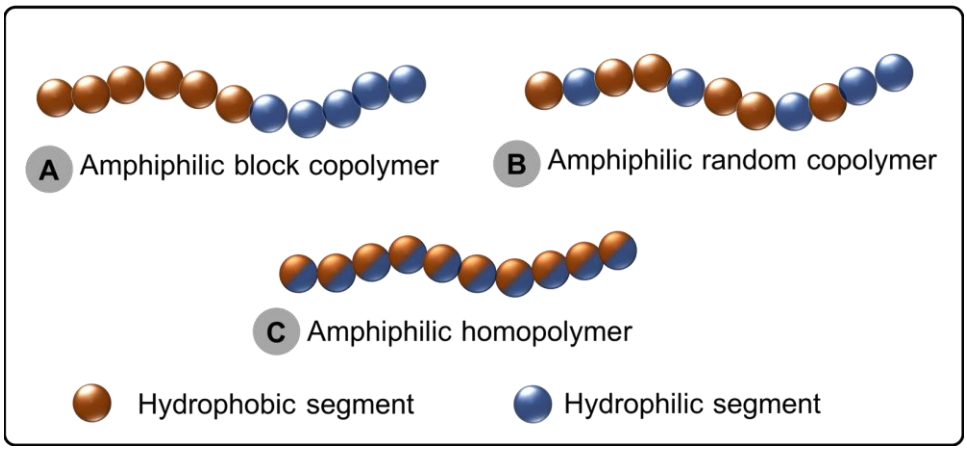

Scheme 1.1 Overview of amphiphilic polymers with different architectures. A) di-block; B) random; C) homopolymer.

Recently, another amphiphilic polymer, in which both a hydrophilic and hydrophobic group are locating in each repeating unit, has gained broad interest owing to their self-assembly property, imparted from their unique polymer structures. This special polymer is named as an amphiphilic homopolymer. In this introduction, we will focus on block copolymer, random copolymer and amphiphilic homopolymers self-assemble, synthesis, and their applications. (Scheme 1.1).

1.1.1 Amphiphilic block copolymer

A block copolymer, a combination of two or more homopolymers, can possess properties characteristic of each of the homopolymers as well as a set of features due to the polymer structure as a whole[12]. Amphiphilic block copolymer contains both hydrophilic and hydrophobic blocks, in which two distinct blocks have been tethered together through covalent bonds.

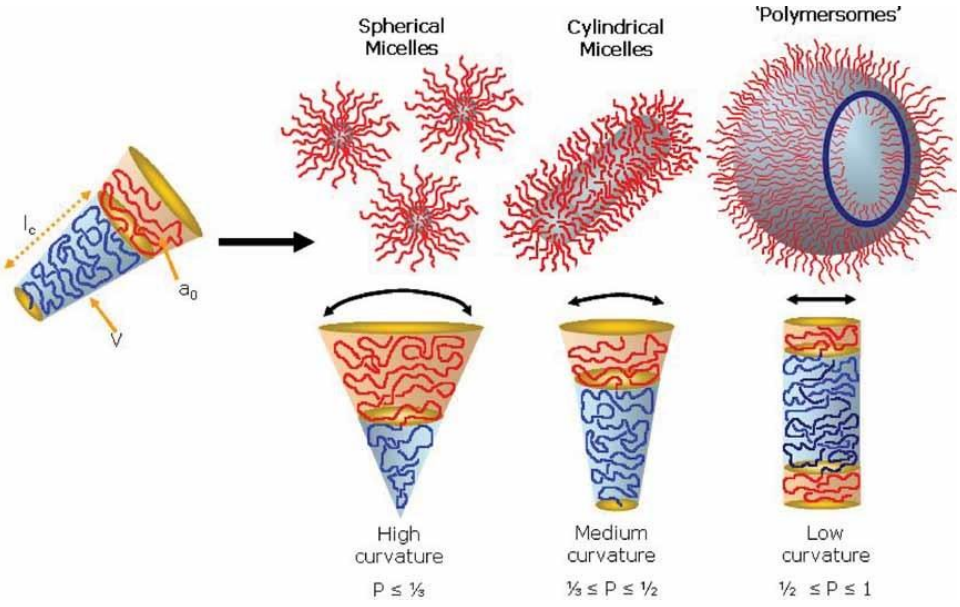

Scheme 1.2 Various self-assembled structures formed by amphiphilic block copolymers in a block-selective solvent. (Reproduced with the permission from ref[12])

Due to the well-defined polymer architectures, their phase separations and morphology transitions in water/organic solvent, as well as solid state have been studied[13]. They can form aggregates with variant morphologies from micelles to vesicles. The type of self-assemble is due to the

hydrophilic/lipophilic balance together with the inherent molecular curvature and how this influences the copolymer chains packing[12]. For example, a spherical micelle-like morphology could obtain if the packing parameter (P) is estimated to be less than 1/3, in which the hydrophilic segment is much larger than hydrophobic segment, and the whole polymer chain tends to self-assemble into energetically favored corn shape. Amphiphilic block copolymers self-assembly behavior and superior physical properties have manifested themselves in various applications, such as biomedicine, microelectronics, and photonic materials[13]. Despite half a century of development of block copolymers, the synthesis of further multi-block copolymer remains tedious and challenging, primarily because the reactive end group after two blocks may be lost during the preparation and purification process, which limits their further applications. Almost at the same time, random copolymers have been developed and could serve as an alternative candidate to overcome the synthetic limitation.

1.1.2 Amphiphilic random copolymer

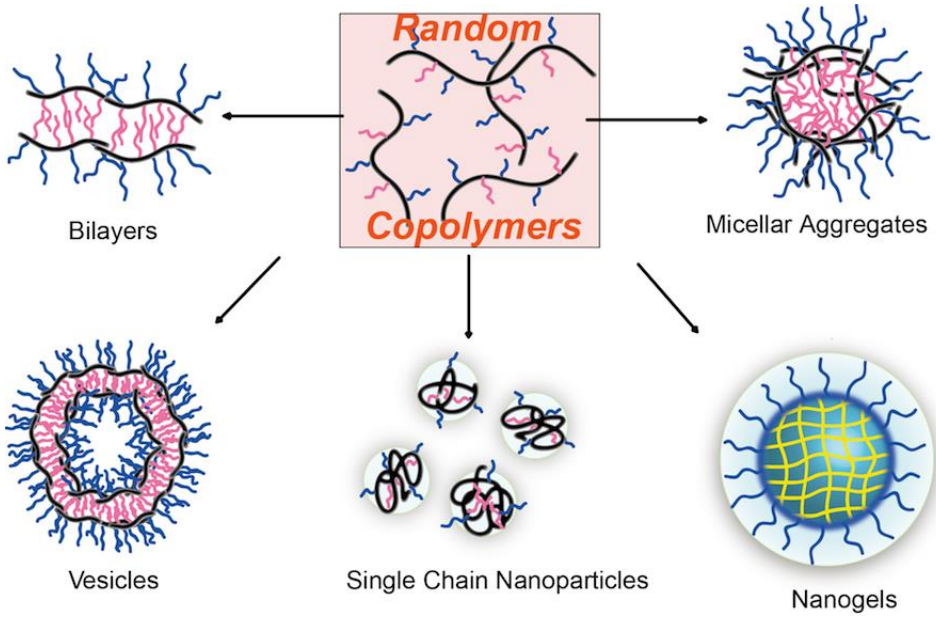

Scheme 1.3 Various self-assembled structures formed by amphiphilic random copolymers. (Reproduced with the permission from ref[14])

Random copolymers contain two or more monomers that have been randomized into a polymer backbone. Monomers with distinct chemical properties can be mixed and matched as required. Paralleling with the block copolymers, random copolymers can also self-assemble into different morphologies, and they are less dense and fast respond if stimuli applied[15]. Different from block copolymers, the sequence of monomers is random and unpredictable. Because of the ill-defined polymer structures, the morphology of amphiphilic random copolymers in aqueous solutions largely depends on their hydrophilic-lipophilic balance (HLB). For example, an amphiphilic random copolymer containing a hydrophobic dodecyl chain and hydrophilic L-glutamic acid was prepared by copolymerization. Through adjusting the feed ratio of decyl group and L-glutamic acid, a rich variety of nanostructures were fabricated, including giant vesicles, vesicles, honeycomb films, and nanoporous spheres[16]. However, compared with block copolymers, random copolymers also have the disadvantage of a crystalline polymer, in which its melting point, modulus, tensile strength and elastic properties will be dramatically compromised[17].

1.1.3 Amphiphilic homopolymer

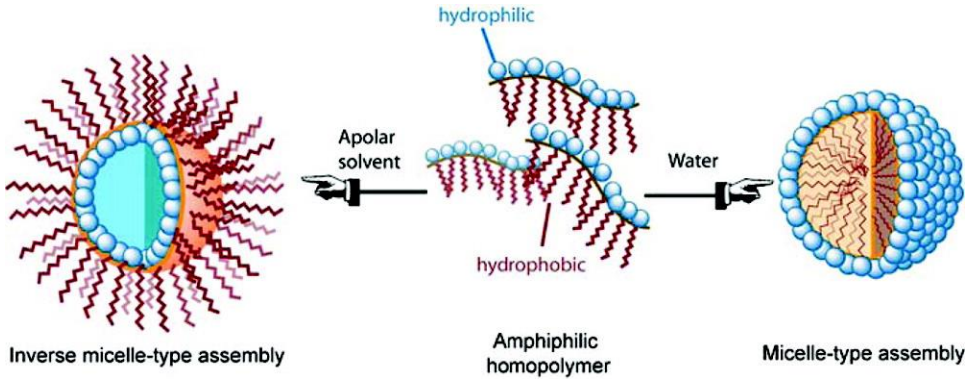

Scheme 1.4 Schematic representation of micelle-type and inverse-micelle-type assemblies[18].

The idea of amphiphilic homopolymer[19] is inspired by the advantage combination of well-defined structure from the block copolymer and facile synthesis of homopolymer. Our group[19–21] together

with others[22–24] have pioneered this area. The specialty of the amphiphilic homopolymer is that both hydrophilic and lipophilic segments possess the same monomer or repeating unit. It can be imaged that amphiphiles or small molecule surfactants have been tethered together using a string. They could self-assemble into a range of nanostructures nano-sized aggregates with different morphologies by changing the nature of monomer chemistry or hydrophobic component. For example, an amphiphilic homopolymer containing (2-hydroxy-3-phenoxypropyl acrylate) (HPPA) has been prepared through RAFT polymerization. Upon merely changing the homopolymer's chain length or co-solvents during self-assembly, large compound micelles (LCMs), simple vesicles, large compound vesicles (LCVs), and hydrated large compound micelles (HLCMs) as a result of the different intensity of inter/intra-polymer hydrogen bonding in the homopolymer self-assemblies[25] were obtained. Besides, morphologies, such as thin film[26], cubic[27], microfibers[28], tubular vesicle[29] were also reported by other researchers.

1.2 Synthesis of amphiphilic polymers

1.2.1 Synthesis of amphiphilic block copolymer

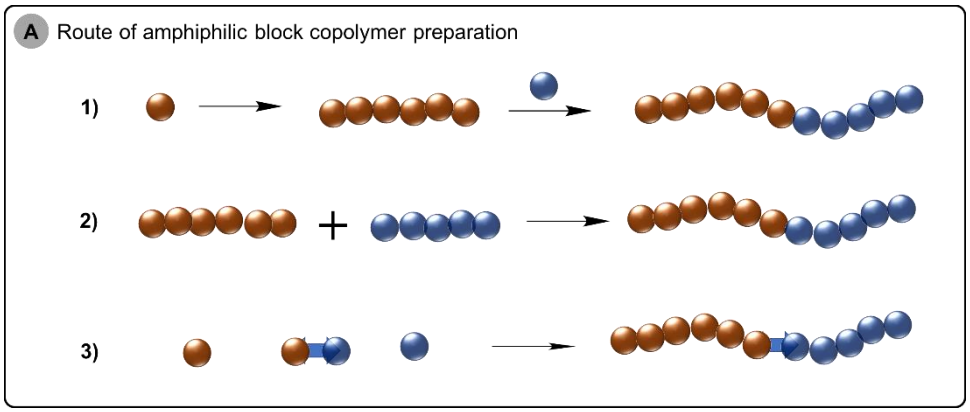

Scheme 1.5 General approaches of preparation of amphiphilic block copolymer**.**

The synthesis of the block copolymer can be generally categorized into three pathways. Firstly, the preparation of block copolymer involves polymerization of one monomer at one time and

sequentially polymerize another monomer with the macroinitiators using atom transfer radical polymerization (ATRP)[30], or with macro-chain transfer reagent by RAFT[31] (Scheme 1.5 (1)). Also, a di-block copolymer can be prepared by linking two blocks of homopolymer together through their end group reactions[32,33](Scheme 1.5 (2)). Another alternative approach is to start with a difunctional initiator with which two different monomers can be polymerized with orthogonal polymerization methods (Scheme 1.5 (3))[34].

1.2.2 Synthesis of amphiphilic random copolymer

Unlike block copolymer, the synthesis of random copolymers is much easier. One could prepare a random copolymer by either copolymerization of two or more monomers in one pot[35] as long as the monomers share similar reactivity (Scheme 1.6 (1)), or post-polymerization modification of precursor polymer with different substitutes (Scheme 1.6 (2))[36]. The advantage of the random copolymer is that their hydrophilic and lipophilic ratio could be tuned easily by changing the feeding ratio of the two or more monomers, which overcomes the synthetic limitation of the block copolymer.

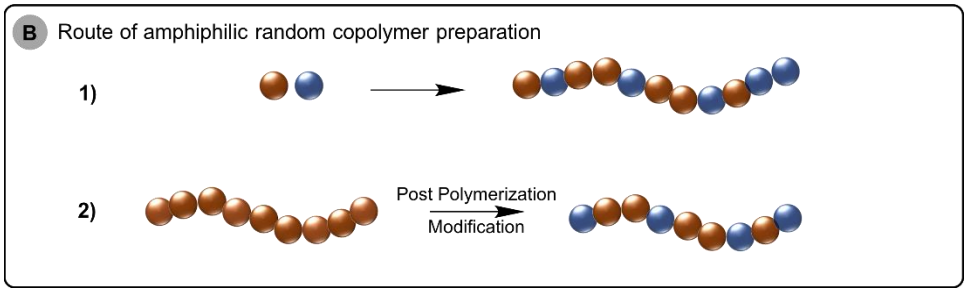

Scheme 1.6 One-step copolymerization one pot post-polymerization treatment for preparing the random copolymer.

1.2.3 Synthesis of amphiphilic homopolymer

The synthesis of the amphiphilic homopolymer is easy compared to a two-step polymerization in block copolymer. To have a homopolymer with amphiphilicity, one could either start with an

amphiphilic monomer or post polymerization modification with an amphiphile. However, rational design and synthesis of monomers with desired amphiphilicity needs to be taken into consideration. Also, the bulky volume of an amphiphilic monomer may prevent it from growing into high molecular weight polymers.

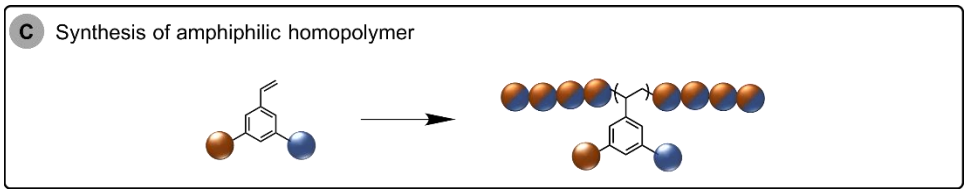

Scheme 1.7 Preparation of amphiphilic homopolymer through amphiphile monomer polymerization.

1.3 Applications

Self-assembly of amphiphilic macromolecules is ubiquitous in nature. Examples include amphiphilic peptide chains self-assembled into water-soluble proteins, and phospholipids self-organized into cell membranes. Synthetic amphiphilic polymers, on the other hand, share similar chemical and physical properties, could also self-assemble into ordered structures with various morphologies. Those morphologies can be tuned through monomer chemical characteristics along with surrounding environments such as temperature, solvent, and additives. This variant along with the morphology transition tunability of polymeric aggregates provide a platform for expanding applications from biomaterials to electronics. In this introduction, we will focus on amphiphilic homopolymer application in responsive therapeutic delivery with micelle aggregates and biomarker sensing with reverse micelle aggregates.

1.3.1 Responsive therapeutic delivery

Micelle, made from amphiphilic polymers, consist of the hydrophilic coronas that afford the solubility in water, and hydrophobic cores that provide an ideal location for encapsulation of water-insoluble molecules such as hydrophobic drugs and fluorescence probes. Increased stability can

also be achieved through coronal or core chain cross-linking. Therefore, amphiphilic homopolymers were widely used as therapeutic delivery carriers. Further, by installing stimuli-responsive functional groups in the polymer, controlled release of the payloads could be realized. Different stimuli have been incorporated into polymers. The stimuli could be: a) biological stimuli, such as protein, enzyme, or sugar; b) physical stimuli, such as magnetic field, electric field, light, ultrasound, or temperature; c) chemical stimuli, such as pH and redox. Therapeutic drugs are allowed to either covalently attached to the polymer through stimuli-responsive linker[37] or non-covalently encapsulated into a nanocarrier interior and released upon the disruption of nanocarrier.

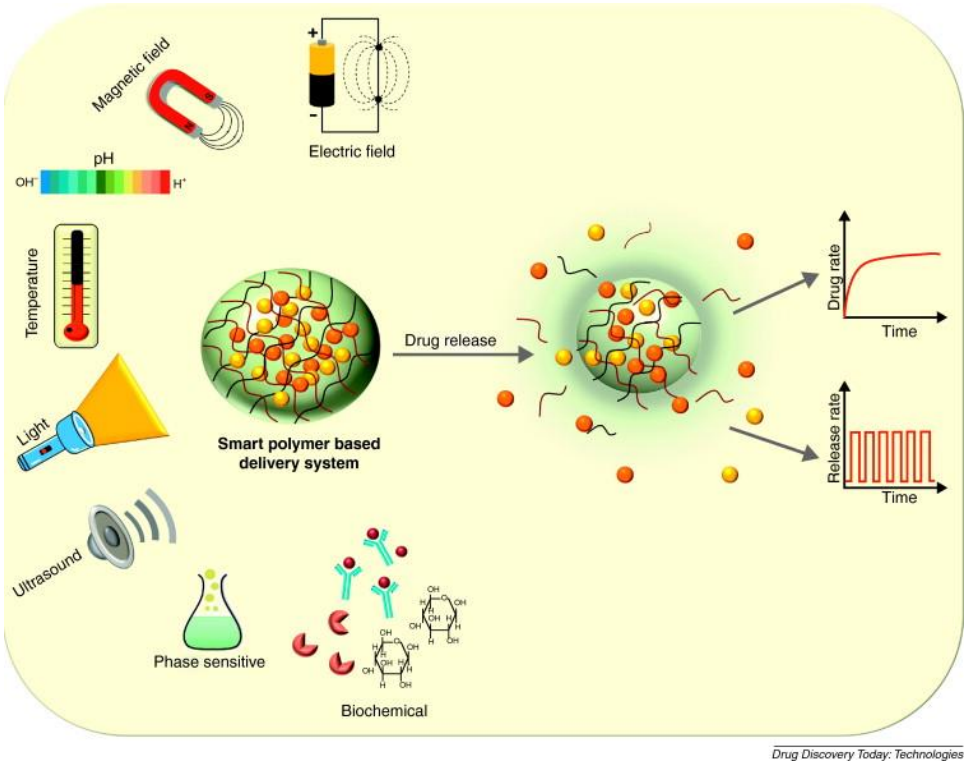

Scheme 1.8 Various stimuli are controlling the drug release from stimuli-responsive polymer-based delivery systems[38].

1.3.2 Biomarker sensing

Biomarkers are biomolecules including peptides, proteins, DNA, RNA or small molecules that have been secreted into body fluid from malfunctioning tissue or cells. They have been identified

as a disease signature. It is imperative to detect those biomarkers in a fast fashion for early diagnosis and disease treatment. Among others, amphiphilic homopolymers were utilized for peptide and protein biomarkers separation and recognition. It is done through a reverse micelle prepared from amphiphilic homopolymer and a sequent liquid-liquid extraction process. Peptides of interest would be extracted and concentrated into reverse micelle interior. Combined with MALDI-MS technique, the extracted peptide could be detected[39–43]. More interestingly, the detection signal could be enhanced more than 100-fold in optimum conditions. Until now, our group has developed a series of polystyrene-based amphiphilic homopolymers with charge moieties as a hydrophilic group and decyl chain as a hydrophobic group. The resultant polymer has demonstrated itself in selectively and sensitively detection of biomarkers with pI higher than aqueous solution pH value.

Scheme 1.9 Selective detection of biomarker peptide from a mixture using reverse micelle combined with MALDI-MS technique.

1.4 Thesis overview

In this thesis, we have demonstrated utilization of nucleophilic click chemistry for preparing amphiphilic polymers. They could be homopolymer as well as random copolymers. These polymers could self-assemble into macro assemblies and later on used for stimuli-responsive therapeutics delivery, peptide detections, and antimicrobial studies. In chapter 2, a sequential

nucleophilic “click” reactions for functional amphiphilic homopolymers are presented. Through the thiol-yne click reaction, a versatile system for preparing of multifactional amphiphilic homopolymer. The fidelity is true to many functionalities. In chapter 3, we developed a methodology for addition polymerization using thiol-yne click reaction. Installing a different thiol sequentially leads to the responsive functionalities in the backbone. The reaction is investigated and demonstrated itself to be efficient, fast and environmentally friendly. In chapter 4, we developed a reverse micelle system composed of a polystyrene base amphiphilic homopolymer which can achieve selective detection of model analytes. In chapter 5, we investigated the signal enhance mechanism underlying peptide detection using reverse micelle system and mass spectrometry technique. In chapter 6, we investigated the antimicrobial ability of silver ion loaded amphiphilic homopolymer against Gram-negative bacteria.

1.5 References

(1) Thomas, E. L.; Anderson, D. M.; Henkee, C. S.; Hoffman, D. Periodic Area-Minimizing Surfaces in Block Copolymers. *Nature* **1988**, *334* (6183), 598–601 DOI: 10.1038/334598a0.

(2) P. Mansky, Y. Liu, E. Huang, T. P. Russell, C. H. Controlling Polymer-Surface Interactions with Random Copolymer Brushes. *Science (80-.).* **1997**, *275* (5305), 1458–1460 DOI: 10.1126/science.207.4435.1073.

(3) Milner, S. T. Polymer Brushes. *Science (80-.).* **1991**, *251* (4996), 898–905 DOI: 10.1126/science.251.4996.898.

(4) Ren, J. M.; McKenzie, T. G.; Fu, Q.; Wong, E. H. H.; Xu, J.; An, Z.; Shanmugam, S.; Davis, T. P.; Boyer, C.; Qiao, G. G. Star Polymers. *Chem. Rev.* **2016**, *116* (12), 6743–6836 DOI: 10.1021/acs.chemrev.6b00008.

(5) Abbasi, E.; Aval, S. F.; Akbarzadeh, A.; Milani, M.; Nasrabadi, H. T.; Joo, S. W.; Hanifehpour, Y.; Nejati-Koshki, K.; Pashaei-Asl, R. Dendrimers: Synthesis, Applications, and Properties. *Nanoscale Research Letters*. Springer 2014, pp 1–10.

(6) Rösler, A.; Vandermeulen, G. W. M.; Klok, H. A. Advanced Drug Delivery Devices via Self-Assembly of Amphiphilic Block Copolymers. *Advanced Drug Delivery Reviews*. Elsevier December 1, 2012, pp 270–279.

(7) Ikkala, O.; ten Brinke, G. Functional Materials Based on Self-Assembly of Polymeric Supramolecules. *Science* **2002**, *295* (5564), 2407–2409 DOI: 10.1126/science.1067794.

(8) Janata, J.; Josowicz, M. Conducting Polymers in Electronic Chemical Sensors. *Nat. Mater.* **2003**, *2* (1), 19–24 DOI: 10.1038/nmat768.

(9) Ouk Kim, S.; Solak, H. H.; Stoykovich, M. P.; Ferrier, N. J.; de Pablo, J. J.; Nealey, P. F. Epitaxial Self-Assembly of Block Copolymers on Lithographically Defined Nanopatterned Substrates. *Nature* **2003**, *424* (6947), 411–414 DOI: 10.1038/nature01775.

(10) Schacher, F. H.; Rupar, P. A.; Manners, I. Functional Block Copolymers: Nanostructured Materials with Emerging Applications. *Angew. Chemie Int. Ed.* **2012**, *51* (32), 7898–7921 DOI: 10.1002/anie.201200310.

(11) Chen, Y.; Thorn, M.; Christensen, S.; Versek, C.; Poe, A.; Hayward, R. C.; Tuominen, M. T.; Thayumanavan, S. Enhancement of Anhydrous Proton Transport by Supramolecular Nanochannels in Comb Polymers. *Nat. Chem.* **2010**, *2* (6), 503–508 DOI: 10.1038/nchem.629.

(12) Blanazs, A.; Armes, S. P.; Ryan, A. J. Self-Assembled Block Copolymer Aggregates: From Micelles to Vesicles and Their Biological Applications. *Macromolecular Rapid Communications*. February 18, 2009, pp 267–277.

(13) Mai, Y.; Eisenberg, A. Self-Assembly of Block Copolymers. *Chem. Soc. Rev.* **2012**, *41* (18), 5969 DOI: 10.1039/c2cs35115c.

(14) Li, L.; Raghupathi, K.; Song, C.; Prasad, P.; Thayumanavan, S. Self-Assembly of Random Copolymers. *Chem. Commun. (Camb).* **2014**, *50* (88), 13417–13432 DOI: 10.1039/c4cc03688c.

(15) Guo, Q.; Zhang, T.; An, J.; Wu, Z.; Zhao, Y.; Dai, X.; Zhang, X.; Li, C. Block versus Random Amphiphilic Glycopolymer Nanopaticles as Glucose-Responsive Vehicles. *Biomacromolecules* **2015**, *16* (10), 3345–3356 DOI: 10.1021/acs.biomac.5b01020.

(16) Zhu, X.; Liu, M. Self-Assembly and Morphology Control of New l -Glutamic Acid-Based Amphiphilic Random Copolymers: Giant Vesicles, Vesicles, Spheres, and Honeycomb Film. *Langmuir* **2011**, *27* (21), 12844–12850 DOI: 10.1021/la202680j.

(17) Kenney, J. F. Properties of Block versus Random Copolymers. *Polym. Eng. Sci.* **1968**, *8* (3), 216–226 DOI: 10.1002/pen.760080307.

(18) Kale, T. S.; Klaikherd, A.; Popere, B.; Thayumanavan, S. Supramolecular Assemblies of Amphiphilic Homopolymers. *Langmuir* **2009**, *25* (17), 9660–9670 DOI: 10.1021/la900734d.

(19) Subhadeep Basu; Dharma Rao Vutukuri, and; Thayumanavan*, S. Homopolymer Micelles in Heterogeneous Solvent Mixtures. **2005** DOI: 10.1021/JA056042A.

(20) Basu, S.; Vutukuri, D. R.; Shyamroy, S.; Sandanaraj, B. S.; Thayumanavan, S. Invertible Amphiphilic Homopolymers. *J. Am. Chem. Soc.* **2004**, *126* (32), 9890–9891 DOI: 10.1021/ja047816a.

(21) Savariar, E. N.; Aathimanikandan, S. V.; Thayumanavan, S. Supramolecular Assemblies from Amphiphilic Homopolymers: Testing the Scope. *J. Am. Chem. Soc.* **2006**, *128* (50), 16224–16230 DOI: 10.1021/ja065213o.

(22) Arnt, L.; Tew, G. N. New Poly(Phenyleneethynylene)s with Cationic, Facially Amphiphilic Structures. *J. Am. Chem. Soc.* **2002**, *124* (26), 7664–7665 DOI: 10.1021/ja026607s.

(23) Arnt, L.; Tew, G. N. Cationic Facially Amphiphilic Poly(Phenylene Ethynylene)s Studied at the Air-Water Interface. *Langmuir* **2003**, *19* (6), 2404–2408 DOI: 10.1021/la0268597.

(24) Ilker, M. F.; Nüsslein, K.; Tew, G. N.; Coughlin, E. B. Tuning the Hemolytic and Antibacterial Activities of Amphiphilic Polynorbornene Derivatives. *J. Am. Chem. Soc.* **2004**, *126* (48), 15870–15875 DOI: 10.1021/ja045664d.

(25) Zhu, Y.; Liu, L.; Du, J. Probing into Homopolymer Self-Assembly: How Does Hydrogen Bonding Influence Morphology? *Macromolecules* **2013**, *46* (1), 194–203 DOI: 10.1021/ma302176a.

(26) Miao, W.-K.; Yan, Y.-K.; Wang, X.-L.; Xiao, Y.; Ren, L.-J.; Zheng, P.; Wang, C.-H.; Ren, L.-X.; Wang, W. Incorporation of Polyoxometalates into Polymers to Create Linear Poly(Polyoxometalate)s with Catalytic Function. *ACS Macro Lett.* **2014**, *3* (2), 211–215 DOI: 10.1021/mz5000202.

(27) Mane, S. R.; Shunmugam, R. Hierarchical Self-Assembly of Amphiphilic Homopolymer into Unique Superstructures. *ACS Macro Lett.* **2014**, *3* (1), 44–50 DOI: 10.1021/mz4005524.

(28) Meizhen, Y.; Jie, S.; Pisula, W.; Minghui, L.; Linjie, Z.; Müllen, K. Functionalization of Self-Assembled Hexa-Peri-Hexabenzocoronene Fibers with Peptides for Bioprobing. *J. Am. Chem. Soc.* **2009**, *131* (41), 14618–14619 DOI: 10.1021/ja9058662.

(29) Xu, J.; Tao, L.; Boyer, C.; Lowe, A. B.; Davis, T. P. Facile Access to Polymeric Vesicular Nanostructures: Remarkable ω-End Group Effects in Cholesterol and Pyrene Functional (Co)Polymers. *Macromolecules* **2011**, *44* (2), 299–312 DOI: 10.1021/ma102386j.

(30) Mühlebach, A.; Gaynor, S. G.; Matyjaszewski, K. Synthesis of Amphiphilic Block Copolymers by Atom Transfer Radical Polymerization (ATRP). *Macromolecules* **1998**, *31* (18), 6046–6052 DOI: 10.1021/ma9804747.

(31) Keddie, D. J. A Guide to the Synthesis of Block Copolymers Using Reversible-Addition Fragmentation Chain Transfer (RAFT) Polymerization. *Chem. Soc. Rev.* **2014**, *43* (2), 496–505 DOI: 10.1039/C3CS60290G.

(32) Dirks, A. J. (Ton); van Berkel, S. S.; Hatzakis, N. S.; Opsteen, J. A.; van Delft, F. L.;

Cornelissen, J. J. L. M.; Rowan, A. E.; van Hest, J. C. M.; Rutjes, F. P. J. T.; Nolte, R. J. M. Preparation of Biohybrid Amphiphiles via the Copper Catalysed Huisgen [3 + 2] Dipolar Cycloaddition Reaction. *Chem. Commun.* **2005**, *0* (33), 4172 DOI: 10.1039/b508428h.

(33) Klaikherd, A.; Nagamani, C.; Thayumanavan, S. Multi-Stimuli Sensitive Amphiphilic Block Copolymer Assemblies. *J. Am. Chem. Soc.* **2009**, *131* (13), 4830–4838 DOI: 10.1021/ja809475a.

(34) Wolf, F. F.; Friedemann, N.; Frey, H. Poly(Lactide)-Block-Poly(HEMA) Block Copolymers: An Orthogonal One-Pot Combination of ROP and ATRP, Using a Bifunctional Initiator. *Macromolecules* **2009**, *42* (15), 5622–5628 DOI: 10.1021/ma900894d.

(35) Ryu, J.-H.; Chacko, R. T.; Jiwpanich, S.; Bickerton, S.; Babu, R. P.; Thayumanavan, S. Self-Cross-Linked Polymer Nanogels: A Versatile Nanoscopic Drug Delivery Platform. *J. Am. Chem. Soc.* **2010**, *132* (48), 17227–17235 DOI: 10.1021/ja1069932.

(36) Liu, X.; Hu, D.; Jiang, Z.; Zhuang, J.; Xu, Y.; Guo, X.; Thayumanavan, S. Multi-Stimuli-Responsive Amphiphilic Assemblies through Simple Postpolymerization Modifications. *Macromolecules* **2016**, *49* (17), 6186–6192 DOI: 10.1021/acs.macromol.6b01397.

(37) Seidi, F.; Jenjob, R.; Crespy, D. Designing Smart Polymer Conjugates for Controlled Release of Payloads. *Chem. Rev.* **2018**, *118* (7), 3965–4036 DOI: 10.1021/acs.chemrev.8b00006.

(38) Oak, M.; Mandke, R.; Singh, J. Smart Polymers for Peptide and Protein Parenteral Sustained Delivery. *Drug Discov. Today Technol.* **2012**, *9* (2), e131–e140 DOI: 10.1016/j.ddtec.2012.05.001.

(39) Rodthongkum, N.; Chen, Y.; Thayumanavan, S.; Vachet, R. W. Matrix-Assisted Laser Desorption Ionization-Mass Spectrometry Signal Enhancement of Peptides after Selective Extraction with Polymeric Reverse Micelles. *Anal. Chem.* **2010**, *82* (9), 3686–3691 DOI: 10.1021/ac1000256.

(40) Rodthongkum, N.; Chen, Y.; Thayumanavan, S.; Vachet, R. W. Selective Enrichment and Analysis of Acidic Peptides and Proteins Using Polymeric Reverse Micelles and MALDI-MS. *Anal. Chem.* **2010**, *82* (20), 8686–8691 DOI: 10.1021/ac101922b.

(41) Combariza, M. Y.; Savariar, E. N.; Vutukuri, D. R.; Thayumanavan, S.; Vachet, R. W. Polymerie Inverse Micelles as Selective Peptide Extraction Agents for MALDI-MS Analysis. *Anal. Chem.* **2007**, *79* (18), 7124–7130 DOI: 10.1021/ac071001d.

(42) Rodthongkum, N.; Ramireddy, R.; Thayumanavan, S.; Richard, W. V. Selective Enrichment and Sensitive Detection of Peptide and Protein Biomarkers in Human Serum Using Polymeric Reverse Micelles and MALDI-MS. *Analyst* **2012**, *137* (4), 1024–1030 DOI: 10.1039/c2an16089g.

(43) Rodthongkum, N.; Washington, J. D.; Savariar, E. N.; Thayumanavan, S.; Vachet, R. W.

Generating Peptide Titration-Type Curves Using Polymeric Reverse Micelles As Selective Extraction Agents along with Matrix-Assisted Laser Desorption Ionization-Mass Spectrometry Detection. *Anal. Chem.* **2009**, *81* (12), 5046–5053 DOI: 10.1021/ac900661e.

CHAPTER

2. SEQUENTIAL NUCLEOPHILIC "CLICK" REACTIONS FOR FUNCTIONAL AMPHIPHILIC HOMOPOLYMERS

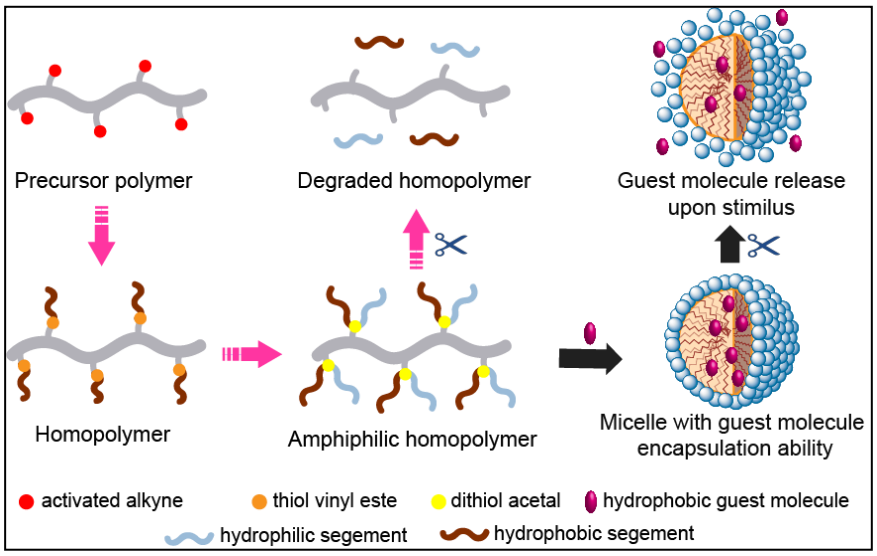

Scheme 2.1 Cartoon representation of sequential nucleophilic click reactions for functional amphiphilic homopolymer preparation, self-assemble and stimuli-responsive disassemble.

2.1 Introduction

Classical homopolymers have been quite featureless by definition, because of their rather monotonous repeat unit patterns. There has been an increased interest in introducing greater functional group diversity in homopolymers. Prominent among this class of polymers are amphiphilic homopolymers that contain both hydrophilic and hydrophobic groups in the same repeating unit[1,2]. These amphiphilic polymers can form micellar or vesicular aggregates in polar solvent[3–7] and reverse micelle-like structures in nonpolar solvent[4,8,9]. Due to their high density of functional groups and stable self-assemblies, amphiphilic homopolymers have been used in materials science for applications in areas such as separations[10,11] and catalysis[12,13] and biology in fields such as protein sensing[14] and DNA detection[1,15].

Moreover, amphiphilic homopolymers with stimuli-responsive features can undergo changes in morphological and physicochemical properties[16] upon external or internal trigger application, which makes them useful for designing stimuli-sensitive drug delivery systems[17–21]. Because of these novel properties, significant effort has been devoted to the syntheses of amphiphilic homopolymers. The commonly used method for amphiphilic homopolymer preparation involves either polymerization of a pre-functionalized amphiphilic monomer[22–24] or post modification of a precursor polymer with functionalities of interest[5,25,26]. In the former case, 100% amphiphilicity in each repeating unit can be potentially achieved. However, the drawbacks of this approach include low polymerization efficiency and low polymeric molecular weights, owing to the steric hindrance effect from the functional groups. Also, significant synthetic challenges involved in making multifunctional monomers may limit their broad applications. On the other hand, post-modification can lead to incomplete functionalization due to inefficient reactions. Therefore, developing an efficient method for the synthesis of homopolymers using an environmentally friendly approach is needed. We envisaged that a synthetic route that can overcome these obstacles would pave the way for expanding the existing polymerization toolbox.

Our solution is to use efficient click chemistry to post-modify the polymer substrate with different functionalities of interest. Click chemistry is increasingly useful in polymer and material science due to its speed, atom economy, easy operation, and high reaction yields. Different click chemistry strategies have been developed for this purpose, e.g., Cu-catalyzed[27,28] or Cu free[29] Huisgen 1,3-dipolar cycloaddition, Staudinger ligation[30] and thiol-ene[31] click chemistry and thiol-yne photo click chemistry[32]. We were inspired by a recent report on a nucleophilic thiol-yne click reaction, involving α,β-unsaturated esters.[33] In this reaction, the electron deficient alkyne group of an α,β-unsaturated ester can readily react with a thiol reagent under mild conditions to form a

mixture of *cis* and *trans* thiol vinyl esters. This functional group is then poised to undergo another thiol-ene addition reaction but only in the presence of a much stronger base. This latter requirement offers the opportunity to attach two different thiol groups on the same carbon to afford a hetero-dithiol adduct. This organocatalytic thiol-yne and a subsequent thiol-ene reaction has been reported for small molecule synthesis, but its use in polymer synthesis has been very limited to the best of our knowledge.[34,35] In this work, we utilize this concept, where the pre-installed electron deficient alkyne groups on polymer side chains are used as a handle for post modification with different thiol species to introduce the functionalities of interest. Furthermore, these customized polymers bearing dithioacetal groups are sensitive to ROS stimulus and degrade in response to it[36,37]. The mechanism of degradation is proposed to occur via nucleophilic attack of the hydroxyl radical to break the C-S bond[38]. In this chapter, we have shown how thiol-alkyne click chemistry is used for efficient post-polymerization modification with different functional groups, both hydrophobic and hydrophilic. We demonstrate the ease of this approach and its potential for the design and syntheses of stimuli-responsive materials.

2.2 Molecular design

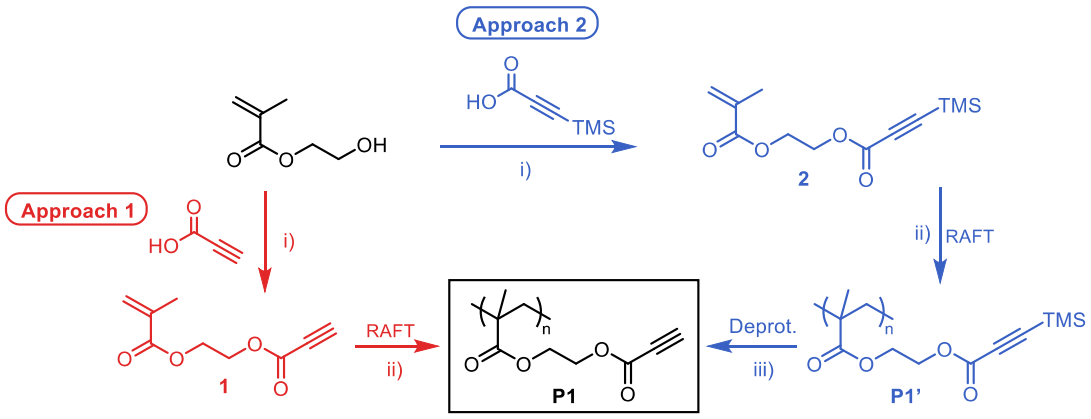

Scheme 2.2 Synthetic approaches for the targeted α,β-alkynoate ester-based polymer P1. Approach 1: i) H_2SO_4 (cat.), toluene, reflux, 42%; ii) CTR, AIBN, THF, 30%. Approach 2: i) DCC, DMAP, DCM, 52%; ii) CTR, AIBN, THF, 80%; iii) AgF, MeCN/THF, then 1M HCl, 99%

2.3 Results and discussions

The precursor polymer for the targeted functionalization with two different functionalities is shown as polymer **P1** in Scheme 2.2. This structure can provide us opportunity for installing functional moieties of interest through addition of thiol species. Two approaches were explored to synthesize the target polymer (**P1**). Approach 1 involved direct polymerization of the unprotected monomer **1**, which was prepared through the esterification reaction of hydroxyethyl methacrylate (HEMA) and propiolate acid (Scheme 2.2, approach 1). **P1** was obtained through RAFT polymerization of monomer **1** with 4-cyano-4-(phenylcarbonothioylthio) pentanoic acid as chain transfer agent. Different solvents (DMF or THF), monomer concentrations (500 mg/mL or 100 mg/mL) and reaction times (12 h or 24 h) were investigated to avoid crosslinking during the polymerization reaction. However, even under the optimized conditions, mildly crosslinked products (10 % crosslinking degree) were still produced. The crosslinking can be identified by the alkene proton peaks (6.12 ppm, 5.63 ppm) from NMR spectrum. Moreover, due to the low monomer concentration and short reaction time used here, the final polymerization yield was relatively low (<30%).

The second approach that we investigated was to use a protection group for the active alkyne group to prevent crosslinking during polymerization. In this process, TMS-protected propiolate acid reacted with hydroxyethyl methacrylate (HEMA) to prepare monomer **2**. By protecting the alkyne group, monomer **2** can be conveniently polymerized with no crosslinking observed from NMR. Note that the esterification reaction in refluxing toluene can produce ethylene glycol dimethacrylate through trans-esterification of HEMA. This byproduct could then act a cross-linker later in the polymerization reaction. Indeed, this byproduct was observed under

the reaction conditions and was also found to exhibit a similar R_f value (R_f = 0.6 in 10% ethyl acetate/hexane) as that of the desired product in chromatography, which made the purification of monomer **2** in this reaction difficult. To address this challenge, a base-catalyzed esterification reaction was utilized with DCC and DMAP as the coupling reagents. After polymer **P1'** was acquired through the polymerization of monomer **2**, several deprotection methods were attempted. The reagent tetra-*n*-butylammonium fluoride (TBAF) yielded insoluble products, presumably due to the strong base-catalyzed crosslinking. Also, the reaction yield under acid conditions (*p*TsOH, MeOH/DCM) was also very poor. We were gratified to find that a metal fluoride (AgF) in MeCN/THF can be used to achieve 100% deprotection. By choosing the protection and deprotection approach, we could successfully obtain the target polymer **P1** with no crosslinking and high overall yield (>70%).

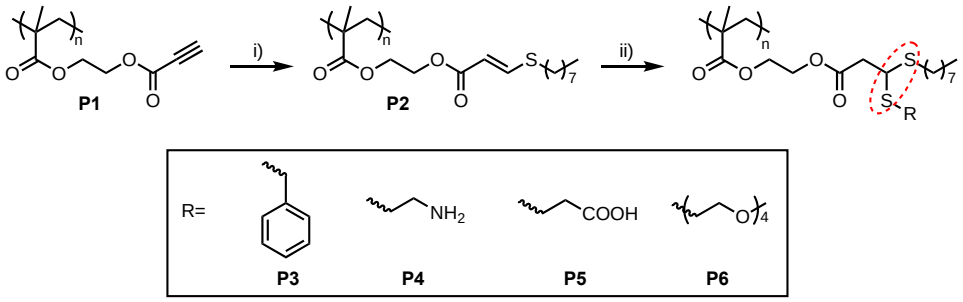

Scheme 2.3 Schematic structure of multifunctional polymers: i) 1st thiol addition reaction with octyl thiol and triethylamine in $CHCl_3$. ii) 2nd thiol addition reaction with different thiol reagents (HS-R) and 1,5,7-Triazabicyclo [4.4.0] dec-5-ene (TBD) in $CHCl_3$.

To test the possibility of sequential nucleophilic addition to **P1**, we treated the polymer with octane-1-thiol (1.0 equiv. respect to alkyne group) as the nucleophile in the presence of triethylamine (0.1 equiv.) as the organocatalyst. The reaction progress was monitored by ^{1}H NMR (Figure 2.1A). The evolution of the alkyne proton signal at 3.01 ppm and the new alkene proton signals at 7.73 ppm and 5.75 ppm were monitored. The former peak decreased in signal intensity with time, while the latter ones concurrently increased in intensity. Complete disappearance of the

alkyne peak and saturation of the alkene peaks within 80 minutes indicated a quantitative conversion within this timeframe (Figure 2.1A). To check whether the thio-vinyl product is available for a second nucleophilic addition under the same reaction conditions, the polymer was reacted with excess octane-1-thiol (2.0 equiv. to alkene group) for much longer reaction time (up to 24 h) with TEA as the catalyst. NMR spectra of these reactions showed that the alkene proton peaks were intact, which suggests that the addition reaction stopped only at the first step and did not go further for a second addition under the mild base conditions (Figure 2.1B). Also, the GPC profiles of polymers from the tested reactions revealed the similar shape and same retention time (Figure 2.6). Together, these results suggested that the degree of the first thiol addition reaction is base-mediated and is independent of the amount of thiol reagent added to the system. This feature is considered critical, as this provides us with the opportunity to attach a different thiol reagent onto the same repeat unit by simply altering the reaction conditions for the second addition.

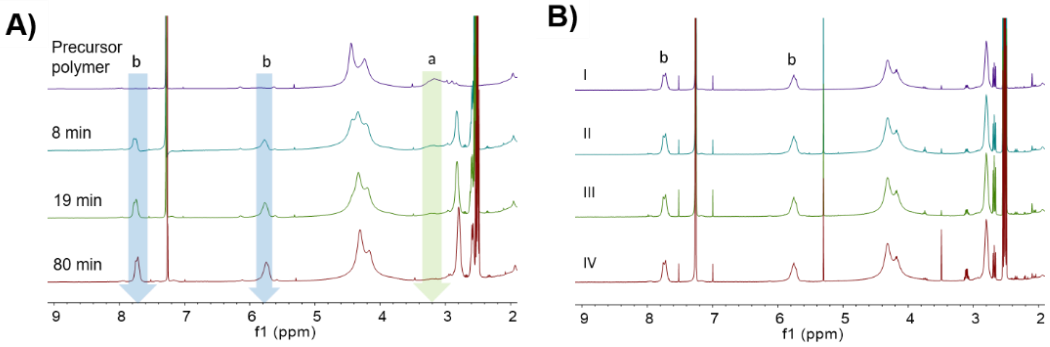

Figure 2.1 (A) ^{1}H NMR spectrum for 1st thiol addition reaction with octyl thiol over time. (B) ^{1}H NMR spectrum for 1st thiol addition with different amount of octyl thiol: (I) 1:1 24 h; (II) 1:2 4 h; (III) 1:2 9 h; (IV) 1:2 24 h. (e.g., 1:1 is respect to the ratio of alkyne to thiol reagent, solvent: $CDCl_3$, base: TEA (0.1 equiv. respect to alkyne))

Next, the possibility of a second addition of a different thiol onto the vinyl side chains of polymer **P2** was tested (Scheme 2.3). The weak electrophilicity of the double bonds in **P2** is attributed to its relatively electron-rich character, owing to the thioether functionality. We envisaged that the use of a stronger base would overcome this reactivity hurdle. Thus, polymer **P2**

was treated with benzyl-thiol in the presence of triazabicyclodecene (TBD) as the organocatalytic base. TBD was chosen as the base, as it is considered a strong base with the pK_a of ~23.5 in DMSO and pK_a of ~15.2 in H_2O. In the presence of this base, the progress of the second addition to **P2** was monitored by ^1H NMR. Total disappearance of the alkene proton signals from the NMR spectrum indicated the complete addition of a second thiol species (Figure 2.2A). Since the double bonds in **P2** are based on an α,β-unsaturated ester, the second thiol is expected to add to the same carbon through a Michael-type addition. Indeed, the proton signals at 4.15 ppm confirm this expectation, where the product is a dithioacetal. The decrease in alkene proton signal was monitored over time in an NMR tube. The complete disappearance of alkene proton signals was considered to be 100% conversion, and the reaction process over time was plotted in figure 2.2B for benzyl mercaptan. The alkene proton signals disappeared within 160 min, showing that the second thiol addition reaction was complete to afford polymer **P3** within 3 h under these reaction conditions. A similar trend was observed when a different thiol nucleophile, cysteamine, was used where the reaction completed in about 120 min (Figure 2.2C).

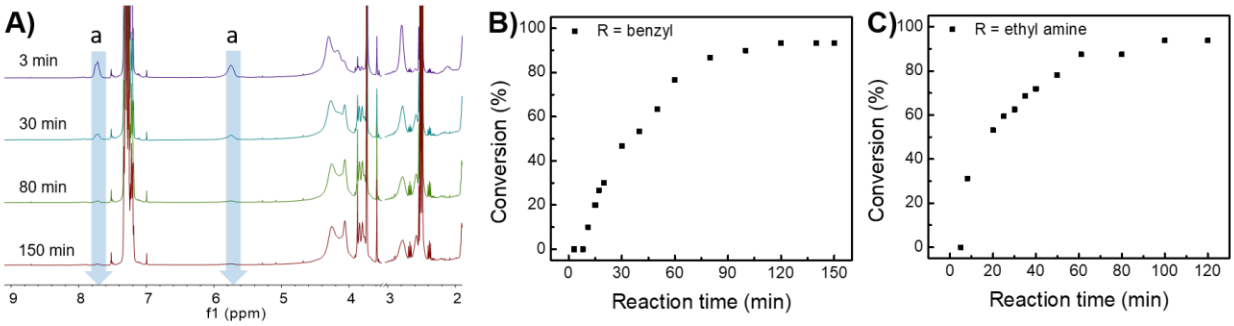

Figure 2.2 (A) ^1H NMR evidence for 2nd thiol addition using benzyl mercaptan. Kinetic study of 2nd addition with benzyl mercaptan (B) and cysteamine (C).

We next sought to examine whether this methodology would translate to useful applications, such as peptide separation and detection. Peptide detection in biological fluids, especially of disease-relevant biomarkers, can be challenging due to their low concentration and

inherent sample complexity.[39,40] There have been several approaches that have used supramolecular chemistry to predictably simplify complex mixtures through selective sequestration of peptides in a liquid-liquid extraction process for detection by matrix-assisted laser desorption ionization mass spectrometry (MALDI-MS)[10,11,41,42]. To demonstrate the potential utility of the bifunctional homopolymers synthesized here, we synthesized a negatively charged amphiphilic homopolymer **P5**. To synthesize this polymer, *tert*-butyl-3-sulfanylpropanoate was used as the second thiol addition reagent. Deprotection of *tert*-butyl group from the resultant polymer using trifluoroacetic acid produced the targeted polymer **P5**, as evidenced by the complete disappearance of *tert*-butyl proton signal at 1.41 ppm (Figure 2.3A).

The negatively charged, amphiphilic homopolymer **P5** is expected to form micelle-like aggregates in water and reverse-micelle-like aggregates in toluene. The size of micellar aggregate was about 190 nm with negative charged zeta potential (-76.8 ± 4.05 mV), while the size of the reverse micelle state in toluene was found to be around 260 nm (Figure 2.8). Reverse micelles of such polymers can be used to selectively enrich peptides according to charge from an aqueous phase into an organic phase. To identify whether these reverse micelle assemblies would be capable of selectively sequestering molecules, we first investigated the extraction capability and selectivity of **P5** toward water-soluble dyes as the model analyte. A positively charged dye molecule, rhodamine 6G (R6G), and a negatively charged molecule, calcein, were chosen as the candidates for this study due to their distinct absorption spectrum. A 200 µL toluene solution with a 2.3 mM concentration of **P5** was used as the apolar phase, while the aqueous phase contained 1 mL of 4 µM calcein or 2.5 µM R6G in PBS buffer (pH = 7.4, 150 mM NaCl). After a two-phase liquid-liquid extraction procedure, the apolar organic and the aqueous phases were separated. The UV-visible absorption spectra of the aqueous solutions before and after the liquid-liquid extraction

procedure were compared, and the overall efficiency of dye extraction was estimated based on the amount of dye molecule left in the aqueous phase. The binding efficiency and the amount of dye molecule remaining in the aqueous phase are expected to be inversely correlated. As discerned from the data in figures 2.3B and 2.3C, the **P5** reverse micelle could efficiently extract the complementarily charged analyte R6G from the aqueous phase to organic phase. In contrast, a negligible amount of calcein is extracted by the same polymer **P5**. These data indicate that the amphiphilic homopolymer **P5** could also be used to selectively separate analyte molecules of interest.

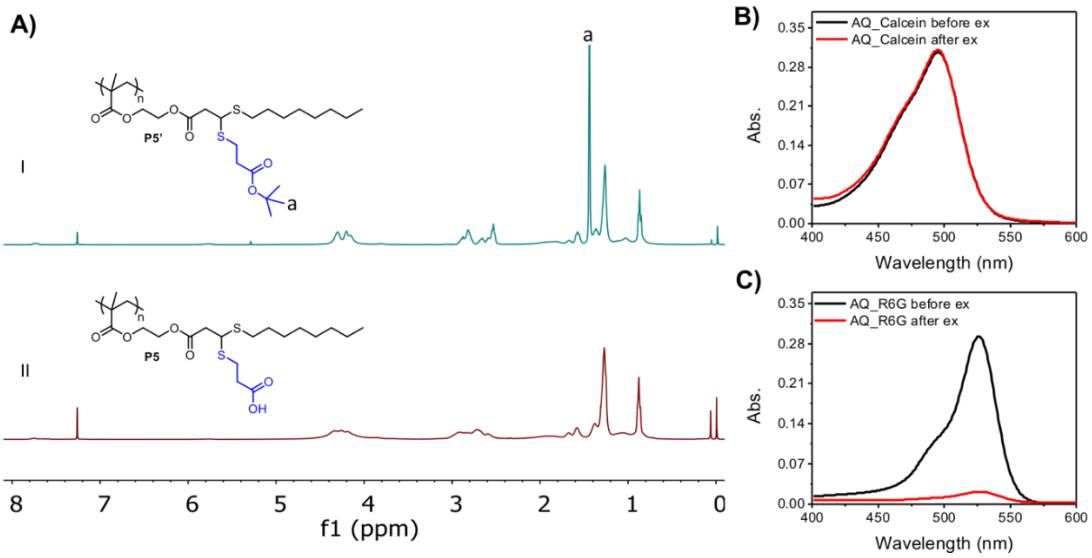

Figure 2.3 (A) ^{1}H NMR spectrum of polymer **P5** before (I) and after (II) deprotection. UV-Vis spectrum of Calcein (B) and Rhodamine 6G (C) in aqueous solution before (black line) and after (red line) extraction with reverse micelles made from **P5**.

After testing the selectivity with dye molecules, we evaluated the potential peptide enrichment selectivity of polymer **P5**. The peptides preproenkephalin, β-amyloid (1-11), kinetensin and bradykinin were chosen as candidate peptides for their different pI values. These peptides were dissolved in MOPS buffer at pH 7. A toluene solution containing the reverse micelles of **P5** was used as the organic phase. As shown in figure 2.4, after the liquid-liquid

extraction process, only peptides with pI values higher than 7.0, *viz.* kinetensin (pI 10.84) and bradykinin (pI 12.0) (Figure 2.4C), were selectively extracted into the organic phase and detected by MALDI-MS. The more negatively charged peptides with pI values lower than 7, *viz.* preproenkephalin (pI 3.71) and β-amyloid (1-11) (pI 4.31) (Figure 2.4B), remained in the aqueous phase. This experiment shows that polymer **P5** could be potentially useful in peptide separation and detection.

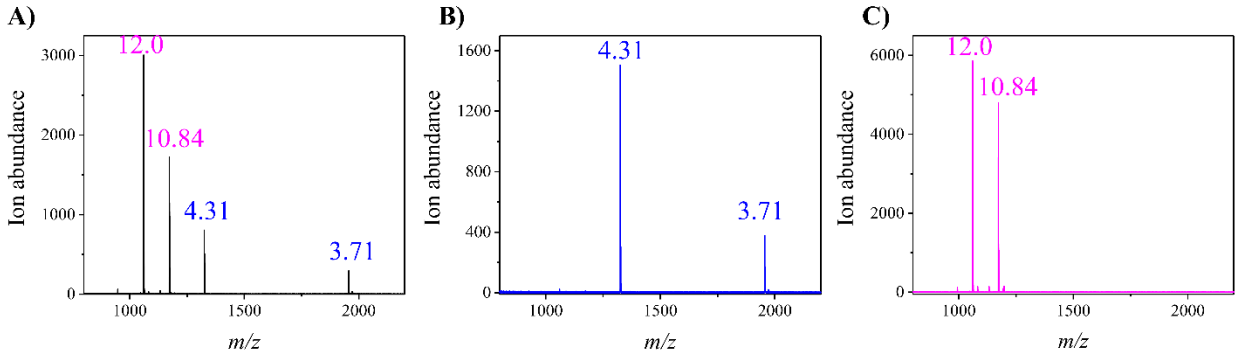

Figure 2.4 MALDI mass spectra of selective extraction of peptides in a mixture with reverse micelles made from **P5**. A) A mixture of four peptides labeled with their pIs in a buffer of pH 7 (Bradykinin *m/z* 1060.5, Kinetensin *m/z* 1172.7, β-amyloid (1-11) *m/z* 1326.3 and Preproenkephalin *m/z* 1954.7). B) Peptides left in aqueous solution after extraction using reverse micelles made by polymer **P5**. C) Peptides extracted by **P5**. * pI numbers are calculated by ExPASy

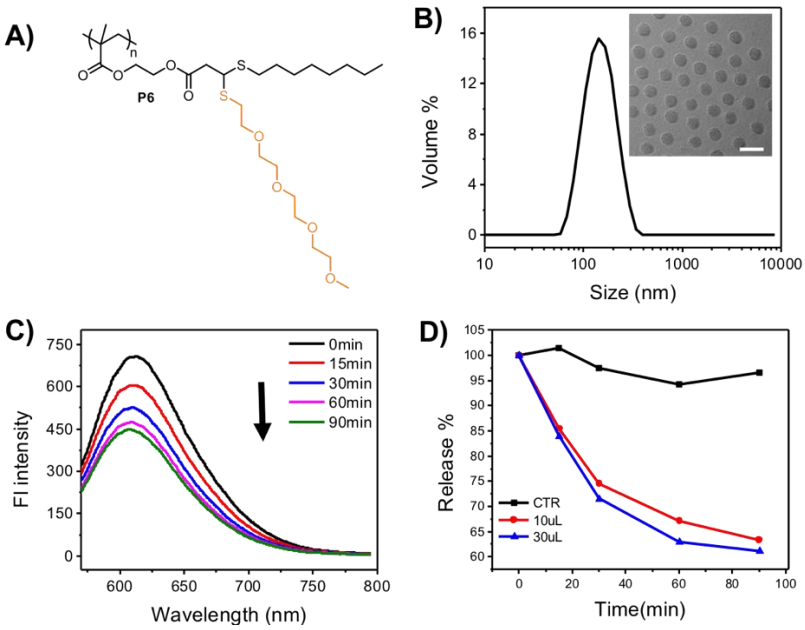

Figure 2.5 (A) Chemical structure of polymer **P6**. (B) DLS size distribution curve and TEM image (insert) of **P6** micelle in aqueous solution. (scale bar =100 nm). (C) Fluorescence emission spectra of Nile Red (NR) at different intervals in the presence of H_2O_2 of an aqueous solution of **P6**. (D) NR release profile at different time intervals in the presence of different amount of H_2O_2 in **P6**.

Finally, a charge neutral amphiphilic homopolymer **P6** was prepared using tetra-ethylene glycol monothiol (TEG-SH) as a second thiol agent (Figure 2.5A). The amphiphilic polymer **P6** bears TEG as the hydrophilic moiety and octyl chain as hydrophobic moiety in each repeating unit. This polymer, too, forms micelle-like aggregates in aqueous solution. These aggregates can encapsulate water-insoluble guest molecules, such as small molecule drugs, in their hydrophobic pockets. We were interested in utilizing this feature to test whether the ROS-sensitive nature of the dithioacetal moiety can be utilized to cause molecular release from these aggregates. Accordingly, Nile red (NR) was utilized as the model guest molecule due to its hydrophobic and fluorescent nature. Also, NR is more fluorescent when present inside the hydrophobic core of the micellar aggregate, whereas very little fluorescence would be observed if NR is in a more polar environment, such as in water[43]. This property could be used for monitoring NR release in response to ROS stimulus. First of all, the morphological characterization of **P6** micelle showed that they form spherical aggregates with size ~130 nm (Figure 2.5B). The assembly was found to be stable in solution for over a month. When 10 μL of H_2O_2 was added as the ROS trigger to a solution of 250 μM concentration of **P6** in water, the fluorescence of the encapsulated NR was found to decrease with time (Figure 2.5C). The control sample, on the other hand, showed very little change in fluorescence properties if any over the same timeframe (Figure 2.5D). When the amount of H_2O_2 was increased to 30 μL, the kinetics of NR release was only moderately higher. Overall, the highest molecular release obtained was ~40%. Moreover, the size of the aggregate was found to slightly increase with time upon exposure to H_2O_2. These observations suggest that the degradation of the dithioacetal bond itself by H_2O_2 occurs but is very slow. This slow degradation results in

incomplete cleavage of the amphiphilic moieties from the aggregates, which causes the aggregates to swell. The fact that there is molecular release shows that the host-guest capacity of these swollen assemblies is much worse than the parent assembly.

2.4 Summary

In summary, a novel method for the convenient preparation of bifunctional polymers using sequential thiol-yne nucleophilic addition reactions is used in a post-polymerization modification process. We have developed a procedure for introducing an activated terminal alkyne as the polymer side chain functionality. This moiety can then be sequentially reacted with two different thiols under mild reaction conditions. Since the base strength requirement for the first step and the second step are considerably different and since the first addition is quantitative under the optimized conditions, this sequential addition paved the way for introducing two different side chain functional groups in every repeat unit of the polymer. The utility of this methodology has been demonstrated by generating amphiphilic homopolymers, where hydrophilic and hydrophobic functional groups have been introduced as the two different side chains. In addition to the functional utility of these amphiphilic homopolymers, we have also provided a preliminary demonstration of the possible ROS-induced degradation of the polymeric aggregates, as the synthetic methodology naturally lends itself to the introduction of dithioacetal moieties in each of the repeat units in the polymer. Overall, the syntheses of highly functional polymeric materials using the environmentally-friendly nucleophilic thiol-yne click approach could pave the way for expanding the functional polymer toolbox.

2.5 Experimental details

2.5.1 Materials and methods

Unless mentioned, all chemicals were used as received from Sigma-Aldrich. ^{1}H-NMR spectra were recorded on a 400 MHz Bruker NMR spectrometer. Molecular weight of the polymers was measured by gel permeation chromatography (GPC, Waters) using a PMMA standard with a refractive index detector. THF was used as eluent with a flow rate of 1 mL/min. Dynamic light scattering (DLS) measurements were performed using a Malvern Nano zetasizer. UV-visible absorption spectra were recorded on a Varian (model EL 01125047) spectrophotometer. The fluorescence spectra were obtained from a JASCO FP-6500 Spectro fluorometer. TEM images were recorded on a JEOL-2000FX machine operating at an accelerating voltage of 100 kV.

Synthesis of monomer **1:**

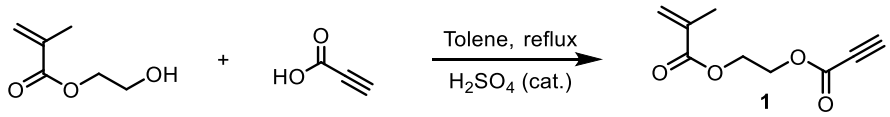

Propiolic acid (1.0 g, 7.04 mmol) and 2-Hydroxyethyl methacrylate (1.008 g, 7.74 mmol) were mixed in 40 mL toluene. After the temperature was increased to 80 ^{o}C, 2 drops of sulfuric acid were added to the above solution. The system was heated to reflux for 36 h with a Dean-Stark apparatus for collecting the condensed water. After the reaction was cooled to room temperature, $NaHCO_3$(Sat.) solution was added to quench the reaction. The crude product was extracted by EtOAc three times. The combined organic phase was washed by brine, dried under sodium sulfate and further condensed under vacuum. The crude was further purified by Combiflash with elute of 0~10% ethyl acetate/hexane to give the liquid product. (yield: 42%, 2.66 g). ^{1}H NMR (400 MHz, Chloroform-*d*) δ 6.15 (d, *J* = 1.3 Hz, 1H), 5.61 (d, *J* = 1.6 Hz, 1H), 4.47-4.44 (m, 2H), 4.39 (m, 2H), 2.93 (s, 1H), 1.95 (s, 3H).

Synthesis of monomer **2:**

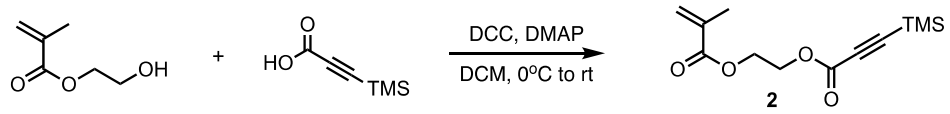

3-(Trimethylsilyl) propynoic acid (1.00 g, 7.04 mmol), 2-Hydroxyethyl methacrylate (1.01 g, 7.74 mmol) and dicyclohexylcarbodiimide (DCC, 1.45 g, 7.04 mmol) were mixed in cold dichloromethane (50 mL). The solution was kept in an ice bath through the time of addition of DMAP (0.43 g, 3.52 mmol) solution (in 2 mL DCM) dropwise. The temperature was brought to r.t. when DMAP solution was finished adding. The system was kept in 40 °C for an overnight before checking TLC. The product was purified by precipitating in cold Et_2O to get rid of DHU by-product. The crude product was further purified using Combiflash: 0~10% ethyl acetate/hexane to give the liquid product. (yield: 52%, 0.94 g). ^{1}H NMR (400 MHz, Chloroform-d) δ 6.15 (d, *J* = 1.3 Hz, 1H), 5.61 (d, *J* = 1.6 Hz, 1H), 4.46-4.43 (m, 4H), 1.96 (s, 3H), 0.25 (s, 9H). ^{13}C NMR (400 MHz, Chloroform-*d*) δ 166.84, 152.54, 135.73, 126.12, 94.10, 63.29, 61.99, 18.16, -0.98. ESI-MS m/z calculated for $C_{12}H_{18}O_4Si$+Na+: 277.09; found: 277.13.

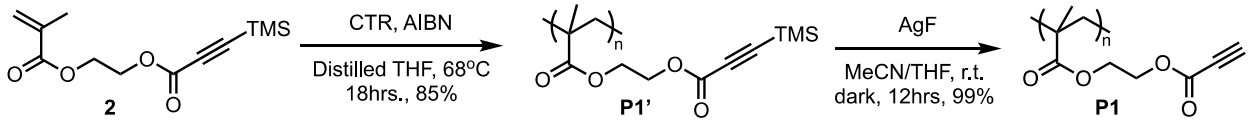

Synthesis of polymer **P1':**

The polymer was prepared through RAFT polymerization[44]. Typical procedure for the polymer P1' with DP=70: in a 10 mL Schlenk flask monomer **2** (770 mg, 2.75 mmol) was added to AIBN (1.29 mg, 0.01 mmol), 4-cyano-4-((thiobenzoyl)-sulfanyl) pentanoic acid (10.98 mg, 0.04 mmol) and distilled THF (1.4 mL). The solution mixture was then de-gassed using four freeze-pump-thaw cycles. The flask was sealed and immersed in a preheated oil bath at 68 °C for 18 h. The polymer was precipitated in hexane. The precipitant was dissolved in minimum amount of

DCM and precipitated in hexane. The same procedure was repeated for two more times to afford the pure polymer. The other polymer prepared from monomer **1** was prepared by the same procedure. ^{1}H NMR (500 MHz, Chloroform-*d*) δ 4.39 (s, 2H), 4.23 (s, 2H), 2.16-1.79 (m, 2H), 1.19-0.84 (m, 3H), 0.29 (s, 8H). ^{13}C NMR (400 MHz, Chloroform-*d*) δ 177.88, 176.30, 155.00, 153.39, 100.82, 97.27, 96.06, 94.92, 63.97, 62.89, 54.58, 45.55, 32.56, 31.77, 30.08, 19.93, 17.58, 0.84, 0.00, -0.09.

Synthesis of polymer **P1:**

Polymer **P1** was prepared through deprotection of **P1'** using modified procedure[45]. Typically, to a degassed solution (acetonitrile/THF) of **P1'** (100 mg, 0.39 mmol), AgF (60 mg, 0.47 mmol) was added in the dark, covering the reaction flask with aluminum foil. The reaction mixture was stirred at room temperature. 1 M HCl (3 equiv.) was added. The mixture was stirred for 10 min. Polymer supernatant was separated by centrifuging out AgCl precipitant. Polymer residue was collected by extensive rinsing precipitant with DCM (twice) and centrifuge. The polymer was purified by evaporating solvent and precipitating into hexane to get rid of small molecules. The polymer was dried in high vacuum for overnight and gave a yield of 71 mg (99%). ^{1}H NMR (400 MHz, Chloroform-*d*) δ 4.46-4.38 (m, 2H), 4.20 (s, 2H), 3.20 (d, *J* = 38.9 Hz, 1H), 2.15-1.65 (m, 2H), 1.50-0.71 (m, 3H). ^{13}C NMR (400 MHz, Chloroform-*d*) δ 207.81, 178.10, 153.14, 77.52, 75.11, 64.03, 63.07, 55.28, 45.60, 31.77, 19.64, 17.77, 0.83.

Synthesis of polymer **P2:**

Polymer **P2** was prepared through nucleophilic reaction. Typically, **P1** (63 mg, 0.35 mmol) was dissolved in degassed $CHCl_3$ (2 mL) in a 7 mL vial. Triethylamine (4.82 μL, 0.03 mmol) and 1-thiol octyl (60 μL, 0.35 mmol) was dissolved in a separate vial in $CHCl_3$ and added into the above polymer solution. The reaction was carried out at room temperature for 4 hours. Resulting

polymer was purified by precipitation in methanol (90 mg, 80%). ^{1}H NMR (400 MHz, Chloroform-*d*) δ 7.74 (d, *J* = 14.6 Hz, 1H), 5.79 – 5.69 (m, 1H), 4.34 – 4.29 (m, 4H), 4.20 – 4.14 (m, 2H), 2.79 (d, *J* = 8.2 Hz, 2H), 1.71 – 1.62 (m, 2H), 1.40 (t, *J* = 7.4 Hz, 2H), 1.28 (p, *J* = 6.0, 4.8 Hz, 8H), 1.04 (s, 3H), 0.88 (t, *J* = 6.6 Hz, 3H). ^{13}C NMR (500 MHz, Chloroform-*d*) δ 177.11, 176.04, 166.21, 164.88, 148.42, 148.25, 112.83, 62.98, 61.31, 54.55, 50.86, 45.02, 44.67, 31.80, 30.36, 29.71, 29.16, 28.84, 28.65, 22.65, 14.12.

Synthesis of polymer P3-6:

Polymer **P3-6** were prepared through a sequential nucleophilic reaction using a stronger base. Typically, **P2** (1.0 equiv.) was dissolved in degassed $CHCl_3$ (30 mg/mL) in a 1 mL vial. TBD (0.1 equiv.) and 2nd thiol reagent (Benzyl mercaptan for **P3**, Cysteamine for **P4**, *tert*-butyl 3-sulfanylpropanoate for **P5'**, TEG-SH for **P6**) (1.1 equiv.) was dissolved in a separate vial in $CHCl_3$ and added into the above polymer solution under argon. The reaction was stirred at room temperature for 4~6 hrs. For polymer **P3** and **P4**, they were designed for monitoring the reaction in NMR tubes, and no further purification steps were applied. For polymer **P5'** and **P6**, they were purified by precipitation either in methanol (**P5'**) or hexane (**P6**).

P5': Yield (90%). ^{1}H NMR (400 MHz, Chloroform-*d*) δ 4.30-4.16 (m, 5H), 4.20-4.14 (m, 1H), 2.90-2.82 (m, 2H), 2.66-2.53 (m, 3H), 1.82 (m, 2H), 1.67-1.56 (m, 2H), 1.44 (s, 8H), 1.36-1.26 (m, 10H), 1.02 (m, 2H), 0.88-0.85 (m, 3H). ^{13}C NMR (400 MHz, Chloroform-*d*) δ 176.79, 170.92, 169.72, 80.74, 61.89, 44.62, 41.39, 35.67, 31.82, 30.52, 29.21, 29.07, 25.82, 22.65, 14.14.

P6: Yield (77%). ^{1}H NMR (400 MHz, Chloroform-*d*) δ 4.34-4.29 (m, 4H), 4.20-4.14 (m, 1H), 3.66-3.64 (m, 11H), 3.56-3.55 (m, 2H), 3.38 (s, 3H), 2.90-2.82 (m, 3H), 2.71-2.60 (m, 2H), 1.83 (m, 2H), 1.69-1.57 (m, 4H), 1.37-1.28 (m, 10H), 1.04 (m, 2H), 0.88 (m, 3H).

P5 was prepared by deprotecting the *tert*-butyl group using TFA. Typically, **P5'** (41 mg, 0.08 mmol) was dissolved in degassed $CHCl_3$ (1.2 mL) in a 7 mL vial. TFA solution (0.8 mL in 1.2 mL of DCM) was added into the above solution. Argon was purged for 20min. Then the reaction was carried out at room temperature for 4 hrs. The resulting polymer **P5** was purified by evaporating the TFA and byproduct to give a yield of 36.4 mg (92%). ^{1}H NMR (400 MHz, Chloroform-*d*) δ 4.33-4.19 (m, 5H), 2.91-2.59 (m, 5H), 1.88 (m, 2H), 1.68-1.58 (m, 2H), 1.37-1.27 (m, 10H), 1.05 (m, 2H), 0.88-0.86 (m, 3H). ^{13}C NMR (400 MHz, Chloroform-*d*) δ 176.74, 62.66, 31.79, 29.17, 22.63, 14.10.

2.5.2 GPC profiles for first additions

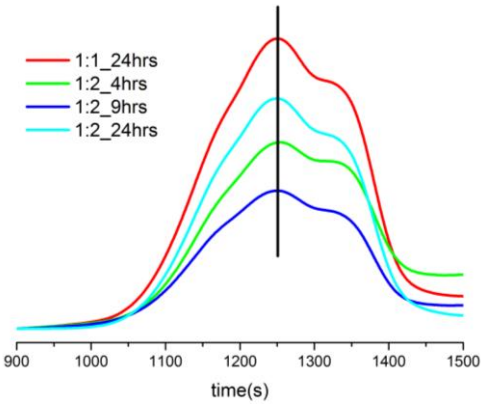

Figure 2.6 GPC profiles of polymer **P2** with longer reaction time and more thiol reagents under TEA base catalyst.

2.5.3 NMR spectrum and GPC profiles for sequential additions

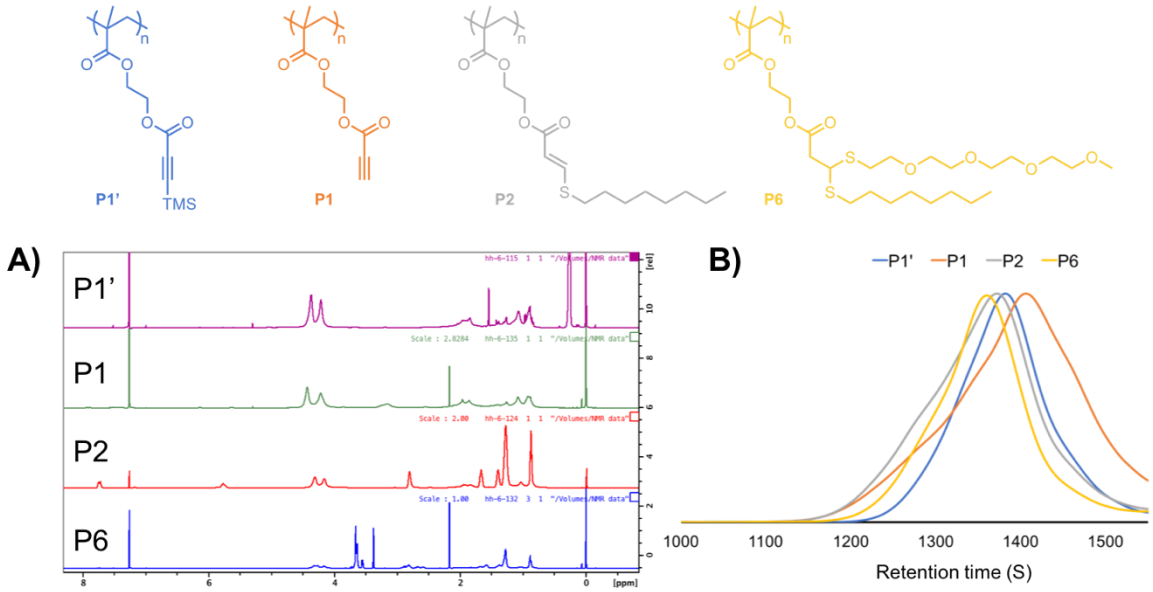

Figure 2.7 ^{1}H NMR spectrum (A) and GPC profiles (B) of four steps of polymer **P1'**, **P1**, **P2**, and **P6**.

2.5.4 Micelle preparation

Polymer (10 mg) was dissolved in minimum amount of acetone. Distilled water (2 mL) was added to the above solution. The acetone was then dialysis out against water for two days. The exact concentration of micelle solution was determined by lyophilizing certain amount of solution and measure the weight of solid residue. Typically, the final concentration of **P6** micelle solution is 3.5 mg/mL.

2.5.5 Reverse micelle preparation

Reverse micelle was prepared following the previous literature[10]. Typically, 1mg of polymer **P5** was dissolved in toluene to make 1 mg/mL concentration solution. Different amount of $NaHCO_3$ (0.1M pH=8.2) solution was added into the toluene solution to deprotonate COOH and make them more hydrophilic. Addition of trace amount of $NaHCO_3$ solution helps to make water pool inside reserve micelle. Sonication has applied at least 3 hrs until a homogeneous solution was obtained.

2.5.6 Peptide extraction experiment

One micromolar of each peptide was dissolved in MOPS buffer of pH 7. Two hundred microliters of the reverse micelle solution made from polymer **P5** was added to 1 mL of the peptide solution. Extraction was done under vigorous vortex for two hours. Centrifugation at 14 000 rcf for 20 min was followed to separate the two phases. The aqueous phase was removed, and the organic phase was dried by blowing N_2 gas. Ten microliters of aqueous solution was taken and mixed with 10 µL of a DHB matrix solution (25 mg/mL in 70% (v/v) acetonitrile containing 1% (v/v) TFA). The dried organic residue was re-dissolved in 20 µL of THF and mixed with 30 µL of the matrix solution. One microliter of this solution was spotted on the matrix-assisted laser desorption/ionization (MALDI) target for analysis.

MALDI-MS analyses were performed on a Bruker Autoflex III time-of-flight mass spectrometer. All mass spectra were obtained in positive mode and represent an average of 300 shots acquired at 40% laser power with an accelerating voltage of 19kV.

2.5.7 DLS of P5 aggregates

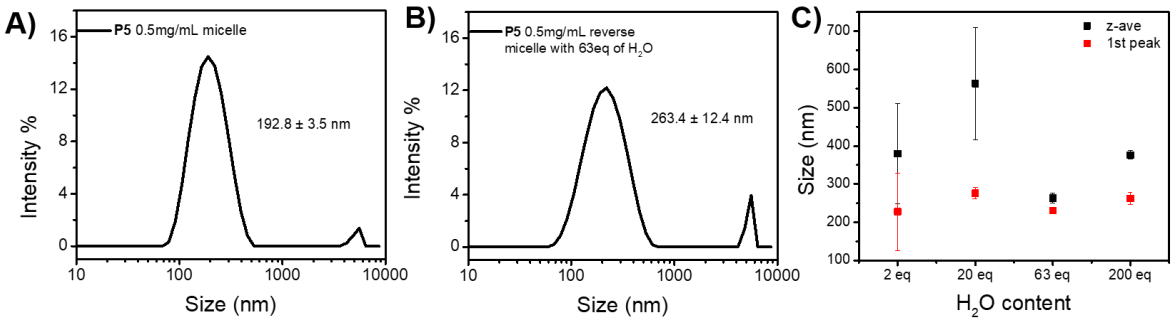

Figure 2.8 Size distribution of micelle (A) and reverse micelle (B) made from polymer **P5**. (C) Size distribution of reverse micelle with different equivalents of H_2O content addition respect to COOH group.

2.5.8 DLS measurements of P6 in response to H_2O_2

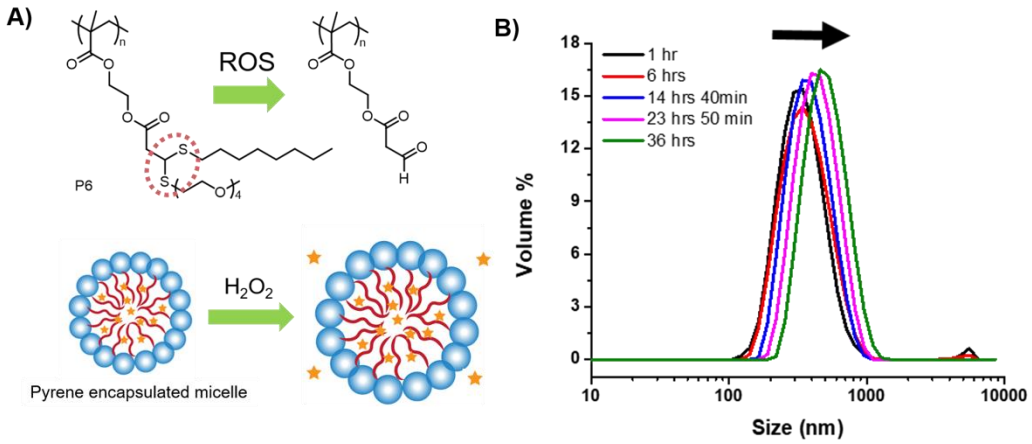

Figure 2.9 (A) Schematic representative of polymer **P6** degrades in response to ROS. (B) Size distribution changes of micelle made from polymer **P6** in response to H_2O_2.

2.5.9 NMR spectra

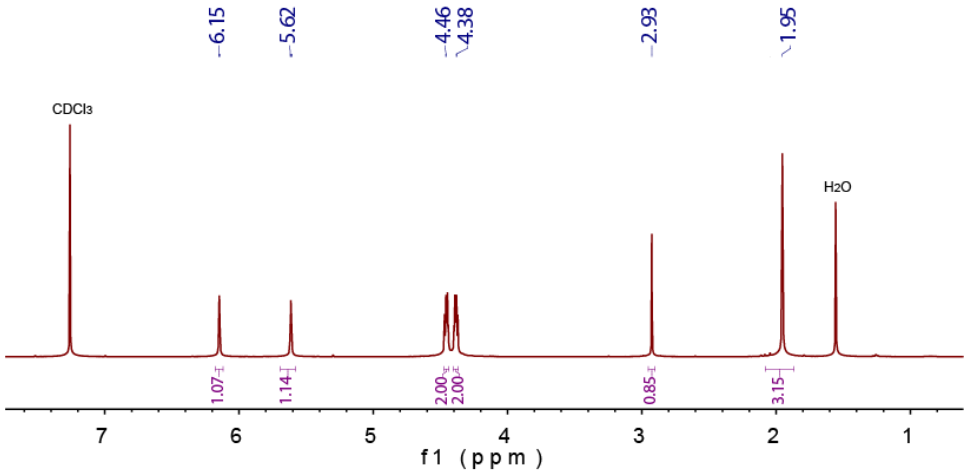

Figure 2.10 ^{1}H NMR spectrum of monomer **1**. Solvent: Chloroform-*d*.

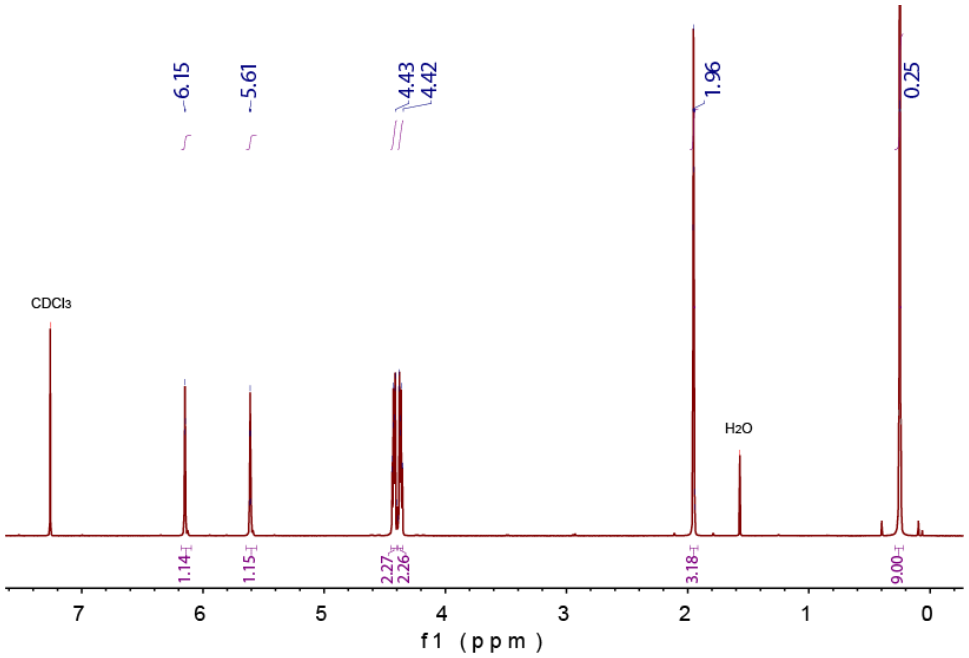

Figure 2.11. [1]H NMR spectrum of monomer **2**. Solvent: Chloroform-*d*.

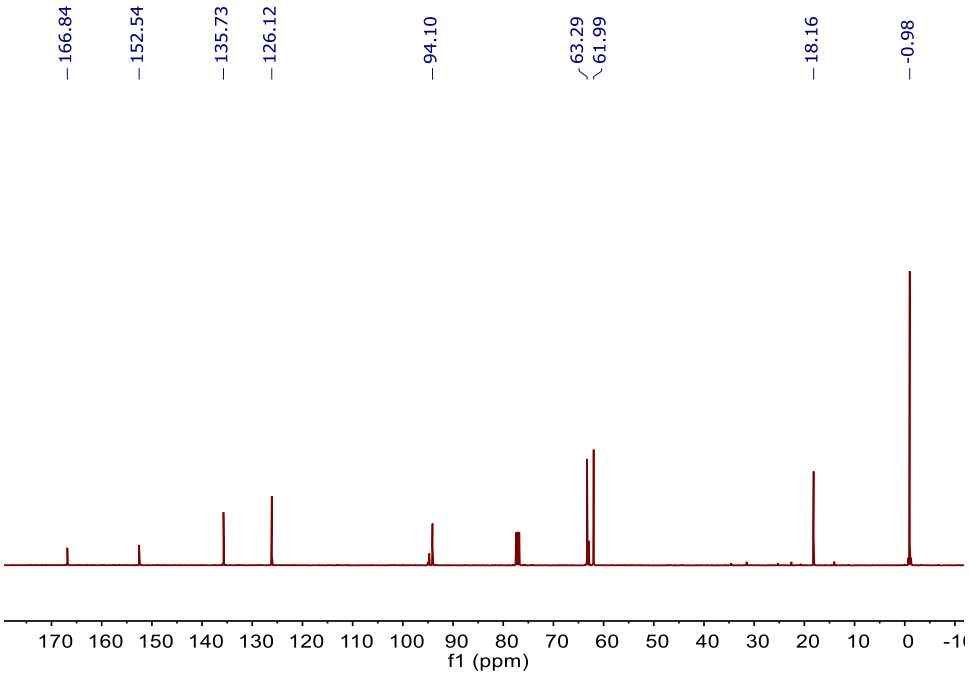

Figure 2.12. [13]C NMR spectrum of monomer **2**. Solvent: Chloroform-*d*

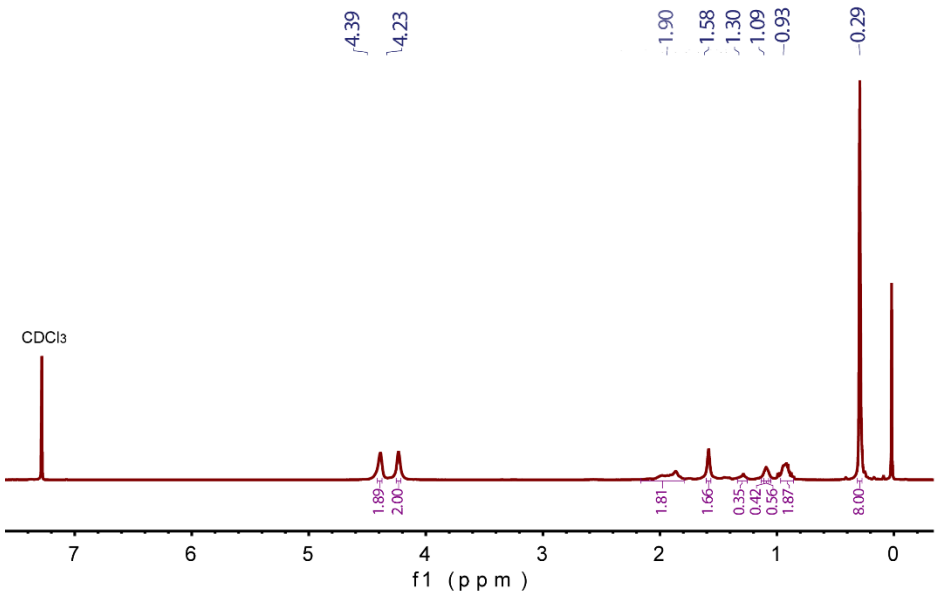

Figure 2.13. [1]H NMR spectrum of polymer **P1'**. Solvent: Chloroform-*d*.

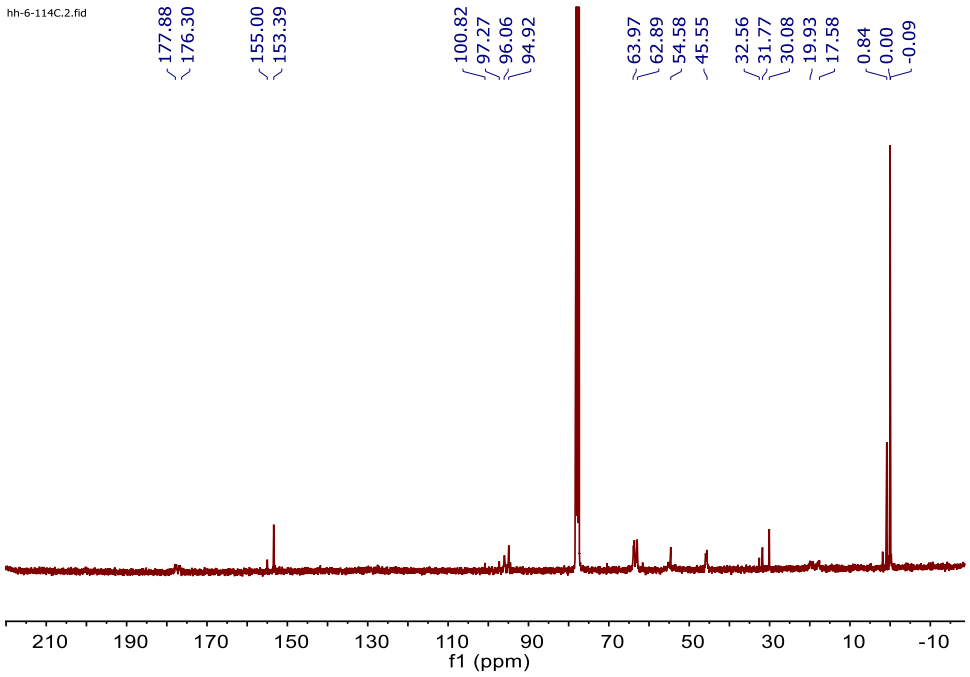

Figure 2.14. [13]C NMR spectrum of polymer **P1'**. Solvent: Chloroform-*d*.

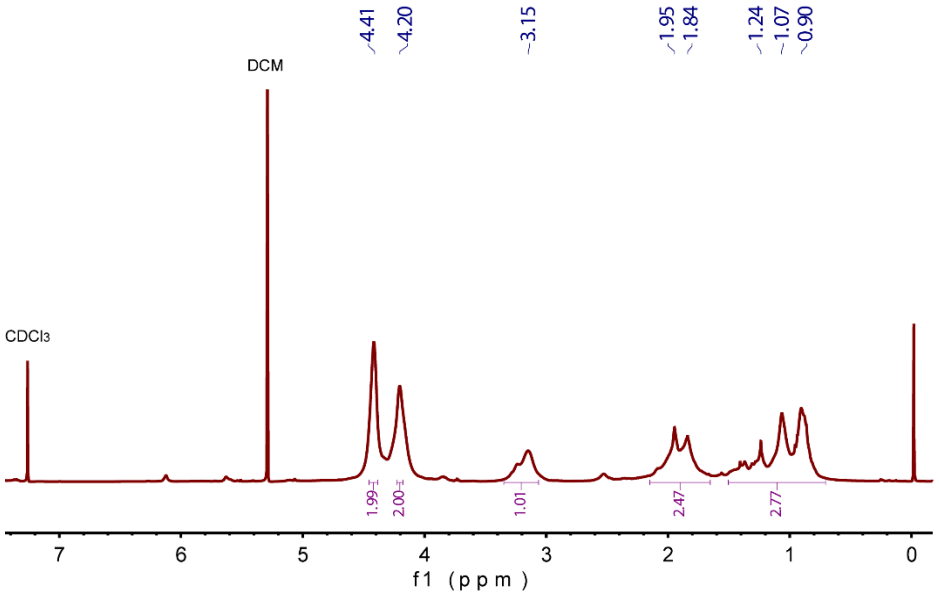

Figure 2.15. ^{1}H NMR spectrum of polymer **P1**. Solvent: Chloroform-*d*.

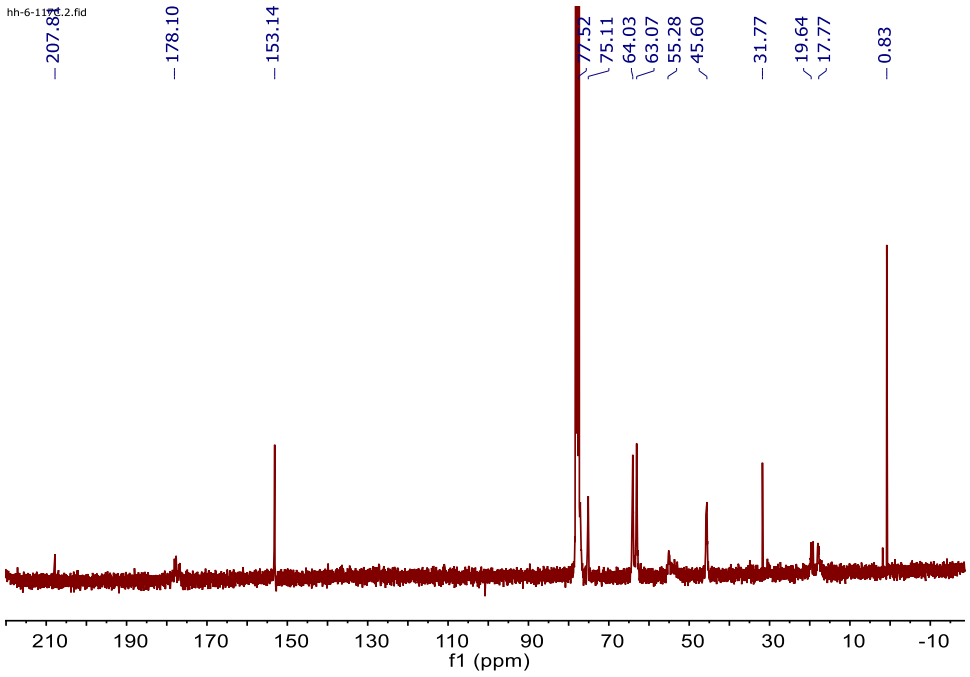

Figure 2.16. ^{13}C NMR spectrum of polymer **P1**. Solvent: Chloroform-*d*.

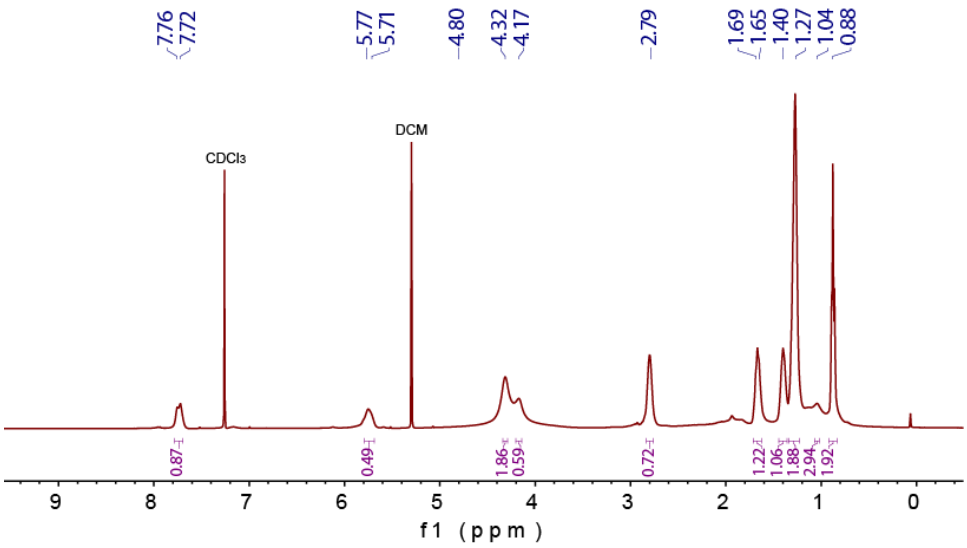

Figure 2.17. [1]H NMR spectrum of polymer **P2**. Solvent: Chloroform-*d*.

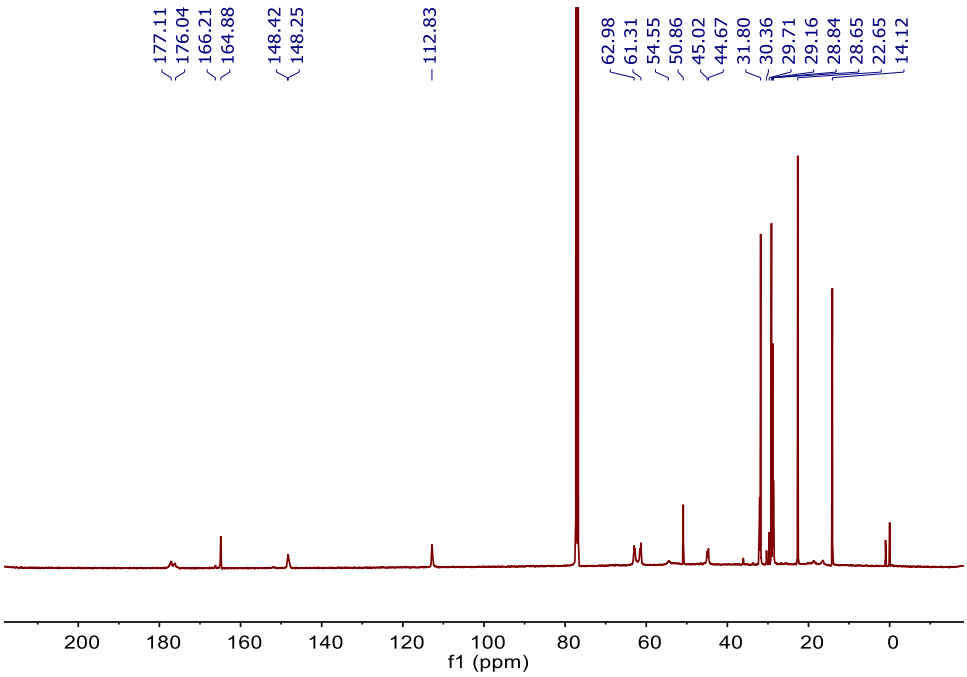

Figure 2.18 [13]C NMR spectrum of polymer **P2**. Solvent: Chloroform-*d*.

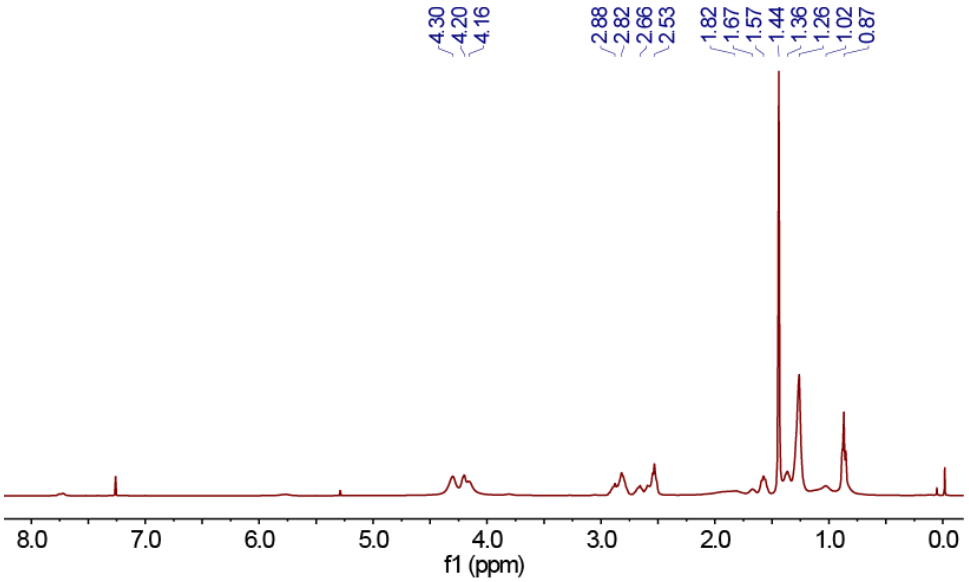

Figure 2.19. [1]H NMR spectrum of polymer **P5'**. Solvent: Chloroform-*d*.

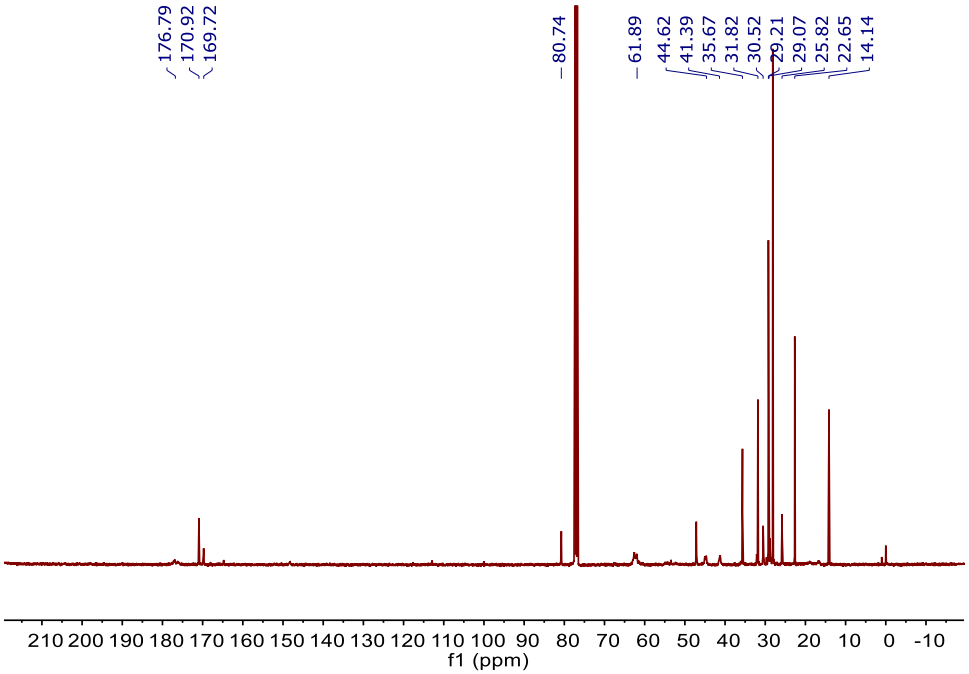

Figure 2.20. [13]C NMR spectrum of polymer **P5'**. Solvent: Chloroform-*d*.

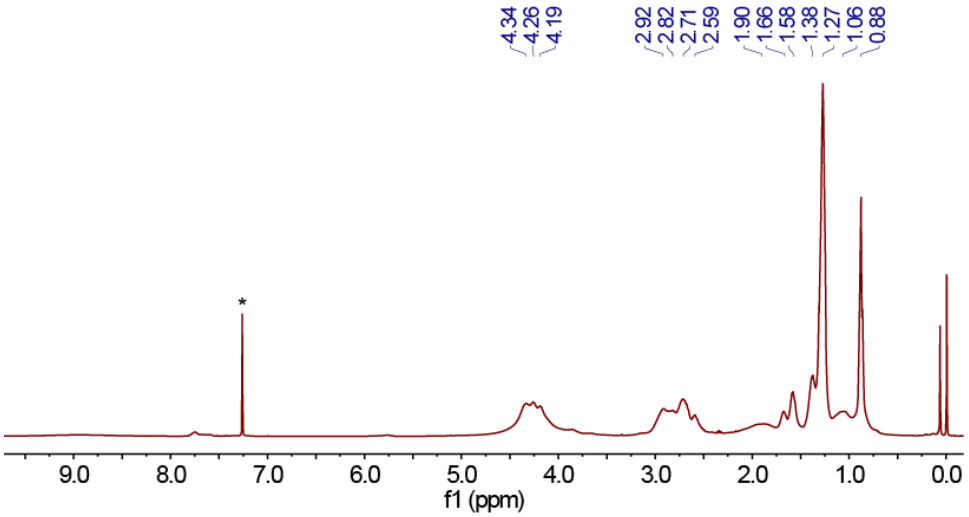

Figure 2.21. [1]H NMR spectrum of polymer **P5**. Solvent: Chloroform-*d*.

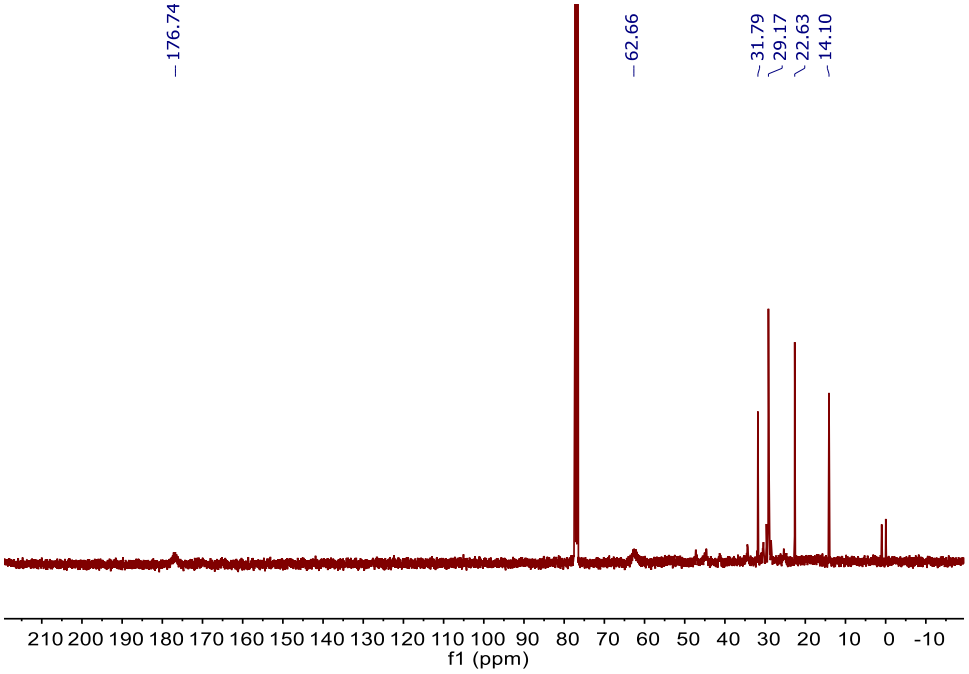

Figure 2.22. [13]C NMR spectrum of polymer **P5**. Solvent: Chloroform-*d*.

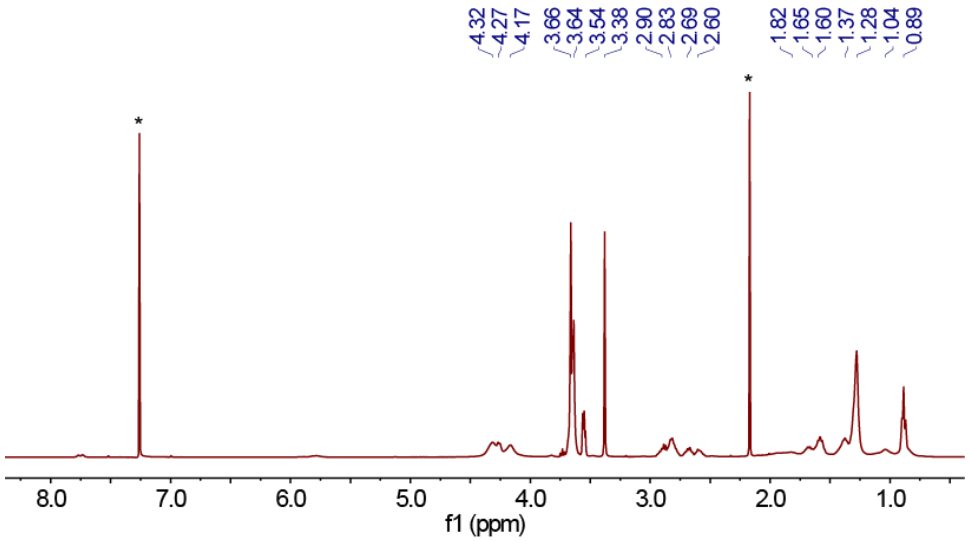

Figure 2.23. ^{1}H NMR spectrum of polymer **P6**. Solvent: $CDCl_3$. * indicated solvent peaks: Chloroform-*d* (7.26ppm), Acetone (2.17ppm).

2.6 References

(1) Zhang, J.; Liu, K.; Müllen, K.; Yin, M. Self-Assemblies of Amphiphilic Homopolymers: Synthesis, Morphology Studies and Biomedical Applications. *Chem. Commun.* **2015**, *51* (58), 11541–11555 DOI: 10.1039/C5CC03016A.

(2) Kale, T. S.; Klaikherd, A.; Popere, B.; Thayumanavan, S. Supramolecular Assemblies of Amphiphilic Homopolymers. *Langmuir* **2009**, *25* (17), 9660–9670 DOI: 10.1021/la900734d.

(3) Cha, J. N.; Birkedal, H.; Euliss, L. E.; Bartl, M. H.; Wong, M. S.; Deming, T. J.; Stucky, G. D. Spontaneous Formation of Nanoparticle Vesicles from Homopolymer Polyelectrolytes. *J. Am. Chem. Soc.* **2003**, *125* (27), 8285–8289 DOI: 10.1021/ja0279601.

(4) Savariar, E. N.; Aathimanikandan, S. V.; Thayumanavan, S. Supramolecular Assemblies from Amphiphilic Homopolymers: Testing the Scope. *J. Am. Chem. Soc.* **2006**, *128* (50), 16224–16230 DOI: 10.1021/ja065213o.

(5) Laurent, B. A.; Grayson, S. M. Synthesis of Cyclic Amphiphilic Homopolymers and Their Potential Application as Polymeric Micelles. *Polym. Chem.* **2012**, *3* (7), 1846–1855 DOI: 10.1039/C1PY00378J.

(6) Zhou, Y.; Liu, B.; Wang, X. Self-Assembly of Homopolymers through Strong Dipole-Dipole Interaction in Their Aqueous Solutions. *Polymer (Guildf).* **2016**, *97*, 1–10 DOI: 10.1016/J.POLYMER.2016.05.011.

(7) Manojkumar, K.; Mecerreyes, D.; Taton, D.; Gnanou, Y.; Vijayakrishna, K. Self-Assembly of Poly(Ionic Liquid) (PIL)-Based Amphiphilic Homopolymers into Vesicles and Supramolecular Structures with Dyes and Silver Nanoparticles. *Polym. Chem.* **2017**, *8* (22), 3497–3503 DOI: 10.1039/C7PY00453B.

(8) Kohut, A.; Hevus, I.; Voronov, S.; Voronov, A. Amphiphilic Invertible Polymers and Their Applications. In *Industrial Applications for Intelligent Polymers and Coatings*; Springer International Publishing: Cham, 2016; pp 399–415.

(9) Qiu, L.; Zhang, J.; Yan, M.; Jin, Y.; Zhu, K. Reverse Self-Assemblies Based on Amphiphilic Polyphosphazenes for Encapsulation of Water-Soluble Molecules. *Nanotechnology* **2007**, *18* (47), 475602 DOI: 10.1088/0957-4484/18/47/475602.

(10) Rodthongkum, N.; Chen, Y.; Thayumanavan, S.; Vachet, R. W. Selective Enrichment and Analysis of Acidic Peptides and Proteins Using Polymeric Reverse Micelles and MALDI-MS. *Anal. Chem.* **2010**, *82* (20), 8686–8691 DOI: 10.1021/ac101922b.

(11) Rodthongkum, N.; Ramireddy, R.; Thayumanavan, S.; Richard, W. V. Selective Enrichment and Sensitive Detection of Peptide and Protein Biomarkers in Human Serum Using Polymeric Reverse Micelles and MALDI-MS. *Analyst* **2012**, *137* (4), 1024–1030 DOI: 10.1039/c2an16089g.

(12) Arumugam, S.; Vutukuri, D. R.; Thayumanavan, S.; Ramamurthy, V. Amphiphilic Homopolymer as a Reaction Medium in Water: Product Selectivity within Polymeric Nanopockets. *J. Am. Chem. Soc.* **2005**, *127* (38), 13200–13206 DOI: 10.1021/ja051107v.

(13) Miao, W.-K.; Yan, Y.-K.; Wang, X.-L.; Xiao, Y.; Ren, L.-J.; Zheng, P.; Wang, C.-H.; Ren, L.-X.; Wang, W. Incorporation of Polyoxometalates into Polymers to Create Linear Poly(Polyoxometalate)s with Catalytic Function. *ACS Macro Lett.* **2014**, *3* (2), 211–215 DOI: 10.1021/mz5000202.

(14) Sandanaraj, B. S.; Demont, R.; Thayumanavan, S. Generating Patterns for Sensing Using a Single Receptor Scaffold. *J. Am. Chem. Soc.* **2007**, *129* (12), 3506–3507 DOI: 10.1021/ja070229f.

(15) Yu, Y.; Yin, M.; Müllen, K.; Knoll, W. LbL-Assembled Multilayer Films of Dendritic Star Polymers: Surface Morphology and DNA Hybridization Detection. *J. Mater. Chem.* **2012**, *22* (16), 7880–7886 DOI: 10.1039/c2jm15931g.

(16) Li, N.; Ye, G.; He, Y.; Wang, X. Hollow Microspheres of Amphiphilic Azo Homopolymers: Self-Assembly and Photoinduced Deformation Behavior. *Chem. Commun.* **2011**, *47* (16), 4757–4759 DOI: 10.1039/c0cc05010e.

(17) Changez, M.; Kang, N. G.; Lee, C. H.; Lee, J. S. Reversible and pH-Sensitive Vesicles from Amphiphilic Homopolymer Poly(2-(4-Vinylphenyl)Pyridine). *Small* **2010**, *6* (1), 63–68 DOI: 10.1002/smll.200901670.

(18) Liu, J.; Huang, W.; Pang, Y.; Huang, P.; Zhu, X.; Zhou, Y.; Yan, D. Molecular Self-Assembly of a Homopolymer: An Alternative to Fabricate Drug Delivery Platforms for Cancer Therapy. *Angew. Chemie Int. Ed.* **2011**, *50* (39), 9162–9166 DOI: 10.1002/anie.201102280.

(19) Mane, S. R.; Rao, V. N.; Shunmugam, R. Reversible pH- and Lipid-Sensitive Vesicles from

Amphiphilic Norbornene-Derived Thiobarbiturate Homopolymers. *ACS Macro Lett.* **2012**, *1* (4), 482–488 DOI: 10.1021/mz2002092.

(20) Mane, S. R.; Rao N, V.; Chaterjee, K.; Dinda, H.; Nag, S.; Kishore, A.; Das Sarma, J.; Shunmugam, R. Amphiphilic Homopolymer Vesicles as Unique Nano-Carriers for Cancer Therapy. *Macromolecules* **2012**, *45* (19), 8037–8042 DOI: 10.1021/ma301644m.

(21) Zhuang, J.; Garzoni, M.; Torres, D. A.; Poe, A.; Pavan, G. M.; Thayumanavan, S. Programmable Nanoassemblies from Non-Assembling Homopolymers Using Ad Hoc Electrostatic Interactions. *Angew. Chemie Int. Ed.* **2017**, *56* (15), 4145–4149 DOI: 10.1002/anie.201611688.

(22) Basu, S.; Vutukuri, D. R.; Shyamroy, S.; Sandanaraj, B. S.; Thayumanavan, S. Invertible Amphiphilic Homopolymers. *J. Am. Chem. Soc.* **2004**, *126* (32), 9890–9891 DOI: 10.1021/ja047816a.

(23) Luo, C.; Liu, Y.; Li, Z. Thermo- and pH-Responsive Polymer Derived from Methacrylamide and Aspartic Acid. *Macromolecules* **2010**, *43* (19), 8101–8108 DOI: 10.1021/ma1015227.

(24) Wang, Y.; Alb, A. M.; He, J.; Grayson, S. M. Neutral Linear Amphiphilic Homopolymers Prepared by Atom Transfer Radical Polymerization. *Polym. Chem.* **2014**, *5* (2), 622–629 DOI: 10.1039/c3py00916e.

(25) Ramireddy, R. R.; Prasad, P.; Finne, A.; Thayumanavan, S. Zwitterionic Amphiphilic Homopolymer Assemblies. *Polym. Chem.* **2015**, *6* (33), 6083–6087 DOI: 10.1039/C5PY00879D.

(26) Kubo, T.; Bentz, K. C.; Powell, K. C.; Figg, C. A.; Swartz, J. L.; Tansky, M.; Chauhan, A.; Savin, D. A.; Sumerlin, B. S. Modular and Rapid Access to Amphiphilic Homopolymers via Successive Chemoselective Post-Polymerization Modification. *Polym. Chem.* **2017**, *8* (39), 6028–6032 DOI: 10.1039/C7PY01585B.

(27) Moses, J. E.; Moorhouse, A. D. The Growing Applications of Click Chemistry. *Chem. Soc. Rev.* **2007**, *36* (8), 1249–1262 DOI: 10.1039/B613014N.

(28) Meldal, M.; Tornøe, C. W. Cu-Catalyzed Azide−Alkyne Cycloaddition. *Chem. Rev.* **2008**, *108* (8), 2952–3015 DOI: 10.1021/cr0783479.

(29) Jewett, J. C.; Bertozzi, C. R. Cu-Free Click Cycloaddition Reactions in Chemical Biology. *Chem. Soc. Rev.* **2010**, *39* (4), 1272–1279.

(30) Schilling, C. I.; Jung, N.; Biskup, M.; Schepers, U.; Bräse, S. Bioconjugation via Azide–Staudinger Ligation: An Overview. *Chem. Soc. Rev.* **2011**, *40* (9), 4840 DOI: 10.1039/c0cs00123f.

(31) Hoyle, C. E.; Bowman, C. N. Thiol-Ene Click Chemistry. *Angew. Chemie Int. Ed.* **2010**, *49* (9), 1540–1573 DOI: 10.1002/anie.200903924.

(32) Lowe, A. B. Thiol-Yne 'Click'/Coupling Chemistry and Recent Applications in Polymer and Materials Synthesis and Modification. *Polym. (United Kingdom)* **2014**, *55* (22), 5517–5549 DOI: 10.1016/j.polymer.2014.08.015.

(33) Truong, V. X.; Dove, A. P. Organocatalytic, Regioselective Nucleophilic 'Click' Addition of Thiols to Propiolic Acid Esters for Polymer-Polymer Coupling. *Angew. Chemie Int. Ed.* **2013**, *52* (15), 4132–4136 DOI: 10.1002/anie.201209239.

(34) Kuroda, H.; Tomita, I.; Endo, T. A Novel Polyaddition of Bifunctional Acetylenes Containing Electron-Withdrawing Groups. 2. Synthesis of Polymers Having B-Alkylmercaptoenoate Moieties by the Reaction with Dithiols. *Macromolecules* **1995**, 6020–6025 DOI: 10.1021/ma00122a006.

(35) Yao, B.; Sun, J.; Qin, A.; Tang, B. Z. Thiol-Yne Click Polymerization. *Chinese Sci. Bull.* **2013**, *58* (22), 2711–2718 DOI: 10.1007/s11434-013-5892-1.

(36) Wilson, D. S.; Dalmasso, G.; Wang, L.; Sitaraman, S. V; Merlin, D.; Murthy, N. Orally Delivered Thioketal Nanoparticles Loaded with TNF-α-siRNA Target Inflammation and Inhibit Gene Expression in the Intestines. *Nat. Mater.* **2010**, *9* (11), 923–928 DOI: 10.1038/nmat2859.

(37) Shim, M. S.; Xia, Y. A Reactive Oxygen Species (ROS)-Responsive Polymer for Safe, Efficient, and Targeted Gene Delivery in Cancer Cells. *Angew. Chemie Int. Ed.* **2013**, *52* (27), 6926–6929 DOI: 10.1002/anie.201209633.

(38) Martin, J. R.; Gupta, M. K.; Page, J. M.; Yu, F.; Davidson, J. M.; Guelcher, S. A.; Duvall, C. L. A Porous Tissue Engineering Scaffold Selectively Degraded by Cell-Generated Reactive Oxygen Species. *Biomaterials* **2014**, *35* (12), 3766–3776 DOI: 10.1016/j.biomaterials.2014.01.026.

(39) Hanash, S. M.; Pitteri, S. J.; Faca, V. M. Mining the Plasma Proteome for Cancer Biomarkers. *Nature* **2008**, pp 571–579.

(40) Liotta, L. A.; Petricoin, E. Cancer Biomarkers: Closer to Delivering on Their Promise. *Cancer Cell*. **2011**, pp 279–280.

(41) Serrano, M. A. C.; He, H.; Zhao, B.; Ramireddy, R. R.; Vachet, R. W.; Thayumanavan, S. Polymer-Mediated Ternary Supramolecular Interactions for Sensitive Detection of Peptides. *Analyst* **2016**, *142* DOI: 10.1039/c6an01591c.

(42) Combariza, M. Y.; Savariar, E. N.; Vutukuri, D. R.; Thayumanavan, S.; Vachet, R. W. Polymeric Inverse Micelles as Selective Peptide Extraction Agents for MALDI-MS Analysis. *Anal. Chem.* **2007**, *79* (18), 7124–7130 DOI: 10.1021/ac071001d.

(43) Greenspan, P.; Fowler, S. D. Spectrofluorometric Studies of the Lipid Probe, Nile Red. *J. Lipid Res.* **1985**, *26* (7), 781–789.

(44) Liu, B.; Thayumanavan, S. Substituent Effects on the pH Sensitivity of Acetals and Ketals

and Their Correlation with Encapsulation Stability in Polymeric Nanogels. *J. Am. Chem. Soc.* **2017**, *139* (6), 2306–2317 DOI: 10.1021/jacs.6b11181.

(45) Escamilla, I. V.; Ramos, L. F. R.; Escalera, J. S.; Hernández, A. Á. Studies on the Deprotection of Triisopropylsilylarylacetylene Derivatives. *J. Mex. Chem. Soc.* **2011**, *55* (3), 133–136.

CHAPTER

3. NUCLEOPHILIC "CLICK" REACTION FOR POLYMERIZATION AND SEQUENTIAL BACKBONE MODIFICATION

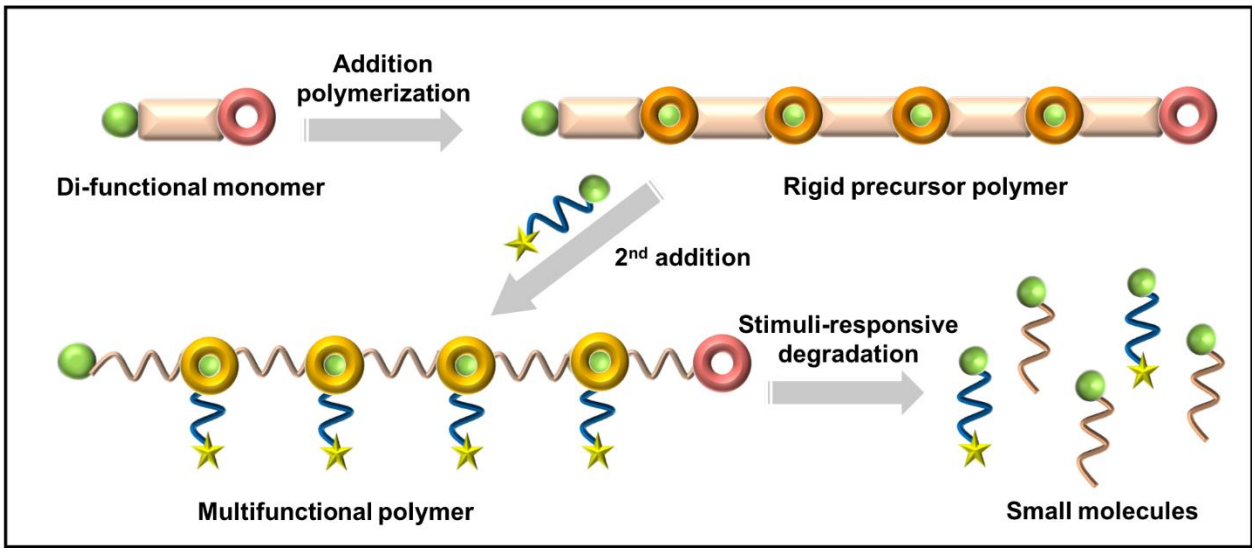

Scheme 3.1 Cartoon representation of addition polymerization of the bifunctional monomer, 2nd thiol addition, and degradation upon stimuli.

3.1 Introduction

Polymers have been widely used in materials science. The current polymerization methods are well established, such as radical polymerization (ATRP[1], RAFT[2], and NMP[3]), ionic polymerization (anionic[4] and cationic[5] polymerization), condensation polymerization[6], as well as addition polymerization. They typically involve harsh reaction conditions, such as oxygen-free atmosphere, high temperature and the use of transition metal catalysts. All these factors add up to the total manufacturing cost in an industrial set up while posing significant safety issues. Therefore, developing simple synthetic protocols to prepare polymeric materials is of marked interest.

Polymers with a stereo backbone have gained lots of interest due to their optical and mechanical properties[7]. They have huge implications in plastics, fibers, rubbers and adhesive industries. For example, the *cis* isomer of polybutadiene is elastic while the *trans* isomer has highly ordered structure and are microcrystalline, which is an important property used in plastics. Therefore, a sufficient *cis* stereoregularity is essential for synthetic rubber to maintain its elasticity. Tunability of stereoisomers in polymers, however, has remained a challenge. Few literature reports suggest that it can be controlled by using stereoselective catalysts and appropriate reaction conditions[8]. For instance, Ziegler-Natta catalyst such as dialkyl-aluminum chloride-cobalt (II) halide combinations was utilized to prepare high *cis*-1,4-PB with approximately 92% cis-1,4 content[9]. Yet, techniques to achieve stereoregularity on diverse polymers remains elusive.

Thiol group is a versatile functional group from a synthetic chemistry perspective as it takes part in a variety of reactions. Thiol-ene chemistry is a widely utilized reaction that proceeds in a click manner under the assistance of UV light and a photo initiator[10]. Additionally, thiol moieties participate in Michael addition, leading to the formation of a sulfur-carbon bond. Recently, it has been shown that thiol groups can readily react with electron deficient triple bonds under mild conditions, yielding stereo-selective products[11,12]. These considerations suggest that a bifunctional monomer with a thiol group at one terminus and an electron-deficient alkyne moiety at the other could result in polymers with stereoregularity.

Furthermore, this polymer possesses thiol vinyl groups on its backbone, which is reported to react with another thiol reagent to form dithiol acetal structure only in the presence of a much stronger base. This latter requirement for preparing linear polymer architecture. Its capability of post-polymerization modification allows us to incorporate new backbone characteristics and multifunctionalities while also controlling the functional groups on the side chain. By doing this,

the amphiphilic side chain could be easily incorporated onto polymer backbone to generate amphiphilic polymers.

Moreover, the addition polymer with dithiol acetal structures on its backbone is considered to be sensitive to ROS stimulus. The mechanism of ROS responsiveness is proposed to break the C-S bond via hydroxyl radical nucleophilic attacking. Since the dithiol acetal functional groups are located on the polymer backbone, we envision that the degradation of the final polymer upon ROS stimulus would be accelerated.

In this work, we have developed a "click" addition polymerization method by using a bi-functional monomer bearing both electron-deficient alkyne and thiol groups. The addition polymerization reaction happens between alkyne and thiol groups to form linear polymers with thiol vinyl group in its backbone (Scheme 3.2). Furthermore, a post-functionalization of the linear polymer can be carried out with another thiol reagent via Michael addition with a stronger base, providing the opportunity to prepare more complicated polymers. Finally, the multifunctional polymer is ROS responsive due to the dithiol acetal structure. This property could allow us to design new material for drug delivery field.

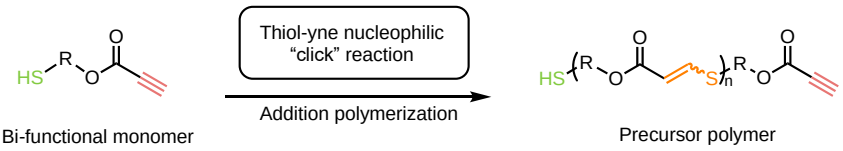

Scheme 3.2 Schematic representation of addition polymerization of the bi-functional monomer.

3.2 Results and discussions

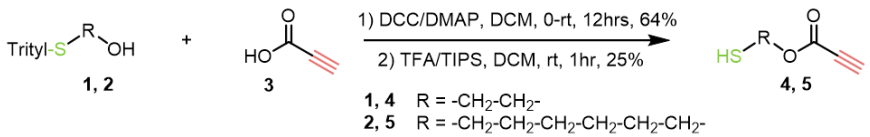

Scheme 3.3 Synthetic scheme of bi-functional monomer **4** and **5**.

In order to test the idea of polymerization using a bifunctional monomer, we synthesized two monomers with two-carbon (**4**) as well as six-carbon (**5**) linkers in between thiol and alkyne

end groups (Scheme 3.3). These bi-functional monomers were synthesized through an esterification reaction between **1** or **2** and **3** (propiolic acid) to install electron deficient alkyne end group. Subsequent deprotection of the trityl group using TFA/TIPS yielded the monomers **4** or **5** with the free thiol terminus.

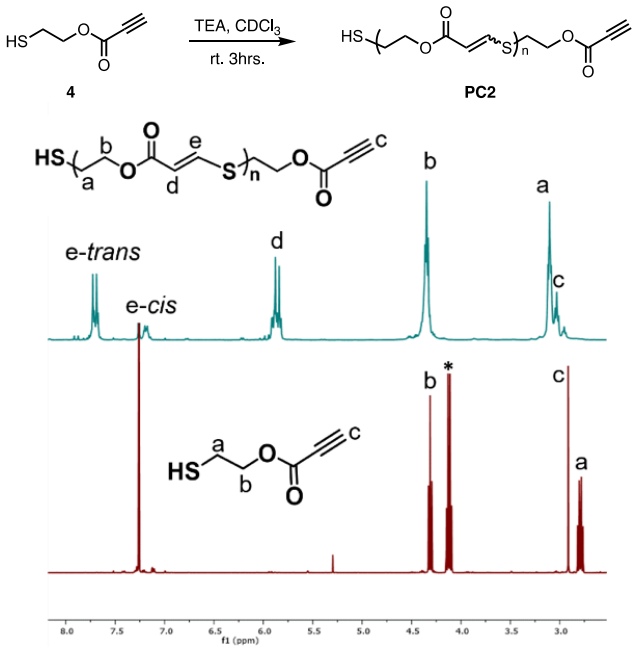

Figure 3.1 ^{1}H NMR spectrum of monomer **4**, 2-mercaptoethyl propiolate and precursor polymer **PC2** prepared by monomer **4**. *Ethyl acetate solvent peak.

Monomer **4** was subjected to polymerization using TEA as a catalyst. To our surprise, a polymer with an Mw as high as 15 000 g/mol and an acceptable PDI of 1.73 was obtained without any pre-treatment. More importantly, the ^{1}H NMR spectrum revealed that majority of the stereoisomers in the polymer backbone were in *trans* state (Figure 3.1). It is to be noted that the polymerization here was carried out at room temperature in the open air without any transition metal catalyst. To further optimize the conditions, we studied the parameters that could affect the Mw and PDI, including the nature and the amount of the base solvent, monomer concentration, reaction time and temperature.

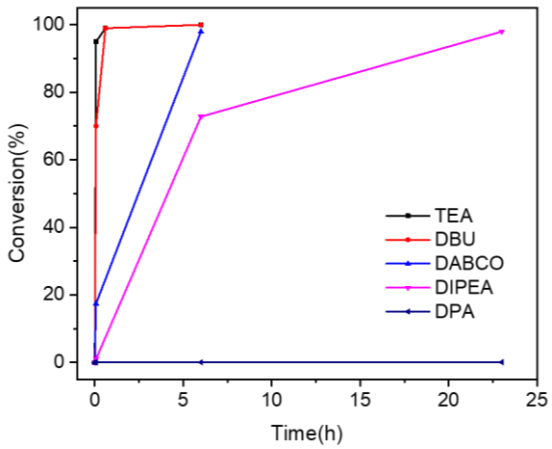

Figure 3.2 Reaction rate with different organic bases. TEA: triethylamine; DBU: 1, 8-Diazabicyclo (5.4.0) undec-7-ene; DABCO: 1,4-diazabicyclo [2.2.2] octane; DIPEA: *N, N*-Diisopropylethylamine; DPA: Diphenylamine.

Five organic bases were chosen with different basicity and nucleophilicity. Polymerization process was monitored by NMR spectroscopy. Monomer conversion was calculated by comparing the integration of alkyne peak before and after adding base over time. Among the bases used, TEA (pK_a=10.5) and DBU (pK_a=14.2) performed better as catalysts (Figure 3.2). In their presence, polymerization was completed (~95%) within an hour. The catalytic efficiency decreased significantly while using DABCO (pK_a=8.8) and DIPEA (pK_a=11.4) due to the steric hindrance of the base. Although surprised by the fact that DPA was considered as a reasonable base for this type of reaction in the literature, we also tried DPA in our case, nonetheless. Not surprisingly, DPA, with a low pKa of 0.79, didn't result in polymerization in our hands. Therefore, for the following studies, we chose TEA as the catalyst.

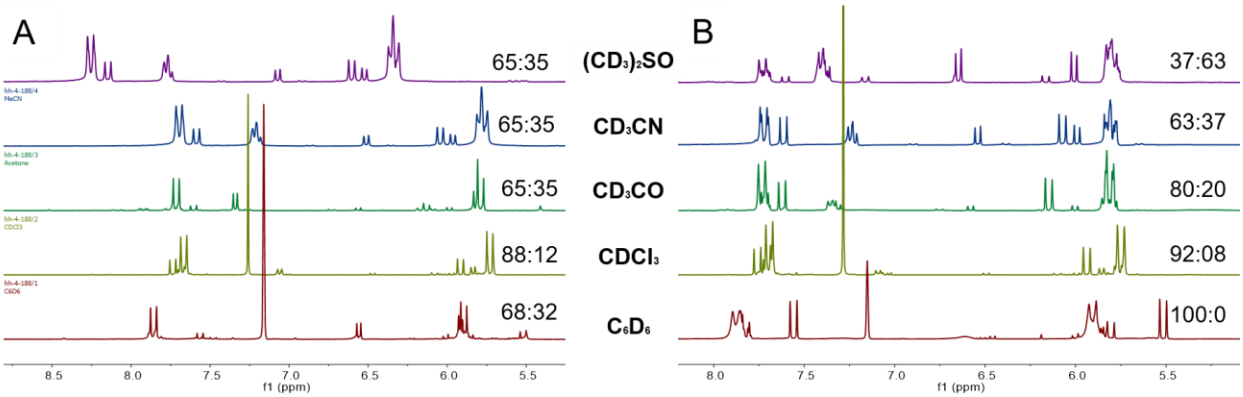

Figure 3.3 Precursor polymer stereo-selectivity upon different solvents. Number ratio represents the isomer ratio between *trans* and *cis*.

Next, we focused our attention on the stereoselectivity effect provided by different solvents[13]. The polymerization reaction was conducted in an NMR tube with identical monomer concentration and TEA dosage. The reaction was carried out for 30 min (Figure 3.3A) as well as 24 hours (Figure 3.3B) to ensure complete monomer conversion and temperature was maintained at 25 ^{o}C throughout. The ratio between *trans* (J_{HH} = 15~20 Hz) and *cis* (J_{HH} = 10~12 Hz) isomers was calculated by comparing the integration of alkene peaks in ^{1}H NMR spectrum. In the reaction at 30 min, total disappearance of alkyne peak from the NMR spectrum indicated the completion of the reaction. It is interesting to see that the ratio between trans/cis has changed from 30 min to 24 hrs. This data suggests that the isomer ratio changes with time, which may due to the reversibility naturean of the reaction. And it is the reversibility that causes the shift from an initial kinetic control ratio toward a thermodynamically controlled ratio. Interestingly, the thermodynamic ratio is different in different solvents. For example, in DMSO the thermodynamic ratio favors cis; while as in benzene, the thermodynamic ratio favors more trans than what we started with. By varying the deuterium solvents from DMSO to benzene, the trans/cis ratio changed from 37:63 to 100:0. One reason behind this phenomenon is that the polarity of the solvents has been changed from 7.2 to 2.7 (with respect to water as 9.0 and pentane as 0.0), and this polarity change may cause the addition mechanism in favor of *cis* over *trans*[12]. This tunability in

stereoselectivity may provide us access to control the stereo structures in polymers by merely changing the reaction solvents.

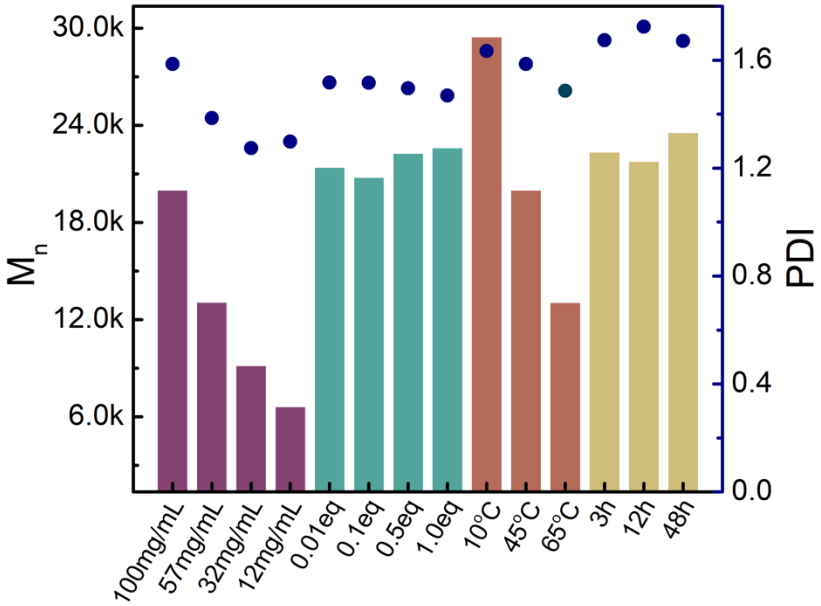

Figure 3.4 Effect of monomer concentration, base amount, reaction temperature and time on polymer weight (bar) and PDI (dot).

Next, we investigated the effect of monomer concentrations, catalyst loading, reaction temperature and time on polymerization using **5** as a model monomer. Firstly, we carried out the polymerization using 12 mg/mL, 32 mg/mL, 50 mg/mL and 100 mg/mL of monomer in $CDCl_3$. The polymer Mw ranged from 3 500 g/mol up to 20 000 g/mol. The sample with high monomer concentration (100 mg/mL) provided the higher Mw (~20 000 g/mol) polymer. Secondly, varying amounts of TEA was used to check its effect on polymerization. Specifically, we used 0.01 equiv., 0.1 equiv., 0.5 equiv. and 1.0 equiv. of TEA relative to the monomer (100 mg/mL) ($CDCl_3$, 45°C, 24 hrs.). As shown in figure 3.4, 1.0 equiv. of TEA gave the highest Mw polymer, while, the PDI of the polymers remained similar in all cases. Thirdly, the temperature effect on polymerization was studied by performing reactions under different temperatures. The reaction was carried out with 100 mg/mL monomer concentration and 0.1 equiv. of TEA dosage. As shown in figure 3.4, Mw decreases with an increase in the reaction temperature. This interesting phenomenon could be

attributed to two possible reasons: 1) the nuclei formation theory suggests that at higher temperatures, more nuclei formation is favored resulting in short chain length; 2) the thiol vinyl bond is labile and is dynamically exchanging with another thiol group. Under high temperatures, thiol groups in the polymer chain tend to have more thiol exchange compared to the case at lower temperatures. This more frequent exchange could result in shorter chain length. Finally, the effect of reaction time on polymerization was studied by quenching reactions at a different time (3 hrs., 12 hrs., and 48 hrs.). As illustrated in figure 3.4, reaction time showed little effect on polymer molecular weight after 3hrs, achieving a Mw of 22 500g/mol. A slightly higher molecular weight (~24 000 g/mol) was obtained when reaction went on to 48 hrs. It is important to note that the PDI increases when the molecular weight increases.

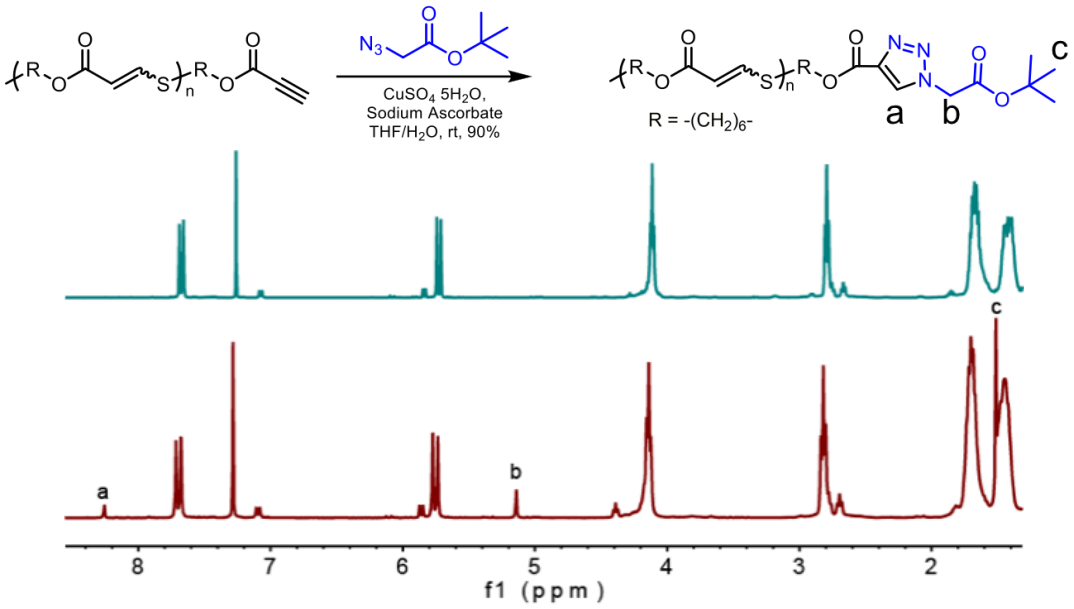

Figure 3.5 End group functionalization on precursor polymer **PC6**.

Since the polymerization was conducted by using a bi-functional monomer, the resulting polymer should have both thiol and alkyne functional groups at the end. To test the availability of alkyne end group, a precursor polymer **PC6** was prepared using monomer **5**. The end group functionalization of **PC6** was realized by reacting the polymer terminal alkyne with *tert*-butyl 2-

azidoacetate through Huisgen cycloaddition click reaction. The resonance around 8.0 ppm (peak a) in the ^{1}H NMR spectrum corresponds to the (=C*H*-) from the triazole ring indicates the successful incorporation of the triazole unit. Furthermore, resonances at 5.17 ppm and 1.49 ppm also confirm the addition of *tert*-butyl 2-azidoacetate to the polymer.

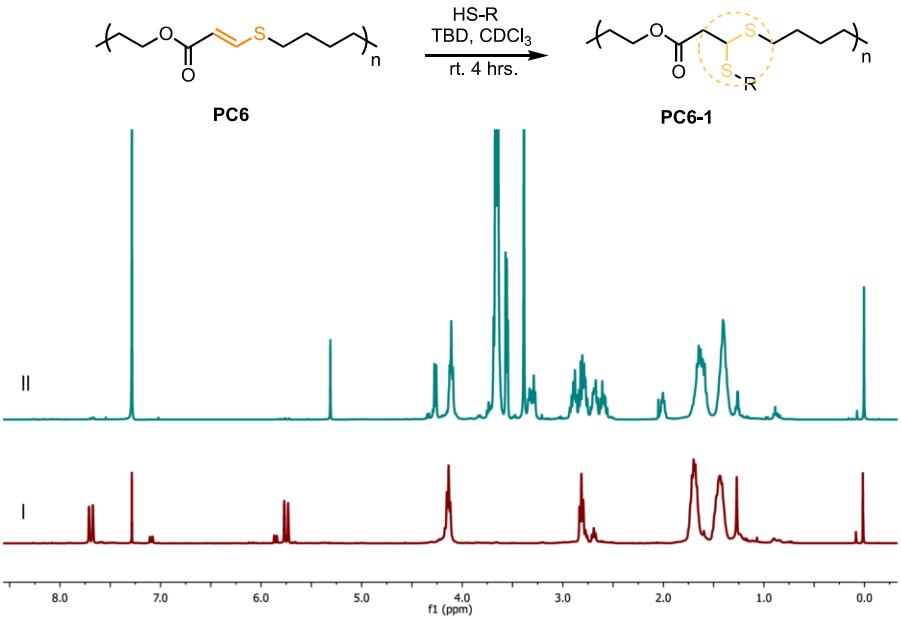

Figure 3.6 Scheme of backbone functionalization of polymer **PC6** with 1-thiol octyl.

The precursor polymer **PC6** with thiol vinyl group in its backbone could undergo post modification with a second thiol agent under more basic conditions[12]. The reaction was carried out under room temperature with TBD (0.1 equiv.) as the catalyst. The complete disappearance of akene proton signals at 5.88 and 7.71 ppm after modification in ^{1}H NMR spectrum (I) and the appearance of acetal proton signals at 4.26 and TEG proton signals at 3.65 ppm after modification in 1H NMR spectrum (II) indicated the success of addition (Figure 3.6). It is a Michael addition reaction and could form hetero dithiol acetal on the polymer backbone. It has been reported that polymers with dithiol ketal structure could be degraded when subjected to ROS[14,15]. We thereby assume that the dithiol acetal adduct obtained here will also possess the ROS responsiveness since

it shares similarity with dithiol ketal structure. This responsiveness could be used for potential cancer therapeutics delivery.

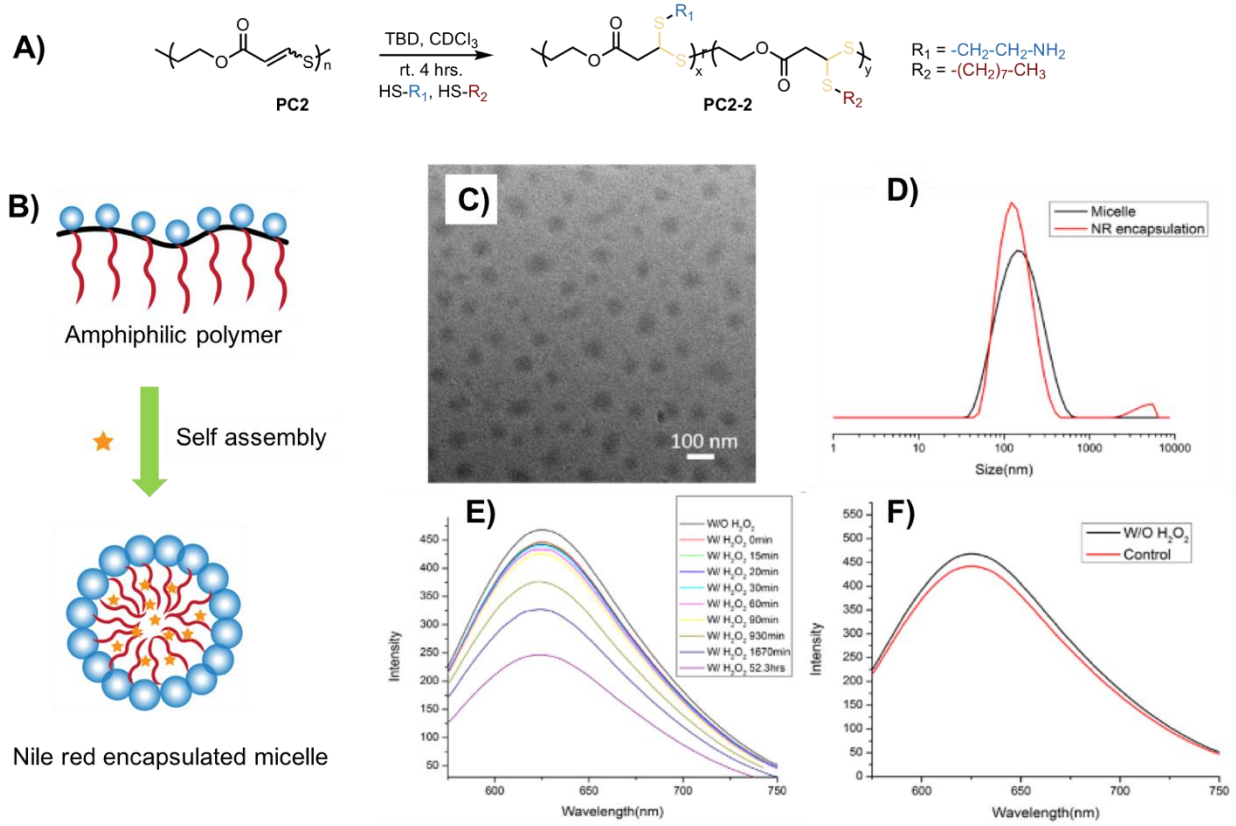

Figure 3.7 (A) Scheme of backbone functionalization of polymer **PC2** with 1-thiol octyl and cysteamine. (B) Schematic representative of self-assembly behavior of backbone functionalized amphiphilic polymer **PC2-2**; (C) TEM image and (D) DLS measurements of micelle aggregates in aqueous solution; (E) Nile Red release upon adding H_2O_2; (F) Control of NR without H_2O_2.

To test whether the dithiol acetal adduct obtained also possess ROS responsiveness, we prepared a random copolymer by adding 1-octane thiol (0.5 equiv.) and cysteamine (0.5 equiv.) in one pot onto the polymer backbone with TBD (0.1 equiv. respect to thiol vinyl unit). The hydrophilic amine group and hydrophobic octyl thiol group could endow amphiphilicity onto polymer **PC2**, which could help the resultant polymer **PC2-2** self-assemble into stable aggregates in aqueous solution. TEM image and DLS measurements suggested that the aggregates are spherical with a size around 100 nm (Figure 3.7C and 3.7D). The cargo encapsulation ability of

the polymeric micelle solution was tested with a hydrophobic dye molecule. Nile Red (NR) was chosen as a model guest in this study. It is reported that the fluorescence intensity of NR would stay if the molecules are in the non-polar microenvironment. However, fluorescence intensity would drop drastically when they are exposed into polar solvent[16]. This property could help us to test the ROS responsiveness of polymer micelle aggregates. The hypothesis is that, when the polymer backbone is degraded by ROS trigger, the micelle aggregates are no longer stable and therefore the capacity to hold the encapsulated molecule decreases. NR as the guest molecule will be released from the non-polar micelle interior to the aqueous polar environment. The degradation process could be monitored by looking at its fluorescence intensity change before and after applying the ROS trigger to the micelle solution. Indeed, the fluorescence spectrum in Figure 3.7E indeed showed a decrease of the fluoresces intensity after subjected to H_2O_2 compared to a negligible decrease in the control experiment (no H_2O_2 added, Figure 3.7F). Another control experiment also has been done, in which the NR was encapsulated in a non-ROS responsive polymeric micelle aggregates. Upon treatment with H_2O_2, a negligible amount of NR fluorescence intensity decrease was observed (Figure 3.15). All these results suggest that the decreasing of fluorescence intensity was attributed to the destabilized micelle stage and release of NR from interior to outside of micelle aggregates upon H_2O_2 stimuli.

Interestingly, when we were trying to monitor the Mw of the polymer from GPC after the post-modification reaction with a second thiol and TBD, instead of an increase, a decrease of polymer Mw was observed (from 34 000 g/mol to 7 000 g/mol). To understand that, we studied the second addition reaction with small molecule analogies (Figure 3.16-3.19) and analyze the product. Finally, we found out that there is thiol exchange happening during the 2nd thiol adding process, which is also mentioned in another researcher's work[17]. However, it is not considered as

an issue in our case since the exchange is thermodynamic control (Figure 3.20-3.21) and the percentage is significantly low.

3.3 Summary

In conclusion, we have developed a novel polymerization method with thiol and electron-deficient alkyne reactions. The polymerization method has been optimized, and all parameters have been investigated. The resulting polymer backbone is subject to further post modification to yield a hetero thiol acetal structure in the polymer, which is responsive and cleaved under ROS. This polymerization method is mild, fast and efficient. The unique property of post-modification and then cleavage can be used in potential applications, such as protein modification via thiol group and delivery into cell and release from polymer by ROS differences.

3.4 Materials and experiments

3.4.1 Materials

All the reagents were purchased from commercial sources and used as such without further purification. ^{1}H NMR spectra were recorded on a Bruker 400 MHz NMR spectrometer using the residual proton resonance of the solvent as the internal standard. Chemical shifts (δ) are reported in parts per million (ppm) and Hertz, respectively. The following abbreviations are used for the peak multiplicities: s, singlet; d, doublet; t, triplet; q, quartet; m, multiplet; dd, doublet of doublet; bs, broad singlet; bd, broad doublet; bm, broad multiplet. ^{13}C-NMR spectra were recorded on a 400MHz Bruker NMR spectrometer using carbon signal of the deuterated solvent as the internal standard. Dynamic Light Scattering (DLS) measurements were carried out on a Malvern Nanozetasizer. TEM images were recorded on a JEOL-2000FX machine operating at an accelerating voltage of 100 kV. Molecular weights of the polymers were estimated by gel permeation chromatography (GPC) using PMMA standard with a refractive index detector.

Fluorescence measurements were performed on a fluorescence plate reader (Molecular Devices, SpectraMax M5).

3.4.2 Synthesis of molecules

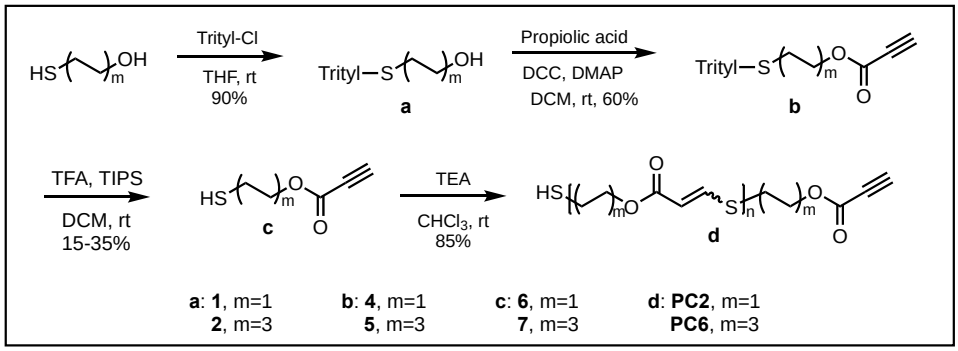

General procedure for the synthesis of molecule **1** & **4:**

Molecule **1** & **4** were prepared trough same procedure1. Typically, trityl chloride (2.78 g, 10 mmol) in DCM (50 mL) was added dropwise to a stirred solution of 6-mercapto-hexan-1-ol (2 mL, 15 mmol) in DCM (20 mL) over 30 min at room temperature. The mixture was stirred for 30 min and washed with an aqueous solution of NaOH (0.1 M). The organic layer was dried over anhydrous Na2SO4, gravity filtered, and concentrated in vacuo. Flash chromatography was used to purify the compound with a step gradient from 9:1 (v:v) to 3:1 (v:v) hexane:EtOAc.

Synthesis of molecule **2** & **5:**

Molecule **2** & **5** were prepared through the same procedure. Typically, compound **1** (7g, 21.8 mmol), DCC (4.5g, 21.8 mmol), and DMAP (0.26g, 2.18 mmol) were added into a 500 mL RB. The mixture was dissolved with DCM and stirred over Argon for 10min. Propiolic acid (3.25g, mmol) was added the above mixture drop wised at ice bath. The temperature was brought to room temperature after finishing adding propiolic acid. The whole system was allowed to react 6 hrs. under argon and followed by workup with brine. The organic layer was collected and recrystallized

in ether to get rid of DCC and its derivative byproduct. Flash chromatography with a step gradient EA in Hexane (0~10%) was used for purifying compound.

Synthesis of molecule **3 & 6:**

Molecule **3** & **6** were prepared through the same procedure. Typically, compound **2** (1.0 equiv.) was dissolved in 100mL RB with DCM followed by addition of TFA (10 equiv.) and TIPS (1.5 equiv.). The solution turned to yellow when adding TFA and turned back to colorless when finish adding TIPS. The reaction was carried out under room temperature for 1hr under argon. The crude product was purified by running combiflash (0~10% EA in Hexane).

Synthesis of polymer **PC2** & **PC6:**

Molecule **PC2** & **PC6** were prepared trough similar procedure. Typically, compound **6** (1.0 equiv.) was dissolved in 7 mL vial $CHCl_3$ followed by addition of TEA (0.1 equiv.). The reaction was carried out under room temperature for 3 h. For parameter screen studies, the monomer concentration, base, solvent, temperature, and time were changed accordingly. The crude polymer was purified by precipitation in hexane and dried in high vacuum.

Post modification of polymer **PC6-1** & **PC2-2:**

Polymer **PC6-1** and **PC2-2** were prepared trough similar procedures. Typically, compound **PC6** (1.0 equiv.) was dissolved in 7 mL vial $CHCl_3$ followed by addition of TBD (0.1 equiv.) and thiol agents (1.0 equiv.). The reaction was carried out under room temperature for 4 h. The crude polymer was purified by either precipitation in hexane and dried in high vacuum or dialysis against water to remove small molecules.

Compound **4:**

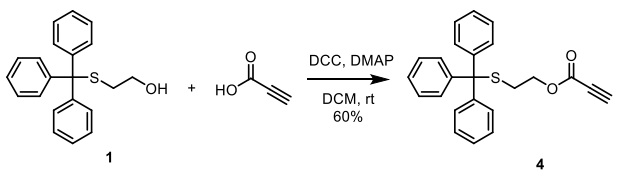

1 4

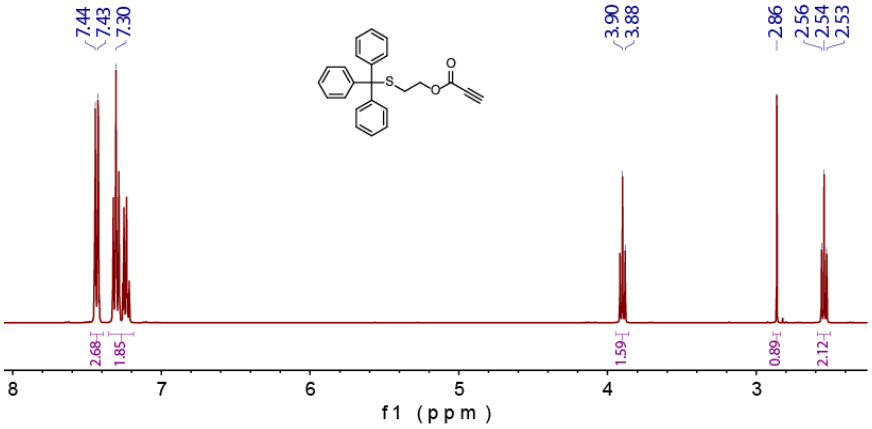

Figure 3.8 ^{1}H NMR spectrum of compound **4**. Solvent chloroform-*d*.

Compound **6:**

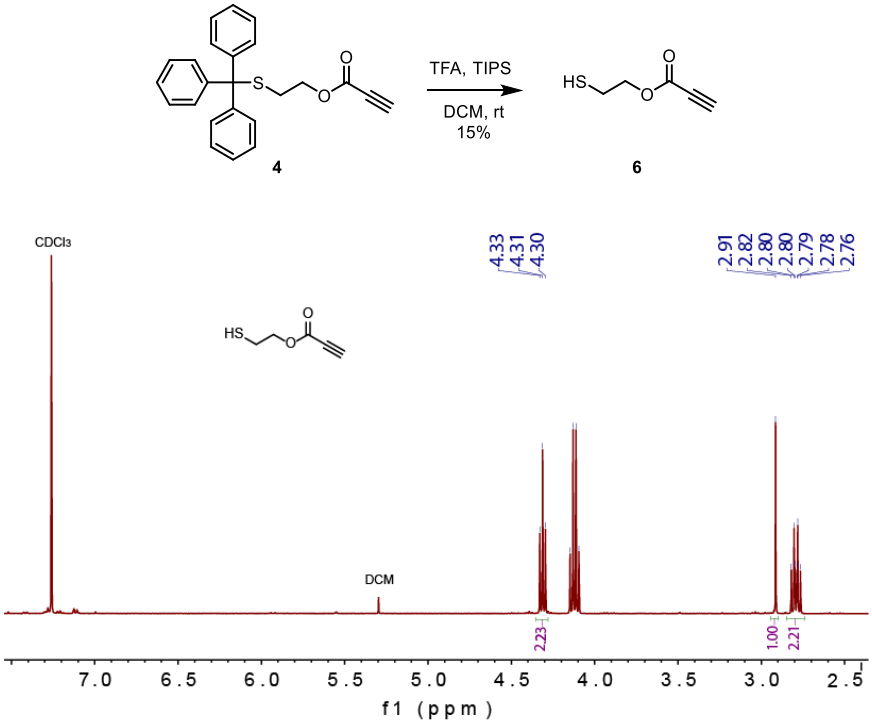

Figure 3.9 ^{1}H NMR spectrum of compound **6**. Solvent chloroform-*d*.

Compound **2:**

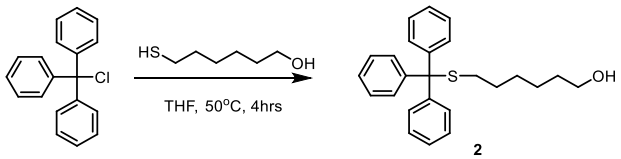

Compound **2** was obtained as a white solid with a yield of 3.2 g (85%). ^{1}H NMR: δ 7.45 – 7.15 (m, 15H), 3.58 (t, J = 6.6, 2H), 2.15 (t, J = 7.3, 2H), 1.48 (m, 2H), 1.40 (m, 2H), 1.26 (m, 5H); ESI-LRMS calculated. for $(C_{25}H_{28}OS \cdot H)^{+}$ 377.2, found 377.2.

Compound **5:**

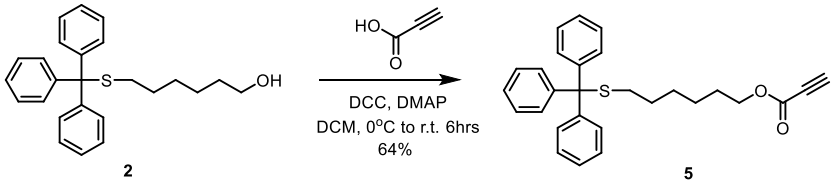

Compound **5** was obtained as a white solid with a yield of 64%. ^{1}H NMR (400 MHz, Chloroform-*d*) δ 7.54 – 7.46 (m, 6H), 7.34 (dd, *J* = 8.5, 7.1 Hz, 7H), 7.30 – 7.22 (m, 3H), 4.23 – 4.15 (m, 2H), 2.89 (d, *J* = 1.0 Hz, 1H), 2.23 (t, *J* = 7.2 Hz, 2H), 1.71 – 1.61 (m, 2H), 1.46 (m, 2H), 1.33 (m, 4H).

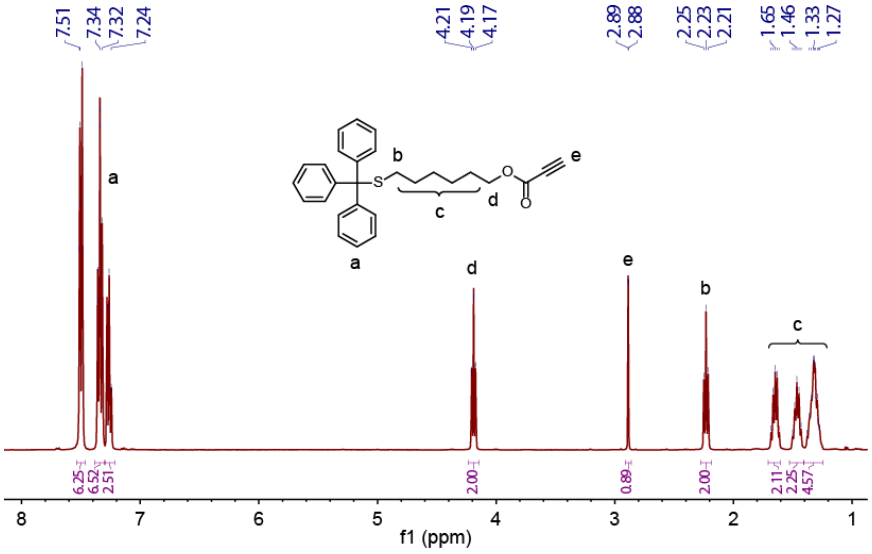

Figure 3.10 ^{1}H NMR spectrum of compound **5**. Solvent chloroform-*d*.

Compound **7:**

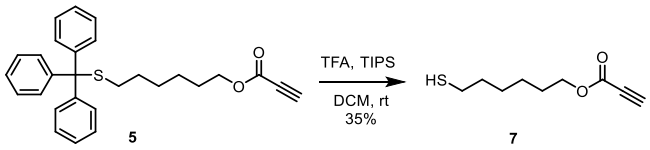

^{1}H NMR (400 MHz, Chloroform-d) δ 4.20 (t, J = 6.7, 1.1 Hz, 2H), 2.87 (s, 1H), 2.53 (q, J = 6.9 Hz, 2H), 1.66 (m, 4H), 1.50 – 1.21 (m, 2H), 1.05 (m, 2H), 0.92 – 0.81 (m, 1H).

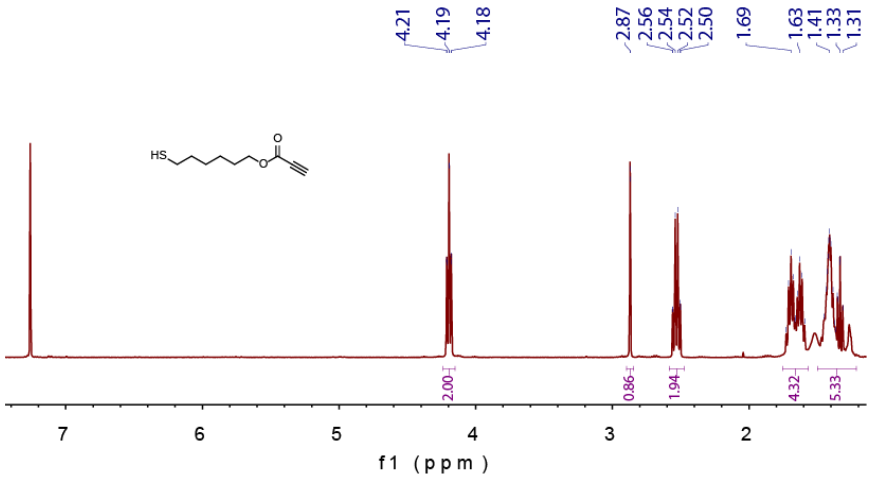

Figure 3.11 ^{1}H NMR spectrum of compound **7**. Solvent chloroform-*d*.

Polymer **PC2:**

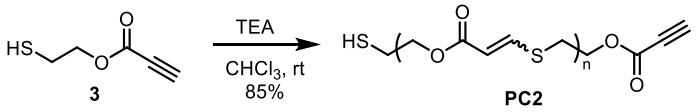

^{1}H NMR (400 MHz, Chloroform-*d*) δ 7.78 - 7.62 (m, 0.8H), 7.24 - 7.14 (m, 0.2H), 5.95 - 5.79 (m, 1H), 4.35 (m, 2H), 3.17 - 2.91 (m, 2H).

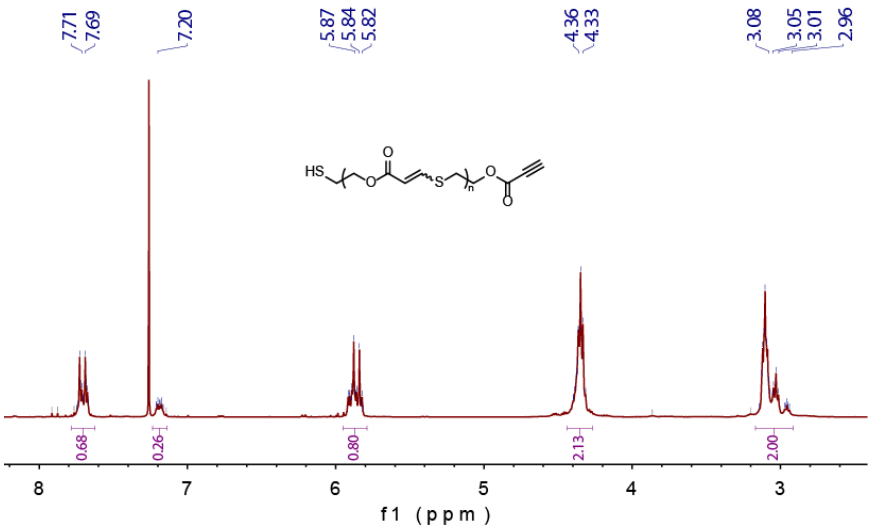

Figure 3.12 [1]H NMR spectrum of polymer **PC2**. Solvent chloroform-*d*.

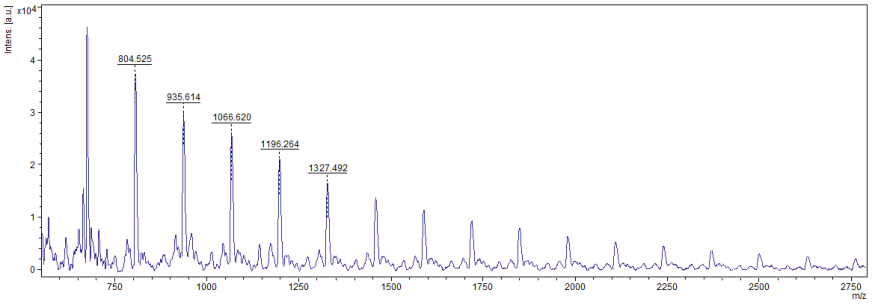

Figure 3.13 MALDI-TOF spectrum of polymer **PC2**.

Polymer **PC6:**

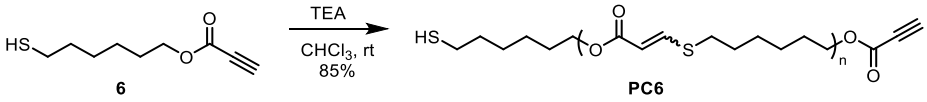

[1]H NMR (500 MHz, Chloroform-*d*) δ 7.67 (dd, *J* = 15.1, 1.9 Hz, 0.8H), 7.07 (d, *J* = 10.2 Hz, 0.1H), 5.84 (d, *J* = 10.1 Hz, 0.1H), 5.73 (d, *J* = 15.1 Hz, 0.8H), 4.11 (t, *J* = 6.7 Hz, 2H), 2.79 (t, *J* = 7.4 Hz, 2H), 2.67 (t, *J* = 7.4 Hz, 0H), 1.67 (m, *J* = 19.2, 11.7, 7.0 Hz, 4H), 1.42 (m, *J* = 23.6,

8.4 Hz, 5H). ^{13}C NMR (400 MHz, $CDCl_3$) δ 165.42, 146.90, 113.64, 64.11, 63.99, 31.88, 30.20, 29.71, 29.07, 28.60, 28.50, 28.46, 28.43, 28.15, 28.11, 25.54.

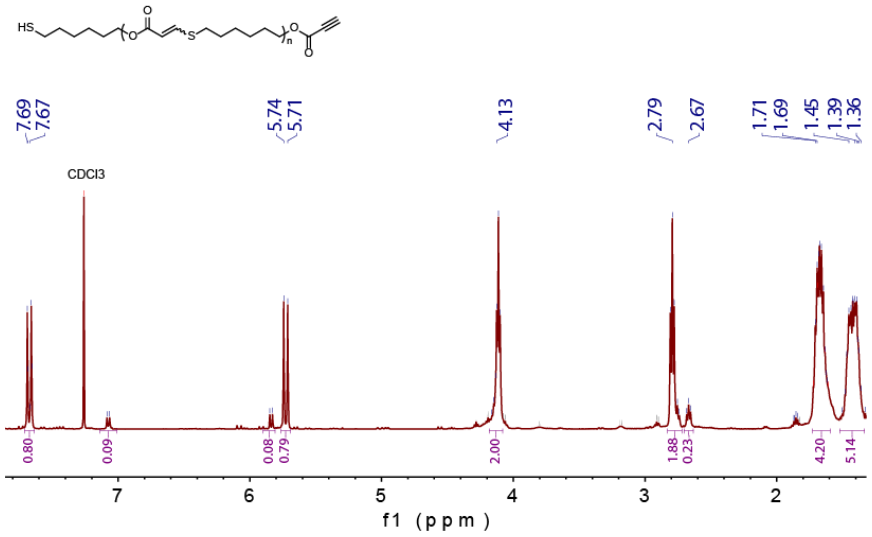

Figure 3.14 ^{1}H NMR spectrum of polymer **PC6**. Solvent chloroform-*d*.

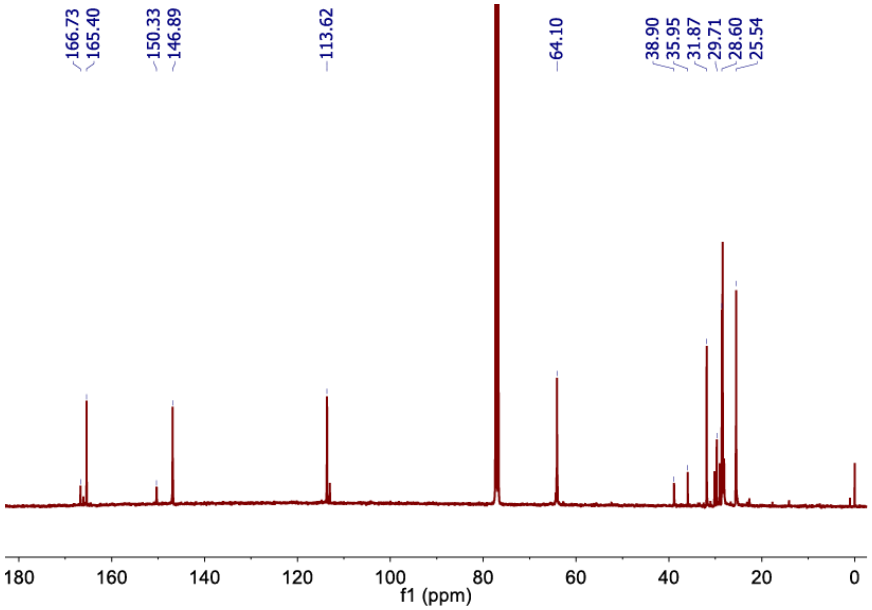

Figure 3.15.^{13}C NMR spectrum of polymer **PC6**. Solvent chloroform-*d*.

Synthesis of Polymer **PC6-1:**

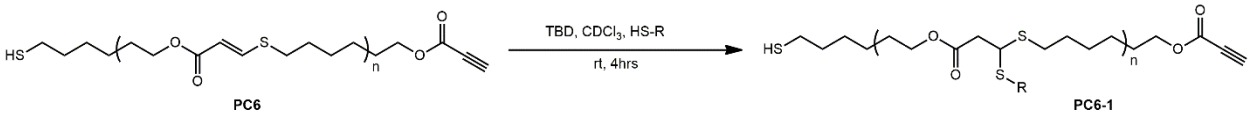

R is TEG thiol in this case. ^{1}H NMR (400 MHz, $CDCl_3$) δ 4.28, 4.26, 4.11, 3.67, 3.65, 3.64, 3.57, 3.56, 3.39, 3.33, 3.29, 2.88, 2.82, 2.67, 2.61, 2.00, 1.65, 1.41, 1.26, 0.89. ^{13}C NMR (400 MHz, $CDCl_3$) δ 170.06, 151.51, 71.94, 70.62, 64.90, 59.04, 47.50, 46.87, 37.69, 30.26, 28.47, 25.53, 20.80.

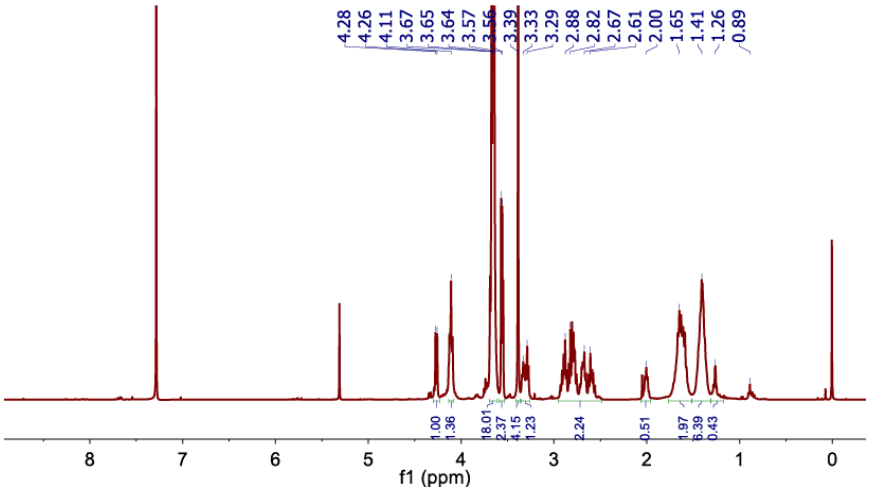

Figure 3.16 ^{1}H NMR spectrum of polymer **PC6-1**. Solvent chloroform-*d*.

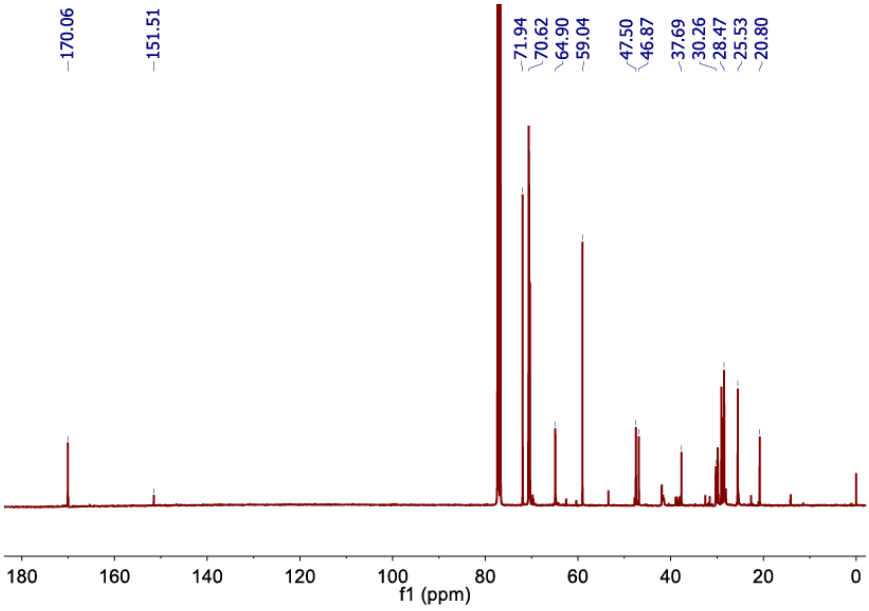

Figure 3.17 ^{13}C NMR spectrum of polymer **PC6-1**. Solvent chloroform-*d*.

3.4.3. Other experimental protocols

3.4.3.1 Micelle preparation:

Amphiphilic polymer was dissolved in minimum amount of acetone. Distilled water was added to the above solution(10X). The acetone was then dialysis out against DI water for two days. The exact concentration of micelle solution was determined by lipolyzing certain amount of solution and measure the weight of solid residue.

3.4.3.2 Dynamic Light Scattering (DLS) Study:

DLS was performed on a Malvern Nano-zeta sizer instrument with a 637 nm laser source with non-invasive backscattering technology detected at 173^0. All sizes are reported as the hydrodynamic diameter (D_H) and were repeated in triplicate. For the DLS measurements, the concentration of the polymer solution was 0.5 mg/mL. The solution was filtered using a hydrophilic membrane (pore size 0.450 μm) before experiment was performed.

3.4.3.3 Transmission Electron Microscope (TEM) Study:

For the TEM measurements the nanogel solution was prepared in 0.5 mg/mL concentration. One drop of the sample (10 μL) was drop casted on carbon coated Cu grid, 400 mesh size and left to dry overnight.

3.4.3.4 NR releasing with control polymer:

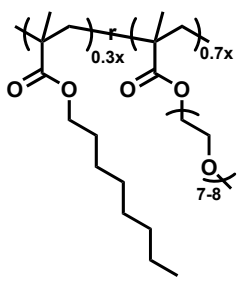

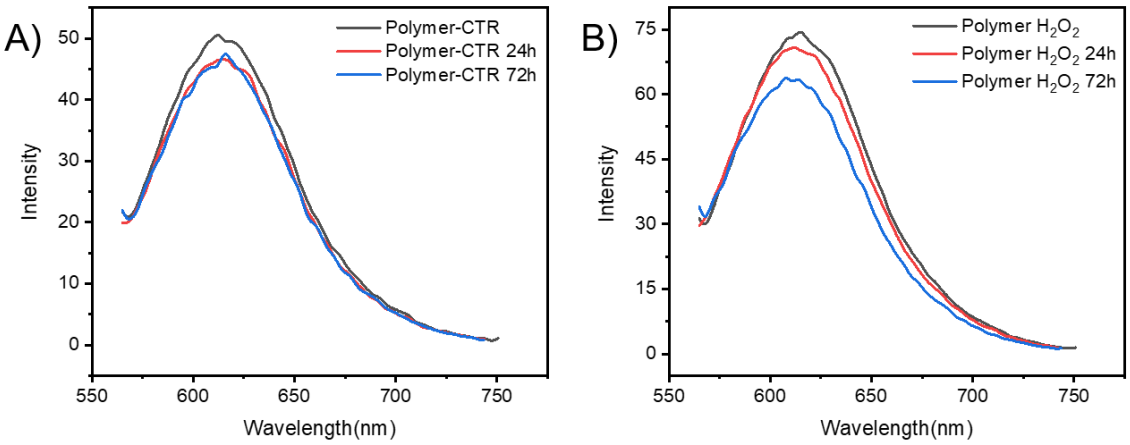

Figure 3.18. The fluorescence intensity of Nile Red in control non-ROS responsive polymeric micelle over time. (A) without H_2O_2. (B) with H_2O_2.

3.4.3.5 Thiol Exchange thermodynamic:

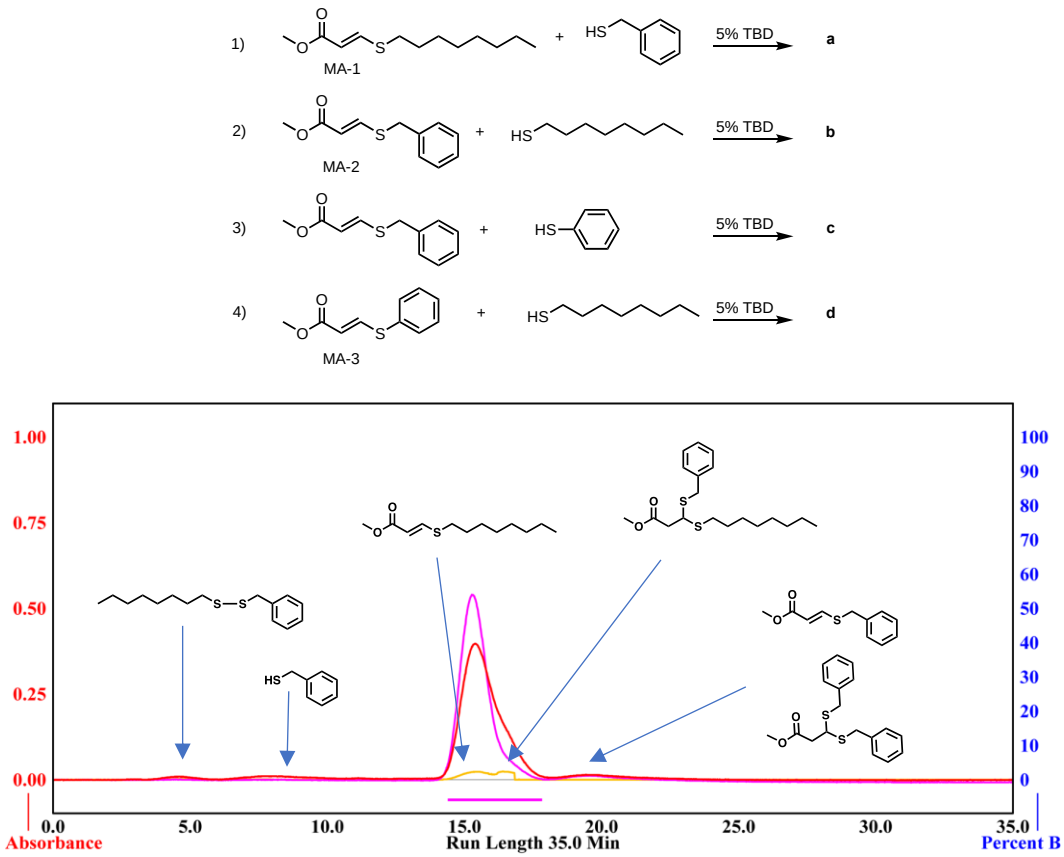

Figure 3.19. An example of CombiFlash profile of crude product **a** from reaction 1.

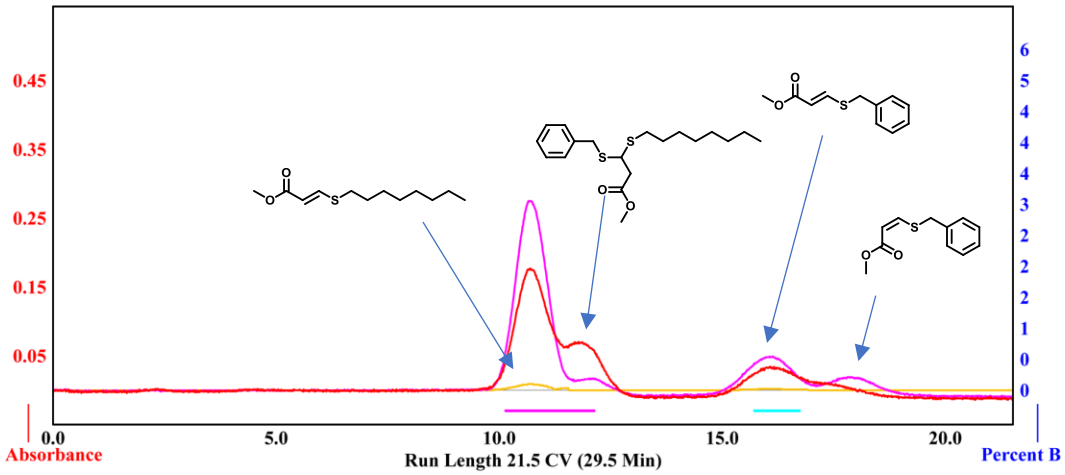

Figure 3.20. An example of CombiFlash profile of crude product **b** from reaction 2.

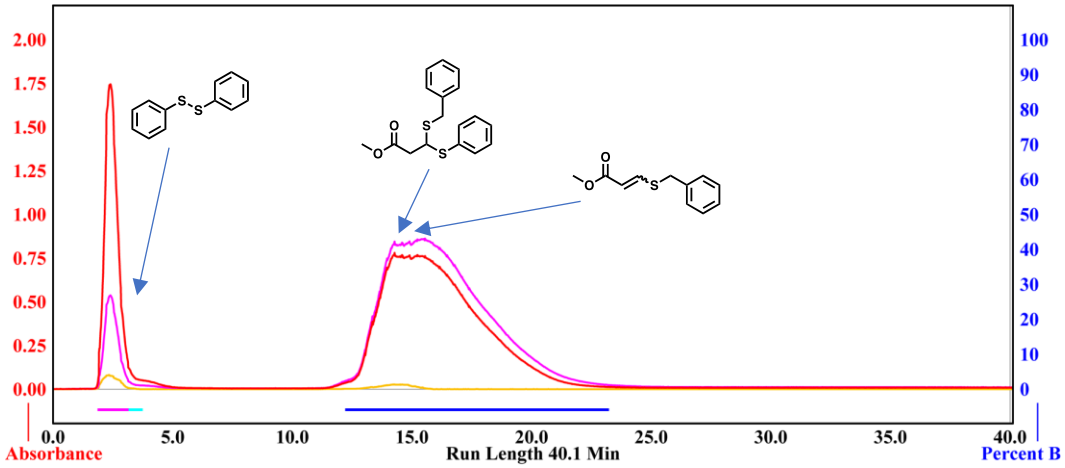

Figure 3.21. An example of CombiFlash profile of crude product **c** from reaction 3.

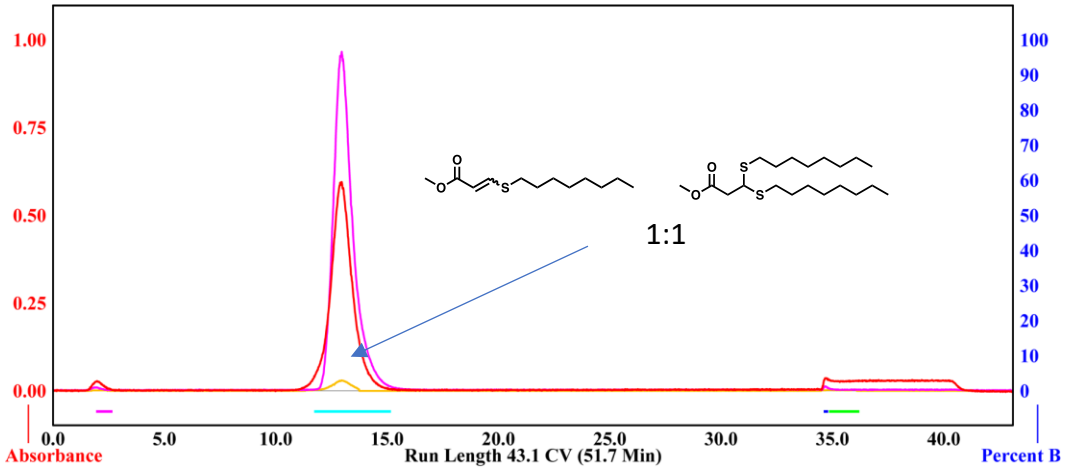

Figure 3.22. An example of CombiFlash profile of crude product **d** from reaction 4.

Thiol exchange study with small molecules was done. Three Michael Acceptors (MA) were prepared through addition reaction of the propiolic acid with thiol reagents (1-octanethiol for MA-1, benzyl mercaptan for MA-2, thiophenol for MA-3) with TEA as a base. Figure 3.15 showed an example of how the crude product looks like from reaction 2 after separation via CombiFlash. The reaction condition for all four reactions is the same (5% TBD, r.t., 12h in $CDCl_3$).

3.4.3.6 Thiol Exchange kinetic:

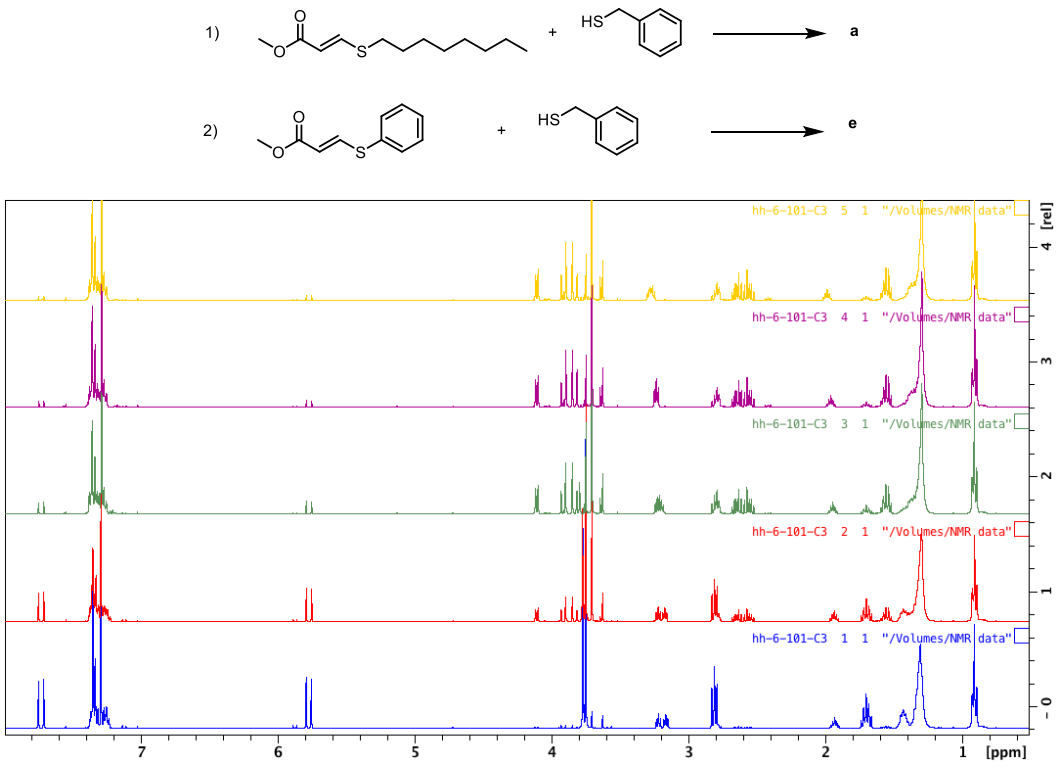

Figure 3.23. Summary of NMR spectra monitoring reaction 1. (blue: 4min; red: 50 min; green: 3h; purple: 5h; yellow: 8h.)

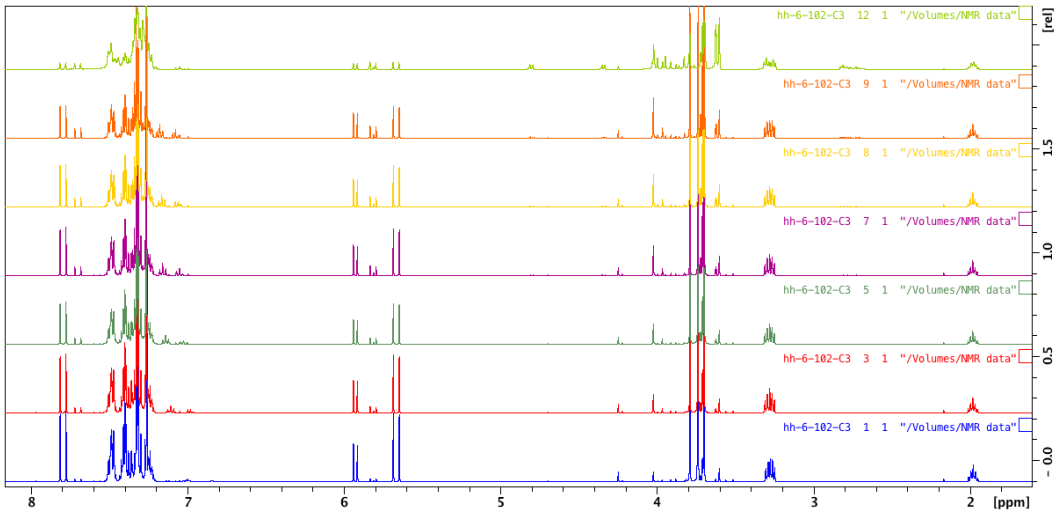

Figure 3.24. Summary of NMR spectra monitoring reaction 2. (blue: 4min; red: 50 min; green: 3h; purple: 5h; yellow: 8h; orange: 14h; light green: 24)

3.5 References

(1) Wang, J.-S.; Matyjaszewski, K. Controlled/"living" Radical Polymerization. Atom Transfer Radical Polymerization in the Presence of Transition-Metal Complexes. *J. Am. Chem. Soc.* **1995**, *117*, 5614–5615.

(2) Chiefari, J., Chong, Y.K., Ercole, F., Krstina, J., Jeffery, J., Mayadunne, L. T. A. Living Free-Radical Polymerization by Reversible Addition-Fragmentation Chain Transfer: The RAFT Process. *Macromolecules* **1998**, *31* (16), 5559–5562.

(3) Julien Nicolas; Yohann Guillaneuf; Catherine Lefay; Denis Bertin; Didier Gigmes; Charleux, and B. Nitroxide-Mediated Polymerisation. *Prog. Polym. Sci.* **2013**, *38* (1), 63–235 DOI: 10.1016/j.progpolymsci.2012.06.002.

(4) Nikos Hadjichristidis, *; Marinos Pitsikalis; Stergios Pispas, and; Iatrou, H. Polymers with Complex Architecture by Living Anionic Polymerization. **2001** DOI: 10.1021/CR9901337.

(5) Matyjaszewski, K. *Cationic Polymerizations: Mechanisms, Synthesis & Applications*; Plastics Engineering; Taylor & Francis, **1996**.

(6) Yokozawa, T.; Ohta, Y. Transformation of Step-Growth Polymerization into Living Chain-Growth Polymerization. *Chem. Rev.* **2016**, *116* (4), 1950–1968 DOI: 10.1021/acs.chemrev.5b00393.

(7) Schildknecht, C. E. Stereoregulation and Stereoregular Polymers. *Polym. Eng. Sci.* **1966**, *6* (3), 240–243 DOI: 10.1002/pen.760060311.

(8) Feldman, D.; Barbalata, A. *Synthetic Polymers : Technology, Properties, Applications*; Chapman & Hall, 1996.

(9) Ulrich, H. Introduction to Industrial Polymers. *Hanser Publ. 1993*, **1993**, 188.

(10) Hoyle, C. E.; Bowman, C. N. Thiol-Ene Click Chemistry. *Angew. Chemie Int. Ed.* **2010**, *49* (9), 1540–1573 DOI: 10.1002/anie.200903924.

(11) Jim, C. K. W.; Qin, A.; Lam, J. W. Y.; Mahtab, F.; Yu, Y.; Tang, B. Z. Metal-Free Alkyne Polyhydrothiolation: Synthesis of Functional Poly(Vinylenesulfide)s with High Stereoregularity by Regioselective Thioclick Polymerization. *Adv. Funct. Mater.* **2010**, *20* (8), 1319–1328 DOI: 10.1002/adfm.200901943.

(12) Truong, V. X.; Dove, A. P. Organocatalytic, Regioselective Nucleophilic "Click" Addition of Thiols to Propiolic Acid Esters for Polymer-Polymer Coupling. *Angew. Chemie - Int. Ed.* **2013**, *52* (15), 4132–4136 DOI: 10.1002/anie.201209239.

(13) Truce, W. E.; Tichenor, G. J. W. Effect of Activating Group on Trans Stereoselectivity of Thiolate Additions to Activated Acetylenes. *J. Org. Chem.* **1972**, *37* (15), 2391–2396 DOI: 10.1021/jo00980a007.

(14) Wilson, D. S.; Dalmasso, G.; Wang, L.; Sitaraman, S. V; Merlin, D.; Murthy, N. Orally Delivered Thioketal Nanoparticles Loaded with TNF-α-siRNA Target Inflammation and Inhibit Gene Expression in the Intestines. *Nat. Mater.* **2010**, *9* (11), 923–928 DOI: 10.1038/nmat2859.

(15) Shim, M. S.; Xia, Y. A Reactive Oxygen Species (ROS)-Responsive Polymer for Safe, Efficient, and Targeted Gene Delivery in Cancer Cells. *Angew. Chemie - Int. Ed.* **2013**, *52* (27), 6926–6929 DOI: 10.1002/anie.201209633.

(16) Greenspan, P.; Fowler, S. D. Spectrofluorometric Studies of the Lipid Probe, Nile Red. *J. Lipid Res.* **1985**, *26* (7), 781–789.

(17) Joshi, G.; Anslyn, E. V. Dynamic Thiol Exchange with β-Sulfido-α,β-Unsaturated Carbonyl Compounds and Dithianes. *Org. Lett.* **2012**, *14* (18), 4714–4717 DOI: 10.1021/ol301781u.

CHAPTER

4. DEVELOPING A CLICKABLE PLATFORM FOR ANALYTES SEPARATION AND ENRICHMENT WITH POLYMERIC REVERSE MICELLE ASSEMBLIES

4.1 Introduction

As we have introduced in Chapter 1, detection of biomarkers in a biological system is imperative due to their significant bio-relevancy with malfunction tissue or cells[1-3]. The trace amount of biomarker presenting, and the complexity of the surrounding mixture makes it difficult to detect the biomarkers successfully. The current detection method for biomarker detection is enzyme-linked immunosorbent assay (ELISA), which has high sensitivity and specificity[4,5]. However, development of ELISA is costly, and false positive data may generate since it can only detect one biomarker at one time.

Our group has developed a technique in which an amphiphilic homopolymer reverse micelle combine with MALDI-MS was utilized for selective and sensitive detection of biomarkers in complex mixture[6–10]. More importantly, by doing these liquid-liquid extractions followed by MALDI-MS, we have observed a signal enhancement compared to the one without reverse micelle extraction. The molecular basis mechanism will be discussed in detail in the next chapter[11]. Because of its signal enhancement feature of this technique, much lower peptide concentration can be detected. In an ideal case, we could push the biomarker detection limit to pM range.

However, within this method, the polymeric reverse micelle was made of a polymer styrene base amphiphilic homopolymer, which possesses both hydrophilic groups and hydrophobic groups on both 3, 5-position of the styrene ring. To prepare a polymer with a different functional group, one has to change the synthetic procedure from the beginning. We thought whether we could design an easy way to prepare functional polymers in one step instead of going from the very first starting material to the tedious synthesis for amphiphilic homopolymers.

Click chemistry is widely used in material synthesis. It has the advantage of fast reaction rate, efficient yield, environmentally friendly[12]. We sought to borrow this concept and develop a clickable platform handle so that a variety of functionalities could be installed onto the polymer at the very last step. By doing so, one could dramatically simplify the synthesis of amphiphilic homopolymers. Moreover, the parent (precursor) clickable polymers share similar polymer molecular weight and poly distribution. Thus reasonable comparison could be made between the polymer modified final polymers.

In this chapter, we will introduce a method in which a clickable handle was installed on one side of polystyrene ring and use it for post modifications with different functionalities of interest. We will also test the assembly behaviors using those amphiphilic homopolymers. Finally, these polymers are used to test their selective extraction ability toward analytes mixtures, including small molecules and protein.

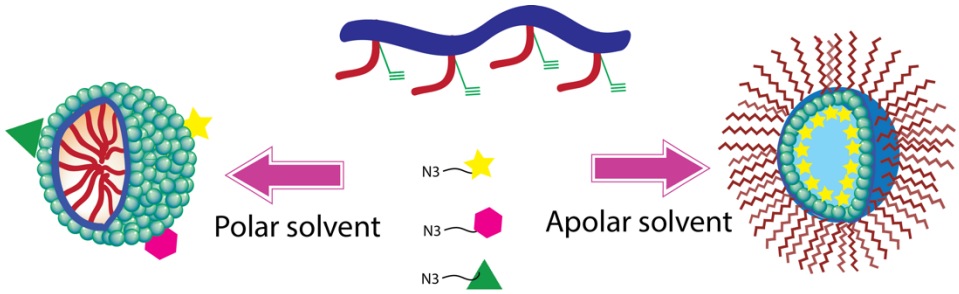

Scheme 4.1 Schematic illustrating analytes detection using amphiphilic polymeric reverse micelles.

4.2 Molecular design

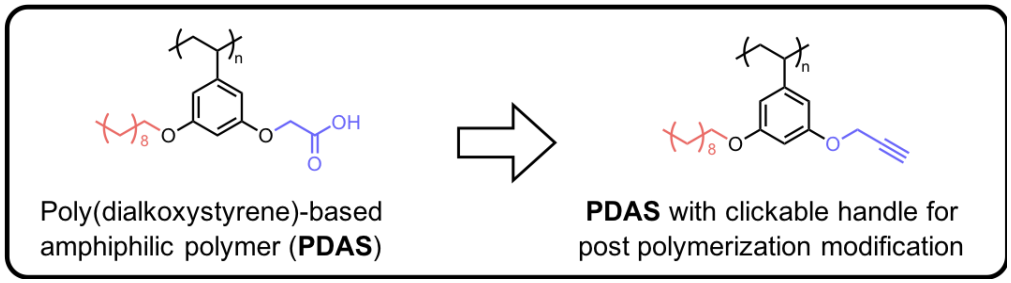

Scheme 4.2 Chemical structure of homopolymer with a clickable triple bond as a handle.

The molecular design for the clickable polymer platform is shown in the Scheme 4.2. Hydrophilic moiety in the polymer contributes to the analytes selectivity and sensitivity. Installing a clickable triple bond on the polymer allows us to vary the hydrophilic groups easily through click reactions. To do that, we have introduced a triple bond instead of any charged functional groups kept the hydrophobic decyl group constant. Protection of the triple bond is highly needed before the polymerization since it may react with a triple bond also. The propargyl group will be liberated after polymerization by cleaving the TMS functionality using a fluoride source to achieve polymer **8**. This polymer will then be treated with appropriate reagents to install the targeted hydrophilic features.

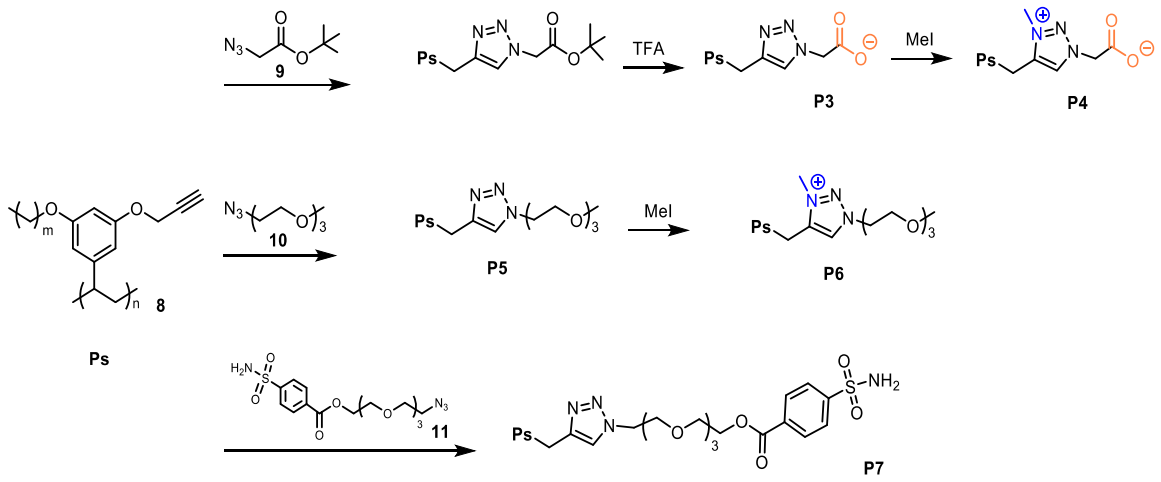

Scheme 4.3 Post-polymerization modifications with Cu-catalyst click reactions to prepare amphiphilic homopolymers. **P3**: negative charge; **P4**: zwitterionic; **P5**: PEG neutral; P6: positive charge; **P7:** carbonic anhydrase ligand

Post modifications were performed on polymer **8**. A negative charged polymer **P3**, charge neutral polymer **P5** and carbonic anhydrase ligand polymer **P7** were synthesized by a Cu-catalyst Huisgen 1,3-dipolar cycloaddition reaction of polymer **8** with corresponding azido reagents. E.g., polymer **P5** was synthesized with molecule **9**, followed by deprotection of *tert*-butyl group using trifluoroacetic acid. For positive charged polymer **P4** and zwitterionic polymer **P6**, they were prepared by methylation of **P5** and **P3**, respectively.

4.3 Results and discussions

Polymer	Size of reverse micelle	Size of micelle	ξ(mV)
P3-COOH(-)	140nm	105nm	-48.2±1.96
P4-COOH(+)	120nm	330nm	-16±1.93
P5-PEG	190nm	900nm	-0.04±1.02
P6-PEG(+)	500nm	120nm	45.9±0.51
P7-ligand	700nm	140nm	-20±1.65

Table 4.1. Summary of DLS measurements and zeta potential of the micelle and reverse micelle solutions made from five amphiphilic homopolymers.

After all, five polymers were successfully prepared, we next started to study them self-assemble behavior. Because of their amphiphilicity, all five polymers were expected to form micelle-like aggregates in water and reverse-micelle-like aggregates in toluene. Also, different charge moiety should be available for selective extraction. To test the charge availability, the zeta potential of micelle-like aggregates was measured. Indeed, we have observed that, with COOH as hydrophilic moiety, Polymer **P3** could form micellar aggregates with a size of about 105 nm with negatively charged zeta potential (-48.28 mV), while the size of the reverse micelle state in toluene was found to be ~190 nm. Reverse micelles of such polymers can be used to selectively enrich peptides according to charge from an aqueous phase into an organic phase. This property could provide us access to extract positive analytes (e.g., a peptide with pI higher than solution pH). Similarly, with methylated polymer **P6**, we do observe a more positive number (+45.9 mV), which indicated that the overall micelle is surrounded by positive charges and they could be used for extracting analytes with negative charges (e.g., peptides with pI lower than solution pH). The PEG polymer **P5** carries no charge which gives a number close to 0 mV zeta potential.

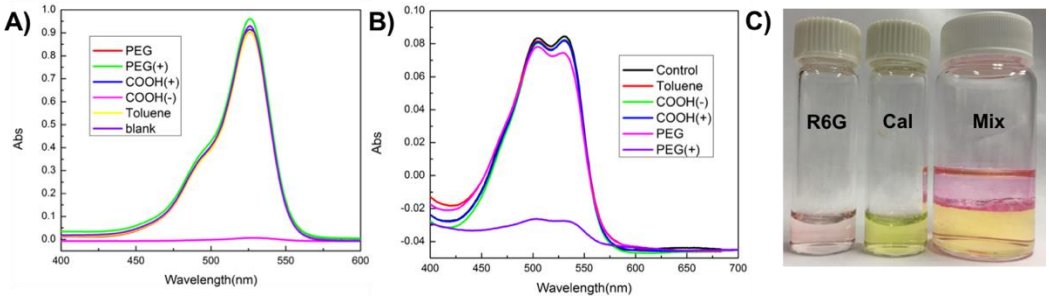

Figure 4.1. UV-Vis spectra of (A) Rhodamine 6G (R6G) and (B) Calcein in aqueous solution after extraction. (C) photo images of two dye molecules individual R6G (left), Calcein (mid) in aqueous solution and mixture (right) after liquid-liquid extraction.

To test whether these reverse micelles could be able to sequester molecules, we first investigated the extraction ability of all five polymers toward water soluble charged dye molecules as model analytes. A positive charge dye molecule, rhodamine 6G (R6G) and a negative charge dye molecule, Calcein, were chosen as the candidates for their distinct absorption spectrum. A 200 μL of reverse micelle toluene solution with a 2.3M concentration of **P3**-**P6** was added into 1 mL of dye aqueous solution. A liquid-liquid extraction process was performed followed by separation of two phases. The amount of dye molecules left in the aqueous after extraction was measured by UV-vis. The selectivity of the polymeric reverse micelle was evidenced by extraction of same dye molecule with different polymers. As shown in figure 4.1A, R6G was completed depleted with the negative charged polymer **P3**. In contrast, negligible amount of R6G is extracted by the other four polymers (**P4**-**P6**). Similarly, as for the case of Calcein, only a positive charged polymer P6 can selectively remove a large amount of negatively charged analyte from its original aqueous solution, while other four polymers (**P3**-**P5**) didn't show any extraction capability. A photo image of the extraction experiment evidence that, using reverse micelle prepared from **P3**, R6G with red color was extracted into the apolar phase while leaving behind the green colored Calcein in polar solution.

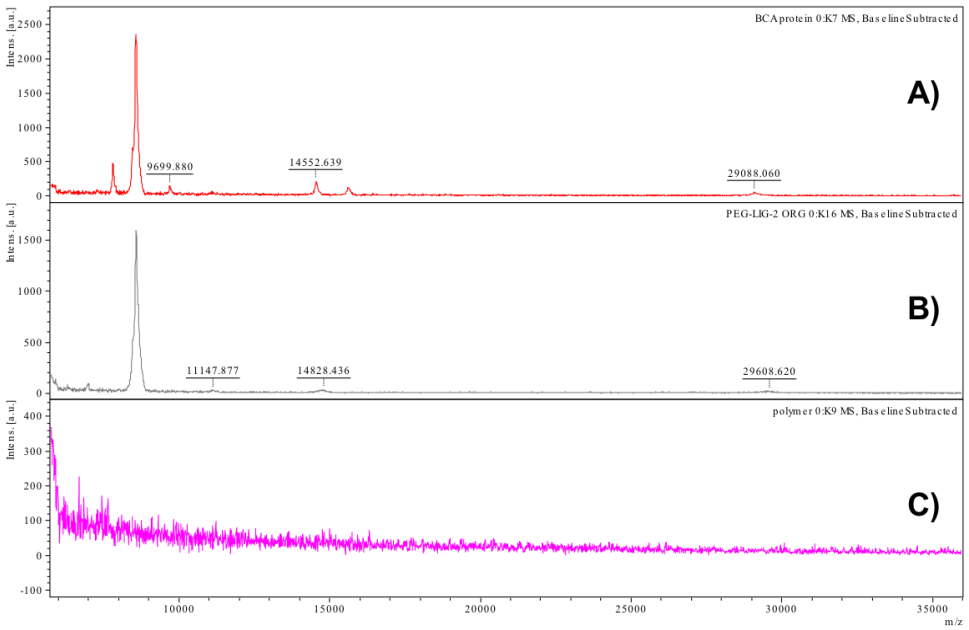

Figure 4.2. Mass spectra of (A) Bovine carbonic anhydrase in PBS buffer; (B) Bovine carbonic anhydrase in organic phase after extraction using **P7**. (C) polymer **P7** after extraction in the aqueous phase.

After testing the selectivity with dye molecules, we evaluated the potential protein enrichment selectivity of polymer **P7**. The protein bovine carbonic anhydrase was chosen as a candidate protein for their high binding affinity toward benzyl sulfonamide ligand. The protein was dissolved in PBS buffer at pH 7.4. A toluene solution containing the reverse micelles of **P7** was used as the organic phase. As shown in Figure 4.2 (gray line), after the liquid-liquid extraction process, bovine carbonic anhydrase was extracted into the organic phase and detected by MALDI-MS. The MALDI-MS of bovine carbonic anhydrase in aqueous and polymer control spectra were shown in Figure 4.2 red and purple line. This experiment suggests that polymer **P7** could be potentially useful in protein separation and detection through ligand binding interaction.

4.4 Summary

In this chapter, a clickable platform was developed for easily preparing amphiphilic polymeric reverse micelle with variant functionalities through click chemistry. The capacity of amphiphilic polymeric reverse micelle made from click reactions has been tested using small

molecule model as well as protein analyte. It is promising that by combining with MALDI-MS method, polymeric reverse micelle could be utilized for biomarker detection with high sensitivity and selectivity.

4.5 Experimental details

4.5.1 Materials and methods

Unless mentioned, all chemicals were used as received from Sigma-Aldrich. ^{1}H-NMR spectra were recorded on a 400 MHz Bruker NMR spectrometer. The molecular weight of the polymers was measured by gel permeation chromatography (GPC, Waters) using a PMMA standard with a refractive index detector. THF was used as eluent with a flow rate of 1 mL/min. Dynamic light scattering (DLS) measurements were performed using a Malvern Nano zetasizer. UV-visible absorption spectra were recorded on a Varian (model EL 01125047) spectrophotometer.

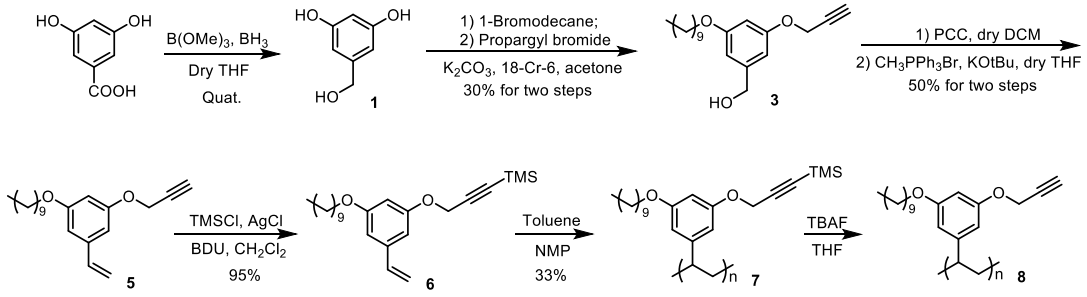

Synthesis of molecule **5**

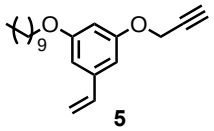

Commercially available CH_3PPh_3Br (3.78g, 10.57 mmol) was taken in dry THF (50 mL), and K-O^{t}Bu (1.18 g, 10.57 mmol) was added to this under argon atmosphere in an ice bath. This reaction mixture was stirred for 30 min with yellow color generated. A solution of compound 4

(2.38 g, 7.55 mmol) in 50 mL of dry THF was added slowly using dropping funnel. The reaction mixture was further stirred at room for 4 hours. The process of the reaction was monitored by TLC. The reaction mixture was filtered, and the filtrate evaporated and purified by silica gel column chromatography (2-3% ethyl acetate in hexane) to afford 1.9 g of compound **5**. ^{1}H NMR (400 MHz, Chloroform-*d*) δ 6.70 – 6.57 (m, 3H), 6.45 (t, *J* = 2.3 Hz, 1H), 5.72 (d, *J* = 17.5 Hz, 1H), 5.25 (d, *J* = 10.8 Hz, 1H), 4.68 (d, *J* = 2.4 Hz, 2H), 3.94 (t, *J* = 6.6 Hz, 2H), 2.53 (t, *J* = 2.4 Hz, 1H), 1.83 – 1.71 (m, 2H), 1.44 (p, *J* = 6.8 Hz, 2H), 1.29 (d, *J* = 16.6 Hz, 13H), 0.88 (t, *J* = 6.6 Hz, 3H).

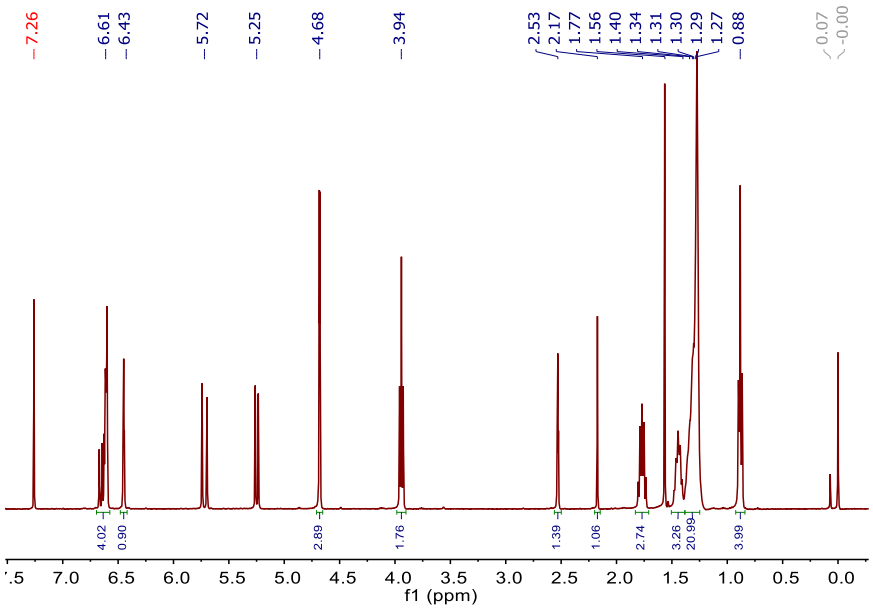

Figure 4.3 ^{1}H NMR spectrum of molecule **5**. Solvent: chloroform-*d*.

Synthesis of molecule **6**

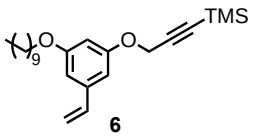

6

To a solution of compound **5** (1.2 g, 3.8 mmol), AgCl (60 mg, 0.42) and DBU (684 μL, 4.5 mmol) in 5 mL of DCM was added commercially available TMSiCl (630 μL, 4.96 mmol). The reaction mixture was further stirred reflux for 12 hours. The process of the reaction was monitored by TLC. The reaction mixture was filtered, and the filtrate evaporated and purified by silica gel column chromatography (1% ethyl acetate in hexane) to afford 1.4 g of compound **6**. yield:95%; ^{1}H NMR (400 MHz, Chloroform-*d*) δ 6.71 – 6.40 (m, 4H), 5.71 (dd, *J* = 17.5, 0.9 Hz, 1H), 5.24 (dd, *J* = 10.8, 0.9 Hz, 1H), 4.74 (d, *J* = 10.0 Hz, 0H), 4.66 (s, 2H), 3.94 (t, *J* = 6.6 Hz, 2H), 1.77 (dq, *J* = 7.9, 6.6 Hz, 2H), 1.51 – 1.19 (m, 15H), 0.97 – 0.85 (m, 3H), 0.17 (d, *J* = 3.7 Hz, 9H).

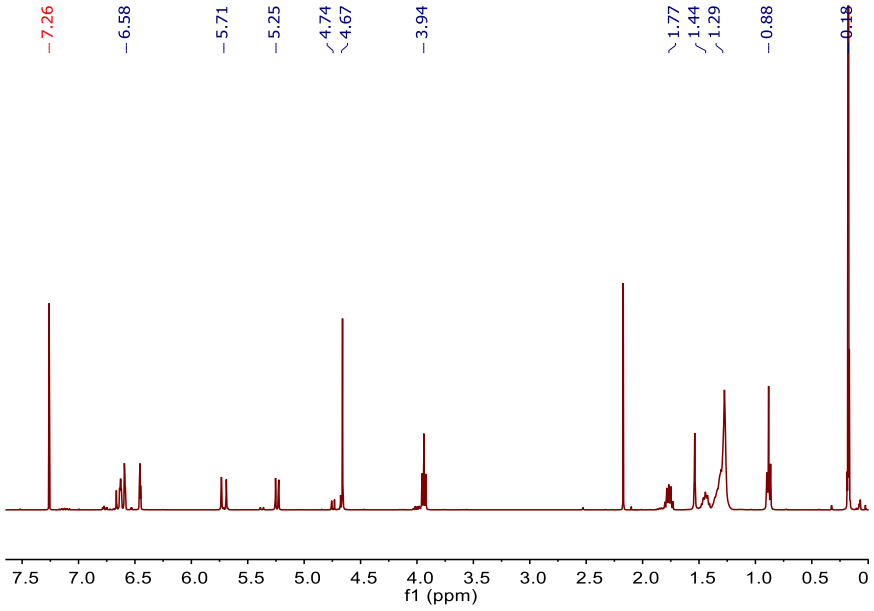

Figure 4.4 ^{1}H NMR spectrum of molecule **6**. Solvent: chloroform-*d*.

Synthesis of polymer **7**

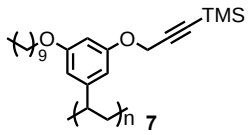

To the solution of compound **6** (700 mg, 1.8mmol) in Toluene (1 mL) was added N-tert-Butyl-N-(2-methyl-1-phenylpropyl)-O-(1-phenylethyl)hydroxylamine (NMP) (6.4mg, 0.2 mmol)

and the resulting mixture was degassed by three freeze/pump/thaw cycles, sealed under argon and heated at 100 °C for 24 h. The reaction mixture is cooled and precipitated three time in methanol to get 420 mg of pure polymer **P7**. GPC (Polystyrene/THF): M_n=14.4K, M_w=17.2K, PDI=1.19; ^{1}H NMR (400 MHz, Chloroform-*d*) δ 6.12-5.68 (m, 3H), 4.36 (m, 2H), 3.63 (m, 2H), 1.66 (m, 2H), 1.29 (m, 15H), 0.88 (d, 3H), 0.21-0.13 (m, 9H).

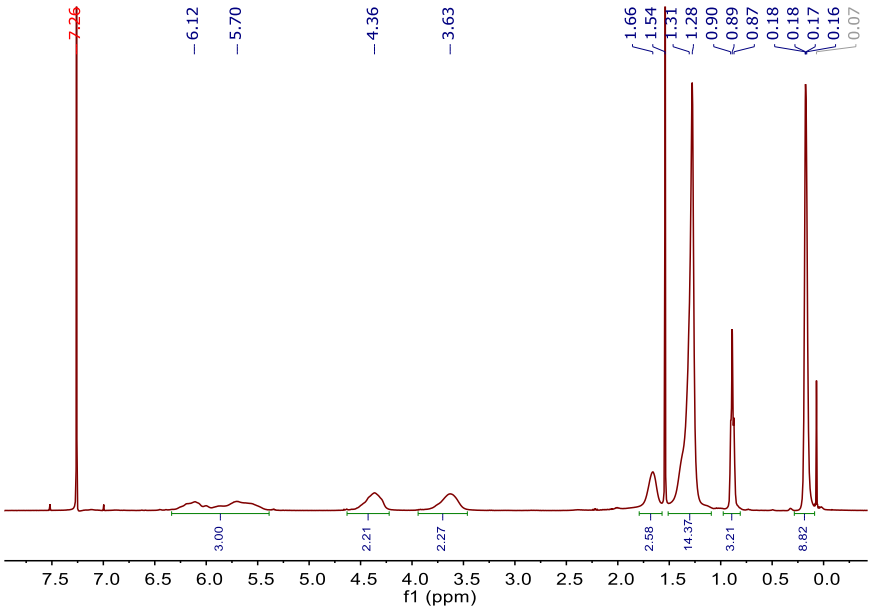

Figure 4.5 ^{1}H NMR spectrum of molecule **7**. Solvent: chloroform-*d*.

Synthesis of polymer **8**

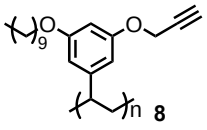

To a solution of polymer **P7** (265 mg 0.67 mmol) in THF (1 mL) was added TBAF (4 mL, 4 mmol) and the resulting mixture was allowed to be stirred under room temperature for 2 hours. Final polymer was purified by three times precipitation in MeOH. The yield is 88% with 190 mg of polymer **P8**. GPC: Mn=13.9K, PDI=1.7; ^{1}H NMR (400 MHz, Chloroform-*d*): δ 6.14 - 5.65 (m, 3H), 4.40 (m, 2H), 3.64 (m, 2H), 2.40 (s, 1H), 1.66 (m, 2H), 1.29 (m, 15H), 0.88 (m, 3H).

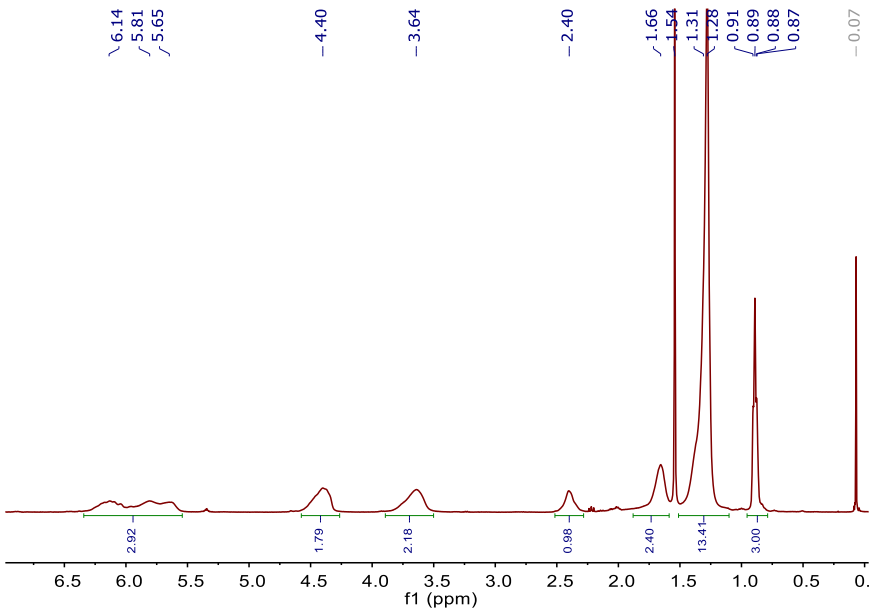

Figure 4.6 ^{1}H NMR spectrum of polymer **8**. Solvent: chloroform-*d*.

Synthesis of molecule **9**

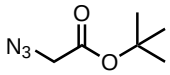

9

tert-Butyl bromoacetate (1.0 equiv.) and sodium azide (2.0 equiv.) was added into DMSO and reacting for overnight. The crude product was extracted EtOAc and H_2O three times. Unreacted sodium azide will be washed away. The combined organic phase was dried under sodium sulfate and further condensed under vacuum. No further purified is needed. Yield: 92%. ^{1}H NMR (400 MHz, Chloroform-d) δ 3.74 (s, 2H), 1.50 (s, 9H).

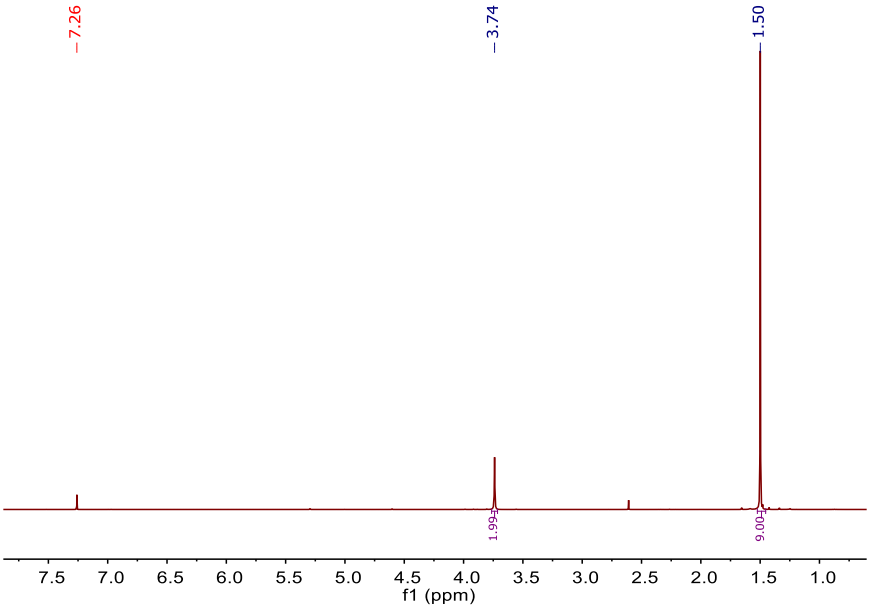

Figure 4.7 ^{1}H NMR spectrum of molecule **9**. Solvent: chloroform-*d*.

Synthesis of molecule **10**

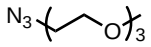

10

Molecule **10** is prepared by Bin Liu from triethylene glycol monomethyl ether. The alcohol was converted to tysol group using tysol chloride. Followed by reacting with sodium azide in DMF solution. The crude product was extracted with DCM three times. The combined organic phase was dried under sodium sulfate and further condensed under vacuum. No further purified is needed. Yield: 99%.^{1}H NMR (400 MHz, Chloroform-*d*) δ 3.71 – 3.61 (m, 6H), 3.54 (m, 2H), 3.42 – 3.34 (m, 3H),

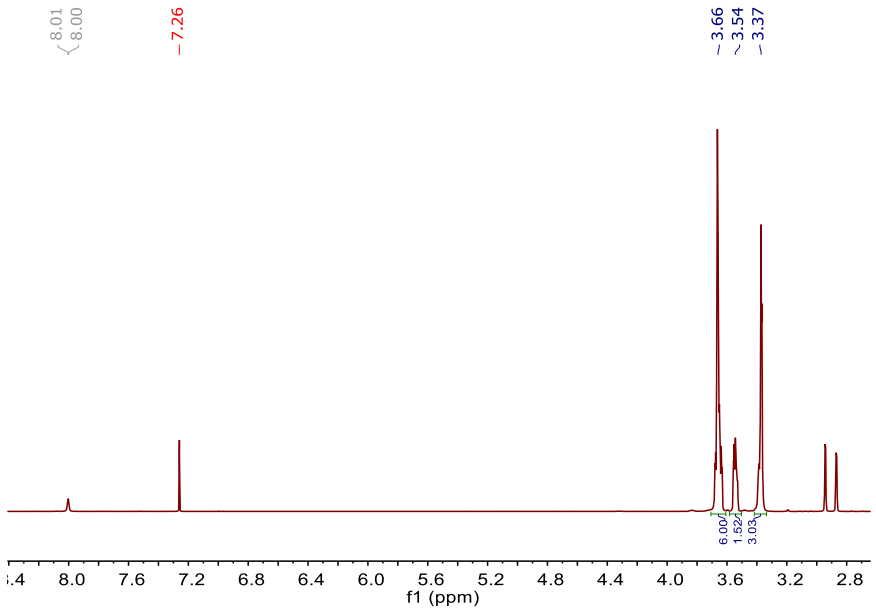

Figure 4.8 [1]H NMR spectrum of molecule **10**. Solvent: chloroform-*d*.

Synthesis of molecule **11**

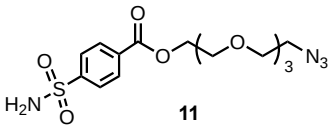

11

Molecule **11** (hh-3-89) was prepared through esterification reaction of HO-TEG-N_3 and 4-sulfamoylbenzoic acid. Typically, HO-TEG-N_3 (1.26g, 5.74 mmol), 4-sulfamoylbenzoic acid (2.31g, 11.48 mmol), 1-Ethyl-3-(3-dimethylaminopropyl) carbodiimide (EDC) (2.42g, 12.63 mmol) were dissolved in anhydrase DMF (20 mL). The mixture solution was kept in 0^{o}C using an ice bath for 20 mins. During that time, DMAP was added. The reaction was carried at room temperature overnight followed by evaporating DMF *in vacuo*. The crude product was extracted by DCM three times. The combined organic phase was washed by brine, dried under sodium sulfate and further condensed under vacuum. The crude was further purified by Combiflash with eluting of 0~10% methanol/dichloromethane to give the liquid product. [1]H NMR (400 MHz, Chloroform-*d*) δ 8.09 – 8.02 (m, 1H), 7.96 – 7.87 (m, 1H), 5.77 (s, 1H), 4.56 – 4.44 (m, 1H), 3.92 – 3.79 (m, 1H), 3.74 – 3.54 (m, 5H), 3.36 (t, *J* = 5.0 Hz, 1H).

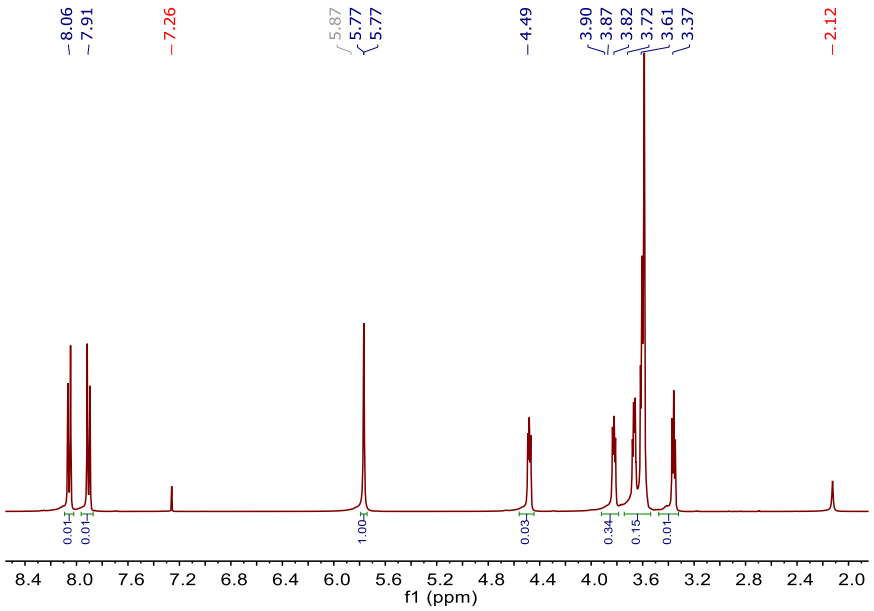

Figure 4.9 ^{1}H NMR spectrum of molecule **11**. Solvent: chloroform-*d*.

Synthesis of polymer **P3-P7**:

P3, **P5**, and **P7** were prepared through the same procedure[13]. Typically, polymer **8** (1.0 equiv.) and azido reagents (2.0 equiv.) were dissolved in THF (100 mg/mL) in a scintillation vial. To this solution, an equal amount of water to THF was added while stirring vigorously at room temp. Sodium ascorbate (10 mol%) and $CuSO_4 \bullet 5H_2O$ (5 mol%) were added to the reaction mixture from a freshly prepared aqueous solution (1.0 M). Upon the addition of copper, the reaction mixture turned brown for a few seconds and then changed to a yellow-orange color, which turned blue-green after the overnight reaction. THF was removed *in vacuo*. The aqueous layer was decanted, and the residue was washed several times with sat. NH_4Cl until no color was observed.

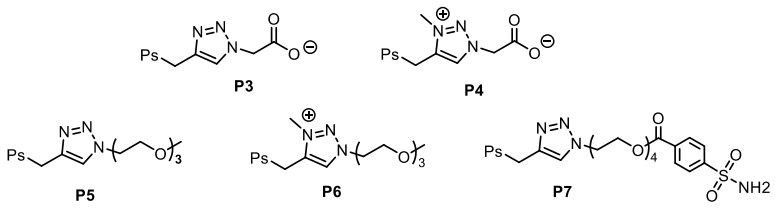

P3': ^{1}H NMR (400 MHz, Chloroform-*d*) δ, 7.74(s, 1H), 6.10-5.78(m, 3H), 5.02-4.81(m, 3H), 3.74-3.61(m, 2H), 1.59-1.24(m, 29H), 0.88(s, 3H).

P3 was prepared by the deprotection of *tert*-butyl group from polymer **P3'** using LiOH in MeOH/THF/H_2O solvents. The polymer was allowed to be stirred in reflux for overnight. The crude polymer residue was dried *in vacuo*. Polymer residue was rinsed with water several times to get rid of LiOH.

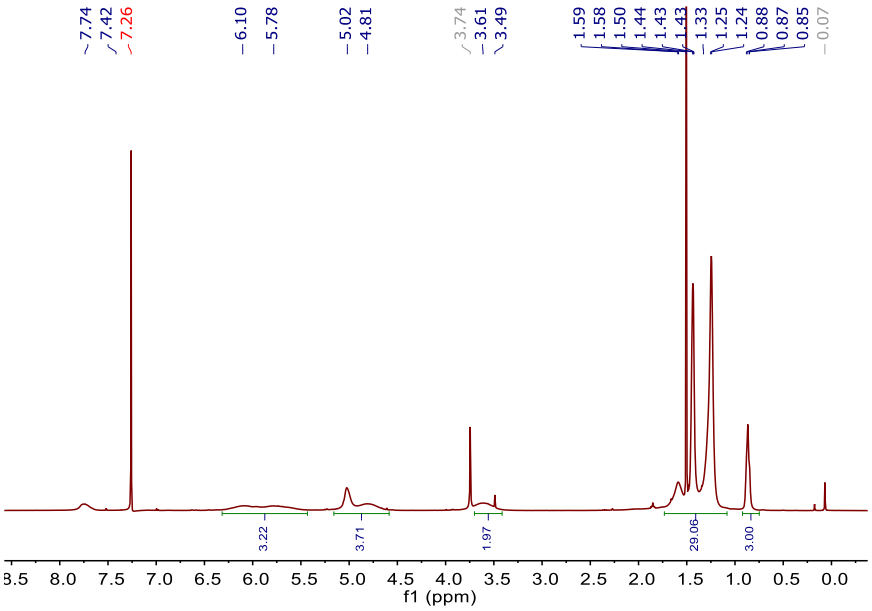

Figure 4.10 ^{1}H NMR spectrum of polymer **P3**. Solvent: chloroform-*d*.

P5: ^{1}H NMR (400 MHz, Chloroform-*d*) δ 7.80, 6.13, 5.77, 4.83, 4.48, 3.84, 3.57, 3.49, 3.31, 1.25, 0.87.

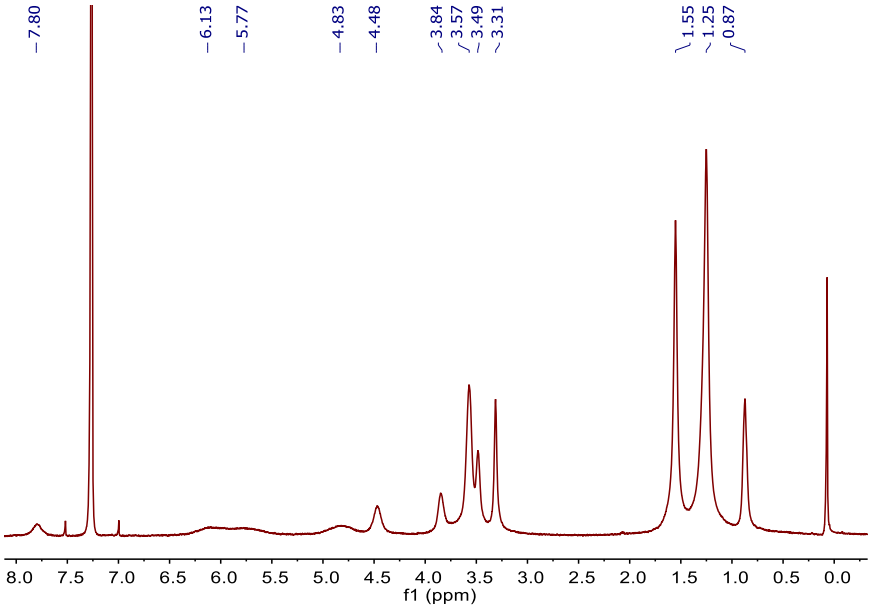

Figure 4.11 [1]H NMR spectrum of polymer **P5**. Solvent: chloroform-*d*.

P7:[1]H NMR (500 MHz, THF) δ 8.09-7.94(d, 4H), 6.73(s, 1H), 6.11(m, 3H), 4.40(m, 3H), 3.72(m, 4H), 3.50, 2.49-2.45(m, 2H), 1.28(m, 14H), 0.88(m, 3H).

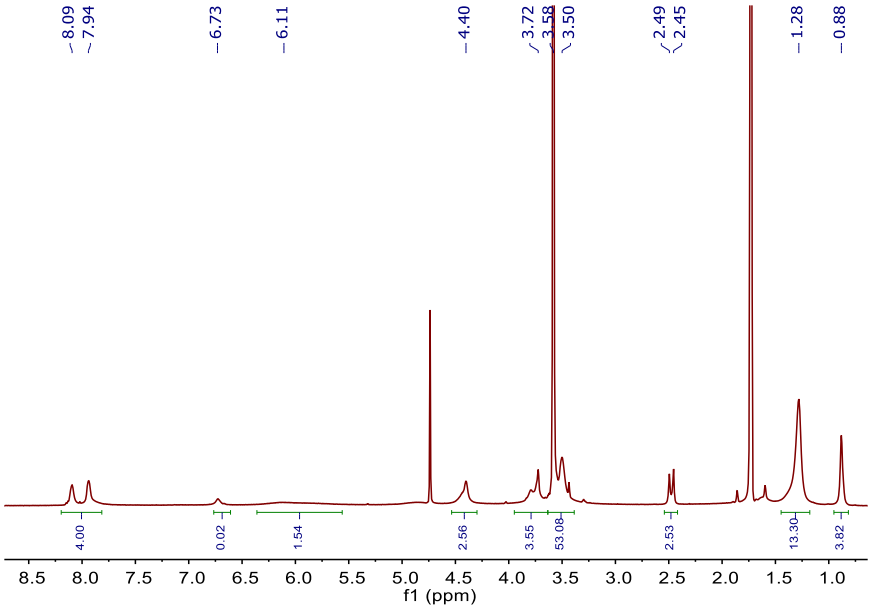

Figure 4.12 [1]H NMR spectrum of polymer **P7**. Solvent: chloroform-*d*.

P4 and **P6** were prepared by methylation of triazole ring from **P3** and **P5**, respectively, using Methyl Iodide in dry dichloromethane for overnight. Because of the solubility issue of these

amphiphilic homopolymers in pure organic solvents or inorganic solvents, we couldn't perform NMR for them.

4.5.2 Other experimental protocols

4.5.2.1 Reverse micelle preparation:

Reverse micelle was prepared following the previous literature. 1 mg of the polymer was dissolved in toluene to make 1 mg/mL concentration solution. Different amount of water (2 equiv. of the hydrophilic group) was added into toluene solution to form water pool inside reserve micelle. Sonication was applied at least three hours until a homogeneous solution was obtained.

4.5.2.2 Protein extraction experiment:

One micromolar of each peptide was dissolved in PBS buffer of pH 7.4. Two hundred microliters of the reverse micelle solution made from polymer **P7** was added to 1 mL of the protein solution. Extraction was done under vigorous vortex for 2 h. Centrifugation at 14 000 rcf for 20 min was followed to separate the two phases. The aqueous phase was removed, and the organic phase was dried by blowing N_2 gas. Ten microliters of aqueous solution was taken and mixed with 10 µL of a CHCA matrix solution (25 mg/mL in 70% (v/v) THF/H_2O containing 1% (v/v) TFA). The dry organic residue was re-dissolved in 20 µL of THF and mixed with 30 µL of the matrix solution. One microliter of this solution was spotted on the matrix-assisted laser desorption/ionization (MALDI) target for analysis. MALDI-MS analyses were performed on a Bruker Autoflex III time-of-flight mass spectrometer. All mass spectra were obtained in positive mode and represent an average of 200 shots acquired at 40% laser power with an accelerating voltage of 19kV.

4.6 References

(1) Hanash, S. M.; Pitteri, S. J.; Faca, V. M. Mining the Plasma Proteome for Cancer

Biomarkers. *Nature*. April 3, 2008, pp 571–579.

(2) Sahab, Z. J.; Semaan, S. M.; Sang, Q.-X. A. Methodology and Applications of Disease Biomarker Identification in Human Serum. *Biomark. Insights* **2007**, *2*, 117727190700200 DOI: 10.1177/117727190700200034.

(3) Liotta, L. A.; Petricoin, E. Cancer Biomarkers: Closer to Delivering on Their Promise. *Cancer Cell*. 2011, pp 279–280.

(4) Buss, H.; Chan, T. P.; Sluis, K. B.; Domigan, N. M.; Winterbourn, C. C. Protein Carbonyl Measurement by a Sensitive ELISA Method. *Free Radic. Biol. Med.* **1997**, *23* (3), 361–366 DOI: 10.1016/S0891-5849(97)00104-4.

(5) Engvall, E.; Perlmann, P. Quantitation of Specific Antibodies by Enzyme-Labeled Anti-Immunoglobulin in Antigencoated Tubes. *Curr. Contents* **1989**, *109* (1), 16 DOI: 10.1038/npg.els.0004021.

(6) Rodthongkum, N.; Chen, Y.; Thayumanavan, S.; Vachet, R. W. Matrix-Assisted Laser Desorption Ionization-Mass Spectrometry Signal Enhancement of Peptides after Selective Extraction with Polymeric Reverse Micelles. *Anal. Chem.* **2010**, *82* (9), 3686–3691 DOI: 10.1021/ac1000256.

(7) Rodthongkum, N.; Chen, Y.; Thayumanavan, S.; Vachet, R. W. Selective Enrichment and Analysis of Acidic Peptides and Proteins Using Polymeric Reverse Micelles and MALDI-MS. *Anal. Chem.* **2010**, *82* (20), 8686–8691 DOI: 10.1021/ac101922b.

(8) Combariza, M. Y.; Savariar, E. N.; Vutukuri, D. R.; Thayumanavan, S.; Vachet, R. W. Polymeric Inverse Micelles as Selective Peptide Extraction Agents for MALDI-MS Analysis. *Anal. Chem.* **2007**, *79* (18), 7124–7130 DOI: 10.1021/ac071001d.

(9) Rodthongkum, N.; Ramireddy, R.; Thayumanavan, S.; Richard, W. V. Selective Enrichment and Sensitive Detection of Peptide and Protein Biomarkers in Human Serum Using Polymeric Reverse Micelles and MALDI-MS. *Analyst* **2012**, *137* (4), 1024–1030 DOI: 10.1039/c2an16089g.

(10) Rodthongkum, N.; Washington, J. D.; Savariar, E. N.; Thayumanavan, S.; Vachet, R. W. Generating Peptide Titration-Type Curves Using Polymeric Reverse Micelles As Selective Extraction Agents along with Matrix-Assisted Laser Desorption Ionization-Mass Spectrometry Detection. *Anal. Chem.* **2009**, *81* (12), 5046–5053 DOI: 10.1021/ac900661e.

(11) Serrano, M. A. C.; He, H.; Zhao, B.; Ramireddy, R. R.; Vachet, R. W.; Thayumanavan, S. Polymer-Mediated Ternary Supramolecular Interactions for Sensitive Detection of Peptides. *Analyst* **2016**, *142* DOI: 10.1039/c6an01591c.

(12) Moses, J. E.; Moorhouse, A. D. The Growing Applications of Click Chemistry. *Chem. Soc. Rev.* **2007**, *36* (8), 1249–1262 DOI: 10.1039/B613014N.

(13) Helms, B.; Mynar, J. L.; Hawker, C. J.; Fréchet, J. M. J. Dendronized Linear Polymers via

"Click Chemistry." *J. Am. Chem. Soc.* **2004**, *126* (46), 15020–15021 DOI: 10.1021/ja044744e.

CHAPTER

5. TERNARY INTERACTION FACILITY OF SIGNAL ENHANCEMENT IN MALDI-TOF PEPTIDE DETECTION

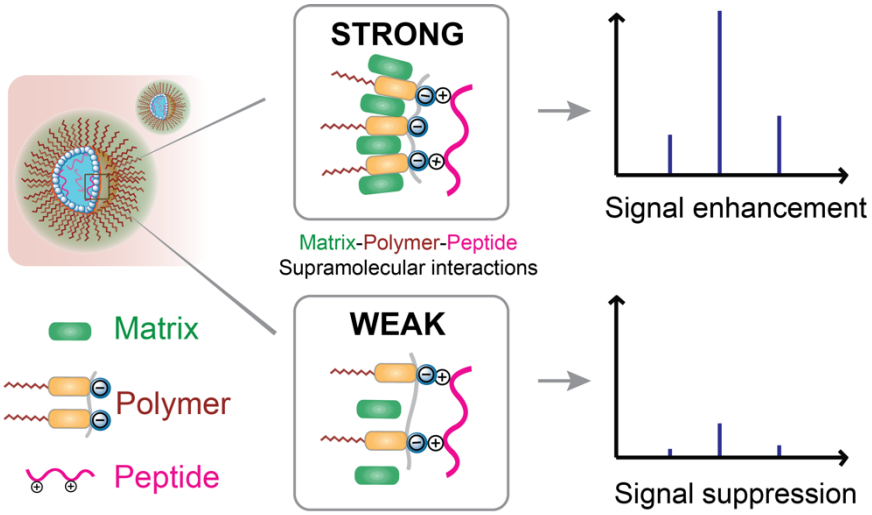

Scheme 5.1 Schematic representation of ternary interactions involving an amphiphilic homopolymer assembly with the analyte peptide through ionic complementarity and with the detection matrix through aromatic donor-acceptor interactions.

5.1 Introduction

Inspired by the complexity of non-covalent interactions in Nature and how they control the structure and function of biomolecules, artificial supramolecular assemblies have been designed with demonstrated applications in chemistry, materials science, and biology[1]. Among the various scaffolds in supramolecular chemistry, amphiphilic polymer-based assemblies that form organized structures such as micelles, vesicles, and nanogels have attracted a lot of interest in recent years for their use in biomimetics[2–4], targeted drug delivery[5–7], biomolecule activity modulation[8,9], sensing[10,11], and separations[12–14]. Recently, our group has developed amphiphilic homopolymers that self-assemble into reverse micelles and selectively enrich molecules, particularly peptides, based on their electrostatic interactions with the hydrophilic interior of the reverse micelle[15–17]. The utility of this method has been illustrated by the highly sensitive detection of picomolar

concentrations of peptides in serum samples when combined with matrix-assisted laser desorption ionization mass spectrometry (MALDI-MS) detection[17].

These low detection limits are achieved from the selective enrichment that occurs upon moving peptides from an aqueous phase to an organic phase, but also from an order of magnitude enhancement in the MALDI ion signal that arises in the presence of certain polymers, such as the dialkoxystyrene-based amphiphilic homopolymer (**PDAS**) (Chart 5.1). Interestingly, signal enhancement is not observed when a polyacrylamide-based amphiphilic control polymer (**PAm**) is used (Chart 5.1), despite having the same enrichment capability as the **PDAS** polymer. This difference suggests that the aromatic ring plays a vital role in the signal enhancement process. The increased MALDI signal in the case of the PDAS polymer is explained by the formation of peptide "hotspots" that contain higher local peptide concentrations and hence increased ion fluxes from these sites. Comparable hotspots are not formed in the absence of the polymer or in the presence of the **PAm** control polymer. The molecular basis for the formation of these hotspots in the presence of **PDAS**, however, is not understood. The fluorescence images reveal that the **PDAS** polymer causes the coalescence of the peptides and the matrix, thereby likely facilitating effective co-crystallization between the two into enriched zones. This observation led us to hypothesize that a donor-acceptor interaction between these two species forms the basis for the hotspot formation and the corresponding signal enhancement as the aromatic ring of the **PDAS** polymer is electron-rich (due to the alkoxy substituents), and the aromatic ring of the MALDI matrix is electron-poor. In effect, the polymer serves as the interface in a ternary supramolecular interaction by electrostatically engaging the peptide through its hydrophilic charged group and the matrix through its aromatic ring. Donor-acceptor supramolecular interactions in polymers have been reported to cause the formation of densely packed macrostructures in the solid state[18] and have found

applications in photovoltaics and organic electronics[19], but this is the first study, to our knowledge, that tackles its role in enhancing the signal obtained in MALDI-MS.

5.2 Molecular design

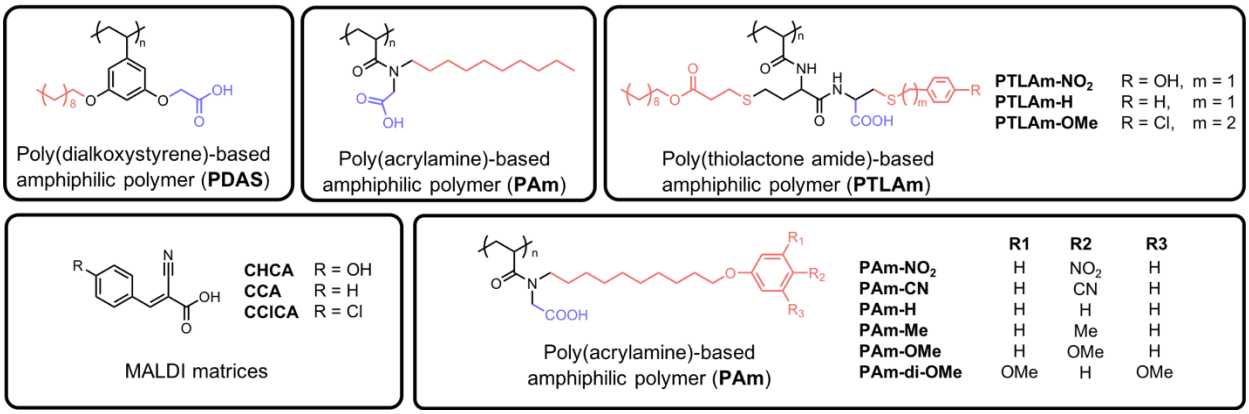

Chart 5.1 Chemical structures of poly(dialkoxystyrene)-based, polyacrylamide-based and poly(thiolactone amide)-based amphiphilic polymers and MALDI matrices.

5.3 Results and discussions

To test our hypothesis, we introduced various electron donating or withdrawing groups (EDG or EWG) to the aromatic ring of the matrix and of the polymer, making them either more electron-rich or more electron-poor (Chart 5.1), and examined how this would affect the hotspot formation and the MALDI-MS signal. For these experiments, we used bradykinin (RPPGFSPFR) and its TAMRA-labeled form (TMR-bradykinin) as the model peptides because of their positive charge at neutral pH.

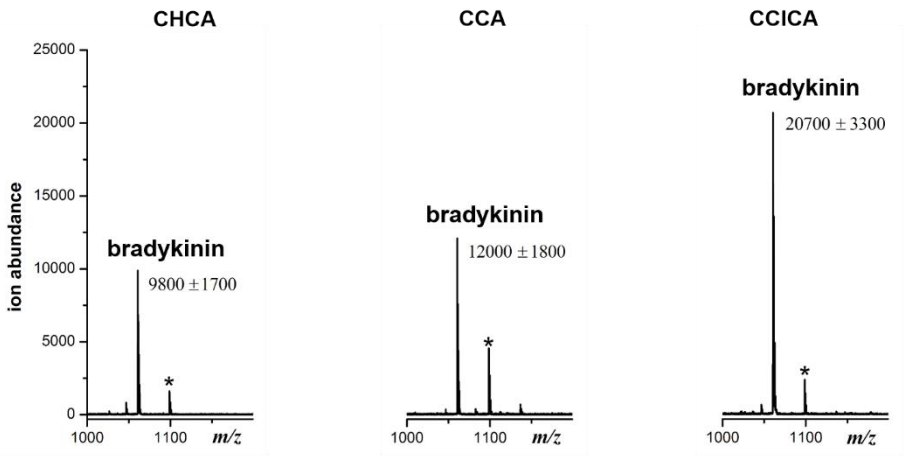

Figure 5.1 MALDI mass spectra of the different MALDI matrices in the order of increasing electron deficiency on the ring, obtained for 100 nM bradykinin extracted using the PDAS polymer (Chart 5.1) and analyzed using these three MALDI matrices. Peaks with asterisks are potassium adducts of the peptides, $[M + K]^+$.

First of all, we started with a variant of the MALDI matrix and kept the polymer same. α-cyano-4-hydroxycinnamic acid (CHCA) is the most commonly used MALDI matrix for peptides. Because of its extended conjugation and electron withdrawing cyano and carboxylate groups, CHCA's aromatic ring is electron-deficient. By replacing the hydroxyl substituent on the aromatic ring with –H (as in α-cyanocinnamic acid, CCA) and –Cl (as in α-cyano-4-chlorocinnamic acid, CClCA), the ring becomes more electron-poor (Chart 5.1). If the donor-acceptor interaction between the polymer and matrix indeed helps in better matrix-peptide clustering and enhanced MALDI-MS signal, then using a more electron-poor MALDI matrix with the electron-rich **PDAS** polymer should result in higher ion abundances in MALDI. Indeed, the expected result is observed upon extraction and analysis of the peptide bradykinin with CHCA, CCA, and CClCA as MALDI matrices (Figure 5.1). Compared to CHCA, the signal is enhanced by 20% when CCA was used, and more than 100% when the most electron-poor matrix, CClCA, is used. Moreover, corresponding fluorescence images reveal that clustering of the extracted peptide is the densest with the CClCA matrix (data not shown here).

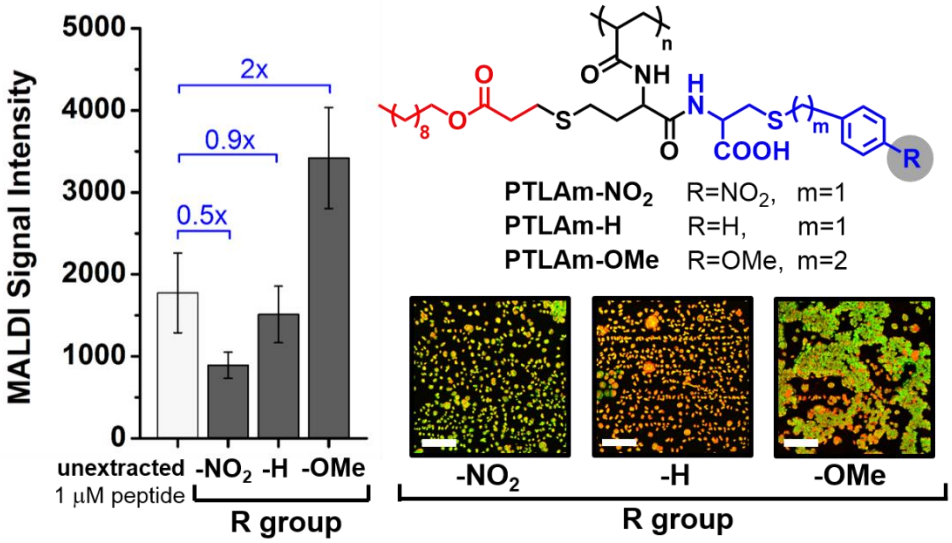

Figure 5.2 MALDI signal intensity of 10 nM bradykinin extracted by polythiolactone amide (PTLAm)-based carboxylate polymers with different R groups compared with 1 μM of unextracted bradykinin (100-fold higher concentration to account for 100-fold enrichment during extraction). Fluorescence images show the degree of clustering of the peptide (red) and matrix (green).

Next, we also investigated the effect of the electron density on the aromatic ring of the polymer on MALDI signal enhancement and hotspot formation. For these experiments, we used the **PTLAm** polymer design shown in Chart 5.1, which also forms reverse micelles and selectively extracts positively-charged peptides (see information in experimental details). A constant MALDI matrix CHCA was used for all the three polymers. Consistent with our hypothesis, using the **PTLAm** polymer with the electron-donating methoxy substituent (**PTLAm-OMe**) resulted in a two-fold enhancement in MALDI signal relative to the unextracted peptide, whereas suppression in signal was observed when the polymer with an electron-withdrawing nitro group (**PTLAM-NO_2**) was used (Figure 5.2). The unsubstituted PTLAm polymer (**PTLAm-H**) did not show a significant difference in MALDI signal relative to the unextracted one. Furthermore, clustering of peptide and matrix into hotspots is apparent in the presence of the **PTLAm-OMe**, but not for either **PTLAm-H** or **PTLAm-NO_2**, suggesting that a polymer with an electron-rich aromatic ring is needed for hotspot formation and MALDI signal enhancement.

To further test our hypothesis, we sought to investigate whether the polymer scaffold is essential for the hotspot formation and signal enhancement. We then designed and synthesized (see information in experimental details) a new set of amphiphilic homopolymers with a polyacrylamide (**PAm**) scaffold that enabled us to conveniently introduce subtle changes, such as a wide range of electron-donating or withdrawing substituents on the ring, while keeping the overall structure consistent (Chart 5.1). These polymers self-assemble into nanometer-sized reverse micelles and selectively extract oppositely charged peptides the same as the **PDAS** and **PTLAm** polymers. A similar trend in signal enhancement is also be observed with a different set of polyacrylamide carboxylate polymer with the aromatic ring positioned at the hydrophobic arm, far away from the carboxylate group.

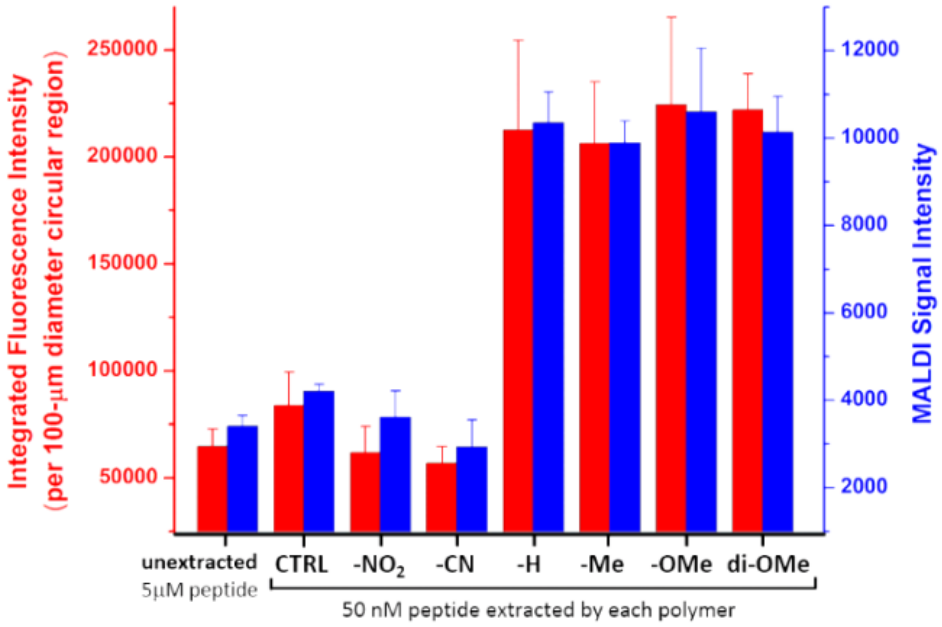

Figure 5.3 Correlation of the degree of clustering, as measured by fluorescence microscopy, with the MALDI-MS signal (average ± SEM of 90 spectra obtained from 3 replicate extractions with 3 spots each).

The degree of matrix-peptide clustering and MALDI signal enhancement after extraction was monitored by fluorescence microscopy (data not shown here) and mass spectrometry, respectively. Through mere visual inspection, it is evident that a higher degree of clustering is

present in samples extracted by polymers with EDG (**PAm-Me**, **PAm-OMe**, **PAm-di-OMe**) compared with those extracted by polymers with EWG (**PAm-NO_2** and **PAm-CN**) (Figure 5.3). At first glance, we would expect **PAm-H** to behave similarly to the control (unextracted) sample, because of the –H substituent. Note, however, that the base aromatic ring is based on an alkoxyarene, making PAm-H a relatively electron-rich aromatic ring. We quantitatively assessed the degree of hotspot formation by measuring the fluorescence intensity per area using the software *ImageJ*[20] and correlated this with the MALDI-MS signal obtained for samples extracted by each polymer, which verifies that the clustering phenomenon indeed translates to enhanced signals in MALDI-MS and that this only occurs when polymers with EDG are used. An approximately 3-fold MALDI signal enhancement is observed for peptides extracted using polymers with EDG in their aromatic ring compared to unextracted samples. In contrast, peptides extracted by polymers with EWG do not exhibit any appreciable enhancement in MALDI signal. These results taken together support our hypothesis that signal enhancement occurs when a good electron donor-acceptor interaction exists between the polymer and the matrix, respectively.

5.4 Summary

In summary, we have investigated the molecular basis for the observed MALDI signal enhancement of peptides after they are extracted using reverse micelles of amphiphilic polymers. An important point to recognize from all the data presented here is that the electrostatic interaction between the polymer and the peptide is not enough to cause hotspot formation and signal enhancement. Via systematic variations to the electron character of the amphiphilic polymer and matrix, we find that favorable donor-acceptor interactions are necessary to assemble the polymer, peptide, and matrix in such a way to produce peptide-rich zones that maximize ion signal during MALDI-MS. Overall, these results reveal that amphiphilic polymers can self-pack (or fold) in such

a way that they mediate favorable interactions between peptides and matrix, so that ionization is enhanced. Such interactions are reminiscent of proteins that upon folding position other biomolecules in just the right way to perform chemistry that is impossible with the ternary interaction. Learning from nature Mother using ternary supramolecular interaction forming high hierarchical structures and performing biological functionalities, the third component in ternary supramolecular interaction is usually indeed essential. Such as chaperones in protein folding, ribosomal in RNA translation, the reaction happened and accelerated in the presence of those important third compartment. This phenomenon and mechanism study from molecular level could provide us with guidelines for further designing molecules resulting in more powerful tools for the low-level concentration of MALDI detection.

5.5 Materials and experiments

5.5.1 Materials

All the reagents were purchased from a commercial source and used as such without further purification. ^{1}H NMR spectra were recorded on a Bruker 400 MHz NMR spectrometer using the residual proton resonance of the solvent as the internal standard. Chemical shifts (δ) are reported in parts per million (ppm) and Hertz, respectively. The following abbreviations are used for the peak multiplicities: s, singlet; d, doublet; t, triplet; q, quartet; m, multiplet; dd, a doublet of doublet; bs, broad singlet; bd, broad doublet; bm, broad multiplet. ^{13}C-NMR spectra were recorded on a 400MHz Bruker NMR spectrometer using a carbon signal of the deuterated solvent as the internal standard. Dynamic Light Scattering (DLS) measurements were carried out on a Malvern Nanozetasizer. TEM images were recorded on a JEOL-2000FX machine operating at an accelerating voltage of 100 kV. Molecular weights of the polymers were estimated by gel permeation chromatography (GPC) using PMMA standard with a refractive index detector.

Fluorescence measurements were performed on a fluorescence plate reader (Molecular Devices, SpectraMax M5). High-performance liquid chromatography was conducted using a Shimadzu Prominence Modular reverse phase

5.5.2 Synthesis of molecules

5.5.2.1 Synthesis of polythiolactone amide (PTLAm)-based amphiphilic polymers

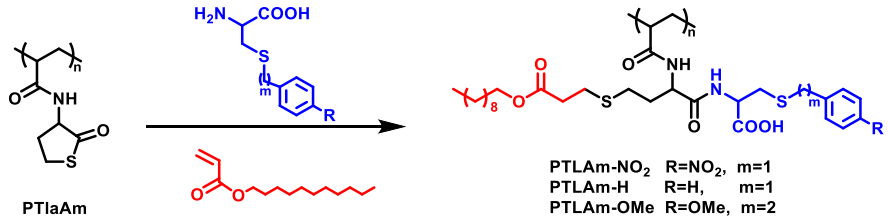

The PTLAm polymer synthesis was initiated by RAFT polymerization of thiolactone acrylamide[21], followed by thiolactone ring opening with different amines (blue) and reaction with decyl acrylate (red) in a one-pot reaction in DCM/MeOH solvent. GPC of precursor polymer PTlaAm: M_n=14.4K, M_w=18.5K, Đ=1.28. ^{1}H-NMR (500 MHz, Chloroform-*d*) δ 4.92 (m, 1H), 3.27 (m, 2H), 2.84-1.11 (m, 5H). Due to aggregation issues, NMR for the final product is not available. IR spectrum peak around 1699cm^{-1} belongs to the C=O of thiolactone disappeared after conjugation showed the completion of modification reaction.

5.5.2.2 Synthesis of polyacrylamide (PAm)-based amphiphilic polymers:

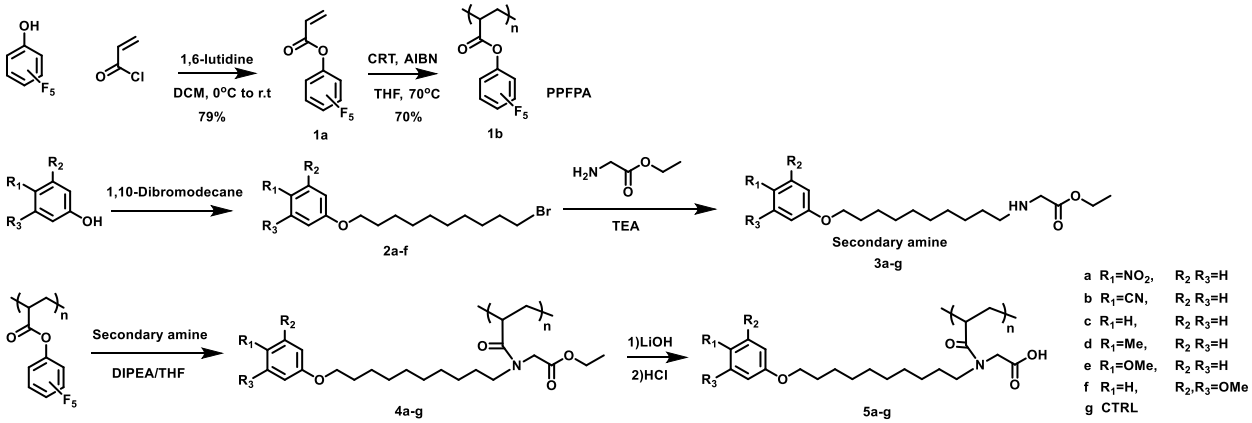

5.5.2.3 Synthesis of compound **1a**

The pentafluorophenylacrylate monomer (PFPA) **1a** was synthesized following the published paper[22] using acryloyl chloride and pentafluorophenol in the presence of 1,6-lutidine as the base.

Synthesis of polymer **1b**

The precursor polymer PPFPA was synthesized by following the reported literature[23]. The PFPA monomer (1.0 g, 4.2 mmol) was added to a 10-mL Schlenk flask containing dry THF (1 mL), chain transfer agent cyanomethyl dodecyl trithiocarbonate (14 mg, 0.044 mmol), and AIBN (1.7 mg, 0.11 mmol). The resulting reaction mixture was degassed using three freeze-pump-thaw cycles for 10 minutes. This reaction mixture is stirred at 70 ºC for 20 hours and then precipitated in MeOH to obtain the product as a white powder (60% yield). GPC (PMMA/THF): M_n=13K, M_w=18.8K, Đ=1.28. ^{1}H-NMR (400 MHz; $CDCl_3$): δ 3.20-3.00 (br s, 1H), 2.20-1.90 (br s, 2H). ^{19}F-NMR (500 MHz; $CDCl_3$): 153.04 (s, 2F), 156.54 (s, 1F), -161.90 (s, 2F).

5.5.2.4 Synthesis of compound **2a**

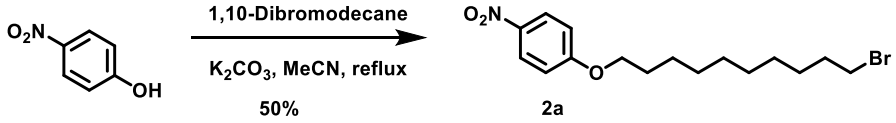

To a solution of acetonitrile (MeCN) mixed with K_2CO_3 (5.45 g, 39.49 mmol) and 18-crown-6 (0.52 g, 1.973 mmol), a solution of 4-nitrophenol (2.74 g, 19.73 mmol) was added. 1,10-dibromodecane (12.0 g, 39.47 mmol) in 150 mL was added via a funnel within 1hr. Then the system was heated under reflux for 24 h with a $CaCl_2$ guard. The reaction mixture was allowed to cool to room temperature and then was concentrated in vacuo . Water was added, and the aqueous layer was extracted thrice with 50-mL portions of ethyl acetate (EtOAc). The combined organic layers were washed with brine (20 mL), dried with $MgSO_4$, filtered and the solvent was removed in vacuo, yielding a white solid as the crude product. The solid was dissolved in minimal amounts

of CH_2Cl_2 and absorbed onto silica followed by purification via silica gel column chromatography (gradient elution: 0 to 30% EtOAc in hexane, increase in increments of 5% EtOAc per 100 ml of eluent used). The solvent was removed in vacuo to yield a white solid (3.50 g, 50%). ^{1}H-NMR (400 MHz, $CDCl_3$) δ 8.16 – 8.14 (d, *J* = 9.2 Hz, 2H), 6.93 – 6.90 (d, *J* = 9.2 Hz, 2H), 4.02 (t, *J* = 6.5 Hz, 2H), 3.38 (t, *J* = 6.9 Hz, 2H), 1.80 (m, 4H), 1.50 – 1.25 (m, 12H).

5.5.2.5 Synthesis of compound **2b**

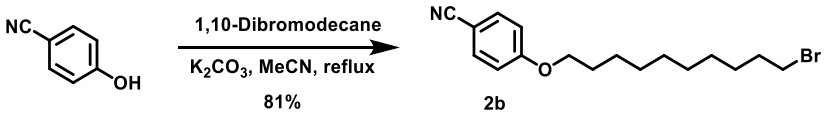

A suspension of K_2CO_3 (3.00 g, 21.71 mmol) in a solution of 4-cyanophenol (1.3 g, 10.91 mmol), 1,10-dibromodecane (12.75 g, 42.49 mmol) in MeCN (150 mL) was heated under reflux for 24 h under argon. The reaction progress was monitored by TLC. The reaction mixture was allowed to cool to room temperature, filtered through celite and concentrated in vacuo. Water (100 mL) was added, and the aqueous layer was extracted with EtOAc (3 x 50 mL). The combined organic layers were washed with brine (50 mL), dried in $MgSO_4$, filtered and the solvent was removed in vacuo. The white solid was dissolved in minimal amounts of CH_2Cl_2 and absorbed onto silica followed by purification via silica gel column chromatography (gradient elution: 0 to 30% EtOAc in hexane, increase in increments of 5% EtOAc per 100 mL of eluent used). The solvent was removed in vacuo to yield a white solid (2.99 g, 81%). ^{1}H-NMR (500 MHz, $CDCl_3$) δ 7.56 – 7.54 (d, *J* = 8.7 Hz, 2H), 6.92 – 6.91 (d, *J* = 8.8 Hz, 2H), 3.97 (t, J = 6.5 Hz, 2H), 3.39 (t, J = 6.8 Hz, 2H), 1.88 – 1.73 (m, 4H), 1.48 – 1.24 (m, 12H).

5.5.2.6 Synthesis of compound **2c**

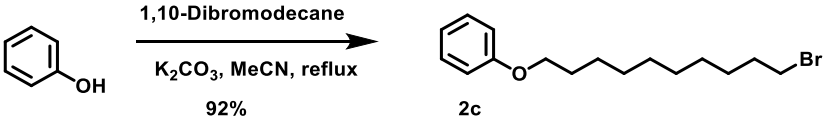

A suspension of K_2CO_3 (5.45 g, 39.49 mmol) in a solution of phenol (1.00 g, 10.6 mmol), 1,10-dibromodecane (12.75 g, 42.5 mmol) in MeCN (150 mL) was heated under reflux for 24 h under argon. The reaction mixture was run through celite pad and concentrated in vacuo. The white solid obtained was dissolved in minimal amounts of CH_2Cl_2 and absorbed onto silica followed by purification via silica gel column chromatography (gradient elution: 0 to 10% EtOAc in hexane, increase in increments of 1% EtOAc per 100 mL of eluent used). The solvent was removed in vacuo to yield a white solid (3.00 g, 92%). ^{1}H-NMR (400 MHz, $CDCl_3$) δ 7.28 (m, 2H), 6.92 (m, 3H), 3.96 (t, *J* = 6.4 Hz, 2H), 3.42 (t, *J* = 6.8Hz, 2H), 1.86 -1.78 (m, 4H), 1.53 – 1.28 (m, 12H).

5.5.2.7 Synthesis of compound **2d**

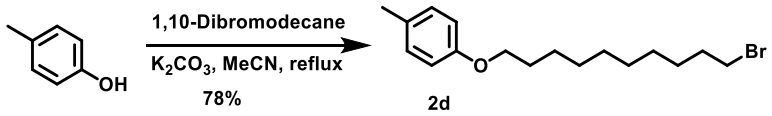

A solution of *p*-cresol (1.00 g, 9.24 mmol), 1,10-dibromodecane (11.10 g, 36.98 mmol) and K_2CO_3 (2.56 g, 18.5 mmol) in 100 mL of MeCN was refluxed overnight at 70 °C under argon. After the reaction was completed, the salt was filtered through celite pad; the MeCN was removed by evaporation. The reaction product was purified by column chromatography on silica gel with EtOAc/hexane (1:5) as the eluent. Yield: 78% (2.00 g). ^{1}H-NMR ($CDCl_3$): δ7.08 (d, *J*= 8.2 Hz, 2H,), 6.80 (d, *J*= 8.4 Hz, 2H,), 3.92 (t, *J*= 6.4 Hz, 2H,), 3.41 (t, *J*= 6.8 Hz 2H,), 2.28 (s, 3H), 1.82 (m, 4H), 1.30 (m, 12H).). FAB-MS (expected: 326.12m/z, obtained: 326.13, 328.12)

Synthesis of compound **2e**

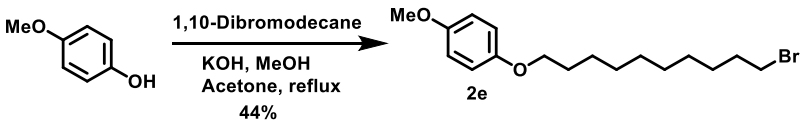

Potassium hydroxide (1.35 g, 23.9 mmol) in 100 mL of methanol was mixed with 4-methoxyphenol (2.48 g, 20.0 mmol) in 20 mL of methanol. The resulting solution was added using

an addition funnel within 1.5 h to 1,10-dibromodecane (12.0 g, 40.0 mmol) in 200 mL of acetone. The mixture was refluxed overnight, concentrated, and diluted with water/diethyl ether. The ether extract was then filtered, washed with dilute water and brine, dried, condensed, and recrystallized from hexane, giving **2e** as a white crystal (3.0g, 44%). ^{1}H-NMR (500 MHz, $CDCl_3$) δ 6.76 (s, 4H), 3.82 (t, J = 6.6 Hz, 2H), 3.69 (s, 3H), 3.46 (t, J = 6.8 Hz, 2H), 1.69 (m, 4H), 1.41 –1.24 (m, 12H).

5.5.2.8 Synthesis of compound **2f**

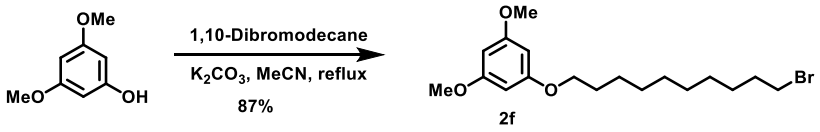

A mixture of 3,5-dimethoxyphenol (1.02 g, 6.67 mmol), and K_2CO_3(1.84 g, 13.3 mmol) in MeCN (50mL) was added to 1,10-dibromodecane (8.0 g, 26.6 mmol) in MeCN (50 mL) solution dropwise and the solution was heated at reflux overnight. After filtration, the solvent was evaporated, and the residue was extracted with EtOAc/H_2O twice. The combined organic layers were washed with brine and dried over Na_2SO_4, the filtrate was concentrated and purified by column chromatography (silica gel, hexane/ EtOAc, 10:1) to give **2f** as a white solid.(2.16 g, 87%). ^{1}H-NMR (400 MHz, $CDCl_3$) δ 6.08 (s, 3H), 3.91 (t, J = 6.6 Hz, 2H), 3.77 (s, 6H), 3.41 (t, J = 6.9 Hz, 2H), 1.85 (q, J = 6.9 Hz, 2H), 1.76 (q, J = 6.7 Hz, 2H), 1.47 – 1.31 (m, 12H).

5.5.2.9 Synthesis of compound **3a-f**

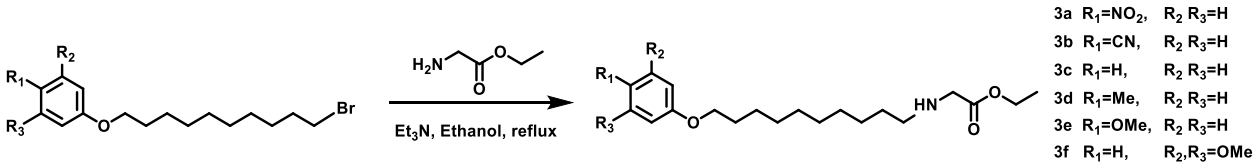

Glycine ethyl ester hydrochloride (2 equiv.), triethylamine (4 equiv.), and the appropriate aliphatic methyl bromoacetate or aliphatic alkyl halide (1 equiv.) were mixed together in ethanol and the reaction mixture was refluxed for 24 h under argon. After the solvent was removed, the residue

was added to water and extracted using CH_2Cl_2. Solvent was removed and the crude reaction mixture was purified through silica-gel column chromatography to get the monoalkylated glycine ester. Yield: 23%~45%.

3a: ^{1}H-NMR (500 MHz, $CDCl_3$) δ 8.15 – 8.13 (d, *J* = 9.2 Hz, 2H), 6.90 – 6.88 (d, *J* = 9.3 Hz, 2H), 4.15 (q, *J* = 7.1 Hz, 2H), 4.01 (t, *J* = 6.5 Hz, 2H), 3.36 (s, 2H), 2.56 (t, *J* = 7.2 Hz, 2H), 1.78 (m, 2H), 1.52 (s, 1H), 1.43 (m, 4H), 1.36 – 1.21 (m, 13H); ESI-MS: expected 380.23, obtained 381.24. **3b**: ^{1}H-NMR (500 MHz, $CDCl_3$) δ 7.55 (d, *J* = 8.8 Hz, 2H), 6.91 (d, *J* = 8.8 Hz, 2H), 4.17 (q, *J* = 7.1 Hz, 2H), 3.97 (t, *J* = 6.5 Hz, 2H), 3.37 (s, 2H), 2.57 (t, *J* = 7.2 Hz, 2H), 1.82 – 1.72 (m, 2H), 1.46 (m, 4H), 1.27 (m, 13H). **3c**: ^{1}H NMR (500 MHz, $CDCl_3$) δ 7.30 – 7.22 (m, 2H), 6.89 (dd, *J* = 16.2, 7.8 Hz, 3H), 4.17 (q, *J* = 7.1 Hz, 2H), 3.92 (t, *J* = 6.6 Hz, 2H), 3.37 (s, 2H), 2.57 (t, *J* = 7.2 Hz, 2H), 1.76 (p, *J* = 6.8 Hz, 2H), 1.55 – 1.39 (m, 4H), 1.38 – 1.21 (m, 13H); ESI-MS expected 335.25, obtained 335.25. **3d**: ^{1}H-NMR (500 MHz, $CDCl_3$) δ 7.07 (d, *J* = 8.2 Hz, 2H), 6.83 – 6.76 (d, *J* = 8.5 Hz, 2H), 4.19 (q, *J* = 7.2 Hz, 2H), 3.92 (t, *J* = 6.6 Hz, 2H), 3.39 (s, 2H), 2.59 (t, *J* = 7.2 Hz, 2H), 2.28 (s, 3H), 1.80 – 1.71 (m, 2H), 1.58 – 1.39 (m, 4H), 1.38 – 1.25 (m, 13H). **3e**: ^{1}H-NMR (500 MHz, $CDCl_3$) δ 6.83 (s, 4H), 4.19 (q, *J* = 7.2 Hz, 2H), 3.90 (t, *J* = 6.6 Hz, 2H), 3.77 (s, 3H), 3.39 (s, 2H), 2.59 (t, *J* = 7.2 Hz, 2H), 1.80 – 1.70 (m, 2H), 1.46 (m, 4H), 1.37 – 1.24 (m, 13H); FAB-MS expected 365.26, obtained 366.2. **3f**: ^{1}H-NMR (500 MHz, $CDCl_3$) δ 6.10 (s, 3H), 4.21 (q, *J* = 7.1 Hz, 2H), 3.93 (t, *J* = 6.6 Hz, 2H), 3.79 (s, 6H), 3.42 (s, 2H), 2.61 (t, *J* = 7.2 Hz, 2H), 1.82 – 1.74 (m, 2H), 1.48 (m, 4H), 1.32 (m, 13H).

5.5.2.10 Synthesis of compound **3g**

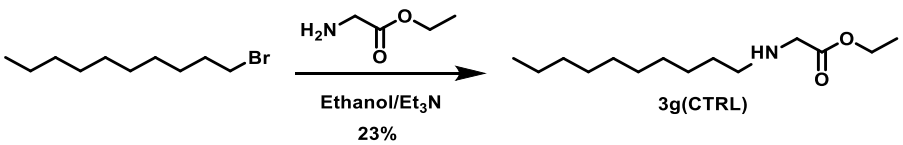

Glycine ethyl ester hydrochloride (12.4 g, 96 mmol), trimethylamine (16.2 mL, 192 mmol), and 1-bromodecane (10.62 g, 48 mmol) were mixed together in ethanol (200 mL), and the reaction mixture was refluxed for 36 h under argon. After solvent removal, the residue was added to water and extracted using EtOAc. The solvent was removed, and the crude product was purified through silica-gel column chromatography to get the monoalkylated glycine ester **3g**. Yield: 23%. The low yield is due to the possible bis-alkylated byproduct. ^{1}H-NMR (400 MHz, $CDCl_3$) δ 4.19 (q, *J* = 7.1 Hz, 2H), 3.40 (s, 2H), 2.59 (t, *J* = 7.2 Hz, 2H), 1.87 (s, 1H), 1.49 (m, 2H), 1.35 – 1.23 (m, 17H), 0.87 (t, *J* = 6.7 Hz, 3H).

5.5.2.11 Synthesis of polymer **4a-g**

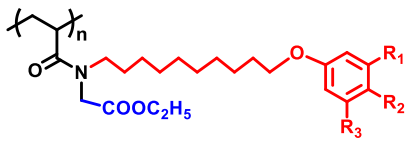

		R_1	R_2	R_3
4a	PAm-NO_2	H	NO_2	H
4b	PAm-CN	H	CN	H
4c	PAm-H	H	H	H
4d	PAm-Me	H	Me	H
4e	PAm-OMe	H	OMe	H
4f	PAm-di-OMe	OMe	H	OMe
4g	PAm-CTRL	no aromatic ring		

50 mg (0.21 mmol) of polypentafluorophenylacrylate (PPFPA), 146.3 µL (0.84 mmol) of DIPEA and 4 equivalents of a secondary amine with respect to PFPA unit, was dissolved in freshly distilled THF (500 mg polymer/mL). The mixture was stirred overnight at 65 °C. The resulting polymer was isolated by precipitation in n-hexane and was then dried in vacuo. Yield: ~70%. ^{1}H-NMR shows corresponding peaks with the same chemical shift as the secondary amine. ^{19}F NMR shows no peak left from the fluorinated precursor polymer, indicating 100% conversion of PPFPA polymer to polyacrylamide polymers **4a-g**.

5.5.2.12 Synthesis of compound **5a-g**

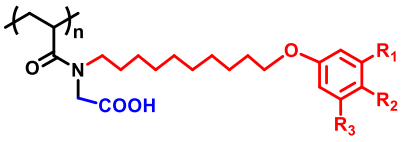

		R_1	R_2	R_3
5a	PAm-NO_2	H	NO_2	H
5b	PAm-CN	H	CN	H
5c	PAm-H	H	H	H
5d	PAm-Me	H	Me	H
5e	PAm-OMe	H	OMe	H
5f	PAm-di-OMe	OMe	H	OMe
5g	PAm-CTRL	no aromatic ring		

The final polymer was obtained by deprotection of the carboxylate group. Lithium hydroxide was added to each polymer dissolved in THF, methanol, and water (8 mL: 2 mL: 1 mL). The reaction was then allowed to take place overnight at room temperature. The solvents were evaporated, and 10 mL of water was then added, followed by neutralization with 3 M HCl solution to precipitate the polymer. The polymer was filtered and vacuum-dried. Molecular weight cannot be obtained by GPC due to solubility issues. Conversion of the ester to the free carboxylic acid was confirmed by IR (vibration at 3100 cm^{-1} for O-H and 1730 cm^{-1} for C=O of carboxylic acid).

5.5.3 Other experimental protocols

5.5.3.1 Dynamic Light Scattering (DLS) Study

DLS was performed on a Malvern Nano-zeta sizer instrument with a 637 nm laser source with non-invasive backscattering technology detected at 173^0. All sizes are reported as the hydrodynamic diameter (D_H) and were repeated in triplicate. For the DLS measurements, the concentration of the polymer and nanogel solution was 1 mg/mL. The solution was filtered using a hydrophilic membrane (pore size 0.450 µm) before the experiment was performed.

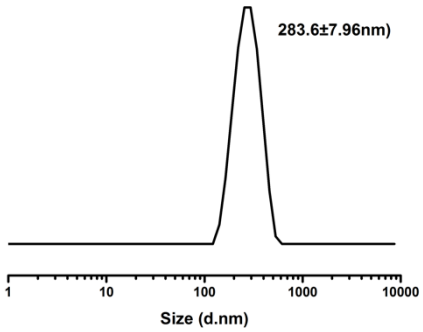

Figure 5.4 Representative DLS measurement of micelle aggregates made from PAm-H.

5.5.3.2 Transmission Electron Microscope (TEM) Study

For the TEM measurements, the nanogel solution was prepared in 1 mg/mL concentration. One drop of the sample (10 μL) was drop cast on carbon-coated Cu grid, 400 mesh size and left to dry overnight.

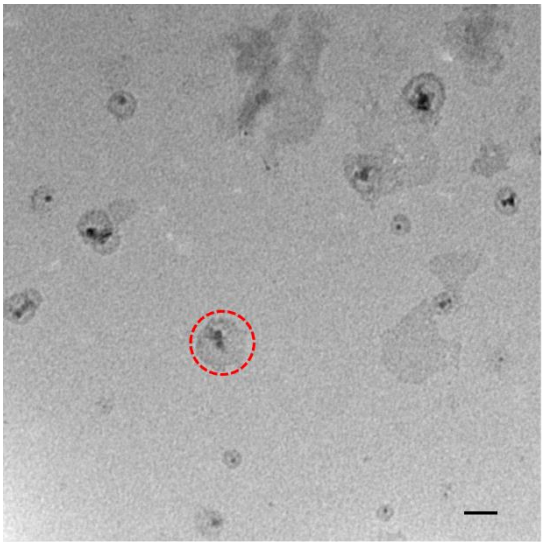

Figure 5.5 Representative TEM image of micelle aggregates made from PAm-H.

5.5.3.3 Critical Aggregation Concentration (CAC) measurements

Different concentrations of the polymeric reverse micelles were prepared by dissolving polymer in toluene and sonicating for 2hrs to obtain clear solutions. The surface tensions of these solutions were recorded using a tensiometer and plotted against the reverse micelle concentration. As an example, the CAC measurement of polymer PAm-H is shown below.

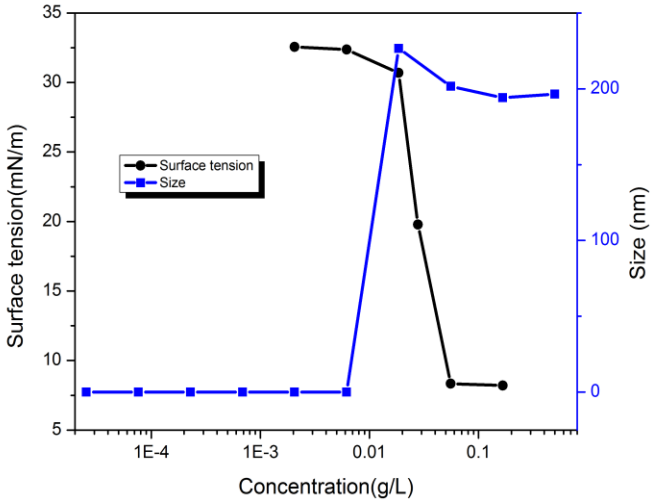

Figure 5.6 Example surface tension (black dots) and particle size (blue square) measurements vs. concentration of polymer PAm-H. A CAC of ~0.055mg/mL was identified as the concentration at which the surface tension and size changes.

5.5.3.4 Matrix-Assisted Laser Desorption/Ionization Mass Spectrometry (MALDI-MS) Analysis. A Bruker Autoflex III time-of-flight mass spectrometer was used for the MALDI- MS analysis of all samples. Acquisition of all mass spectra was measured in reflectron mode with an accelerating voltage of 19 kV. Each spectrum is the average of 300 laser shots at 25% laser power.

5.5.4 NMR spectra

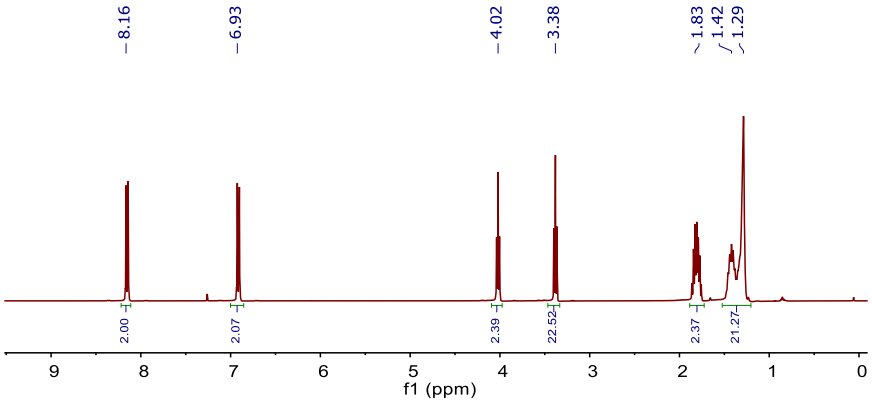

Figure 5.7 ^{1}H NMR spectrum of compound **2a**. Solvent: chloroform-*d*.

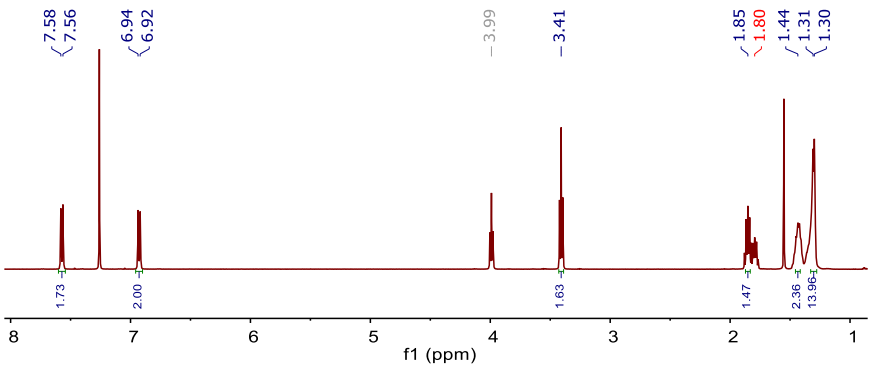

Figure 5.8 ^{1}H NMR spectrum of compound **2b**. Solvent: chloroform-*d*.

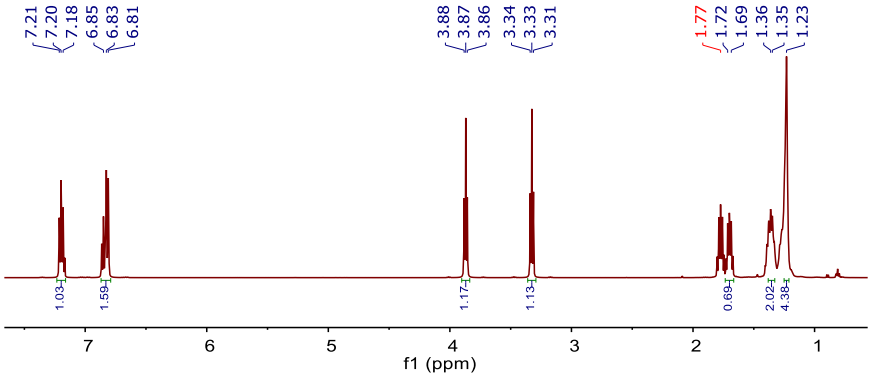

Figure 5.9 ^{1}H NMR spectrum of compound **2c**. Solvent: chloroform-*d*.

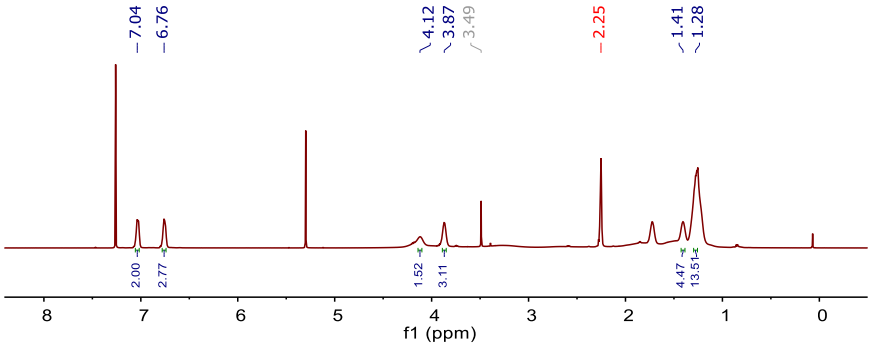

Figure 5.10 ^{1}H NMR spectrum of compound **2d**. Solvent: chloroform-*d*.

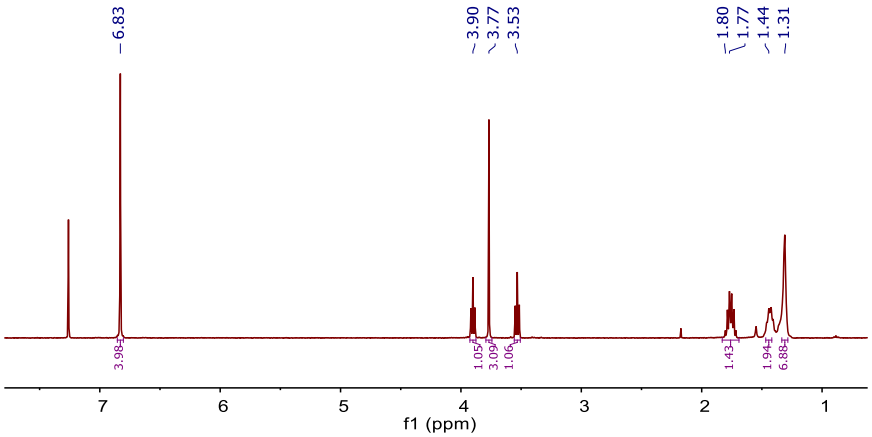

Figure 5.11 ^{1}H NMR spectrum of compound **2e**. Solvent: chloroform-*d*.

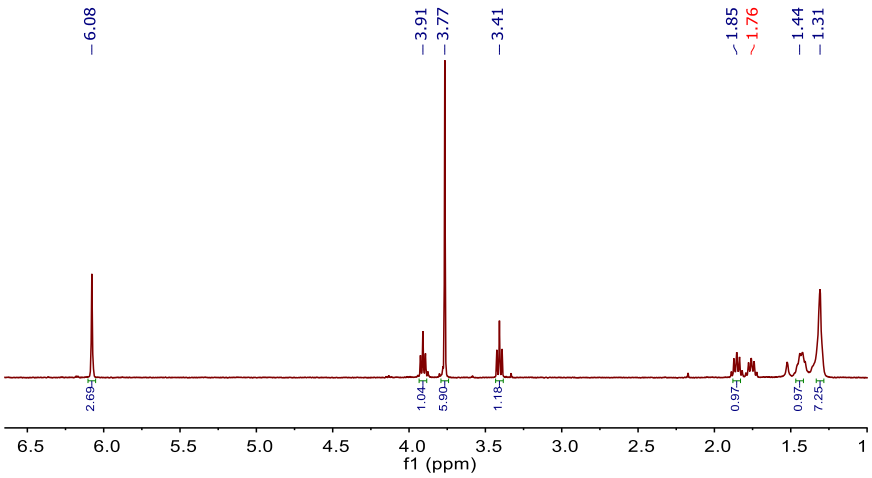

Figure 5.12 ^{1}H NMR spectrum of compound **2f**. Solvent: chloroform-*d*.

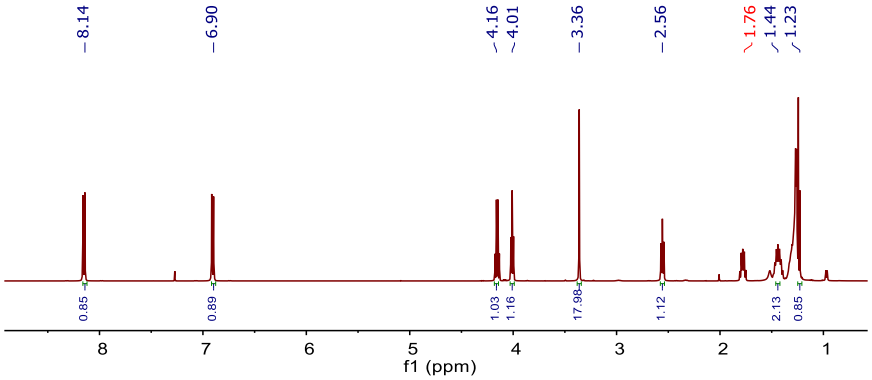

Figure 5.13 ^{1}H NMR spectrum of compound **3a**. Solvent: chloroform-*d*.

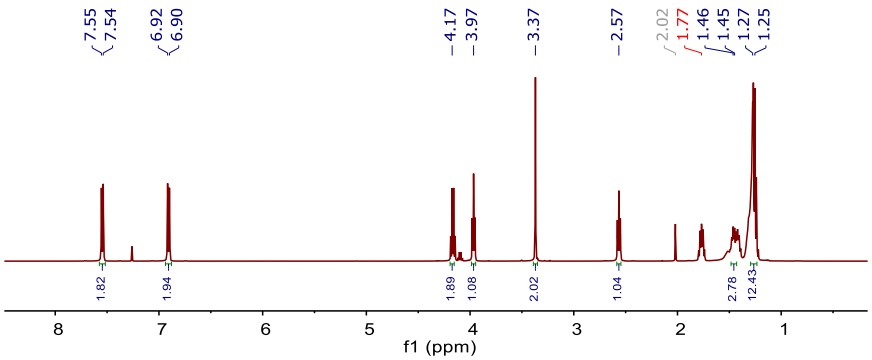

Figure 5.14 [1]H NMR spectrum of compound **3b**. Solvent: chloroform-*d*.

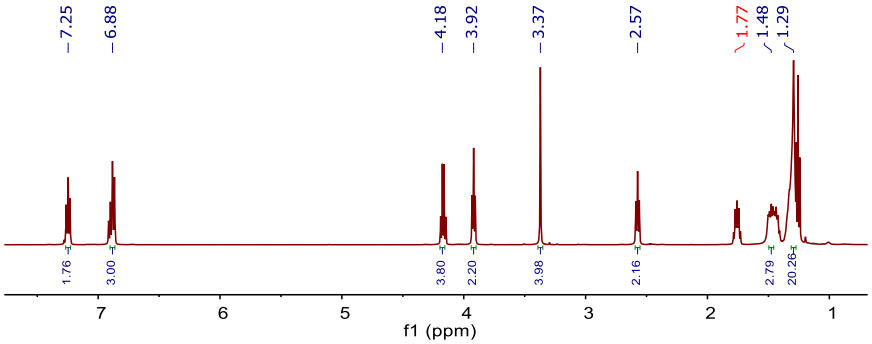

Figure 5.15 [1]H NMR spectrum of compound **3c**. Solvent: chloroform-*d*.

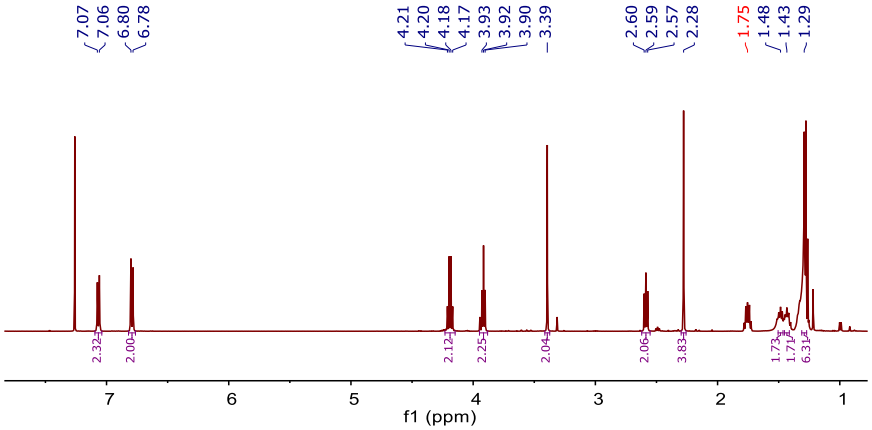

Figure 5.16 [1]H NMR spectrum of compound **3d**. Solvent: chloroform-*d*.

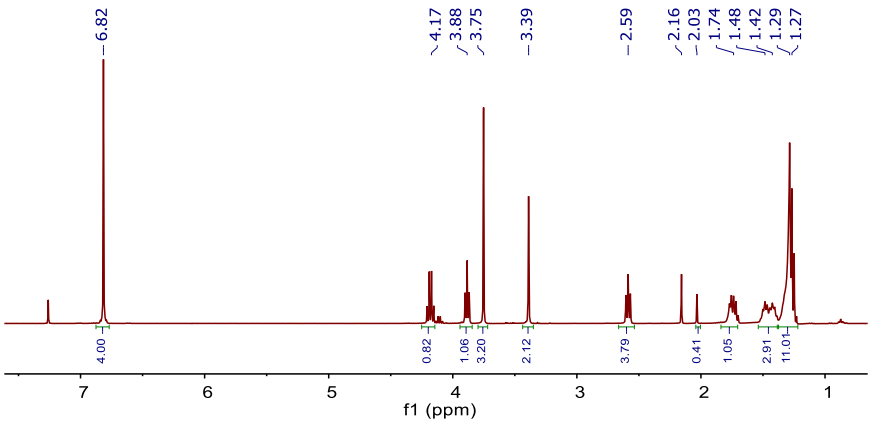

Figure 5.17 ^{1}H NMR spectrum of compound **3e**. Solvent: chloroform-*d*.

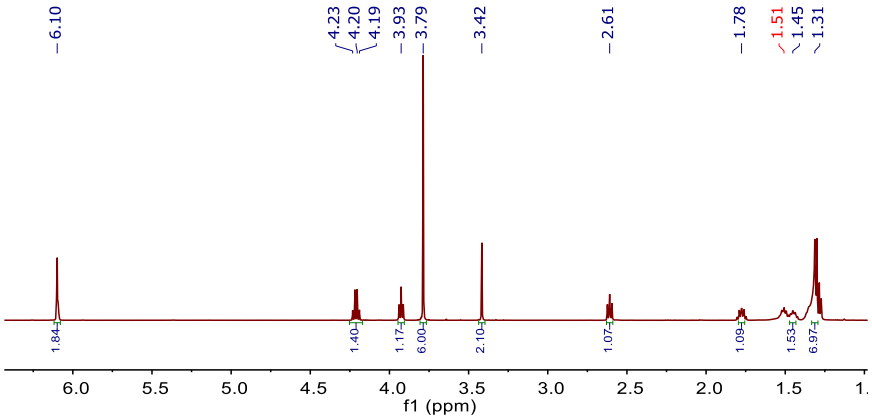

Figure 5.18 ^{1}H NMR spectrum of compound **3f**. Solvent: chloroform-*d*.

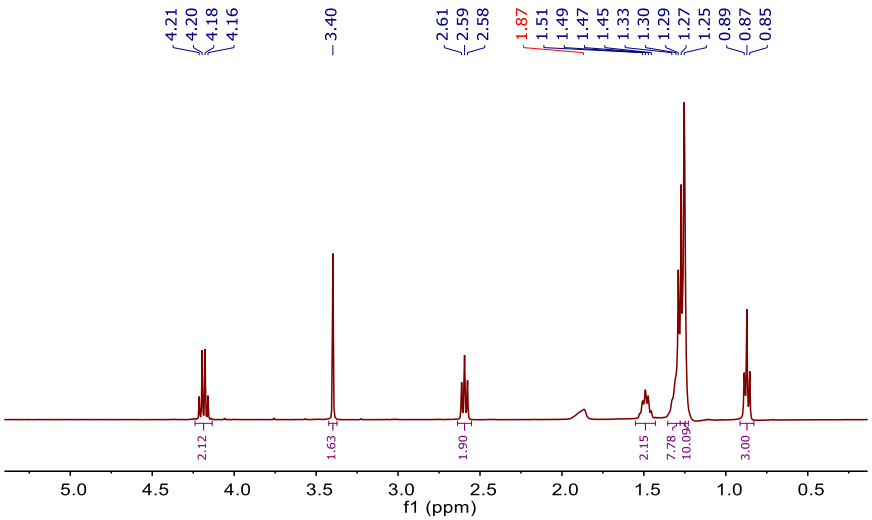

Figure 5.19 ^{1}H NMR spectrum of compound **3g**. Solvent: chloroform-*d*.

5.6 References

(1) Busseron, E.; Ruff, Y.; Moulin, E.; Giuseppone, N. Supramolecular Self-Assemblies as Functional Nanomaterials. *Nanoscale* **2013**, *5* (16), 7098 DOI: 10.1039/c3nr02176a.

(2) Isimjan, T. T.; de Bruyn, J. R.; Gillies, E. R. Self-Assembly of Supramolecular Polymers from β-Strand Peptidomimetic−Poly(Ethylene Oxide) Hybrids. *Macromolecules* **2010**, *43* (10), 4453–4459 DOI: 10.1021/ma100444b.

(3) Jin, H.; Huang, W.; Zhu, X.; Zhou, Y.; Yan, D. Biocompatible or Biodegradable Hyperbranched Polymers: From Self-Assembly to Cytomimetic Application. *Chem. Soc. Rev* **2012**, *41*, 5986–5997 DOI: 10.1039/c2cs35130g.

(4) Tu, Y.; Peng, F.; Adawy, A.; Men, Y.; Abdelmohsen, L. K. E. A.; Wilson, D. A. Mimicking the Cell: Bio-Inspired Functions of Supramolecular Assemblies. *Chem. Rev.* **2016**, *116* (4), 2023–2078 DOI: 10.1021/acs.chemrev.5b00344.

(5) Bae, Y.; Fukushima, S.; Harada, A.; Kataoka, K. Design of Environment-Sensitive Supramolecular Assemblies for Intracellular Drug Delivery: Polymeric Micelles That Are Responsive to Intracellular PH Change. *Angew. Chemie* **2003**, *115* (38), 4788–4791 DOI: 10.1002/ange.200250653.

(6) Zhang, J.; Sun, H.; Ma, P. X. Host−Guest Interaction Mediated Polymeric Assemblies: Multifunctional Nanoparticles for Drug and Gene Delivery. *ACS Nano* **2010**, *4* (2), 1049–1059 DOI: 10.1021/nn901213a.

(7) Jia, H.-Z.; Zhang, W.; Zhu, J.-Y.; Yang, B.; Chen, S.; Chen, G.; Zhao, Y.-F.; Feng, J.; Zhang, X.-Z. Hyperbranched–Hyperbranched Polymeric Nanoassembly to Mediate Controllable Co-Delivery of SiRNA and Drug for Synergistic Tumor Therapy. *J. Control. Release* **2015**, *216*, 9–17 DOI: 10.1016/J.JCONREL.2015.08.006.

(8) Lee, M.; Jang, C.-J., and; Ryu, J.-H. Supramolecular Reactor from Self-Assembly of Rod−Coil Molecule in Aqueous Environment. *J. Am. Chem. Soc.* **2004** *126* (26), pp 8082–8083 DOI: 10.1021/JA048264Z.

(9) Wang, Z. P.; van Oers, M. C. M.; van Hest, J. C. M.; Rutjes, F. Polymersome Pickering Emulsion for Enzyme Catalysis in a Biphasic System. *Abstr. Pap. Am. Chem. Soc.* **2014**, *247* (43), 10904–10908 DOI: 10.1002/ange.201206555.

(10) Azagarsamy, M. A.; Gomez-Escudero, A.; Yesilyurt, V.; Vachet, R. W.; Thayumanavan, S. Amphiphilic Nanoassemblies for the Detection of Peptides and Proteins Using Fluorescence and Mass Spectrometry. *Analyst* **2009**, *134* (4), 635 DOI: 10.1039/b818484d.

(11) Gillissen, M. A. J.; Voets, I. K.; Meijer, E. W.; Palmans, A. R. A. Single Chain Polymeric Nanoparticles as Compartmentalised Sensors for Metal Ions. *Polym. Chem.* **2012**, *3* (11), 3166–3174 DOI: 10.1039/c2py20350b.

(12) Subhadeep Basu; Dharma Rao Vutukuri, and; Thayumanavan*, S. Homopolymer Micelles in Heterogeneous Solvent Mixtures. *J. Am. Chem. Soc.* **2005**, *127* (48), pp 16794–16795 DOI: 10.1021/JA056042A.

(13) Combariza, M. Y.; Savariar, E. N.; Vutukuri, D. R.; Thayumanavan, S.; Vachet, R. W. Polymeric Inverse Micelles as Selective Peptide Extraction Agents for MALDI-MS

Analysis. *Anal. Chem.* **2007**, *79* (18), 7124–7130 DOI: 10.1021/ac071001d.

(14) Rodthongkum, N.; Chen, Y.; Thayumanavan, S.; Vachet, R. W. Matrix-Assisted Laser Desorption Ionization-Mass Spectrometry Signal Enhancement of Peptides after Selective Extraction with Polymeric Reverse Micelles. *Anal. Chem.* **2010**, *82* (9), 3686–3691 DOI: 10.1021/ac1000256.

(15) Rodthongkum, N.; Washington, J. D.; Savariar, E. N.; Thayumanavan, S.; Vachet, R. W. Generating Peptide Titration-Type Curves Using Polymeric Reverse Micelles As Selective Extraction Agents along with Matrix-Assisted Laser Desorption Ionization-Mass Spectrometry Detection. *Anal. Chem.* **2009**, *81* (12), 5046–5053 DOI: 10.1021/ac900661e.

(16) Rodthongkum, N.; Chen, Y.; Thayumanavan, S.; Vachet, R. W. Selective Enrichment and Analysis of Acidic Peptides and Proteins Using Polymeric Reverse Micelles and MALDI-MS. *Anal. Chem.* **2010**, *82* (20), 8686–8691 DOI: 10.1021/ac101922b.

(17) Rodthongkum, N.; Ramireddy, R.; Thayumanavan, S.; Richard, W. V. Selective Enrichment and Sensitive Detection of Peptide and Protein Biomarkers in Human Serum Using Polymeric Reverse Micelles and MALDI-MS. *Analyst* **2012**, *137* (4), 1024–1030 DOI: 10.1039/c2an16089g.

(18) Reczek, J. J.; Iverson, B. L. Using Aromatic Donor Acceptor Interactions to Affect Macromolecular Assembly. *Macromolecules* **2006**, *39*, 5601–5603 DOI: 10.1021/ma0611669.

(19) Beaujuge, P. M.; Fréchet, J. M. J. Molecular Design and Ordering Effects in π-Functional Materials for Transistor and Solar Cell Applications. *J. Am. Chem. Soc.* **2011**, *133* (50), 20009–20029 DOI: 10.1021/ja2073643.

(20) Rasband, W. S. ImageJ. US National Institutes of Health: Bethesda, Maryland, USA

(21) Reinicke, S.; Espeel, P.; Stamenović, M. M.; Du Prez, F. E. One-Pot Double Modification of p(NIPAAm): A Tool for Designing Tailor-Made Multiresponsive Polymers. *ACS Macro Lett.* **2013**, *2* (6), 539–543.

(22) Zhuang, J.; Jiwpanich, S.; Deepak, V. D.; Thayumanavan, S. Facile Preparation of Nanogels Using Activated Ester Containing Polymers. *ACS Macro Lett.* **2012**, *1* (1), 175–179.

(23) Eberhardt, M.; Mruk, R.; Zentel, R.; Théato, P. Synthesis of Pentafluorophenyl(Meth)Acrylate Polymers: New Precursor Polymers for the Synthesis of Multifunctional Materials. *Eur. Polym. J.* **2005**, *41* (7), 1569–1575.

CHAPTER

6. ANTIMICROBIAL STUDIES WITH SLIVER LOADED AMPHIPHILIC HOMOPOLYMERS

6.1 Introduction

Antibiotic resistanc[1] evolution and spread, generally caused by overuse or misuse of antibiotics, is now the greatest threat to successful antibiotic coverage and hence the driving force behind the development of new therapies[2]. To overcome the antibiotic resistance, one needs to either increase the dosage or change to another kind of antibiotics or develop new antibiotics. However, raising the antibiotic dosage without targeting or focusing on disease sites may harm other bacteria that benefit the body. Changing to another antibiotic or a combination of different antibiotics may eventually evolve multi-drug resistance. Unfortunately, development of new antibiotics requires decades to obtain clinical approval. Silver, a broad-spectrum antibiotic, has been known for centuries for its ability to kill bacterial and relatively low toxicity to human tissues. The mode of antibacterial action of silver is reported to be: i) interacting with the bacterial cell envelope[3]; ii) interacting with molecules inside the cells[4]; iii) producing reactive oxygen species[5]. However, using silver salt or silver particle alone may end up with a homogeneous distribution into the whole body and dramatically reduce the outcome efficacy. Enough silver components need to be accumulated into a target site at a short period to make it effective. Polymer delivery carriers, which are easily functionalized and bind with therapeutics, can be used to address this problem. In this chapter, we have designed the polymer with dithiol acetal structure, in which the approximate close position of the two thiol atoms and strong coordination interaction between thiol and silver ion could help to load silver onto the polymer. In the meantime, the polymer could also protect silver ion from destabilizing of the active moiety within an organometallic complex[6] and achieve sustained release[7].

6.2 Molecular design

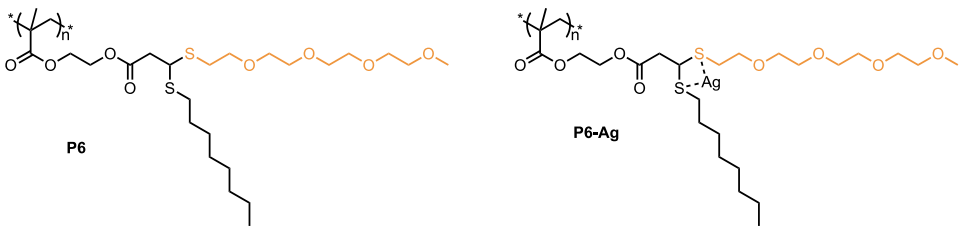

Scheme 6.1 Schematic chemical structure of polymer **P6** and **P6**-Ag.

With the dithiol acetal polymer prepared, we notice that it may have the ability to load silver ion onto the polymer due to the di-thiol structure and high binding affinity between thiol and silver. The further direction for the chapter 2 is to use amphiphilic homopolymer **P6** for silver loading and their subsequent antimicrobial studies.

6.3 Results and discussions

The **P6** polymer could self-assemble into spheric aggregates in aqueous solution (Figure 6.1B) with a size of 130 nm. The critical aggregation concentration (CMC) of **P6** is done by serial dilution of polymer solution and measurement of hydrodynamic size using DLS. The CMC for polymer **P6** is determined to be 10^{-8} M (Figure 6.1 A). Micelle at a concentration lower than 10^{-8} M shows unstable aggregates.

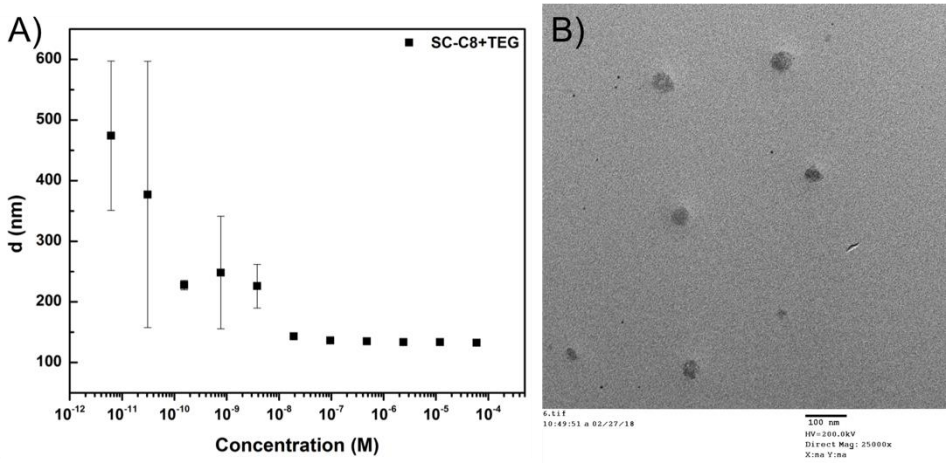

Figure 6.1 Self-assemble behavior study of polymer **P6**. A) TEM image of micelle-like aggregates; B) DLS size average with different micelle concentrations.

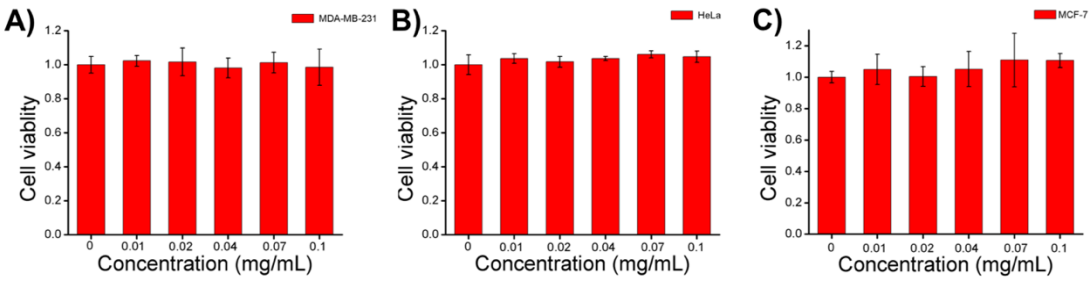

Figure 6.2 Cytotoxicity study of polymer **P6** with three different human cell lines: A) MDA-MB-231; B) HeLa; C) MCF-7.

Firstly, we have tested the toxicity of the polymer itself using three different cell lines including MDA-MB-231, HeLa and MCF-7. All three cell lines good viability (>90%) suggested that the polymer is biocompatible and no harm to human cells up to 0.1mg/mL concentration after 24 h incubation (Figure 6.2). (courtesy of Bin)

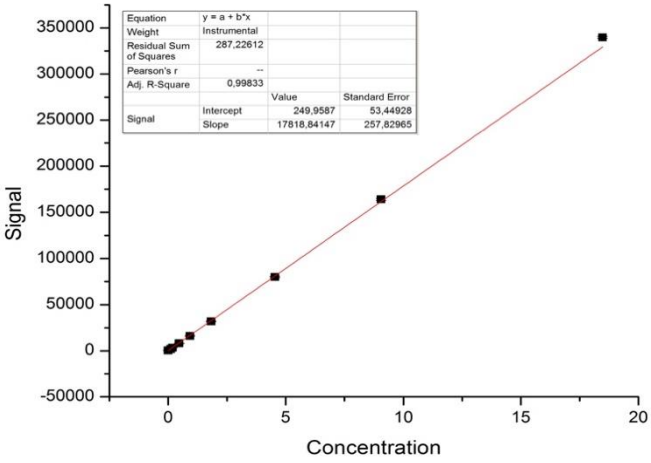

Item	ppm	ug/mL
6-155-1	109.8513	109.8513
6-155-2	103.6074	103.6074
6-155-3	91.9970	91.9970
Average	101.82±9.06	

Figure 6.3 Standard curve of ICP-MS for silver ion. The table is the triplicate ICP data.

Next, triple loading experiments were done at different dates and different times to make sure the data's reliability and repeatability. Typically, to 1 mL solution of 3.5 mg/mL of micelle prepared

from polymer P6, 200 μL of $AgNO_3$ solution (4 mg/mL) was added dropwise. The mixture was kept in the dark and stirred for overnight at room temperature. To remove the free unloaded Ag^+, the solution was washed thoroughly with nanopore water by using Amicon Ultra-4 centrifugal filter devices (3 kDa MWCO) more than four cycles. The absence of free Ag^+ was confirmed by checking the no formation of AgCl precipitates upon adding a saturated NaCl solution to the filtrate. The silver loading capacity was determined by ICP-MS (courtesy of Laura). Silver concentration standard curve was obtained first by measuring the ion signal of the prepared silver solution against different concentrations. The average loading capacity is about 101.8 ppm, and the loading efficiency is 2.5% based on the ICP results. The ratio of thiol: Ag^+ is calculated by comparing the moles of each in 1mL. It is around 10% of thiol monomers have been loaded with Ag^+. This data could provide guidance for the later on antimicrobial study.

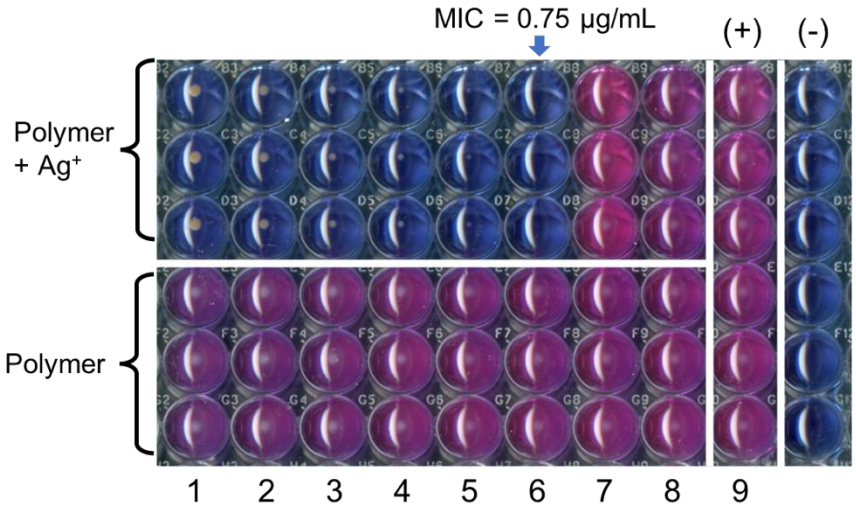

Figure 6.4 Antimicrobial study of polymer **P6** vs. **P6-Ag**. (Blue color represents dead bacteria; purple color represents live bacteria.

Next, the silver-loaded micelle was evaluated using minimal inhibition concentration (MIC) assay to determine its antimicrobial capability. The study based on the concentration of silver ion using MH broth. *E. coli* BL21 was used as model bacteria. *E. coli* was diluted to a final concentration of 2×10^5 CFU/mL in each well. Micelles with or without Ag^+-loading was tested with the final silver

concentrations ranging from 24 μg/mL to 0.47 μg/mL (serial half-fold dilution). The positive control was bacteria growth without any treatment, and the negative control was medium only. However, no visible MIC was detected for micelles without silver loaded after overnight incubation at 37 ºC. MIC for micelles with silver loaded was determined to be 0.75 μg/mL (Figure 6.6), which is comparable to free Ag+ MIC against E. *coli*[8]. The result was further confirmed by the alamarBlue assay (Figure 6.7). (courtesy of Ziwen)

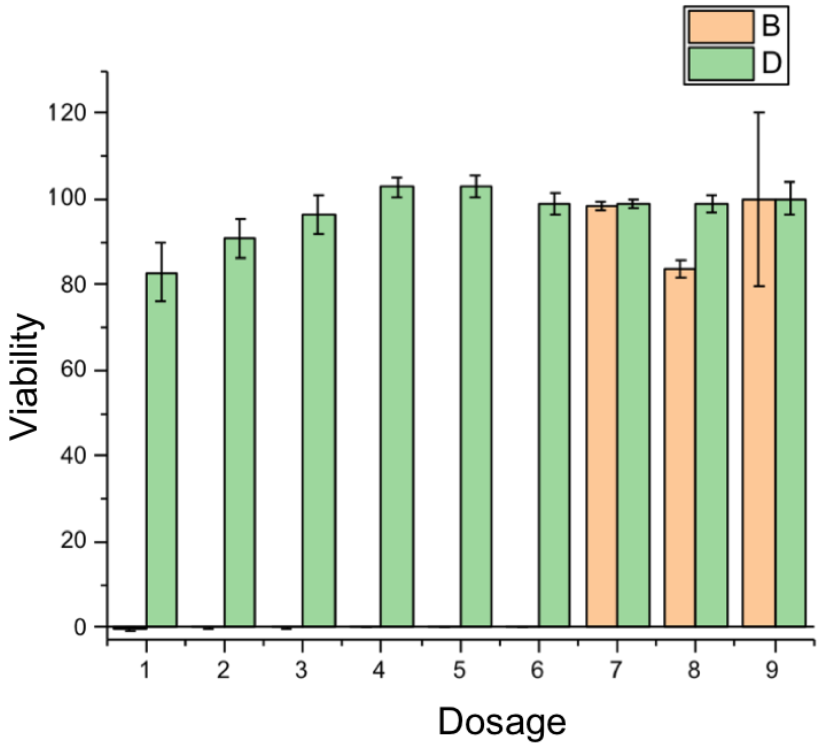

Figure 6.5 AlamarBlue assay of antimicrobial study for polymer **P6 (D)** vs. **P6-Ag (B)**.

6.4 Summary and further plans

In this chapter, the antimicrobial ability of polymer synthesized with dithiol structures loaded with silver ions was investigated. The polymer material is biocompatible with human cells and no harm to bacteria. While loaded with Ag^{+}, polymer **P6-Ag** has shown a MIC of 0.75 μg/mL against Gram-negative *E. Coli* bacteria. This preliminary data showed polymer could be used as a delivery carrier for potential antimicrobial applications.

Next, COOH is known to bind with Ag^+ through electrostatic interaction. Positive charged functional groups have been utilized for antimicrobial studies for decades. It will be interesting to investigate whether putting charged moieties on polymers will increase antimicrobial efficacy. For this purpose, polymers with a different charge, a positive charged polymer **P7** as well as negative charged polymer **P5** and their corresponding Ag^+ loading experiments need to be done to give a comparison with **P6**.

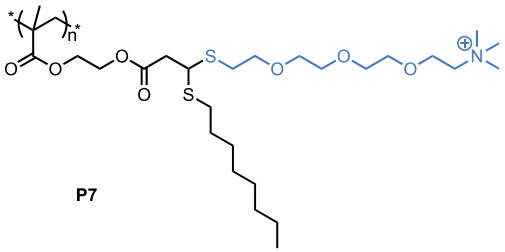

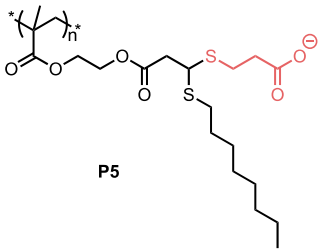

Other evidence of thiol-Ag coordination needs to be done: a) ICP-MS for the amount of Ag^+ loaded for **P5** and **P7**; b) XPS experiment for polymer loaded with silver ion and silver ion itself to determine the binding interaction between thiol and Ag^+. c) antimicrobial study with gram-negative bacteria (*E Coli*) and gram-positive bacteria (*B sub*) using polymer **P5**, **P6**, **P7,** and their efficacy comparison. d) a biocompatibility study of polymers and Ag^+ loaded polymers in mammalian cells to study the selectivity toward bacteria.

6.5 References

(1) Antibiotic Resistance Questions and Answers | Community | Antibiotic Use | CDC https://www.cdc.gov/antibiotic-use/community/about/antibiotic-resistance-faqs.html (accessed Aug 25, 2018).

(2) Silver, L. L.; Bostian, K. A. Discovery and Development of New Antibiotics: The Problem of Antibiotic Resistance. *Antimicrob. Agents Chemother.* **1993**, *37* (3), 377–383 DOI: 10.1128/AAC.37.3.377.

(3) Jung, W. K.; Koo, H. C.; Kim, K. W.; Shin, S.; Kim, S. H.; Park, Y. H. Antibacterial Activity and Mechanism of Action of the Silver Ion in Staphylococcus Aureus and Escherichia Coli. *Appl. Environ. Microbiol.* **2008**, *74* (7), 2171–2178 DOI: 10.1128/AEM.02001-07.

(4) Khadka, P.; Rao Krishnamurthi, V.; Alqahtany, M.; Wang, Y. New Insights into the Antimicrobial Mechanism of Silver Ions Revealed by Super-Resolution Fluorescence Microscopy. *Biophys. J.* **2018**, *114* (3), 347a DOI: 10.1016/j.bpj.2017.11.1938.

(5) Kędziora, A.; Speruda, M.; Krzyżewska, E.; Rybka, J.; Łukowiak, A.; Bugla-Płoskońska, G. Similarities and Differences between Silver Ions and Silver in Nanoforms as Antibacterial Agents. *Int. J. Mol. Sci.* **2018**, *19* (2), 444 DOI: 10.3390/ijms19020444.

(6) Lim, Y. H.; Tiemann, K. M.; Heo, G. S.; Wagers, P. O.; Rezenom, Y. H.; Zhang, S.; Zhang, F.; Youngs, W. J.; Hunstad, D. A.; Wooley, K. L. Preparation and in Vitro Antimicrobial Activity of Silver-Bearing Degradable Polymeric Nanoparticles of Polyphosphoester-Block-Poly(l-Lactide). *ACS Nano* **2015**, *9* (2), 1995–2008 DOI: 10.1021/nn507046h.

(7) Hindi, K. M.; Ditto, A. J.; Panzner, M. J.; Medvetz, D. A.; Han, D. S.; Hovis, C. E.; Hilliard, J. K.; Taylor, J. B.; Yun, Y. H.; Cannon, C. L.; Youngs, W. J. The Antimicrobial Efficacy of Sustained Release Silver-Carbene Complex-Loaded l-Tyrosine Polyphosphate Nanoparticles: Characterization, in Vitro and in Vivo Studies. *Biomaterials* **2009**, *30* (22), 3771–3779 DOI: 10.1016/j.biomaterials.2009.03.044.

(8) Radzig, M. A.; Koksharova, O. A.; Khmel', I. A. Antibacterial Effects of Silver Ions on Growth of Gram-Negative Bacteria and Biofilm Formation. *Mol. Genet. Microbiol. Virol.* **2009**, *24* (4), 194–199 DOI: 10.3103/S0891416809040065.

CHAPTER

7. SUMMARY AND FUTURE DIRECTIONS

7.1 Summary

In summary, we have successfully designed, synthesized and studied multifunctional amphiphilic polymers. In chapter 2, we have utilized thiol-yne nucleophilic click reactions to prepare amphiphilic homopolymers with the di-thiol acetal functional group on the polymer side chain. The resultant polymers were tested for different applications ranging from analytes detection, responsive therapeutic delivery to antimicrobial activity. In chapter 3, dithiol acetal functional groups were incorporated onto polymer backbone by polymerizing a bi-functional monomer with both thiol and alkyne group at termini and post modification of backbone with a different thiol species. This polymer structure was found to possess enhanced ROS responsiveness. In chapter 4, a clickable polystyrene-based polymer was synthesized, and its feasibility of being a clickable platform was tested by post modification of various polar functional groups. The outcome polymers were demonstrated to be used for bio analytes detection in a complex mixture. In chapter 5, a mechanism underlying the signal enhancement phenomenon was investigated by varying of the electron density of matrix and polymer. We have found that a complementary electron pair on aromatic rings between the MALDI matrix and amphiphilic homopolymer could help to form large aggregate and therefore enhance the signal in the mass spectrum. In chapter 6, a preliminary antimicrobial study was performed using silver loaded amphiphilic homopolymer. The amphiphilic homopolymer showed good biocompatibility with mammalian cells by itself. Antimicrobial activity against bacterial of polymers after binding with silver ion was confirmed.

7.2 Further direction

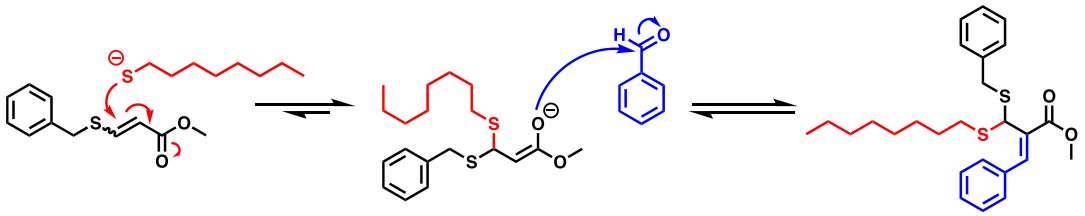

Scheme 7.1 Molecular design of tri-functional molecule design through enol trapping.

Multifunctional materials have been attracting significant attention. Recently, we have found that vinyl thiol structure could display dynamic thiol exchange, and we sought whether we could transfer this phenomenon to a broad range of material synthesis. The kinetics of thiol exchange has been reported before, but the thermodynamic nature of the exchange has not yet been explored. Our preliminary data (Figure 3.20-21) show that aliphatic thiols are more stable, while aromatic thiols are more dynamic and easier to be swapped with another thiol group. After the investigation of potential thiol exchange mechanism, we are interested to see the intermedia that might be present during the exchange process. If our hypothesis is correct, adding an enol trapper should be able to yield a trifunctional molecule. This approach could open a new way for multifunctional materials preparation. In the meantime, this enol trapper could help to stop potential thiol exchange and generate a more stable product.

APPENDIX

INVESTIGATION OF BETA ATOM EFFECT ON HYDROLYSIS RATE OF ESTERS IN ACIDIC CONDITIONS

INTRODUCTION

Material stability under different pH has always been considered as a big issue in the material industry. The pH-responsive property has been long utilized in material science and chemistry therapeutic delivery[1,2] field due to its simplicity and biological relevant[3]. pH-responsive materials often fall into two categories: (i) non-cleavable charge conversion (protonation and deprotonation); (ii) cleavable functional group (hydrazine linkages[4], cis-aconityl linkages[5], ortho esters[6], ketal/acetal linkages[7]). Among the pH-responsive functional groups, cleavable function groups under low pH are more attractive because of their biologic relevancy. For an instant, tumor tissue environment has pH~5.0. A low pH responsive material could be used for tumor therapeutics delivery, imaging diagnosis, and cancer treatment.

Despite all of the cleavable functional groups, ester function group hasn't been treated as a pH-responsive moiety in acidic condition. Their cleavages or hydrolytic behaviors haven't been considered either as a pH-responsive manner. Since water is such a poor nucleophile[8] compare to a hydroxyl group, the rate of nucleophilic addition with an ester is generally very slow, meaning under acidic condition, ester materials are known to be relatively stable. However, recently, researchers have found out that with the help of thiol atom at the beta position to ester especially, the resulting beta thiol ester will possess pH responsiveness and can be cleaved easily at acidic pH[9]. This kind of ester is known as a beta-thiol ester or beta thiol propionate. Beta-thiol ester has been considered to be pH responsive (acid-labile functional group) and shown as a promising candidate since then about one and a half decade ago[9,10]. Also, because of its ease to synthesize

through Michael addition of a thiol reagent to an electron deficient vinyl group, a large number of papers has been published utilizing beta-thiol ester as a linker to introduce pH sensitivity to their molecules. Our group[11] as well as other research groups[12–16] have involved in developing acid labile beta thiol ester materials for therapeutics delivery for cancer treatment or other applications based on this feature. Those delivery carriers were designed to be temporarily inactive and serve as a drug reservoir for pH-responsive controlled release.

One of the possible mechanisms for the pH responsiveness is thought to be the inductive effect from the sulfur atom, which makes the carbonyl carbon more charge positive and electrophilic. This will further favor water molecule attacking and hydrolysis on the ester bond. Another possible mechanism is that thiol atom at the beta position could facilitate a six-member ring[13,17] formation with proton (Figure 1B), and this six-member ring could be stabilized by thiol atom and then allow water molecule to attack efficiently. However, in most of the cases, beta-thiol ester pH responsiveness has been tested or proven true through indirect ways within complicated systems, either by monitoring the release of the encapsulated cargo from a micelle aggregate or the degradation of the material (e.g., weight loss, mass swelling, aggregates size change)[18]. Though its hydrolytically behavior has been studied under basic condition[19] (pH 7.4 and pH 8.0), single ester bond cleavage study in small molecules under acidic condition has not been done yet. In another case, a comparison hydrolysis rate of an ester between sulfide, sulfoxide, and sulfone locating at beta-position was performed, and results have shown that due to the inductive effect, hydrolysis rate of sulfonate is faster than the one with sulfone than sulfur at physiological pH[20]. In a linker length effect study, Hubbell group[21] has conjugated a drug molecule on to PEG-based hydrogel through ester bond with sulfur near it. Hydrolytic study of drug molecule from ester bond has shown that due to the inductive effect of the sulfide on the ester bond, under physiological pH,

increasing number if methylene units on the ester would slow down the hydrolysis rate[19]. The similar hydrolytic study has done on thiol esters in a polymeric hydrogel at pH 7.4 and pH 9.8. Results showed that esters are prone to be cleaved faster under more basic conditions [22]. Until now, to the best of our knowledge, there is no direct and comprehensive study has shown to compare the hydrolysis behavior of esters under acidic condition with a variant atom at the beta position to examine their effect. Driven by the desire to uncover the mystery of beta-thiol ester acid labile property, herein, we would like to investigate all the beta-X ester hydrolysis progress using NMR directly and investigate the mechanism of hydrolysis behavior. In the end, we will challenge the well-accepted conception: beta-thiol ester is pH sensitive. Fast hydrolysis rate for beta thiol ester under acidic pH is found to be unlikely true in our study. More mechanism study will be needed to help explain the reason behind other people's cases.

In this chapter, we attempt to show that nonetheless valuable mechanistic information can be obtained from a study of ester hydrolysis kinetics in acid condition from three libraries of ester molecules (totally seven small molecules, six amphiphiles, and four polymers). Moreover, with the help of molecular modeling and calculation, we hope in this chapter we could gain some insight into the difference of hydrolysis behaviors of the ester with beta hetero atoms in acidic pH.

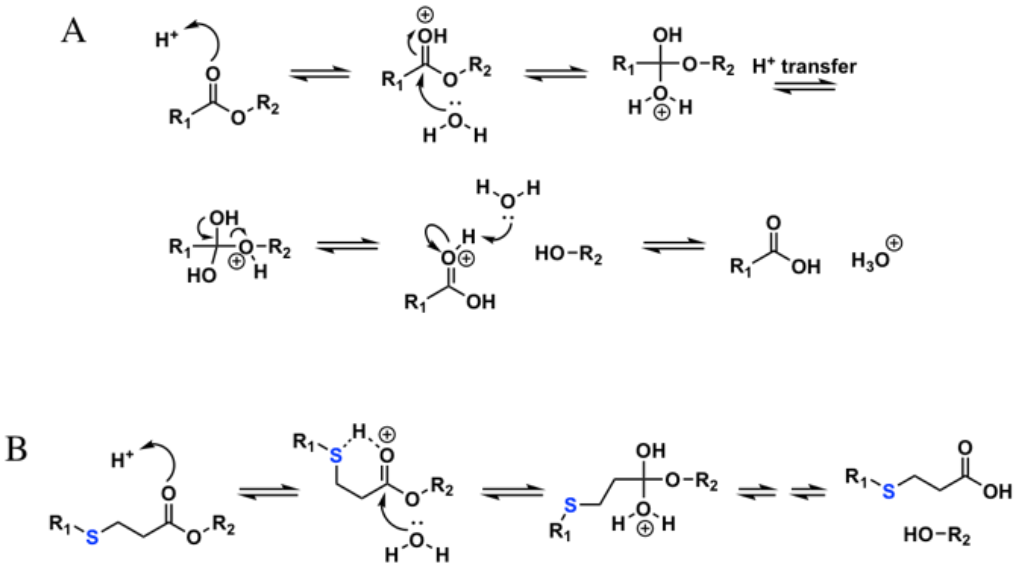

Scheme 1. Well-established mechanism of the hydrolysis of ester at acid pH. (A) generalized mechanism of hydrolysis (slow). (B) mechanism of hydrolysis for beta-thiol ester (fast).

RESULTS AND DISCUSSIONS

Firstly, the small molecule library (**1**-**7**) were designed and utilized for the acid catalyst hydrolysis study. Esters (**1**-**5**) with identical chemical structures were used to compare the different beta atoms effect on acidic hydrolysis rate. The esters investigated here are methyl esters, chosen to vary one structural parameter at one time. The atoms we chose are Carbon (**1**), Nitrogen (**2**), Oxygen (**3**), Sulfur (**4**), Selenium (**5**). A conjugated sulfur ester (**6**) and bis-sulfur ester (**7**) were added to the list to further test the hypothesis, which is if beta-thiol ester acid lability is due to the inductive effect[21] or facilitated six-member ring formation[17] from the sulfur atom, a bis-sulfur (**7**) structure should have an even more significant effect and therefore hydrolyzed faster than one sulfur ester (**4**). The hydrolyzed process was performed in an NMR tube with acetonitrile-d_3/D_2O as co-solvent and TFA as the acid catalyst. The progress was examined by monitoring the generation of MeOH that being hydrolyzed from methyl ester overtime at peak around 3.31 ppm (Figure 1B). However, to our surprise, the 7 small molecules seem to fall into three groups. As shown in figure 3A, Carbon (**1**) has the fastest hydrolysis rate ($t_{1/2}$~ 400 hrs.), followed by the second group ($t_{1/2}$~ 800 hrs.),

containing Oxygen (**3**), Sulfur (**4**) and Selenium (**5**). The rest three (**2**, **6**, **7**) showed very slow hydrolysis rate. These trends illustrated: 1) If we only compare the three esters with different atoms at beta-position to test the above hypothesis, we would obtain the following order: the hydrolysis rate is Carbon > Sulfur > Bis-Sulfur. 2) Ester with a conjugate structure (**6)** which has the highest inductive effect on the carbonyl carbon among the others showed negligible hydrolysis in acidic condition. 3) Another interesting observation is that ester with nitrogen has a significant slow hydrolysis rate. We assume that, since we use one equivalent of TFA over ester molecule, the proton is prone to protonate nitrogen rather than carbonyl oxygen which leading to not availability for hydrolysis anymore. This hypothesis was tested by adding two equivalents of TFA into the mixture and see whether Nitrogen ester will re-gain some hydrolysis. Not surprisingly, we observed accelerated hydrolysis rate for esters **1**-**5** and **7**. Also, we found that all other six molecules still followed the same trend except the nitrogen ester, which exhibits significant hydrolysis compare to one equivalent amount of TFA condition. Its hydrolysis rate changed from slower than bis-sulfur **7** to faster than it, but still much slower than **1**, **3**, **4**, **5**. To summarize, all seven esters exhibited relatively slow hydrolysis rates in acidic conditions (e.g., $t_{1/2}$ > 400 hrs. with 1eq of TFA; $t_{1/2}$ > 250 hrs. with 2 eq of TFA) compare to basic hydrolysis process. In acidic condition, there is no advantage in hydrolysis for beta-thiol ester (**4**) over carbon ester (**1**) in this comparison.

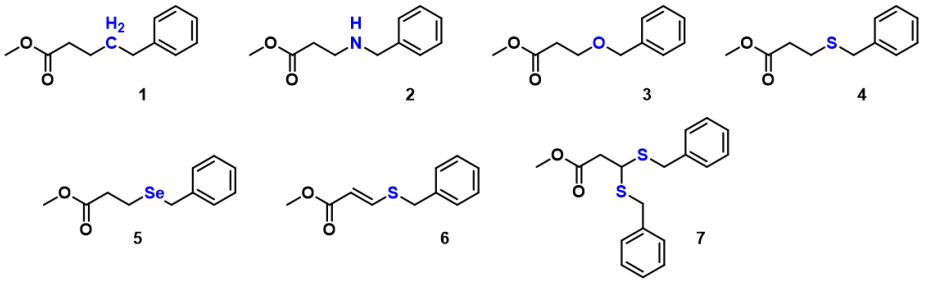

Chart 1. Chemical structures of small molecule series I.

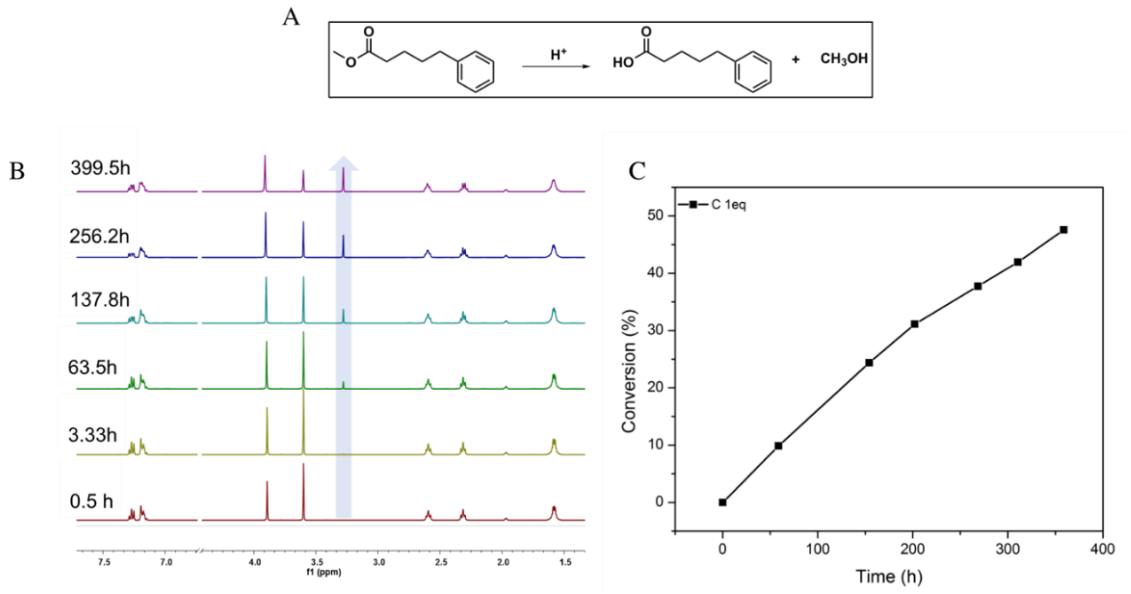

Figure 1. Hydrolysis of molecule **1** at the acidic condition. (A) Hydrolysis reaction studied, (B) NMR spectra of the hydrolytic process (arrow showed methanol generated after hydrolysis), (C) Hydrolysis kinetics.

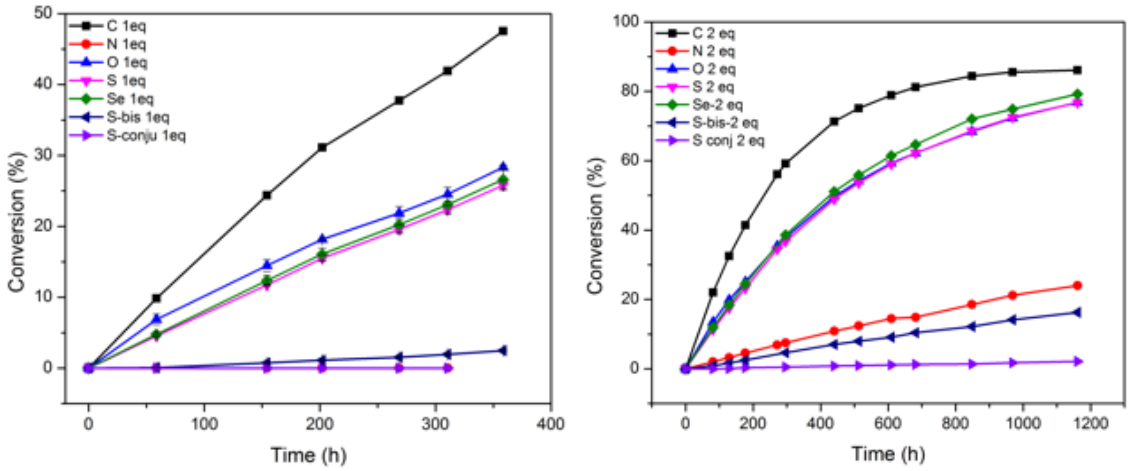

Figure 2. Summary of hydrolysis rate of molecules (**1**~**7**). (A) 1.0 equiv. and (B) 2.0 equiv. of H^+ with respect to ester molecules.

Next, to further investigate the hydrolysis process in an aqueous solution, we have synthesized a series II of six small water-soluble amphiphiles with hydrophilic oligo ethylene glycol moiety and hydrophobic moiety (aliphatic and aromatic) connected with an ester linkage (Chart 2). Doing so, we could be able to study the hydrolysis process in the pure D_2O system which resembles the real case. Besides the acidic TFA/D_2O condition, two buffer solution systems were

added for better control. Totally, 24 samples were prepared, including four conditions: 1.0 eq of TFA, 2.0 eq of TFA, pD = 5.0 and pD = 7.4 for each small amphiphile molecule (80 mM). NMR was used to monitor the hydrolytic process. The integration of methoxyl peak in each amphiphile was used as an internal standard. As shown in Figure 4C and 4D, in an acidic D_2O system with TFA as a proton source, similar phenomena with small molecule series I were observed when comparing between amphiphile **8**, **9** and **10** (or **11**, **12** and **13**): Carbon > Sulfur > Nitrogen. These profiles are consistent with the small molecule hydrolysis behavior. This trend is true for both the alkane chain (**8**~**10**) and aromatic chain (**11**~**13**). Interestingly, for Carbon amphiphiles, aromatic one (**11**) hydrolyzed slowly in the first 200 h, it even slower than Thiol amphiphiles, but accolated fast after that. At 500 hrs., both aromatic amphiphiles (**11**, **13**) hydrolyzed faster than their aliphatic form (**8**, **10**). While as in PB buffer solution (shown in Figure 4A and 4B), we observed an opposite trend, which is Nitrogen amphiphilic esters (**9**, **12**) got hydrolyzed in the fastest rate, both in pD = 5.0 (Figure 4A) and pD = 7.4 (Figure 4B). Nitrogen amphiphilic ester with an aromatic hydrophobic moiety (**12**) exhibited a faster hydrolysis rate than the aliphatic one (**9**) in both pH conditions. This may due to the self-destroyed effect with nucleophilic primary amine located nearby[23,24]. Interestingly, Carbon and Sulfur esters didn't show any significant difference within buffer solvent.

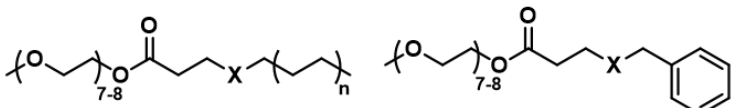

8 X=C, n=3
9 X=N, n=4
10 X=S, n=3
11 X=C
12 X=N
13 X=S

Chart 2. Chemical structure of amphiphiles series II.

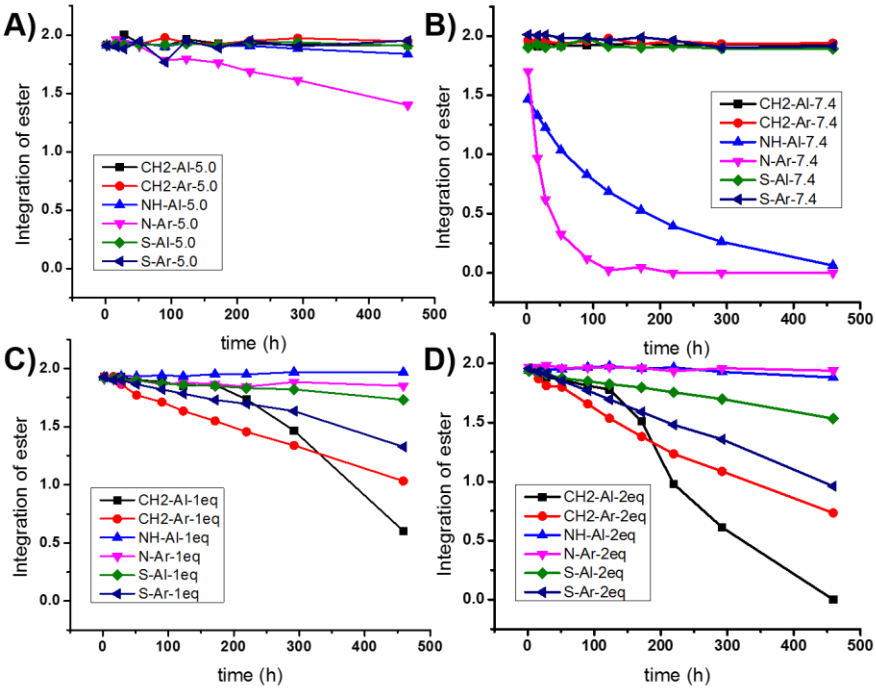

Figure 3. Summary of the hydrolytic process with molecules (**8**~**13**) at different pH. PB buffer with pH=5.0 (A) and pH=7.4 (B) in D_2O. TFA was used as an acid catalyst: 1.0 equiv. (C) and 2.0 equiv. (D) of TFA with respect to the number of moles of amphiphiles.

Since small amphiphiles are known to form micelle-like aggregates and have the capability of encapsulation of hydrophobic guest molecules (such as Nile Red, a dye with UV and fluorescence readout). We then study the ester bond cleavage indirectly by used UV-vis spectrum. Once the ester bond was cleaved, hydrophilic-lipophilic balance (HLB) of the amphiphiles was interrupted to yield less stable micelle assembly. Therefore, their encapsulation capability will be disrupted, and guest molecules will be released out and tested using UV-vis spectroscopy. Releasing profiles showed that within both buffer solutions utilized (PBS and Tris-base: pH 5.0 and pH 7.4), we didn't observe any evidence indicating that beta-thiol amphiphilic ester hydrolyzed faster than other amphiphilic esters (Experimental detail), which ruled out the hydrophobic environment effect on the hydrolysis process.

Moreover, an NMR study of residues from the hydrolysis product of esters was performed[25]. Instead of reacting in an NMR tube, ten folds of TFA was added into water phase containing amphiphilic esters in a small vial with stirring bar. After 24 h reaction, the water phase was lyophilized, and the residue was re-dissolved in $CDCl_3$ and subjected to NMR. However, even in this extreme condition, no ester cleavage evidence was observed either (supportive information).

Meanwhile, amphiphilic ester hydrolytic process in Tris-base buffer was also monitored by ESI-MS. Hydrolytic samples from different time intervals were diluted with methanol and subjected to ESI-MS. New molecular weight was expected after the cleavage. However, during the period the experiment performed, no significant change or new mass/charge peaks have been observed. (experimental detail) This may because: 1) the hydrolytic product is not prone to be ionized; 2) the hydrolytic process is slow to all amphiphilic esters including thiol esters. ESI-MS data have suggested that thiol ester is not showing any specialty over other esters in this reaction condition.

Finally, a series of four PEG polymers were synthesized with a pro fluorophore attached to the end through an ester bond. As scheme 3 showed, the pro fluorophore had little or no fluorescence when it is an ester form and attached to the polymer. When being cleaved from the ester bond to become its pristine hydroxyl form, the fluorophore (4-methylumbelliferone) will re-gain its fluorescence signal[26]. By doing this, we would be able to detect the hydrolysis behavior in the aqueous phase and with significant low concentration, which is hard to realize using the NMR technique. Four PEG polymers were synthesized with a variant of the atom at their beta position to the ester bond which connected to the pro fluorophore. The study was performed under conditions of PB as well as TFA catalyst. Since the starting point of the fluorescence spectrum is different, we normalized all the intensity from the same starting point. From Figure 5A, we could

see that, after normalization, with 1 equiv. of TFA as catalyst, Oxygen > Carbon > Nitrogen > Sulfur. The same phenomenon was observed with 10 equiv. and 100 equiv. of TFA as proton source (data not shown). Hydrolysis of 4-methylumbelliferone from PEG polymer under PB buffer was summarized in Figure 5B, which showed us that Carbon is faster than Sulfur in both pH 7.4 and 5.0 condition.

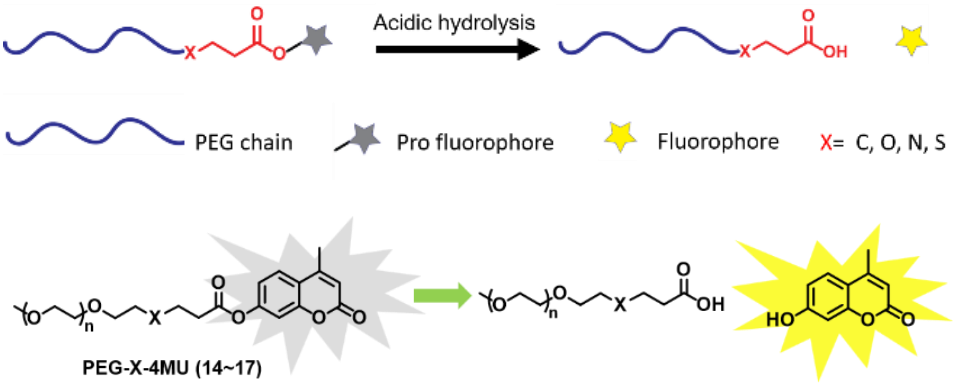

Scheme 2. Illustration of fluorescence turns on by hydrolysis of 4-methylumbelliferone (4MU) from PEG chain.

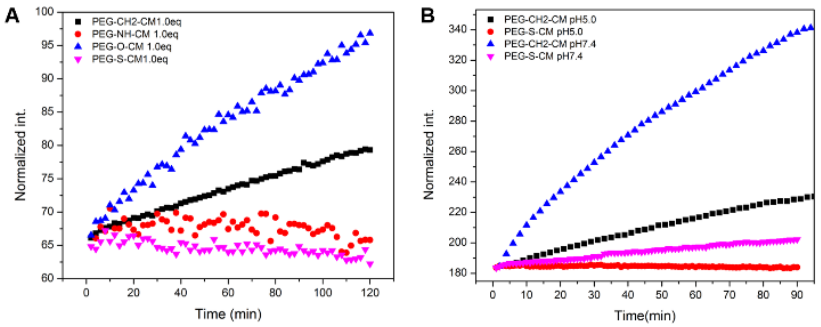

Figure 4. Fluorescence of 4-methylumbelliferone hydrolyzed from PEG over time at A) pH = 5.0 vs. pH = 7.4; B) with 1.0eq of TFA.

SUMMARY

In summary, we have test three molecule libraries from small hydrophobic molecules to small amphiphiles to large hydrophilic PEG molecules. In each series, we have kept the same of molecular structure expect the atom at the beta position. NMR study of those molecules has been done, but on no occasion have we observe any accelerated or fast hydrolysis in Sulfur based

molecules compared to Carbon-based molecules. Beta thiol ester itself is not special in its acid labile behavior, in contrast, it stays stable under all conditions we tested. However, it's working in other people's system may suggest that acid responsiveness may happen when complexed with other molecules. The mechanism underlines the complexed system is still under-investigated. Extensive computational studies are prone to help understand the mechanism of esters hydrolysis process under acidic conditions, the results of which will be released soon in due course.

EXPERIMENTAL SECTION

Reagents. Methyl 5-Phenylvalerate (**1**) (CAS#: 20620-59-1) was purchased from TCI. Methyl 3-(N-Benzylamino) propionate (**2**) (CAS#:23574-01-8) was purchased from Santa Cruz Biotechnology. Methyl 3-(benzyloxy)propanoate (**3**) (CAS#: 4126-60-7) was purchased from Ark Pham, Inc. Dibenzyl diselenide (CAS#: 1482-82-2) and Methyl propiolate (CAS#: 922-67-8) were purchased from Alfa Aesar. Benzyl mercaptan, methyl 3-brompropionate, methyl acrylate, acryloyl chloride, 4-methylumbelliferone and trifluoroacetic acid (TFA) were purchased from Sigma-Aldrich. Sodium borohydride was purchased from Acros Organics. mPEG-SH (Mw=2,000) was purchased from Laysan Bio, Inc. mPEG-COOH (Mw=2,000) and mPEG-NH_2 (Mw=2,000) was purchased from Nanocs. Dichloromethane (DCM), acetonitrile (MeCN), hydrochloric acid (HCl), purified water, Tris(hydroxymethyl)-aminomethane (Tris buffer), were obtained from Fisher Scientific. THF was distilled over Na/Ph_2CO before use.

3 Series of Molecules Synthesis and Characterization. Series I: Four small molecules (**4-7**) were synthesized through either esterification or Michael addition[27] to study the effect of atom on ester hydrolysis in CD_3CN/D_2O mixture using NMR. Series II: six oligo ethylene glycol amphiphiles (**8-13**) were synthesized to study the effect of an atom on ester hydrolysis in D_2O and buffer solution using NMR and UV-vis. Series III: four polyethylene glycol-umbelliferon (**14-17**)

were synthesized study the effect of an atom on ester hydrolysis in H_2O using fluorimeter. Refer to Supplementary Information for synthetic and characterization details.

Hydrolytic Study of Molecule Series 1 and 2[3]. 10 mmol of the ester molecules was dissolved in 0.3 mL of CD_3CN, and then 0.1 mL of TFA solution (in D_2O, 50mM) was added for hydrolysis. The corresponding hydrolytic process was monitored by 400 MHz NMR at room temperature.

REFERENCES

(1) Elsabahy, M.; Wooley, K. L. Design of Polymeric Nanoparticles for Biomedical Delivery Applications. *Chem. Soc. Rev.* **2012**, *41* (7), 2545 DOI: 10.1039/c2cs15327k.

(2) Gao, W.; Chan, J. M.; Farokhzad, O. C. PH-Responsive Nanoparticles for Drug Delivery. *Mol. Pharm.* **2010**, *7* (6), 1913–1920 DOI: 10.1021/mp100253e.

(3) Liu, B.; Thayumanavan, S. Substituent Effects on the pH Sensitivity of Acetals and Ketals and Their Correlation with Encapsulation Stability in Polymeric Nanogels. *J. Am. Chem. Soc.* **2017**, *139* (6), 2306–2317 DOI: 10.1021/jacs.6b11181.

(4) Etrych, T.; Jelínková, M.; Říhová, B.; Ulbrich, K. New HPMA Copolymers Containing Doxorubicin Bound via PH-Sensitive Linkage: Synthesis and Preliminary in Vitro and in Vivo Biological Properties. *J. Control. Release* **2001**, *73* (1), 89–102 DOI: 10.1016/S0168-3659(01)00281-4.

(5) Shen, W.-C.; Ryser, H. J.-P. Cis-Aconityl Spacer between Daunomycin and Macromolecular Carriers: A Model of pH-Sensitive Linkage Releasing Drug from a Lysosomotropic Conjugate. *Biochem. Biophys. Res. Commun.* **1981**, *102* (3), 1048–1054 DOI: 10.1016/0006-291X(81)91644-2.

(6) Heller, J.; Barr, J.; Ng, S. Y.; Abdellauoi, K. S.; Gurny, R. Poly(Ortho Esters): Synthesis, Characterization, Properties and Uses. *Advanced Drug Delivery Reviews*. 2002, pp 1015–1039.

(7) Gillies, E. R.; Goodwin, A. P.; Fréchet, J. M. J. Acetals as pH-Sensitive Linkages for Drug Delivery. In *Bioconjugate Chemistry*; American Chemical Society, 2004; Vol. 15, pp 1254–1263.

(8) Yates, K. Kinetics of Ester Hydrolysis in Concentrated Acid. *Acc. Chem. Res.* **1971**, *4* (4), 136–144 DOI: 10.1021/ar50040a003.

(9) Oishi, M.; Sasaki, S.; Nagasaki, Y.; Kataoka, K. pH-Responsive Oligodeoxynucleotide (ODN) - Poly (Ethylene Glycol) Conjugate through Acid-Labile -Thiopropionate Linkage : Preparation and Polyion Complex Micelle Formation. *Biomacromolecules* **2003**, *4* (5), 1426–1432 DOI: 10.1021/bm034164u.

(10) Oishi, M.; Nagasaki, Y.; Itaka, K.; Nishiyama, N.; Kataoka, K. Lactosylated Poly(Ethylene Glycol)-SiRNA Conjugate through Acid-Labile Beta-Thiopropionate Linkage to Construct PH-Sensitive Polyion Complex Micelles Achieving Enhanced Gene Silencing in Hepatoma Cells. *J. Am. Chem. Soc.* **2005**, *127* (6), 1624–1625 DOI: 10.1021/ja044941d.

(11) Molla, M. R.; Marcinko, T.; Prasad, P.; Deming, D.; Garman, S. C.; Thayumanavan, S. Unlocking a Caged Lysosomal Protein from a Polymeric Nanogel with a pH Trigger. *Biomacromolecules* **2014**, *15* (11), 4046–4053 DOI: 10.1021/bm501091p.

(12) Jamal, S.; Rezaei, T.; Sarbaz, L.; Niknejad, H. Folate-Decorated Redox/PH Dual-Responsive Degradable Prodrug Micelles for Tumor Triggered Targeted Drug Delivery. *RSC Adv.* **2016**, *6*, 62630–62639 DOI: 10.1039/c6ra11824k.

(13) Lv, S.; Tang, Z.; Zhang, D.; Song, W.; Li, M.; Lin, J.; Liu, H.; Chen, X. Well-Defined Polymer-Drug Conjugate Engineered with Redox and PH-Sensitive Release Mechanism for Efficient Delivery of Paclitaxel. *J. Control. Release* **2014**, *194*, 220–227 DOI: 10.1016/j.jconrel.2014.09.009.

(14) Chen, C. K.; Wang, Q.; Jones, C. H.; Yu, Y.; Zhang, H.; Law, W. C.; Lai, C. K.; Zeng, Q.; Prasad, P. N.; Pfeifer, B. A.; Cheng, C. Synthesis of pH-Responsive Chitosan Nanocapsules for the Controlled Delivery of Doxorubicin. *Langmuir* **2014**, *30* (14), 4111–4119 DOI: 10.1021/la4040485.

(15) He, J.; Xia, Y.; Niu, Y.; Hu, D.; Xia, X.; Lu, Y.; Xu, W. PH-Responsive Core Crosslinked Polycarbonate Micelles via Thiol-Acrylate Michael Addition Reaction. *J. Appl. Polym. Sci.* **2017**, *134* (5) DOI: 10.1002/app.44421.

(16) Zhu, L.; Ye, Z.; Cheng, K.; Miller, D. D.; Mahato, R. I. Site-Specific Delivery of Oligonucleotides to Hepatocytes after Systemic Administration. *Bioconjug. Chem.* **2008**, *19* (1), 290–298 DOI: 10.1021/bc070126m.

(17) Zou, J.; Zhang, F.; Zhang, S.; Pollack, S. F.; Elsabahy, M.; Fan, J.; Wooley, K. L. Poly(Ethylene Oxide)- *Block* -Polyphosphoester- *Graft* -Paclitaxel Conjugates with Acid-Labile Linkages as a PH-Sensitive and Functional Nanoscopic Platform for Paclitaxel Delivery. *Adv. Healthc. Mater.* **2014**, *3* (3), 441–448 DOI: 10.1002/adhm.201300235.

(18) Metters, A.; Hubbell, J. Network Formation and Degradation Behavior of Hydrogels Formed by Michael-Type Addition Reactions. *Biomacromolecules* **2005**, *6* (1), 290–301 DOI: 10.1021/bm049607o.

(19) Rydholm, A. E.; Anseth, K. S.; Bowman, C. N. Effects of Neighboring Sulfides and PH on Ester Hydrolysis in Thiol–Acrylate Photopolymers. *Acta Biomater.* **2007**, *3* (4), 449–455 DOI: 10.1016/j.actbio.2006.12.001.

(20) Crielaard, B. J.; Rijcken, C. J. F.; Quan, L.; Van Der Wal, S.; Altintas, I.; Van Der Pot, M.; Kruijtzer, J. A. W.; Liskamp, R. M. J.; Schiffelers, R. M.; Van Nostrum, C. F.; Hennink, W. E.; Wang, D.; Lammers, T.; Storm, G. Glucocorticoid-Loaded Core-Cross-Linked Polymeric Micelles with Tailorable Release Kinetics for Targeted Therapy of Rheumatoid

Arthritis. *Angew. Chemie Int. Ed.* **2012**, *51* (29), 7254–7258 DOI: 10.1002/anie.201202713.

(21) Schoenmakers, R. G.; Van De Wetering, P.; Elbert, D. L.; Hubbell, J. A. The Effect of the Linker on the Hydrolysis Rate of Drug-Linked Ester Bonds. *J. Control. Release* **2004**, *95* (2), 291–300 DOI: 10.1016/j.jconrel.2003.12.009.

(22) Rydholm, A. E.; Anseth, K. S.; Bowman, C. N. Effects of Neighboring Sulfides and PH on Ester Hydrolysis in Thiol-Acrylate Photopolymers. *Acta Biomater.* **2007**, *3* (4), 449–455 DOI: 10.1016/j.actbio.2006.12.001.

(23) Yong-beom Lim; Seon-mi Kim; Hearan Suh, and; Park*, J. Biodegradable, Endosome Disruptive, and Cationic Network-Type Polymer as a Highly Efficient and Nontoxic Gene Delivery Carrier. **2002** DOI: 10.1021/BC025541N.

(24) Yong-beom Lim; Young Hun Choi, and; Park, J. A Self-Destroying Polycationic Polymer: Biodegradable Poly(4-Hydroxy-l-Proline Ester). **1999** DOI: 10.1021/JA984012K.

(25) Dan, K.; Pan, R.; Ghosh, S. Aggregation and PH Responsive Disassembly of a New Acid-Labile Surfactant Synthesized by Thiol−Acrylate Michael Addition Reaction. *Langmuir* **2011**, *27* (2), 612–617 DOI: 10.1021/la104445h.

(26) Chen, S.; Hou, P.; Wang, J.; Liu, L.; Zhang, Q. A Highly Selective Fluorescent Probe Based on Coumarin for the Imaging of N2H4 in Living Cells. *Spectrochim. Acta Part A Mol. Biomol. Spectrosc.* **2017**, *173*, 170–174 DOI: 10.1016/J.SAA.2016.09.013.

(27) Yeom, C. E.; Kim, M. J.; Kim, B. M. 1,8-Diazabicyclo[5.4.0]Undec-7-Ene (DBU)-Promoted Efficient and Versatile Aza-Michael Addition. *Tetrahedron* **2007**, *63* (4), 904–909 DOI: 10.1016/j.tet.2006.11.037.

BIBLIOGRAPHY

Abbasi, E.; Aval, S. F.; Akbarzadeh, A.; Milani, M.; Nasrabadi, H. T.; Joo, S. W.; Hanifehpour, Y.; Nejati-Koshki, K.; Pashaei-Asl, R. Dendrimers: Synthesis, Applications, and Properties. *Nanoscale Research Letters*. Springer 2014, pp 1–10.

Arnt, L.; Tew, G. N. Cationic Facially Amphiphilic Poly(Phenylene Ethynylene)s Studied at the Air-Water Interface. *Langmuir* **2003**, *19* (6), 2404–2408 DOI: 10.1021/la0268597.

Arnt, L.; Tew, G. N. New Poly(Phenyleneethynylene)s with Cationic, Facially Amphiphilic Structures. *J. Am. Chem. Soc.* **2002**, *124* (26), 7664–7665 DOI: 10.1021/ja026607s.

Arumugam, S.; Vutukuri, D. R.; Thayumanavan, S.; Ramamurthy, V. Amphiphilic Homopolymer as a Reaction Medium in Water: Product Selectivity within Polymeric Nanopockets. *J. Am. Chem. Soc.* **2005**, *127* (38), 13200–13206 DOI: 10.1021/ja051107v.

Azagarsamy, M. A.; Gomez-Escudero, A.; Yesilyurt, V.; Vachet, R. W.; Thayumanavan, S. Amphiphilic Nanoassemblies for the Detection of Peptides and Proteins Using Fluorescence and Mass Spectrometry. *Analyst* **2009**, *134* (4), 635 DOI: 10.1039/b818484d.

Bae, Y.; Fukushima, S.; Harada, A.; Kataoka, K. Design of Environment-Sensitive Supramolecular Assemblies for Intracellular Drug Delivery: Polymeric Micelles That Are Responsive to Intracellular PH Change. *Angew. Chemie* **2003**, *115* (38), 4788–4791 DOI: 10.1002/ange.200250653.

Basu, S.; Vutukuri, D. R.; Shyamroy, S.; Sandanaraj, B. S.; Thayumanavan, S. Invertible Amphiphilic Homopolymers. *J. Am. Chem. Soc.* **2004**, *126* (32), 9890–9891 DOI: 10.1021/ja047816a.

Beaujuge, P. M.; Fréchet, J. M. J. Molecular Design and Ordering Effects in π-Functional Materials for Transistor and Solar Cell Applications. *J. Am. Chem. Soc.* **2011**, *133* (50), 20009–20029 DOI: 10.1021/ja2073643.

Blanazs, A.; Armes, S. P.; Ryan, A. J. Self-Assembled Block Copolymer Aggregates: From Micelles to Vesicles and Their Biological Applications. *Macromolecular Rapid Communications*. February 18, 2009, pp 267–277.

Buss, H.; Chan, T. P.; Sluis, K. B.; Domigan, N. M.; Winterbourn, C. C. Protein Carbonyl Measurement by a Sensitive ELISA Method. *Free Radic. Biol. Med.* **1997**, *23* (3), 361–366 DOI: 10.1016/S0891-5849(97)00104-4.

Busseron, E.; Ruff, Y.; Moulin, E.; Giuseppone, N. Supramolecular Self-Assemblies as Functional Nanomaterials. *Nanoscale* **2013**, *5* (16), 7098 DOI: 10.1039/c3nr02176a.

Cha, J. N.; Birkedal, H.; Euliss, L. E.; Bartl, M. H.; Wong, M. S.; Deming, T. J.; Stucky, G. D. Spontaneous Formation of Nanoparticle Vesicles from Homopolymer Polyelectrolytes. *J. Am.*

Chem. Soc. **2003**, *125* (27), 8285–8289 DOI: 10.1021/ja0279601.

Changez, M.; Kang, N. G.; Lee, C. H.; Lee, J. S. Reversible and PH-Sensitive Vesicles from Amphiphilic Homopolymer Poly(2-(4-Vinylphenyl)Pyridine). *Small* **2010**, *6* (1), 63–68 DOI: 10.1002/smll.200901670.

Chen, C. K.; Wang, Q.; Jones, C. H.; Yu, Y.; Zhang, H.; Law, W. C.; Lai, C. K.; Zeng, Q.; Prasad, P. N.; Pfeifer, B. A.; Cheng, C. Synthesis of pH-Responsive Chitosan Nanocapsules for the Controlled Delivery of Doxorubicin. *Langmuir* **2014**, *30* (14), 4111–4119 DOI: 10.1021/la4040485.

Chen, S.; Hou, P.; Wang, J.; Liu, L.; Zhang, Q. A Highly Selective Fluorescent Probe Based on Coumarin for the Imaging of N2H4 in Living Cells. *Spectrochim. Acta Part A Mol. Biomol. Spectrosc.* **2017**, *173*, 170–174 DOI: 10.1016/J.SAA.2016.09.013.

Chen, Y.; Thorn, M.; Christensen, S.; Versek, C.; Poe, A.; Hayward, R. C.; Tuominen, M. T.; Thayumanavan, S. Enhancement of Anhydrous Proton Transport by Supramolecular Nanochannels in Comb Polymers. *Nat. Chem.* **2010**, *2* (6), 503–508 DOI: 10.1038/nchem.629.

Chiefari, J., Chong, Y.K., Ercole, F., Krstina, J., Jeffery, J., Mayadunne, L. T. A. Living Free-Radical Polymerization by Reversible Addition-Fragmentation Chain Transfer: The RAFT Process. *Macromolecules* **1998**, *31* (16), 5559–5562.

Combariza, M. Y.; Savariar, E. N.; Vutukuri, D. R.; Thayumanavan, S.; Vachet, R. W. Polymerie Inverse Micelles as Selective Peptide Extraction Agents for MALDI-MS Analysis. *Anal. Chem.* **2007**, *79* (18), 7124–7130 DOI: 10.1021/ac071001d.

Crielaard, B. J.; Rijcken, C. J. F.; Quan, L.; Van Der Wal, S.; Altintas, I.; Van Der Pot, M.; Kruijtzer, J. A. W.; Liskamp, R. M. J.; Schiffelers, R. M.; Van Nostrum, C. F.; Hennink, W. E.; Wang, D.; Lammers, T.; Storm, G. Glucocorticoid-Loaded Core-Cross-Linked Polymeric Micelles with Tailorable Release Kinetics for Targeted Therapy of Rheumatoid Arthritis. *Angew. Chemie Int. Ed.* **2012**, *51* (29), 7254–7258 DOI: 10.1002/anie.201202713.

Dan, K.; Pan, R.; Ghosh, S. Aggregation and PH Responsive Disassembly of a New Acid-Labile Surfactant Synthesized by Thiol−Acrylate Michael Addition Reaction. *Langmuir* **2011**, *27* (2), 612–617 DOI: 10.1021/la104445h.

Dirks, A. J. (Ton); van Berkel, S. S.; Hatzakis, N. S.; Opsteen, J. A.; van Delft, F. L.; Cornelissen, J. J. L. M.; Rowan, A. E.; van Hest, J. C. M.; Rutjes, F. P. J. T.; Nolte, R. J. M. Preparation of Biohybrid Amphiphiles via the Copper Catalysed Huisgen [3 + 2] Dipolar Cycloaddition Reaction. *Chem. Commun.* **2005**, *0* (33), 4172 DOI: 10.1039/b508428h.

Elsabahy, M.; Wooley, K. L. Design of Polymeric Nanoparticles for Biomedical Delivery Applications. *Chem. Soc. Rev.* **2012**, *41* (7), 2545 DOI: 10.1039/c2cs15327k.

Engvall, E.; Perlmann, P. Quantitation of Specific Antibodies by Enzyme-Labeled Anti-Immunoglobulin in Antigencoated Tubes. *Curr. Contents* **1989**, *109* (1), 16 DOI: 10.1038/npg.els.0004021.

Escamilla, I. V.; Ramos, L. F. R.; Escalera, J. S.; Hernández, A. Á. Studies on the Deprotection of Triisopropylsilylarylacetylene Derivatives. *J. Mex. Chem. Soc.* **2011**, *55* (3), 133–136.

Etrych, T.; Jelínková, M.; Říhová, B.; Ulbrich, K. New HPMA Copolymers Containing Doxorubicin Bound via PH-Sensitive Linkage: Synthesis and Preliminary in Vitro and in Vivo Biological Properties. *J. Control. Release* **2001**, *73* (1), 89–102 DOI: 10.1016/S0168-3659(01)00281-4.

Feldman, D.; Barbalata, A. *Synthetic Polymers : Technology, Properties, Applications*; Chapman & Hall, 1996.

Feng, C.; Lu, G.; Li, Y.; Huang, X. Self-Assembly of Amphiphilic Homopolymers Bearing Ferrocene and Carboxyl Functionalities: Effect of Polymer Concentration, β-Cyclodextrin, and Length of Alkyl Linker. *Langmuir* **2013**, *29* (34), 10922–10931 DOI: 10.1021/la402335d.

Gao, W.; Chan, J. M.; Farokhzad, O. C. PH-Responsive Nanoparticles for Drug Delivery. *Mol. Pharm.* **2010**, *7* (6), 1913–1920 DOI: 10.1021/mp100253e.

Gillies, E. R.; Goodwin, A. P.; Fréchet, J. M. J. Acetals as pH-Sensitive Linkages for Drug Delivery. In *Bioconjugate Chemistry*; American Chemical Society, 2004; Vol. 15, pp 1254–1263.

Gillissen, M. A. J.; Voets, I. K.; Meijer, E. W.; Palmans, A. R. A. Single Chain Polymeric Nanoparticles as Compartmentalised Sensors for Metal Ions. *Polym. Chem.* **2012**, *3* (11), 3166–3174 DOI: 10.1039/c2py20350b.

Greenspan, P.; Fowler, S. D. Spectrofluorometric Studies of the Lipid Probe, Nile Red. *J. Lipid Res.* **1985**, *26* (7), 781–789.

Guo, Q.; Zhang, T.; An, J.; Wu, Z.; Zhao, Y.; Dai, X.; Zhang, X.; Li, C. Block versus Random Amphiphilic Glycopolymer Nanopaticles as Glucose-Responsive Vehicles. *Biomacromolecules* **2015**, *16* (10), 3345–3356 DOI: 10.1021/acs.biomac.5b01020.

Hanash, S. M.; Pitteri, S. J.; Faca, V. M. Mining the Plasma Proteome for Cancer Biomarkers. *Nature*. April 3, 2008, pp 571–579.

He, J.; Xia, Y.; Niu, Y.; Hu, D.; Xia, X.; Lu, Y.; Xu, W. PH-Responsive Core Crosslinked Polycarbonate Micelles via Thiol-Acrylate Michael Addition Reaction. *J. Appl. Polym. Sci.* **2017**, *134* (5) DOI: 10.1002/app.44421.

Heller, J.; Barr, J.; Ng, S. Y.; Abdellauoi, K. S.; Gurny, R. Poly(Ortho Esters): Synthesis, Characterization, Properties and Uses. *Advanced Drug Delivery Reviews*. 2002, pp 1015–1039.

Helms, B.; Mynar, J. L.; Hawker, C. J.; Fréchet, J. M. J. Dendronized Linear Polymers via "Click Chemistry." *J. Am. Chem. Soc.* **2004**, *126* (46), 15020–15021 DOI: 10.1021/ja044744e.

Hoyle, C. E.; Bowman, C. N. Thiol-Ene Click Chemistry. *Angew. Chemie - Int. Ed.* **2010**, *49* (9), 1540–1573 DOI: 10.1002/anie.200903924.

Ikkala, O.; ten Brinke, G. Functional Materials Based on Self-Assembly of Polymeric Supramolecules. *Science* **2002**, *295* (5564), 2407–2409 DOI: 10.1126/science.1067794.

Ilker, M. F.; Nüsslein, K.; Tew, G. N.; Coughlin, E. B. Tuning the Hemolytic and Antibacterial Activities of Amphiphilic Polynorbornene Derivatives. *J. Am. Chem. Soc.* **2004**, *126* (48), 15870–15875 DOI: 10.1021/ja045664d.

Isimjan, T. T.; de Bruyn, J. R.; Gillies, E. R. Self-Assembly of Supramolecular Polymers from β-Strand Peptidomimetic−Poly(Ethylene Oxide) Hybrids. *Macromolecules* **2010**, *43* (10), 4453–4459 DOI: 10.1021/ma100444b.

Jamal, S.; Rezaei, T.; Sarbaz, L.; Niknejad, H. Folate-Decorated Redox/PH Dual-Responsive Degradable Prodrug Micelles for Tumor Triggered Targeted Drug Delivery. *RSC Adv.* **2016**, *6*, 62630–62639 DOI: 10.1039/c6ra11824k.

Janata, J.; Josowicz, M. Conducting Polymers in Electronic Chemical Sensors. *Nat. Mater.* **2003**, *2* (1), 19–24 DOI: 10.1038/nmat768.

Jewett, J. C.; Bertozzi, C. R. Cu-Free Click Cycloaddition Reactions in Chemical Biology. *Chem. Soc. Rev.* **2010**, *39* (4), 1272–1279.

Jia, H.-Z.; Zhang, W.; Zhu, J.-Y.; Yang, B.; Chen, S.; Chen, G.; Zhao, Y.-F.; Feng, J.; Zhang, X.-Z. Hyperbranched–Hyperbranched Polymeric Nanoassembly to Mediate Controllable Co-Delivery of SiRNA and Drug for Synergistic Tumor Therapy. *J. Control. Release* **2015**, *216*, 9–17 DOI: 10.1016/J.JCONREL.2015.08.006.

Jim, C. K. W.; Qin, A.; Lam, J. W. Y.; Mahtab, F.; Yu, Y.; Tang, B. Z. Metal-Free Alkyne Polyhydrothiolation: Synthesis of Functional Poly(Vinylenesulfide)s with High Stereoregularity by Regioselective Thioclick Polymerization. *Adv. Funct. Mater.* **2010**, *20* (8), 1319–1328 DOI: 10.1002/adfm.200901943.

Jin, H.; Huang, W.; Zhu, X.; Zhou, Y.; Yan, D. Biocompatible or Biodegradable Hyperbranched Polymers: From Self-Assembly to Cytomimetic Applicationsw. *This J. is Cite this Chem. Soc. Rev* **2012**, *41*, 5986–5997 DOI: 10.1039/c2cs35130g.

Joshi, G.; Anslyn, E. V. Dynamic Thiol Exchange with β-Sulfido-α,β-Unsaturated Carbonyl Compounds and Dithianes. *Org. Lett.* **2012**, *14* (18), 4714–4717 DOI: 10.1021/ol301781u.

Julien Nicolas; Yohann Guillaneuf; Catherine Lefay; Denis Bertin; Didier Gigmes; Charleux, and B. Nitroxide-Mediated Polymerisation. *Prog. Polym. Sci.* **2013**, *38* (1), 63–235 DOI: 10.1016/j.progpolymsci.2012.06.002.

Kale, T. S.; Klaikherd, A.; Popere, B.; Thayumanavan, S. Supramolecular Assemblies of Amphiphilic Homopolymers. *Langmuir* **2009**, *25* (17), 9660–9670 DOI: 10.1021/la900734d.

Keddie, D. J. A Guide to the Synthesis of Block Copolymers Using Reversible-Addition Fragmentation Chain Transfer (RAFT) Polymerization. *Chem. Soc. Rev.* **2014**, *43* (2), 496–505 DOI: 10.1039/C3CS60290G.

Kenney, J. F. Properties of Block versus Random Copolymers. *Polym. Eng. Sci.* **1968**, *8* (3), 216–226 DOI: 10.1002/pen.760080307.

Klaikherd, A.; Nagamani, C.; Thayumanavan, S. Multi-Stimuli Sensitive Amphiphilic Block Copolymer Assemblies. *J. Am. Chem. Soc.* **2009**, *131* (13), 4830–4838 DOI: 10.1021/ja809475a.

Kohut, A.; Hevus, I.; Voronov, S.; Voronov, A. Amphiphilic Invertible Polymers and Their Applications. In *Industrial Applications for Intelligent Polymers and Coatings*; Springer International Publishing: Cham, 2016; pp 399–415.

Kubo, T.; Bentz, K. C.; Powell, K. C.; Figg, C. A.; Swartz, J. L.; Tansky, M.; Chauhan, A.; Savin, D. A.; Sumerlin, B. S. Modular and Rapid Access to Amphiphilic Homopolymers via Successive Chemoselective Post-Polymerization Modification. *Polym. Chem.* **2017**, *8* (39), 6028–6032 DOI: 10.1039/C7PY01585B.

Kuroda, H.; Tomita, I.; Endo, T. A Novel Polyaddition of Bifunctional Acetylenes Containing Electron-Withdrawing Groups. 2. Synthesis of Polymers Having B-Alkylmercaptoenoate Moieties by the Reaction with Dithiols. *Macromolecules* **1995**, 6020–6025 DOI: 10.1021/ma00122a006.

Laurent, B. A.; Grayson, S. M. Synthesis of Cyclic Amphiphilic Homopolymers and Their Potential Application as Polymeric Micelles. *Polym. Chem.* **2012**, *3* (7), 1846–1855 DOI: 10.1039/C1PY00378J.

Li, L.; Raghupathi, K.; Song, C.; Prasad, P.; Thayumanavan, S. Self-Assembly of Random Copolymers. *Chem. Commun. (Camb).* **2014**, *50* (88), 13417–13432 DOI: 10.1039/c4cc03688c.

Li, N.; Ye, G.; He, Y.; Wang, X. Hollow Microspheres of Amphiphilic Azo Homopolymers: Self-Assembly and Photoinduced Deformation Behavior. *Chem. Commun.* **2011**, *47* (16), 4757–4759 DOI: 10.1039/c0cc05010e.

Liotta, L. A.; Petricoin, E. Cancer Biomarkers: Closer to Delivering on Their Promise. *Cancer Cell*. 2011, pp 279–280.

Liu, B.; Thayumanavan, S. Substituent Effects on the PH Sensitivity of Acetals and Ketals and Their Correlation with Encapsulation Stability in Polymeric Nanogels. *J. Am. Chem. Soc.* **2017**, *139* (6), 2306–2317 DOI: 10.1021/jacs.6b11181.

Liu, J.; Huang, W.; Pang, Y.; Huang, P.; Zhu, X.; Zhou, Y.; Yan, D. Molecular Self-Assembly of a Homopolymer: An Alternative to Fabricate Drug-Delivery Platforms for Cancer Therapy. *Angew. Chemie - Int. Ed.* **2011**, *50* (39), 9162–9166 DOI: 10.1002/anie.201102280.

Liu, X.; Hu, D.; Jiang, Z.; Zhuang, J.; Xu, Y.; Guo, X.; Thayumanavan, S. Multi-Stimuli-Responsive Amphiphilic Assemblies through Simple Postpolymerization Modifications. *Macromolecules* **2016**, *49* (17), 6186–6192 DOI: 10.1021/acs.macromol.6b01397.

Lowe, A. B. Thiol-Yne 'Click'/Coupling Chemistry and Recent Applications in Polymer and Materials Synthesis and Modification. *Polym. (United Kingdom)* **2014**, *55* (22), 5517–5549 DOI: 10.1016/j.polymer.2014.08.015.

Luo, C.; Liu, Y.; Li, Z. Thermo- and PH-Responsive Polymer Derived from Methacrylamide and Aspartic Acid. *Macromolecules* **2010**, *43* (19), 8101–8108 DOI: 10.1021/ma1015227.

Lv, S.; Tang, Z.; Zhang, D.; Song, W.; Li, M.; Lin, J.; Liu, H.; Chen, X. Well-Defined Polymer-Drug Conjugate Engineered with Redox and PH-Sensitive Release Mechanism for Efficient Delivery of Paclitaxel. *J. Control. Release* **2014**, *194*, 220–227 DOI: 10.1016/j.jconrel.2014.09.009.

Mai, Y.; Eisenberg, A. Self-Assembly of Block Copolymers. *Chem. Soc. Rev.* **2012**, *41* (18), 5969 DOI: 10.1039/c2cs35115c.

Mane, S. R.; Rao N, V.; Chaterjee, K.; Dinda, H.; Nag, S.; Kishore, A.; Das Sarma, J.; Shunmugam, R. Amphiphilic Homopolymer Vesicles as Unique Nano-Carriers for Cancer Therapy. *Macromolecules* **2012**, *45* (19), 8037–8042 DOI: 10.1021/ma301644m.

Mane, S. R.; Rao, V. N.; Shunmugam, R. Reversible PH- and Lipid-Sensitive Vesicles from Amphiphilic Norbornene-Derived Thiobarbiturate Homopolymers. *ACS Macro Lett.* **2012**, *1* (4), 482–488 DOI: 10.1021/mz2002092.

Mane, S. R.; Shunmugam, R. Hierarchical Self-Assembly of Amphiphilic Homopolymer into Unique Superstructures. *ACS Macro Lett.* **2014**, *3* (1), 44–50 DOI: 10.1021/mz4005524.

Manojkumar, K.; Mecerreyes, D.; Taton, D.; Gnanou, Y.; Vijayakrishna, K. Self-Assembly of Poly(Ionic Liquid) (PIL)-Based Amphiphilic Homopolymers into Vesicles and Supramolecular Structures with Dyes and Silver Nanoparticles. *Polym. Chem.* **2017**, *8* (22), 3497–3503 DOI: 10.1039/C7PY00453B.

Martin, J. R.; Gupta, M. K.; Page, J. M.; Yu, F.; Davidson, J. M.; Guelcher, S. A.; Duvall, C. L. A Porous Tissue Engineering Scaffold Selectively Degraded by Cell-Generated Reactive Oxygen Species. *Biomaterials* **2014**, *35* (12), 3766–3776 DOI: 10.1016/j.biomaterials.2014.01.026.

Matyjaszewski, K. *Cationic Polymerizations: Mechanisms, Synthesis & Applications*; Plastics Engineering; Taylor & Francis, 1996.

Meizhen, Y.; Jie, S.; Pisula, W.; Minghui, L.; Linjie, Z.; Müllen, K. Functionalization of Self-Assembled Hexa-Peri-Hexabenzocoronene Fibers with Peptides for Bioprobing. *J. Am. Chem. Soc.* **2009**, *131* (41), 14618–14619 DOI: 10.1021/ja9058662.

Meldal, M.; Tornøe, C. W. Cu-Catalyzed Azide−Alkyne Cycloaddition. *Chem. Rev.* **2008**, *108* (8), 2952–3015 DOI: 10.1021/cr0783479.

Metters, A.; Hubbell, J. Network Formation and Degradation Behavior of Hydrogels Formed by Michael-Type Addition Reactions. *Biomacromolecules* **2005**, *6* (1), 290–301 DOI: 10.1021/bm049607o.

Miao, W.-K.; Yan, Y.-K.; Wang, X.-L.; Xiao, Y.; Ren, L.-J.; Zheng, P.; Wang, C.-H.; Ren, L.-X.; Wang, W. Incorporation of Polyoxometalates into Polymers to Create Linear Poly(Polyoxometalate)s with Catalytic Function. *ACS Macro Lett.* **2014**, *3* (2), 211–215 DOI:

10.1021/mz5000202.

Milner, S. T. Polymer Brushes. *Science* **1991**, *251* (4996), 898–905 DOI: 10.1126/science.251.4996.898.

Molla, M. R.; Marcinko, T.; Prasad, P.; Deming, D.; Garman, S. C.; Thayumanavan, S. Unlocking a Caged Lysosomal Protein from a Polymeric Nanogel with a pH Trigger. *Biomacromolecules* **2014**, *15* (11), 4046–4053 DOI: 10.1021/bm501091p.

Moses, J. E.; Moorhouse, A. D. The Growing Applications of Click Chemistry. *Chem. Soc. Rev.* **2007**, *36* (8), 1249–1262 DOI: 10.1039/B613014N.

Mühlebach, A.; Gaynor, S. G.; Matyjaszewski, K. Synthesis of Amphiphilic Block Copolymers by Atom Transfer Radical Polymerization (ATRP). *Macromolecules* **1998**, *31* (18), 6046–6052 DOI: 10.1021/ma9804747.

Lee, M.; Jang, C. J.; Ryu, J.H. Supramolecular Reactor from Self-Assembly of Rod-Coil Molecule in Aqueous Environment *J. Am. Chem. Soc*. **2004**, *126* (26), pp 8082–8083 DOI: 10.1021/JA048264Z.

Hadjichristidis, N.; Pitsikalis, M.; Pispas, S.; Iatrou, H. Polymers with Complex Architecture by Living Anionic Polymerization. *Chem. Rev*. **2001**, *101* (12), pp 3747–3792 DOI: 10.1021/CR9901337.

Oak, M.; Mandke, R.; Singh, J. Smart Polymers for Peptide and Protein Parenteral Sustained Delivery. *Drug Discov. Today Technol.* **2012**, *9* (2), e131–e140 DOI: 10.1016/j.ddtec.2012.05.001.

Oishi, M.; Nagasaki, Y.; Itaka, K.; Nishiyama, N.; Kataoka, K. Lactosylated Poly(Ethylene Glycol)-SiRNA Conjugate through Acid-Labile Beta-Thiopropionate Linkage to Construct PH-Sensitive Polyion Complex Micelles Achieving Enhanced Gene Silencing in Hepatoma Cells. *J. Am. Chem. Soc.* **2005**, *127* (6), 1624–1625 DOI: 10.1021/ja044941d.

Oishi, M.; Sasaki, S.; Nagasaki, Y.; Kataoka, K. pH-Responsive Oligodeoxynucleotide (ODN) - Poly (Ethylene Glycol) Conjugate through Acid-Labile -Thiopropionate Linkage : Preparation and Polyion Complex Micelle Formation. *Biomacromolecules* **2003**, *4* (5), 1426–1432 DOI: 10.1021/bm034164u.

Ouk Kim, S.; Solak, H. H.; Stoykovich, M. P.; Ferrier, N. J.; de Pablo, J. J.; Nealey, P. F. Epitaxial Self-Assembly of Block Copolymers on Lithographically Defined Nanopatterned Substrates. *Nature* **2003**, *424* (6947), 411–414 DOI: 10.1038/nature01775.

Mansky, P.; Liu, Y.; Huang, E.; Russell, T. P.; Hawker, C.; Controlling Polymer-Surface Interactions with Random Copolymer Brushes. *Science* **1997**, *275* (5305), 1458–1460 DOI: 10.1126/science.207.4435.1073.

Qiu, L.; Zhang, J.; Yan, M.; Jin, Y.; Zhu, K. Reverse Self-Assemblies Based on Amphiphilic Polyphosphazenes for Encapsulation of Water-Soluble Molecules. *Nanotechnology* **2007**, *18* (47),

475602 DOI: 10.1088/0957-4484/18/47/475602.

Quémener, D.; Hellaye, M. Le; Bissett, C.; Davis, T. P.; Barner-Kowollik, C.; Stenzel, M. H. Graft Block Copolymers of Propargyl Methacrylate and Vinyl Acetate via a Combination of RAFT/MADIX and Click Chemistry: Reaction Analysis. *J. Polym. Sci. Part A Polym. Chem.* **2008**, *46* (1), 155–173 DOI: 10.1002/pola.22367.

Ramireddy, R. R.; Prasad, P.; Finne, A.; Thayumanavan, S. Zwitterionic Amphiphilic Homopolymer Assemblies. *Polym. Chem.* **2015**, *6* (33), 6083–6087 DOI: 10.1039/C5PY00879D.

Rasband, W. S. ImageJ. US National Institutes of Health: Bethesda, Maryland, USA

Reczek, J. J.; Iverson, B. L. Using Aromatic Donor Acceptor Interactions to Affect Macromolecular Assembly. *Macromolecules* **2006**, *39*, 5601–5603 DOI: 10.1021/ma0611669.

Ren, J. M.; McKenzie, T. G.; Fu, Q.; Wong, E. H. H.; Xu, J.; An, Z.; Shanmugam, S.; Davis, T. P.; Boyer, C.; Qiao, G. G. Star Polymers. *Chem. Rev.* **2016**, *116* (12), 6743–6836 DOI: 10.1021/acs.chemrev.6b00008.

Rodthongkum, N.; Chen, Y.; Thayumanavan, S.; Vachet, R. W. Matrix-Assisted Laser Desorption Ionization-Mass Spectrometry Signal Enhancement of Peptides after Selective Extraction with Polymeric Reverse Micelles. *Anal. Chem.* **2010**, *82* (9), 3686–3691 DOI: 10.1021/ac1000256.

Rodthongkum, N.; Chen, Y.; Thayumanavan, S.; Vachet, R. W. Selective Enrichment and Analysis of Acidic Peptides and Proteins Using Polymeric Reverse Micelles and MALDI-MS. *Anal. Chem.* **2010**, *82* (20), 8686–8691 DOI: 10.1021/ac101922b.

Rodthongkum, N.; Ramireddy, R.; Thayumanavan, S.; Richard, W. V. Selective Enrichment and Sensitive Detection of Peptide and Protein Biomarkers in Human Serum Using Polymeric Reverse Micelles and MALDI-MS. *Analyst* **2012**, *137* (4), 1024–1030 DOI: 10.1039/c2an16089g.

Rodthongkum, N.; Washington, J. D.; Savariar, E. N.; Thayumanavan, S.; Vachet, R. W. Generating Peptide Titration-Type Curves Using Polymeric Reverse Micelles As Selective Extraction Agents along with Matrix-Assisted Laser Desorption Ionization-Mass Spectrometry Detection. *Anal. Chem.* **2009**, *81* (12), 5046–5053 DOI: 10.1021/ac900661e.

Rösler, A.; Vandermeulen, G. W. M.; Klok, H. A. Advanced Drug Delivery Devices via Self-Assembly of Amphiphilic Block Copolymers. *Adv. Drug Deliv. Rev* **2012**, 53, 95-108 DOI: 10.1016/S0169-409X(01)00222-8

Rydholm, A. E.; Anseth, K. S.; Bowman, C. N. Effects of Neighboring Sulfides and pH on Ester Hydrolysis in Thiol–Acrylate Photopolymers. *Acta Biomater.* **2007**, *3*, 449–455 DOI: 10.1016/j.actbio.2006.12.001.

Ryu, J. H.; Chacko, R. T.; Jiwpanich, S.; Bickerton, S.; Babu, R. P.; Thayumanavan, S. Self-Cross-Linked Polymer Nanogels: A Versatile Nanoscopic Drug Delivery Platform. *J. Am. Chem. Soc.* **2010**, *132* (48), 17227–17235 DOI: 10.1021/ja1069932.

Sahab, Z. J.; Semaan, S. M.; Sang, Q. X. A. Methodology and Applications of Disease Biomarker Identification in Human Serum. *Biomark. Insights* **2007**, *2*, 21-43

Sandanaraj, B. S.; Demont, R.; Thayumanavan, S. Generating Patterns for Sensing Using a Single Receptor Scaffold. *J. Am. Chem. Soc.* **2007**, *129* (12), 3506–3507 DOI: 10.1021/ja070229f.

Savariar, E. N.; Aathimanikandan, S. V.; Thayumanavan, S. Supramolecular Assemblies from Amphiphilic Homopolymers: Testing the Scope. *J. Am. Chem. Soc.* **2006**, *128* (50), 16224–16230 DOI: 10.1021/ja065213o.

Schacher, F. H.; Rupar, P. A.; Manners, I. Functional Block Copolymers: Nanostructured Materials with Emerging Applications. *Angew. Chemie Int. Ed.* **2012**, *51* (32), 7898–7921 DOI: 10.1002/anie.201200310.

Schildknecht, C. E. Stereoregulation and Stereoregular Polymers. *Polym. Eng. Sci.* **1966**, *6* (3), 240–243 DOI: 10.1002/pen.760060311.

Schilling, C. I.; Jung, N.; Biskup, M.; Schepers, U.; Bräse, S. Bioconjugation via Azide–Staudinger Ligation: An Overview. *Chem. Soc. Rev.* **2011**, *40* (9), 4840 DOI: 10.1039/c0cs00123f.

Schoenmakers, R. G.; Van De Wetering, P.; Elbert, D. L.; Hubbell, J. A. The Effect of the Linker on the Hydrolysis Rate of Drug-Linked Ester Bonds. *J. Control. Release* **2004**, *95* (2), 291–300 DOI: 10.1016/j.jconrel.2003.12.009.

Seidi, F.; Jenjob, R.; Crespy, D. Designing Smart Polymer Conjugates for Controlled Release of Payloads. *Chem. Rev.* **2018**, *118* (7), 3965–4036 DOI: 10.1021/acs.chemrev.8b00006.

Serrano, M. A. C.; He, H.; Zhao, B.; Ramireddy, R. R.; Vachet, R. W.; Thayumanavan, S. Polymer-Mediated Ternary Supramolecular Interactions for Sensitive Detection of Peptides. *Analyst* **2016**, *142*, 118-122 DOI: 10.1039/c6an01591c.

Shen, W. C.; Ryser, H. J. P. Cis-Aconityl Spacer between Daunomycin and Macromolecular Carriers: A Model of pH-Sensitive Linkage Releasing Drug from a Lysosomotropic Conjugate. *Biochem. Biophys. Res. Commun.* **1981**, *102* (3), 1048–1054 DOI: 10.1016/0006-291X(81)91644-2.

Shim, M. S.; Xia, Y. A Reactive Oxygen Species (ROS)-Responsive Polymer for Safe, Efficient, and Targeted Gene Delivery in Cancer Cells. *Angew. Chemie Int. Ed.* **2013**, *52* (27), 6926–6929 DOI: 10.1002/anie.201209633.

Basu, S.; Vutukuri, D. R. and; Thayumanavan, S. Homopolymer Micelles in Heterogeneous Solvent Mixtures. *J. Am. Chem. Soc.* **2005**, *127* (48), 16794-16795 DOI: 10.1021/JA056042A.

Thomas, E. L.; Anderson, D. M.; Henkee, C. S.; Hoffman, D. Periodic Area-Minimizing Surfaces in Block Copolymers. *Nature* **1988**, *334* (6183), 598-601 DOI: 10.1038/334598a0.

Truce, W. E.; Tichenor, G. J. W. Effect of Activating Group on Trans Stereoselectivity of Thiolate Additions to Activated Acetylenes. *J. Org. Chem.* **1972**, *37* (15), 2391–2396 DOI:

10.1021/jo00980a007.

Truong, V. X.; Dove, A. P. Organocatalytic, Regioselective Nucleophilic “Click” Addition of Thiols to Propiolic Acid Esters for Polymer-Polymer Coupling. *Angew. Chemie Int. Ed.* **2013**, *52* (15), 4132-4136 DOI: 10.1002/anie.201209239.

Tu, Y.; Peng, F.; Adawy, A.; Men, Y.; Abdelmohsen, L. K. E. A.; Wilson, D. A. Mimicking the Cell: Bio-Inspired Functions of Supramolecular Assemblies. *Chem. Rev.* **2016**, *116* (4), 2023-2078 DOI: 10.1021/acs.chemrev.5b00344.

Ulrich, H. Introduction to Industrial Polymers. *Hanser Publ.* **1993**, 188.

Wang, J. S.; Matyjaszewski, K. Controlled/"living" Radical Polymerization. Atom Transfer Radical Polymerization in the Presence of Transition-Metal Complexes. *J. Am. Chem. Soc.* **1995**, *117*, 5614–5615.

Wang, Y.; Alb, A. M.; He, J.; Grayson, S. M. Neutral Linear Amphiphilic Homopolymers Prepared by Atom Transfer Radical Polymerization. *Polym. Chem.* **2014**, *5* (2), 622–629 DOI: 10.1039/c3py00916e.

Wang, Z. P.; van Oers, M. C. M.; van Hest, J. C. M.; Rutjes, F. Polymersome Pickering Emulsion for Enzyme Catalysis in a Biphasic System. *Angew. Chem. Int. Ed.* **2012**, *51*, 10746-10750 DOI: 10.1002/anie.201206555.

Wilson, D. S.; Dalmasso, G.; Wang, L.; Sitaraman, S. V; Merlin, D.; Murthy, N. Orally Delivered Thioketal Nanoparticles Loaded with TNF-α-SiRNA Target Inflammation and Inhibit Gene Expression in the Intestines. *Nat. Mater.* **2010**, *9* (11), 923-928 DOI: 10.1038/nmat2859.

Wolf, F. F.; Friedemann, N.; Frey, H. Poly(Lactide)-Block-Poly(HEMA) Block Copolymers: An Orthogonal One-Pot Combination of ROP and ATRP, Using a Bifunctional Initiator. *Macromolecules* **2009**, *42* (15), 5622-5628 DOI: 10.1021/ma900894d.

Xu, J.; Tao, L.; Boyer, C.; Lowe, A. B.; Davis, T. P. Facile Access to Polymeric Vesicular Nanostructures: Remarkable ω-End Group Effects in Cholesterol and Pyrene Functional (Co)Polymers. *Macromolecules* **2011**, *44* (2), 299-312 DOI: 10.1021/ma102386j.

Yao, B.; Sun, J.; Qin, A.; Tang, B. Z. Thiol-Yne Click Polymerization. *Chinese Sci. Bull.* **2013**, *58* (22), 2711-2718 DOI: 10.1007/s11434-013-5892-1.

Yates, K. Kinetics of Ester Hydrolysis in Concentrated Acid. *Acc. Chem. Res.* **1971**, *4* (4), 136-144 DOI: 10.1021/ar50040a003.

Yeom, C. E.; Kim, M. J.; Kim, B. M. 1,8-Diazabicyclo[5.4.0]Undec-7-Ene (DBU)-Promoted Efficient and Versatile Aza-Michael Addition. *Tetrahedron* **2007**, *63* (4), 904–909 DOI: 10.1016/j.tet.2006.11.037.

Yokozawa, T.; Ohta, Y. Transformation of Step-Growth Polymerization into Living Chain-Growth Polymerization. *Chem. Rev.* **2016**, *116* (4), 1950–1968 DOI:

10.1021/acs.chemrev.5b00393.

Lim, Y.; Kim, S.; Suh, H.; Park, J. Biodegradable, Endosome Disruptive, and Cationic Network-Type Polymer as a Highly Efficient and Nontoxic Gene Delivery Carrier. *Bioconjugate Chem.* **2002**, *13* (5), 952-957 DOI: 10.1021/BC025541N.

Lim, Y.; Choi, Y. H.; Park, J. A Self-Destroying Polycationic Polymer: Biodegradable Poly(4-Hydroxy-l-Proline Ester). **1999** DOI: 10.1021/JA984012K.

Yu, Y.; Yin, M.; Müllen, K.; Knoll, W. LbL-Assembled Multilayer Films of Dendritic Star Polymers: Surface Morphology and DNA Hybridization Detection. *J. Mater. Chem.* **2012**, *22* (16), 7880-7886 DOI: 10.1039/c2jm15931g.

Zhang, J.; Liu, K.; Müllen, K.; Yin, M. Self-Assemblies of Amphiphilic Homopolymers: Synthesis, Morphology Studies and Biomedical Applications. *Chem. Commun.* **2015**, *51* (58), 11541-11555 DOI: 10.1039/c5cc03016a.

Zhang, J.; Sun, H.; Ma, P. X. Host-Guest Interaction Mediated Polymeric Assemblies: Multifunctional Nanoparticles for Drug and Gene Delivery. *ACS Nano* **2010**, *4* (2), 1049-1059 DOI: 10.1021/nn901213a.

Zhang, L.; Eisenberg, A. Multiple Morphologies of "Crew-Cut" Aggregates of Polystyrene-b-Poly(Acrylic Acid) Block Copolymers. *Science* **1995**, *268* (5218), 1728-1731 DOI: 10.1126/science.268.5218.1728.

Zhou, Y.; Liu, B.; Wang, X. Self-Assembly of Homopolymers through Strong Dipole-Dipole Interaction in Their Aqueous Solutions. *Polymer (Guildf).* **2016**, *97*, 1-10 DOI: 10.1016/J.POLYMER.2016.05.011.

Zhu, L.; Ye, Z.; Cheng, K.; Miller, D. D.; Mahato, R. I. Site-Specific Delivery of Oligonucleotides to Hepatocytes after Systemic Administration. *Bioconjug. Chem.* **2008**, *19* (1), 290-298 DOI: 10.1021/bc070126m.

Zhu, X.; Liu, M. Self-Assembly and Morphology Control of New L-Glutamic Acid-Based Amphiphilic Random Copolymers: Giant Vesicles, Vesicles, Spheres, and Honeycomb Film. *Langmuir* **2011**, *27* (21), 12844-12850 DOI: 10.1021/la202680j.

Zhu, Y.; Liu, L.; Du, J. Probing into Homopolymer Self-Assembly: How Does Hydrogen Bonding Influence Morphology? *Macromolecules* **2013**, *46* (1), 194-203 DOI: 10.1021/ma302176a.

Zhuang, J.; Garzoni, M.; Torres, D. A.; Poe, A.; Pavan, G. M.; Thayumanavan, S. Programmable Nanoassemblies from Non-Assembling Homopolymers Using Ad Hoc Electrostatic Interactions. *Angew. Chemie Int. Ed.* **2017**, *56* (15), 4145-4149 DOI: 10.1002/anie.201611688.

Zou, J.; Zhang, F.; Zhang, S.; Pollack, S. F.; Elsabahy, M.; Fan, J.; Wooley, K. L. Poly(Ethylene Oxide)- *Block* -Polyphosphoester- *Graft* -Paclitaxel Conjugates with Acid-Labile Linkages as a PH-Sensitive and Functional Nanoscopic Platform for Paclitaxel Delivery. *Adv. Healthc. Mater.* **2014**, *3* (3), 441-448 DOI: 10.1002/adhm.201300235.